

# **PHYSICO-CHEMICAL BASIS FOR STRUVITE STONE FORMATION**

**Senthy Sellaturay**

MBBS BSc MRCS(Eng)

A thesis submitted to University College London, University of London  
in part fulfilment of the requirement for the degree of

Doctor of Medicine (M.D.)

Department of Applied Physiology

Institute of Urology

University College London

2011

## **Declaration of Authorship**

I, Senthyl Sellaturay, confirm that the work presented in this thesis is my own. Where information has been derived from other sources, I confirm that this has been indicated in the thesis.

**Signed:**

**Date:**

## **ABSTRACT:**

### **Introduction:**

Struvite stones (magnesium ammonium phosphate) account for 10-15% of renal stones and can grow rapidly forming staghorn calculi. With limited medical therapies available and surgery the mainstay of treatment, an understanding of the physico-chemical conditions causing struvite crystallization allows development of strategies to prevent their formation.

At present, very little is known about the physico-chemical conditions that result in struvite crystallisation. This lack of understanding has two bases: i) the particular ionised concentrations of the reactants (e.g.  $Mg^{2+}$ ,  $NH_4^+$ , and phosphate) in the urine are unknown; ii) the prevailing chemical conditions that would modulate crystallisation are also unclear (e.g. pH, osmolality, other urinary constituents). Recent advances in the development of ion-selective electrodes allows accurate determination of urinary constituents in small (<1ml) undiluted samples.

### **Methods:**

We have furthered developed an  $NH_4^+$ -ion selective electrode and magnesium ion-selective electrode to measure the urinary concentrations of each to aid our understanding of struvite deposition.  $[NH_4^+]$  and  $[Mg^{2+}]$  were measured using plastic dip cast ion-selective electrodes dispersed in suitable plasticisers, using nonactin for  $NH_4^+$  and several different neutral ligands for  $Mg^{2+}$ . Data were validated against standardised and developing methodology, including colour spectrophotometry and computational algorithms. Urine samples were also subjected to analysis using clinical biochemical techniques.

### **Results:**

We characterised an  $NH_4^+$ -ion selective electrode and made the first measurements of  $[NH_4^+]$  in undiluted urine samples, in normal subjects and those with stone disease. This technique was validated using colour spectrophotometry and then the technique was used to validate a computational algorithm. We have developed and characterised the  $Mg^{2+}$ -ion-selective electrode but  $Ca^{2+}$  caused significant interference.

### **Conclusions:**

Direct measurement of the urinary  $[NH_4^+]$  has been achieved for the first time with a value of about 25mM. This exciting new technique may now provide clinicians with an important point-of-care investigative tool in diagnosing and monitoring struvite calculogenesis.

## **ACKNOWLEDGEMENTS:**

I would like to thank a number of people who have assisted and encouraged me during my research and am very grateful for all the help I have received, but in particular I would like to thank the following:

Professor Christopher Fry, Professor of Cell Physiology, University College London, whose support and encouragement has been fantastic. He has taught me scientific method, inspired me and become a true great friend.

Mr Simon Choong, Urology Consultant at University College London Hospital, and my clinical supervisor, who guided me into research, and has provided much encouragement and support during this time.

Dr Bill Robertson, Biochemist at University College London, whose enthusiasm for the subject is both inspiring and knows no bounds.

Dr Nathan Davies, Lecturer at the Institute of Hepatology, UCL, who was exceptionally patient with me and assisted hugely in the validation of the ammonium ion-selective electrode.

My colleagues in the laboratory, who provided endless samples of urine for my experiments, without whom this work may not have been possible.

The Royal College of Surgeons (England), for awarding me a Research Fellowship which funded one year of research.

Family and friends who have been supportive and understanding when pressures of work have superseded other events.

Dad, Mum, Haresh, Priya and Nikki, who are the greatest family and have supported me in many ways during my period in research. Their unending enthusiasm has been fantastic and spurred me on during this time.

Our delightful little son, Shuban, who has enlightened our lives with his charming smile and sparkling personality. Born around the time of the Viva examination, he has provided me with immense inspiration in completing the thesis and examination.

And finally, my wonderful wife, Joanna Christine Makepeace, who has been a real pillar of support, very kind and generous. She has been encouraging and enthusiastic throughout and it would not be an understatement to say that this achievement is hers too.

I am grateful to them all.

# TABLE OF CONTENTS

page no

ABSTRACT	iii
ACKNOWLEDGEMENTS	iv
TABLE OF CONTENTS	vi
LIST OF TABLES	xii
LIST OF FIGURES	xiv
CHAPTER 1 INTRODUCTION	1
1.1 URINARY TRACT STONES, THE CLINICAL SITUATION	1
1.1.1 Urinary Tract Stones:	1
1.2 EPIDEMIOLOGY:	2
1.2.1 Intrinsic Factors:	2
1.2.1.1 Age / Sex:	2
1.2.1.2 Genetics:	2
1.2.2 Extrinsic Factors:	2
1.2.2.1 Geography:	2
1.2.2.2 Climate/Season:	3
1.2.2.3 Diet:	3
1.2.2.4 Water intake:	4
1.2.2.5 Occupation / Stress:	4
1.3 STONE TYPE, AETIOLOGY AND INCIDENCE:	5
1.4 CALCIUM STONE FORMATION:	7
1.4.1 Idiopathic Stone Formation:	7
1.4.2 Metabolic Causes for Stone Formation:	8
1.4.3 Management:	10
1.5 URIC ACID AND CYSTINE STONES:	10
1.5.1 Uric acid stones	10
1.5.2 Cystine stones	11
1.6 PHYSICO-CHEMICAL PRINCIPLES OF STONE FORMATION	11
1.6.1 Supersaturation	11
1.6.2 Crystal Formation	12
1.6.3 Modifiers of Crystal Formation	13
1.6.4 Crystalluria	14

1.6.5	Stone Matrix	14
1.7	<b>STRUVITE STONES</b>	15
1.7.1	Struvite Stones	16
1.7.2	Management	18
1.7.3	Struvite Crystal Formation	19
1.7.4	Struvite Crystal Structure	20
1.7.4.1	Struvite Crystals	20
1.7.4.2	In-vitro struvite crystal growth	21
1.7.4.3	In-vivo struvite crystal growth	23
1.7.5	Ultrastructure of human infected stones	24
1.7.6	Manipulating struvite crystallisation in artificial urine	24
1.7.7	Manipulating struvite crystallisation in human urine	25
1.8	<b>BACTERIOLOGY ASSOCIATED WITH STRUVITE STONES</b>	26
1.9	<b>CLINICAL IMPLICATIONS OF STRUVITE STONES</b>	30
1.9.1	Survival rates and sepsis	30
1.9.2	Renal function impairment	32
1.9.3	Encrustation and blockage of urethral catheters	33
1.9.4	Ureteric Stent Encrustation	36
1.9.5	Metabolic syndrome	37
1.9.6	Summary	38
1.10	<b>THE USE OF ION-SELECTIVE ELECTRODES IN MONITORING URINE COMPOSITION</b>	39
1.11	<b>HYPOTHESES, AIMS AND OBJECTIVES OF THE THESIS</b>	41
1.11.1	Hypotheses	41
1.11.2	Aims and experimental objectives of the thesis	41
<b>CHAPTER 2 METHODS AND PATIENT SAMPLES</b>		43
2.1	<b>PATIENT GROUPS</b>	43
2.2	<b>URINE COLLECTION AND CLINICAL BIOCHEMISTRY:</b>	44
2.2.1	Urine collection.	44
2.2.2	Urine storage	44
2.2.3	Clinical Biochemistry	44
2.3	<b>MANUFACTURE OF ION-SELECTIVE ELECTRODES</b>	45
2.3.1	General procedure for the manufacture of ion-selective plastics	45

2.3.2	Manufacture of the electrode template	47
2.3.3	Coating the electrode template with the ion-selective membrane	48
2.3.4	Ion-selective electrode filling solutions	48
2.3.5	Manufacture of reference electrodes	49
2.3.6	Manufacture of the Ag/AgCl electrodes	50
2.3.7	Experimental arrangement	51
2.4	CALIBRATION OF ION-SELECTIVE ELECTRODES	53
2.4.1	Calibration solutions	53
2.4.2	Manufacture of calibrating solutions	54
2.4.3	Experimental protocol	54
2.5	THEORY OF IONIC SOLUTIONS AND THE CALCULATION OF SELECTIVITY COEFFICIENTS.	56
2.5.1	Concentration and ionic activity	56
2.5.2	The relationship between electrode potential and ion activity – the Nikolsky equation.	57
2.5.3	Experimental protocol for calculating potentiometric selectivity coefficients, $k_{ij}^{pot}$ for an ion-selective electrode	61
2.5.4	Effect of pH on ion-selective responses	63
2.5.5	The effects of altered osmolality on ion-selective electrode responses	64
2.5.6	Effect of temperature on ion-selective $\text{NH}_4^+$ and $\text{K}^+$ -selective electrode responses	65
2.6	EXPERIMENTAL PROTOCOLS	65
2.6.1	Estimation of urinary $[\text{NH}_4^+]$ .	65
2.6.1.1	Measurements from the $\text{NH}_4^+$ -selective electrode	65
2.6.1.2	Measurement of urinary $[\text{K}^+]$	66
2.6.1.3	Protocol to measure urinary $[\text{NH}_4^+]$ from calibration curves	68
2.6.1.4	Protocol to measure urinary $[\text{Mg}^{2+}]$ from calibration curves:	70
2.6.2	Effects of storage on urinary $[\text{NH}_4^+]$	70
2.7	VALIDATION OF $\text{NH}_4^+$ -SELECTIVE ELECTRODE DATA AGAINST COLOUR SPECTROPHOTOMETRY	71
2.8	ALGORITHM TO CALCULATE URINARY $[\text{NH}_4^+]$	72

2.9	DATA PRESENTATION AND STATISTICAL ANALYSIS	74
CHAPTER 3	RESULTS:	75
3.1	Calibration of the $\text{NH}_4^+$ -selective electrode	75
3.1.1	Selectivity and sensitivity of the $\text{NH}_4^+$ -selective electrode	75
3.1.2	$\text{Na}^+$ interference	79
3.1.3	$\text{K}^+$ interference	79
3.1.4	$\text{Ca}^{2+}$ interference	84
3.1.5	$\text{H}^+$ ion interference	85
3.1.6	Determination of the effect of osmolality on the $\text{NH}_4^+$ -ISE response	87
3.2	Calibration of the $\text{K}^+$ -selective electrode	91
3.2.1	Calibration of $\text{K}^+$ -selective electrode	91
3.2.2	Selectivity of the $\text{K}^+$ -selective electrode	92
3.2.3	$\text{Na}^+$ interference	92
3.2.4	$\text{NH}_4^+$ interference	93
3.2.5	$\text{Ca}^{2+}$ interference	94
3.2.6	$\text{H}^+$ ion interference	94
3.2.7	Determination of the effect of osmolality on the $\text{K}^+$ -selective electrode	97
3.3	Characteristics of Patient Groups and Normal Subjects	99
3.4	Urinary $[\text{NH}_4^+]$ and $[\text{K}^+]$ measurements using the $\text{NH}_4^+$ - and $\text{K}^+$ -selective electrodes at room temperature	100
3.4.1	Sample calculations. Urinary $[\text{K}^+]$ measurement	100
3.4.2	Urinary $[\text{NH}_4^+]$ measurement	101
3.4.3	Values of urinary $[\text{NH}_4^+]$ and $[\text{K}^+]$ at room temperature	102
3.4.4	The relationship between $[\text{NH}_4^+]$ and $[\text{K}^+]$	103
3.4.5	Effects of storage on urinary $[\text{NH}_4^+]$ and $[\text{K}^+]$	104
3.4.6	Validation of urinary $[\text{NH}_4^+]$ measurements with a $\text{NH}_4^+$ -selective electrode in comparison to colour spectrophotometry	107
3.4.7	The pH-dependence of the $[\text{NH}_4^+]$ at room temperature	110
3.4.8	Summary of results at room temperature	111
3.5	Urinary $[\text{NH}_4^+]$ and $[\text{K}^+]$ measurements using the $\text{NH}_4^+$ - and $\text{K}^+$ -selective electrodes at $37^\circ\text{C}$ .	113
3.5.1	Calibration of $\text{NH}_4^+$ -selective electrode at $37^\circ\text{C}$	113

3.5.2	Selectivity of the $\text{NH}_4^+$ -selective electrode at $37^\circ\text{C}$	115
3.5.3	Calibration and selectivity of $\text{K}^+$ -selective electrode at $37^\circ\text{C}$	117
3.6.	Values of urinary $[\text{NH}_4^+]$ and $[\text{K}^+]$ measured at $37^\circ\text{C}$	121
3.6.1	Urinary values of $[\text{NH}_4^+]$ and $[\text{K}^+]$	121
3.6.2	The relationship between urinary $[\text{NH}_4^+]$ and $[\text{K}^+]$ .	122
3.6.3	The pH dependence of urinary $[\text{NH}_4^+]$ at $37^\circ\text{C}$	122
3.6.4	Effect of adjusting urinary pH to 6.0 on urinary $[\text{NH}_4^+]$ and $[\text{K}^+]$	123
3.6.5	Summary of results at $37^\circ\text{C}$	128
3.7	Urinary $[\text{NH}_4^+]$ and $[\text{K}^+]$ from patients at a Renal Stone Clinic	129
3.7.1	Measured values of urinary $[\text{NH}_4^+]$ and $[\text{K}^+]$ at room temperature and $37^\circ\text{C}$	129
3.7.2	The dependence of urinary $[\text{NH}_4^+]$ and $[\text{K}^+]$ on urine osmolality	133
3.7.3	The dependence of urinary $[\text{NH}_4^+]$ and $[\text{K}^+]$ on urine voided pH	135
3.7.4	Summary of measured urinary $[\text{NH}_4^+]$ and $[\text{K}^+]$ .	136
3.7.5	Validation of the algorithm for calculation of the urinary $[\text{NH}_4^+]$	138
3.7.6	Urinary $[\text{NH}_4^+]$ in 'struvite' vs 'non-struvite' patients	143
3.8	Measurements with a $\text{Mg}^{2+}$ ion-selective electrode:	145
3.8.1	Calibration of the $\text{Mg}^{2+}$ -selective electrode:	145
3.8.2	Selectivity of the $\text{Mg}^{2+}$ -selective electrode and use of a $\text{Ca}^{2+}$ -selective electrode	147
3.8.3	Values of urinary $[\text{Mg}^{2+}]$	154
CHAPTER 4 DISCUSSION		156
4.1	URINARY TRACT STONES	156
4.1.1	The clinical problem.	156
4.1.2	Struvite stones	157
4.2	CHARACTERISATION OF THE $\text{NH}_4^+$ ELECTRODE:	160
4.2.1	The $\text{NH}_4^+$ -selective electrode	160
4.2.2	$\text{K}^+$ -selective electrode	164
4.3	URINARY MEASUREMENT OF $\text{NH}_4^+$	165
4.3.1	Values of urinary $[\text{NH}_4^+]$ at room temperature	165
4.3.2	Comparison with other methods	166
4.4	VALIDATION OF THE $\text{NH}_4^+$ -SELECTIVE ELECTRODE	169

FOR USE IN URINE	
4.5 URINARY MEASUREMENT OF [NH <sub>4</sub> <sup>+</sup> ] AT 37°C	171
4.5.1 Characterisation of the NH <sub>4</sub> <sup>+</sup> -selective electrode at 37°C	171
4.5.2 Characterisation of K <sup>+</sup> -selective electrode at 37°C	172
4.5.3 Urinary measurements of [NH <sub>4</sub> <sup>+</sup> ] at 37°C	172
4.5.4 pH dependence of urinary [NH <sub>4</sub> <sup>+</sup> ]	173
4.6 URINARY MEASUREMENTS FROM PATIENTS ATTENDING A RENAL STONE CLINIC	175
4.6.1 Effect of temperature on urinary measurements of [NH <sub>4</sub> <sup>+</sup> ] and [K <sup>+</sup> ]	176
4.6.2 The dependence of urinary [NH <sub>4</sub> <sup>+</sup> ] and [K <sup>+</sup> ] on urine osmolality	176
4.6.3 The dependence of urinary [NH <sub>4</sub> <sup>+</sup> ] and [K <sup>+</sup> ] on voided pH	177
4.6.4 Differences between stone-formers and non-stone formers	177
4.6.5 Validation of the NH <sub>4</sub> <sup>+</sup> -selective electrode against a standard algorithm	178
4.7 CHARACTERISATION OF MAGNESIUM ELECTRODE	179
4.8 URINARY MEASUREMENT OF [Mg <sup>2+</sup> ] AT 37°C	183
4.8.1 Characterisation of the Ca <sup>2+</sup> -selective electrode at 37°C	183
4.8.2 Urinary measurements of [Mg <sup>2+</sup> ] at 37°C	183
4.8.3 pH dependence of urinary [Mg <sup>2+</sup> ]	183
4.9 CONCLUSION AND FUTURE STUDIES	184
 CHAPTER 5 APPENDIX	
5.1 Patient Consent Form	187
5.2 Patient Information Sheet	189
5.3 Parent Information Sheet	192
5.4 Control Information Sheet	195
5.5 Patient Questionnaire	198
5.6 Ethics Approval	199
 CHAPTER 6 REFERENCES	201

## LIST OF TABLES

Table 1.1	The causes and incidence of stones	6
Table 1.2	A list of urease-producing bacteria	27
Table 2.1	Components of the ion-selective plastics to manufacture ISEs	47
Table 2.2.	Composition of filling solutions used with the different ISEs	50
Table 2.3	Example of a calibration protocol for the $\text{NH}_4^+$ -selective electrode	55
Table 2.4	Composition of solutions to determine potentiometric selectivity coefficients	62
Table 2.5	Solution composition for changes to solution osmolality	64
Table 3.1	Typical $\text{NH}_4^+$ -selective electrode calibration data	76
Table 3.2	$\text{K}^+$ potentiometric selectivity coefficients of $\text{NH}_4^+$ -selective electrodes	80
Table 3.3	Potentiometric selectivity coefficients for $\text{NH}_4^+$ ion-selective electrodes	87
Table 3.4	Values of $\log k_{\text{NH}_4\text{Na}}^{\text{pot}}$ for $\text{NH}_4^+$ -selective electrodes: variable osmolality	88
Table 3.5	Typical $\text{K}^+$ -selective electrode calibration data	91
Table 3.6	$\log k_{\text{Kj}}^{\text{pot}}$ , $k_{\text{Kj}}^{\text{pot}}$ , $1 / k_{\text{Kj}}^{\text{pot}}$ for the $\text{K}^+$ -ISE	96
Table 3.7	$\log k_{\text{KNa}}^{\text{pot}}$ and $k_{\text{KNa}}^{\text{pot}}$ in solutions of varying ionic strength and osmolality	97
Table 3.8	Individual values of urinary $[\text{NH}_4^+]$ and $[\text{K}^+]$ at room temperature	103
Table 3.9	Effects of storage at room temperature and $-20^\circ\text{C}$ on urinary $[\text{NH}_4^+]$	105
Table 3.10	Urinary $[\text{K}^+]$ measured at day 0 and after seven days frozen storage at $-20^\circ\text{C}$	107
Table 3.11	$[\text{NH}_4^+]$ values determined with CS and the ISE	109
Table 3.12	$[\text{NH}_4^+]$ values from frozen samples determined with CS and the ISE	110
Table 3.13	Typical $\text{NH}_4^+$ -selective electrode calibration data at $37^\circ\text{C}$	114
Table 3.14	$k_{\text{NH}_4\text{K}}^{\text{pot}}$ values at room temperature and $37^\circ\text{C}$	115
Table 3.15	Sample $\text{K}^+$ -selective electrode calibration data at $37^\circ\text{C}$	118
Table 3.16	Comparison of $\log k_{\text{KNH}_4}^{\text{pot}}$ at room temperature and $37^\circ\text{C}$	119
Table 3.17	Individual values of urinary $[\text{NH}_4^+]$ , $[\text{K}^+]$ and voided pH at $37^\circ\text{C}$	121
Table 3.18	Values of urinary $[\text{NH}_4^+]$ at voided pH and pH 6.0	125
Table 3.19	Values of urinary $[\text{K}^+]$ at voided pH and pH 6.0	126
Table 3.20	Values of $[\text{NH}_4^+]$ and $[\text{K}^+]$ from patients attending a renal stone clinic	130
Table 3.21	Values of $[\text{NH}_4^+]$ and $[\text{K}^+]$ non-stone formers and stone-formers	137
Table 3.22	Calculated urinary $[\text{NH}_4^+]$ compared to ion-selective electrode values	139
Table 3.23	Urinalysis of patients with struvite and non-struvite stones	144
Table 3.24	Sample $\text{Mg}^{2+}$ -selective electrode calibration data	145
Table 3.25	Sample calibration of a $\text{Ca}^{2+}$ -selective electrode	149

Table 3.26	Values of the $\log k_{ij}^{pot}$ for the $Mg^{2+}$ -selective electrode	152
Table 3.27	Values of urinary $[Mg^{2+}]$ at voided pH and after adjustment to pH 6.0	154

## LIST OF FIGURES

Figure 1.1	Risk factors which lead to calcium stone formation	9
Figure 1.2	A scheme of stone initiation	15
Figure 2.1.	A schematic diagram of the electrochemical cell used for ISEs	52
Figure 2.2	The test chamber used for experiments	53
Figure 2.3	Sample calibration curve for an $\text{NH}_4^+$ -selective electrode	60
Figure 2.4	The experimental arrangement with two ion-selective electrodes	68
Figure 2.5	A sample calibration curve to estimate $[\text{NH}_4^+]$ in a urine sample	69
Figure 3.1	Typical calibration curve of a $\text{NH}_4^+$ -selective electrode	77
Figure 3.2	Calibration curves of an $\text{NH}_4^+$ -selective electrode in low $[\text{K}]$	81
Figure 3.3	Calibration curves of an $\text{NH}_4^+$ -selective electrode in high $[\text{K}]$	82
Figure 3.4	Calibration curves of an $\text{NH}_4^+$ -selective electrode in all $[\text{K}]$	83
Figure 3.5	Calibration curves of an $\text{NH}_4^+$ -selective electrode in variable $[\text{Ca}]$	84
Figure 3.6	Calibration curves of an $\text{NH}_4^+$ -selective electrode in variable pH	85
Figure 3.7	Calibration curves of an $\text{NH}_4^+$ -selective electrode in variable $[\text{K}]$ and pH	86
Figure 3.8	Calibration curves of an $\text{NH}_4^+$ -selective electrode in variable osmolarity	89
Figure 3.9	Calibration curves of an $\text{NH}_4^+$ -selective electrode in variable ionic strength	90
Figure 3.10	Typical calibration curve of a $\text{K}^+$ -selective electrode	92
Figure 3.11	Calibration curves of a $\text{K}^+$ -selective electrode in variable $[\text{NH}_4\text{Cl}]$	93
Figure 3.12	Calibration curves of a $\text{K}^+$ -selective electrode in variable $[\text{Ca}]$	95
Figure 3.13	Calibration curves of a $\text{K}^+$ -selective electrode in variable pH	96
Figure 3.14	Calibration curves of a $\text{K}^+$ -selective electrode in variable osmolarity	98
Figure 3.15	The relationship between urinary $[\text{NH}_4^+]$ and urinary $[\text{K}^+]$	104
Figure 3.16	Urinary $[\text{NH}_4^+]$ in freshly voided and 7-day stored, frozen samples	106
Figure 3.17:	Comparison of urinary $[\text{NH}_4^+]$ measurements using colour spectrophotometry (CS) and ion-selective electrodes (ISE)	108
Figure 3.18	The variation of $[\text{NH}_4^+]$ as a function of voided pH	111
Figure 3.19	Calibration curve for $\text{NH}_4^+$ -selective electrodes at $37^\circ\text{C}$	114
Figure 3.20	Calibration curves of $\text{NH}_4^+$ selective electrode in variable $[\text{K}]$ at $37^\circ\text{C}$	117
Figure 3.21	Mean calibration curves of $\text{K}^+$ -selective electrodes at RT and $37^\circ\text{C}$	118
Figure 3.22	Calibration curves of a $\text{K}^+$ -selective electrode in variable $[\text{NH}_4\text{Cl}]$ at $37^\circ\text{C}$	120
Figure 3.23	The relationship between urinary $[\text{K}^+]$ and urinary $[\text{NH}_4^+]$ at the voided pH	122
Figure 3.24	Urinary $[\text{NH}_4^+]$ as a function of voided pH, measured at $37^\circ\text{C}$	123

Figure 3.25	Change of urinary $[\text{NH}_4^+]$ , $\Delta[\text{NH}_4^+]$ , as a function of alteration of pH, $\Delta\text{pH}$	127
Figure 3.26	Change of urinary $[\text{K}^+]$ , $\Delta[\text{K}^+]$ , as a function of alteration of pH, $\Delta\text{pH}$	128
Figure 3.27	Urinary $[\text{NH}_4^+]$ and $[\text{K}^+]$ at room temperature and $37^\circ\text{C}$	131
Figure 3.28	$[\text{NH}_4^+]$ at $37^\circ\text{C}$ and RT from patients at the Renal Stone Clinic	132
Figure 3.29	$[\text{K}^+]$ at $37^\circ\text{C}$ and RT from patients at the Renal Stone Clinic	133
Figure 3.30	The association between urinary $[\text{NH}_4^+]$ and osmolality	134
Figure 3.31	The association between urinary $[\text{K}^+]$ and osmolality	134
Figure 3.32	The association between urinary $[\text{NH}_4^+]$ and voided pH	135
Figure 3.33	The association between urinary $[\text{K}^+]$ and voided pH	136
Figure 3.34	Urinary $[\text{NH}_4^+]$ and voided pH for stone-formers and non-stone formers	138
Figure 3.35	Calculated values of urinary $[\text{NH}_4^+]$ as a function of measured values	140
Figure 3.36	The difference between calculated and measured values of urinary $[\text{NH}_4^+]$	141
Figure 3.37	pH-dependence of calculated and measured values of urinary $[\text{NH}_4^+]$	142
Figure 3.38	Calculated and measured values of urinary $[\text{NH}_4^+]$ as a function of pH	143
Figure 3.39	Sample calibration curve of a $\text{Mg}^{2+}$ -selective electrode	146
Figure 3.40	Calibration curves of an $\text{Mg}^{2+}$ -selective electrode in variable $[\text{Ca}]$	148
Figure 3.41	Sample calibration curves of a $\text{Ca}^{2+}$ -selective electrode	150
Figure 3.42	Calibration curves of a $\text{Ca}^{2+}$ -selective electrode in high $[\text{K}]$	151
Figure 3.43	Calibration curves of a $\text{Mg}^{2+}$ -selective electrode in variable pH	153
Figure 3.44	Values of $\Delta[\text{Mg}^{2+}]$ as a function of $\Delta\text{pH}$	155
Figure 4.1	The structure of nonactin	160
Figure 4.2	The structure of bis(2-ethylhexyl) sebacate	161
Figure 4.3.	The structure of bis(1-butylpentyl)adipate	162

# **CHAPTER 1**

## **INTRODUCTION**

### **1.1 URINARY TRACT STONES, THE CLINICAL SITUATION**

#### 1.1.1 Urinary Tract Stones:

Urolithiasis is a common disorder with 10% of Caucasian men developing a kidney stone by the age of 70. The risk of recurrence without treatment for a calcium oxalate stone is 10% at one year and 50% at 10 years (Uribarri et al 1989). Multiple factors contribute to urolithiasis.

Up until fairly recently, urinary stones were a major health problem. A large number of patients required extensive surgical procedures and a significant minority had their kidney removed. Since the advent of extracorporeal methods such as lithotripsy and further advances in endoscopic techniques for stone destruction, the management of stones has become more efficient and effective, along with decreased morbidity relating to stone surgery.

However these advances in technology have allowed medical management of stones and research into their prevention to suffer and be left behind. Though surgical procedures may well treat stones, they are unable to prevent them and with stone recurrence being a major issue, preventative strategies are long overdue for the management of stones and certainly for the identifiable group of patients with stone recurrence.

## **1.2 EPIDEMIOLOGY:**

### 1.2.1 Intrinsic Factors:

#### 1.2.1.1 Age / Sex:

The peak incidence of stones is between age 20 and 40. The male to female ratio is 3:1 and this is due in part to lower testosterone levels providing protection for women and children against developing oxalate stones, since testosterone may increase the production of oxalate in the liver (Finlayson 1974).

#### 1.2.1.2 Genetics:

25% of patients with kidney stones have a family history of stones and in a study (of 38,000 male health professionals, a family history of stones was more than three times higher in men with kidney stones than in non-stone formers (Curhan et al, 1997). Renal stones are rare in black-Americans, black-Africans, native-Americans and Australian aborigines, but more common in Asians and Caucasians. Familial renal tubular acidosis, cystinuria and xanthinuria are hereditary disorders that lead to stone formation.

### 1.2.2 Extrinsic Factors:

#### 1.2.2.1 Geography:

High incidence areas include the United States, the British Isles, Scandinavian countries, Mediterranean countries and central Europe. Low incidence areas include Central and South America, and Africa (Finlayson, 1974).

#### 1.2.2.2 Climate/Season:

Renal stones are common in hot climates and the incidence was thought to be increased after the peak temperatures during the hot summer months (Prince et al, 1960). Baker et al (1993) investigated trends in stone formation in residents in South Australia between 1977 and 1991 and found no significant seasonal variation in calcium stone formation. There was however an increase in uric acid stone formation during summer and autumn and a decrease in infectious stone formation during spring and summer.

Hallson et al (1977) showed that crystalluria was greater during summer months in patients who formed stones and postulated that increased sweating during high temperatures led to concentrated urine and urinary crystal formation. Uric acid and cystine stone-formers are further at risk since concentrated urine tends to be more acidic, encouraging these compounds to precipitate. Parry et al (1975) suggested that increased vitamin D production during summer, due to increased exposure to sunlight, may lead to increased stone formation due to increased calcium excretion in the urine.

#### 1.2.2.3 Diet:

Increased incidence of renal calculi is associated with a more 'affluent' diet (increased animal protein, refined sugar and salt). Robertson et al (1978) showed that there was a strong relationship between animal protein consumption and stone occurrence. Animal protein increases urinary calcium, oxalate and uric acid and generates an acidic urine, all contributing to calcium oxalate oversaturation and precipitation. A lower prevalence of stone disease has been observed in vegetarians in the UK (Robertson et al, 1979) and moderation of animal protein intake was suggested.

Interestingly, a higher dietary calcium intake (e.g. 2 glasses milk/day) has been strongly associated with a decreased risk of kidney stones. However dietary calcium supplementation is not protective.

Sucrose has been shown to increase urinary calcium and oxalate concentrations (Thom et al,1981) where sucrose and starch supplements were added to a standard diet in normal subjects, resulting in an increased frequency and magnitude of diurnal peaks of urinary calcium and oxalate concentration in the higher sucrose diet subjects. A lack of dietary fibre is also thought to contribute to stone formation, since fibre traps and decreases the rate and extent of absorption of sucrose and animal protein.

#### 1.2.2.4 Water intake:

Increased water intake causes urinary dilution of the constituents that may otherwise crystallise, as well as reduces the average time of residence of free crystal particles in the urine (Finlayson, 1974). Current opinion suggests that a low fluid intake (<1,200ml/day) predisposes to stone formation. It is also important to consider the trace element content of the water supply of the region. Sierakowski et al (1978) suggested that excessive water hardness (e.g. with calcium and magnesium ions) causes a greater incidence of stone disease.

#### 1.2.2.5 Occupation / Stress:

Sedentary occupations, including professional and managerial groups, have been shown to have a higher incidence of urinary calculi as compared to manual workers (Lonsdale, 1968). Stress has also been associated with stone disease and a case-

control study of 400 patients showed that emotional life events were significantly associated with stone disease (Najem, 1997).

### **1.3 STONE TYPE, AETIOLOGY AND INCIDENCE:**

There are many different type of stones (see Table 1.1) but the most common type of stone consists of a mixture of calcium oxalate and calcium phosphate. 70-80% of these stones are said to be idiopathic, where there is no known metabolic cause. 10-12% are due to metabolic causes (e.g. hyperparathyroidism, renal tubular acidosis, or hyperoxaluria). Struvite stones (or infection stones) account for 15-20% of all stones.

It is important to understand the aetiological factors and current treatments for the different types of stone formation. These may then be applied to devise specific strategies to manage different types of stone that may develop.

The first part of the Introduction will be concerned with the more common calcium-containing stones and some less common stone types, as well as general principles of stone formation. In section 1.7 and after struvite stones, the main subject of this thesis will be discussed in greater detail.

Table 1.1: The causes and incidence of stones.

Disorder	Stone Type	% of all stones
Idiopathic	Calcium oxalate / phosphate	70-80
Hypercalcaemic states: (i) Hyperparathyroidism (ii) Sarcoidosis (iii) Hyperthyroidism	Calcium oxalate / phosphate	5-7
Hyperoxaluric states: (i) 1 <sup>o</sup> - enzyme deficiency (ii) 2 <sup>o</sup> – enteric hyperoxaluria	Calcium oxalate	1
Uric acid lithiasis: (i) Diabetes / Metabolic Syndrome (ii) Gout (iii) Myeloproliferative disorders	Uric acid	8
Renal tubular acidosis	Calcium phosphate	4
Cystinuria	Cystine	1-3
Xanthinuria	Xanthine	0.0001
Urinary tract infections	Magnesium ammonium phosphate	15-20

## 1.4 CALCIUM STONE FORMATION:

Calcium stone formation is really due to a combination of abnormalities. Risk factor analysis shows that the following factors (see Fig 1.1), listed in order of decreasing importance, are involved in calcium stone formation:

1. Low urine volume
2. Mild hyperoxaluria (normal:  $< 450 \mu\text{m} / \text{day}$ )
3. Increased urinary pH
4. Hypercalciuria (normal:  $< 6.2$  (female),  $< 7.5$  (male)  $\text{mmol} / \text{day}$ )
5. Hypocitraturia
6. Hyperuricosuria (normal:  $1.2 - 4.5 \text{ mmol} / \text{day}$ )
7. Hypomagnesiuria

### 1.4.1 Idiopathic Stone Formation:

This is the commonest condition and for calcium stones to form, supersaturation of the urine with calcium is a prerequisite, i.e. if the urine is undersaturated stone formation is impossible. 30%-60% of patients have increased urinary calcium excretion in the absence of raised serum calcium levels – idiopathic hypercalciuria. Hypercalciuria contributes to stone formation by increasing the relative supersaturation of urine. Three types have been described: absorptive hypercalciuria, due to increased intestinal calcium absorption; renal hypercalciuria, due to failure of reabsorption of filtered calcium by nephrons causing hypercalciuria; resorptive hypercalciuria, due to excessive bone resorption of calcium, due to increased parathyroid hormone (PTH).

#### 1.4.2 Metabolic Causes for Stone Formation:

1. Hypercalcaemia: of all patients with hypercalcaemia who form stones, almost all have primary hyperparathyroidism where PTH increases osteoclast activity, calcium reabsorption and vitamin D<sub>3</sub> production in the kidney. The mainstay of treatment is surgical removal of the adenoma with 90% to 100% improvement in stone recurrences.

Other causes include sarcoidosis, hyperthyroidism and vitamin D toxicity.

2. Hyperoxaluria: Primary hyperoxaluria is a rare genetic disorder causing increased oxalate production in the liver. Pyridoxine decreases oxalate production in some patients. Enteric hyperoxaluria due to malabsorption (including small bowel resection) increases exposure of the colon to bile salts, which causes increased permeability of the colon to oxalate. A combination of oral hydration and a low oxalate, low fat diet may be used.
3. Renal tubular acidosis (R.T.A.): this results from a defect of renal tubular secretion of H<sup>+</sup>, which decreases the ability of the kidney to acidify urine. This causes an alkaline urine, which increases calcium phosphate supersaturation, leading to calcium phosphate stones. Treatment is directed at correcting systemic acidosis with alkali therapy and raising urinary citrate levels.
4. Hyperuricosuria: seen in 10%-40% of calcium stone formers. Hyperuricosuria promotes calcium oxalate crystallisation. The main cause is excessive dietary purine intake. Purine restriction by limiting red meat, poultry and fish helps to reduce hyperuricosuria.
5. Hypocitraturia: seen in 15%-63% of patients with calcium stones. Citrate is not only a complexing agent for calcium, creating a more soluble complex than calcium oxalate, but also it inhibits calcium oxalate crystal formation and

growth. The main cause of decreased citrate excretion in the urine is metabolic acidosis.

6. Hypomagnesuria: studies have shown a low urinary magnesium concentration in patients with stones, commonly associated with hypocitraturia. The main cause is malabsorption due to inflammatory bowel disease.

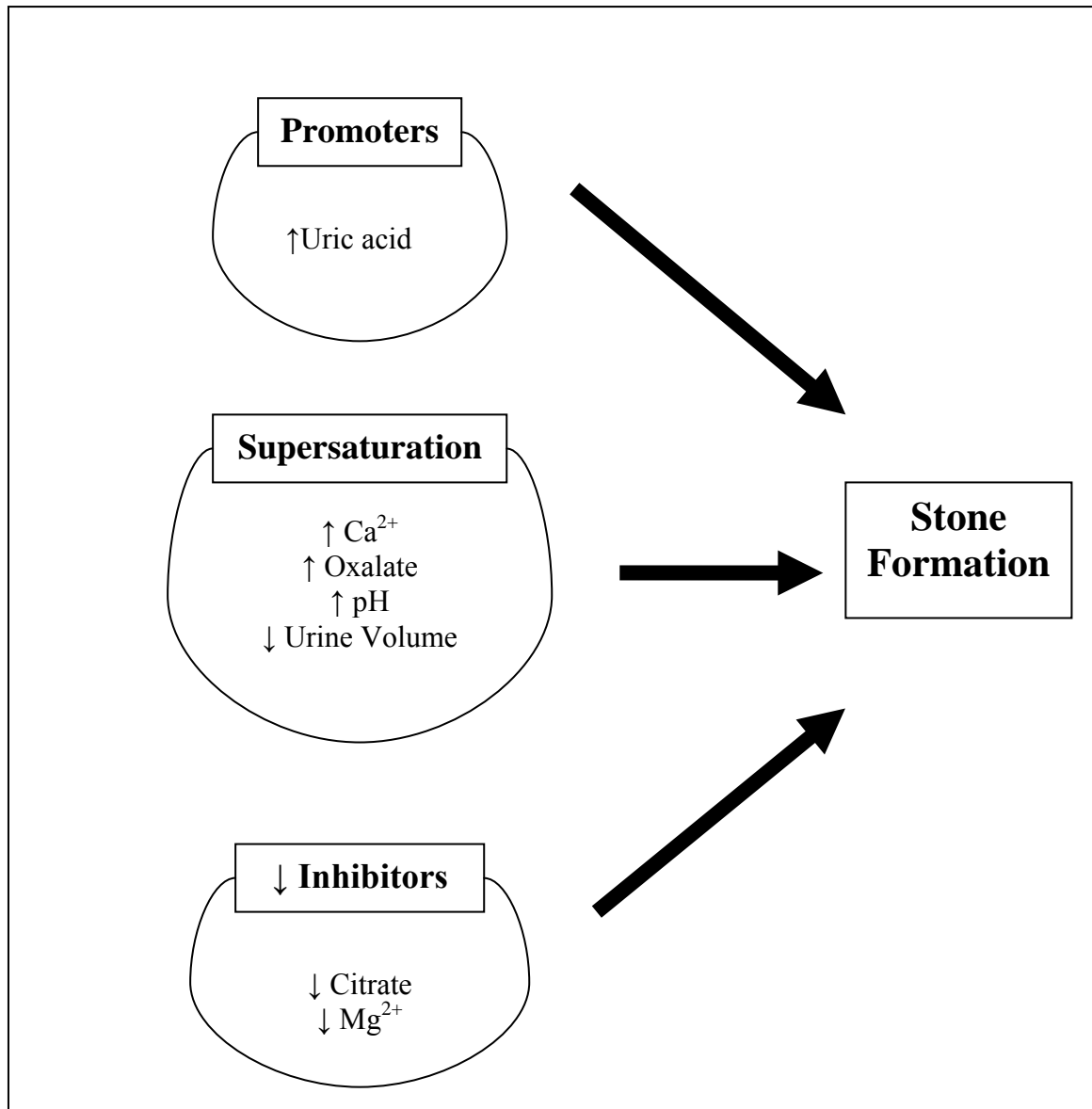


Fig 1.1: Risk factors which lead to calcium stone formation.

### 1.4.3 Management:

It is quite difficult to dissolve calcium stones, and therefore an important aspect of patient management is the prevention of further calcium stones forming once stone clearance has been achieved: Hydration - drink plenty of clear fluids to maintain a urinary output >2 l/day; Diet - limit daily meat (protein) intake, increase dietary fibre intake and limit oxalate-rich foods; Thiazides - promote calcium resorption in the kidney; Orthophosphates - decrease urinary calcium excretion; Sodium cellulose phosphate (not extensively used in the UK) - a non-absorbable resin that binds calcium and decreases calcium absorption from the intestine; Citrate - potassium citrate may be used for treatment of hypocitraturia; Magnesium citrate - to treat hypomagnesiuria and hypocitraturia.

## **1.5 URIC ACID AND CYSTINE STONES:**

### 1.5.1 Uric acid stones

Purines are metabolised to uric acid, which exists in two forms: ionised urate (soluble) and undissociated uric acid (insoluble). The dissociation constant for uric acid is near 5.35 – at this pH, half of the uric acid is present as the ionised urate form and the other half is present as free uric acid. As the pH decreases, more uric acid precipitates out of solution.

Patients with uric acid stones or gout show increased production of uric acid, though the cause is not known. Characteristically patients have acidic urine, increased hyperuricosuria and reduced volumes of urine.

Management: Medical therapy is successful in dissolving renal uric acid stones, and urine alkalinisation (to pH 6.5–7.0) and hydration have been shown to dissolve near completely uric acid staghorn calculi. Allopurinol may be used if the patient has hyperuricaemia or hyperuricosuria, as it will reduce production of uric acid from xanthine.

### 1.5.2 Cystine stones

Cystine stones account for 1% of all stones, and only occur in patients with cystinuria. Cystinuria, an autosomal recessive disease causing a decreased cystine resorption in the proximal tubule of the kidney, affects 1 in 20,000 individuals, and the peak age of stone formation is 20-30 years.

The aim of treatment is to reduce cystine concentration in urine and includes: low methionine diet – since cystine is a breakdown product of methionine, which is present in meat, fish and dairy products; Oral hydration; alkalinise urine to pH >7.5, which allows solubilisation of the stone; acetazolamide - augments alkalinisation, by inhibiting carbonic anhydrase, thereby increasing urinary bicarbonate excretion; D-penicillamine or alpha-mercaptopyrionylglycine (MPG) – these bind cystine making it soluble in urine; and surgery – to debulk / remove the stone.

## 1.6 PHYSICO-CHEMICAL PRINCIPLES OF STONE FORMATION:

### 1.6.1 Supersaturation:

When a substance is dissolved in water, the solution is said to be ‘saturated’ when the concentration of the substance is high enough but crystals have not formed. As the

concentration is increased further, crystals precipitate. The point at which saturation is reached and crystallisation begins is known as the ‘thermodynamic solubility product’ ( $K_{sp}$ ). This is a constant under designated conditions of temperature and pH. Temperature and pH are always specified, since changes in either factor, may change the amount of crystallisation that may occur. It is important to be aware of crystallisation studies performed at room temperature rather than at body temperature.

Urine is a more complex solution, since when the concentration of a substance reaches the point at which crystallisation would occur in water, crystallisation does not occur in urine. This is due to the fact that urine has the capacity to hold more solute than water, since urine has a mixture of many electrically active ions interacting with each other, affecting their solubility. The presence of organic molecules, such as urea, uric acid and citrate also affect the solubility of other substances. Urine is therefore described as being ‘metastable’. As the concentration of the substance is increased further, a point is reached when the substance eventually crystallises and this concentration is known as the ‘formation product’ ( $K_F$ ) of the substance. Therefore the metastable range can be described as the range between the  $K_{sp}$  and the  $K_F$  (Menon et al 2002).

### 1.6.2 Crystal Formation:

There are three processes of crystallisation:

- i) Nucleation (the formation of crystals) of which there are two types; ‘homogeneous nucleation’ which is the formation of the earliest crystal that will not dissolve; and ‘heterogeneous nucleation’ which is the formation of crystals on surfaces (e.g. cells, debris, urinary casts, and other crystals; Brown et al, 1992).

- ii) Crystal growth
- iii) Agglomeration (crystals aggregate together to form larger particles).

Furthermore there are two theories (Robertson, 2004) of crystal formation (Fig 1.2).

- i) The 'free-particle' theory describes the spontaneous precipitation of crystals in supersaturated urine. The crystals grow / aggregate sufficiently during the transit time of urine in the kidney. One of the newly formed nuclei grows sufficiently in size that they become trapped at a narrow point in the renal tract and form a focus around which the stone develops.
- ii) The 'fixed-particle' theory proposes that nuclei cannot grow sufficiently during the transit time of urine in the kidney, but that once a crystal forms, it adheres to the renal epithelium, possibly because of increased stickiness of the epithelium or damage to the cell walls (caused by crystals or by viruses and bacteria).

Once formed, the growing crystals then aggregate with each other by a process known as agglomeration. This is the stage in crystal formation when crystal growth is most rapid. Through further crystal growth and agglomeration the particle becomes a stone.

### 1.6.3 Modifiers of Crystal Formation:

Substances that alter or modify crystal formation exist in urine. They have been described with respect to calcium-containing stones, but not struvite (magnesium ammonium phosphate), cystine or uric acid stones. Types of modifiers include:

1. Inhibitors: these slow or inhibit the rate of growth / aggregation of crystals or reduce the adherence of crystals to the renal epithelium. Examples include

magnesium, citrate, pyrophosphate and urinary glycoproteins, such as nephrocalcin and non-polymerised Tamm-Horsfall protein (also known as uromodulin).

2. Promoters: these stimulate crystallisation and examples include matrix substance A, and other urinary glycoproteins such as the polymerised form of Tamm-Horsfall protein (uromuroid).

#### 1.6.4 Crystalluria:

This is the production of crystals in urine and is an important requirement for stone formation. It occurs more frequently in urine from stone-formers than from controls. The size of crystals within the urine is associated with the severity of the disorder, as defined by stone episode rate.

#### 1.6.5 Stone Matrix:

Renal stones also contain matrix, which is a non-crystalline material. The matrix content of a stone may be between 10%-65% by weight, and tends to be higher when there is an associated urinary tract infection. It has been suggested that an alteration in the secretion of renal enzymes (decreased urokinase and increased sialidase) may increase matrix formation. Certain bacteria, such as *Proteus mirabilis* and *Escherichia coli*, alter urokinase/sialidase activity leading to matrix formation, in turn causing increased crystal adherence to the renal epithelium.

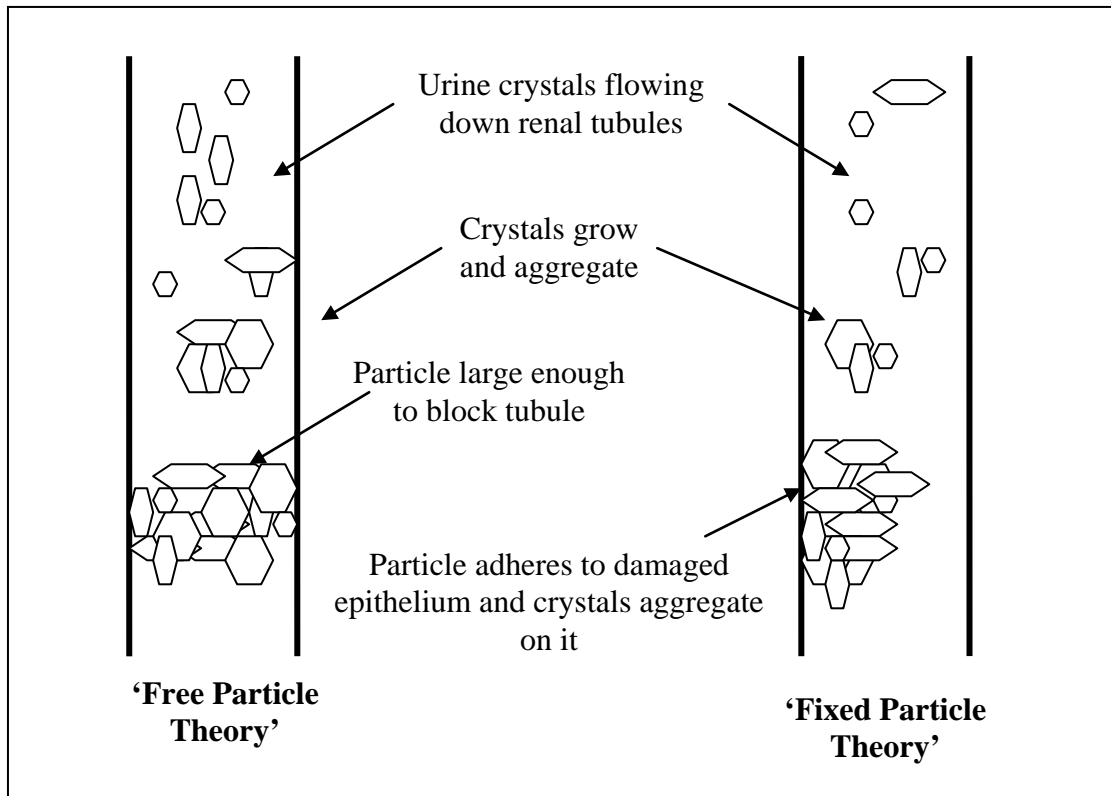


Fig 1.2: a scheme of stone initiation occurring by the 'free-particle theory' or the 'fixed-particle theory'.

### 1.7 STRUVITE STONES:

Struvite stones are composed of magnesium ammonium phosphate, are also known as 'infection stones', and account for 15%-20% of all stones. Certain bacteria, such as *Proteus mirabilis* and *Ureaplasma urealyticum*, secrete the enzyme urease which hydrolyses urea to carbon dioxide and ammonium ions. This reaction causes the urinary pH to rise. As mentioned previously, *E.coli* was shown to decrease urokinase and increase sialidase activity, causing increased matrix production, thereby leading to crystal adherence to the renal epithelium. This explains how non-urease producing bacteria may be associated with struvite stones. Struvite calculi also account for the majority of staghorn stones.

### 1.7.1 Struvite Stones

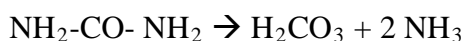
Struvite, a crystalline substance composed of magnesium ammonium phosphate, was first identified by Ulex, a Swedish geologist, in the 18<sup>th</sup> century. He created the term 'struvite' in honour of his friend and mentor H.C.G von Struve (1772-1851), a Russian diplomat and natural scientist (Griffith, 1987). Brown suggested that bacteria split urine and thus caused and facilitated stone formation. He also isolated *Proteus vulgaris* from a stone nucleus and this is known today to secrete urease. However it was Hager and Magath, in 1925, who suggested that 'urease' was the cause of hydrolysis of urine (Griffith, 1978; Bichler KH et al, 2002).

Struvite stones account for 5-20 % of all urinary stones (Griffith, 1978; Sharma et al, 1989). Data from the 1970s indicated that struvite stones constituted 15% of the all stone specimens sent for calculus analysis but Rodman (1998) suggested that this figure over-reported the incidence of infection stones, since many small spontaneously passed calculi are never caught and do not have their chemical composition determined. Bichler et al (2002) suggested that 15-20 % of urinary stones were infection stones in industrial countries and their clinic results showed that out of 4,400 patients with urinary stones, 510 had infection stones (11.6 %).

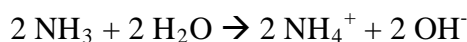
Struvite stones are also referred to as 'infection stones' and 'triple phosphate stones'. The term triple phosphate is derived from the fact that early chemical analyses demonstrated calcium, magnesium, ammonium and phosphate (i.e. three cations and one anion). More recently struvite stones have been shown to be a mixture of struvite and carbonate apatite.

For struvite to form, the urine must contain ammonium and trivalent phosphate ions at the same time. The renal tubule only makes ammonium when the organism is excreting an acid load, however trivalent phosphate is almost not present in acid urine. Thus under normal physiological conditions struvite may not precipitate. For struvite to form, conditions which are non-physiological are required and these are created by urease-secreting bacteria.

Urease splits urea into ammonia and carbonic acid:



Ammonia then mixes with water to produce ammonium hydroxide and under these alkaline conditions, carbonic acid moves toward bicarbonate and carbonate ions.



Thus, the alkalinisation of urine by the urease reaction causes the formation of  $\text{NH}_4^+$ , which favours the formation of carbonate ions ( $\text{CO}_3^{2-}$ ) and trivalent phosphate ions ( $\text{PO}_4^{3-}$ ). This in turn causes struvite and carbonate apatite formation (Rodman, 1999; Miano et al, 2007).



However the explanation for mechanism of action is not definite. Rodman (1999) suggested that struvite could form in the absence of urea-splitting bacteria, since it has been possible to form struvite crystals in vitro in acidic solutions (pH 6) even though

the morphology of the resultant crystals is slightly different. In vivo, no non-urease mechanism has been demonstrated.

#### 1.7.2 Management:

Patients may present acutely with loin pain, haematuria, fever, dysuria and frequency. Alternatively a large number of patients may present with malaise, weakness and loss of appetite. Struvite stones are usually radiopaque on X-ray. Preventive treatment may first be tried. The main aim of medical treatment is firstly to remove the stone completely and then provide medical therapy to prevent recurrent urinary tract infection.

#### Diet – limiting phosphorus in foods

phosphate-poor diet; phosphate found in high protein diets. However, such diets are unpalatable to many and are associated with constipation, neurological dysfunction, osteopathy and muscle weakness.

#### Urease inhibitors

the compound must have high renal clearance and penetrate bacterial cell walls (because most of the urease enzyme is intracellular).

- Acetohydroxamic acid (AHA) similar in structure to urea and a potent irreversible inhibitor of urease. It is effective but severe side-effects limit its usage: there may be problems in patients with concomitant deep vein thrombosis, pulmonary embolism and haemolytic anaemia and low grade intravascular coagulopathies, as well as associated headache and confusion. It must not be used if creatinine clearance is  $<40\text{ml/min}$ .
- Hydroxyurea – not as effective as AHA

- Flurofamide – about 1000-times more potent, but thus far has failed clinical trials

#### Stone Clearance

a combination of percutaneous nephrolithotomy (PCNL) and extracorporeal shock-wave lithotripsy (ESWL) are commonly used.

#### Intermittent bladder catheterisation

#### Better nephrostomy care in patients with diverted urinary tracts

#### Antibiotics

once patients are stone and infection free, then suppressive treatment is often indicated if the patient is prone to recurrent urine infections. Sterilise the urine and prevent stone recurrences/growth after operative procedures.

### 1.7.3 Struvite Crystal Formation

Struvite has been investigated by mineralogists, chemists and physicians. It has been found as a mineral in peat beds, in sediments rich in organic remains and in phosphate caves. It has been suggested that struvite may have formed from evaporating sea water on the primitive earth, and may have been important for prebiotic phosphorylation (Abbona et al, 1979).

More recently struvite has become of clinical relevance due to its presence in renal stones, staghorn calculi, encrustation of urological devices and vesical calculi. However, struvite has also been problematic in wastewater treatment plants where struvite deposition has been found in pumps, aerators and pipe bends. Remediation methods that have been attempted include jet washing, heat treating, and acid washing but not all are successful, and the process for acid washing, which did remove struvite

deposits, is complex and time-consuming. Stratful et al (2001) described ‘the most productive and cost-effective way to remove struvite build-up is manually with a hammer and chisel’. This poignant statement reflects our current still ‘almost primitive’ approach to treating renal staghorn stones and it may be time now for a more elegant treatment strategy. Interestingly there are some potential uses for struvite, such as a slow-release fertiliser, as a raw material to the phosphate industry, for use in fire resistant panels and as a binding material in cements (Stratful et al, 2001).

#### 1.7.4 Struvite Crystal Structure:

##### 1.7.4.1 Struvite Crystals:

In calculi, struvite is rarely found in the pure state but usually is associated with varying amounts of hydroxyapatite ( $\text{Ca}_5(\text{PO}_4)_3\text{OH}$ ) and carbonate apatite ( $\text{Ca}_5(\text{PO}_4, \text{CO}_3, \text{OH})_3\text{OH}$ ) (Leusmann, 1991). Abbona et al (1979) investigated struvite crystal growth and crystal morphology. They described the structure as regular  $\text{PO}_4^{3-}$  tetrahedra,  $\text{Mg}(\text{H}_2\text{O})_6^{2+}$  octahedra and  $\text{NH}_4^+$  groups all held together by hydrogen bonding. They showed that crystal morphology was associated with the rate of growth of crystals: very high supersaturations (i.e. high growth kinetics where  $\text{pH} > 8.0$ ) promoted formation of bidimensional or tridimensional twinned crystals; whereas high supersaturation ( $\text{pH}$  about 7.0) promoted tabular crystals; and decreasing supersaturation ( $\text{pH}$  6.7) promoted crystals that were less tabular and more elongated. In summary their results showed that high growth kinetics promoted flat crystals with large faces, whereas low growth kinetics promoted stick-like crystals, flat and without faces.

#### 1.7.4.2 In-vitro struvite crystal growth:

McLean et al (1985) examined the initial events in the production of infection stones. A culture flask was aseptically filled with artificial urine. A ureolytic strain of *Proteus mirabilis* was isolated from a patient with a urinary calculus and maintained on a slant of tryptic soy agar. The artificial urine was inoculated with a 1% inoculum of *Proteus mirabilis* and the flask was agitated and aerated. Waste urine and air were removed through a side tube in the flask. Fresh artificial urine was added at a rate of 60ml/hr. Several substances were suspended in the culture medium to act as surfaces for bacterial colonisation. These substances included resin blocks, urinary catheter material, glass rods and nichrome wire. The pH increased to between 8.5 and 9.5 within 4 hours and by 6-8 hours optical density had reached maximum turbidity. Scanning electron microscopy of the substances in the culture medium showed progressive colonisation of *Proteus mirabilis*. Crystals, resembling struvite and apatite, were seen covered by an amorphous substance. Energy-dispersive X-ray analysis revealed the presence of  $Mg^{2+}$ ,  $Ca^{2+}$  and  $PO_4^{3-}$  suggesting the presence of struvite and apatite. Transmission electron microscopy examination revealed *Proteus mirabilis* surrounded by an amorphous material stained by ruthenium red and thought to be bacterial glycocalyx. They hypothesised that bacteria, such as *Proteus mirabilis*, colonise the renal epithelium, shed their glycocalyx and form glycocalyx-enclosed micro-colonies. Urease, secreted by these bacteria, causes hydrolysis of urea to ammonia, increasing the pH of the urine and therefore causes struvite and apatite to precipitate. The glycocalyx traps these crystals and mucoproteins and polysaccharides present in the urine. The bacteria are well protected from the body's defences within these glycocalyx-enclosed micro-colonies, which then mature into large renal calculi.

McLean et al (1990) modified this technique by growing crystals in solution, rather than on surfaces, and the solution examined by light microscopy. This revealed a large number of crystals in solution, confirmed to be struvite with X-ray diffraction. The pH,  $[\text{NH}_3]$ , optical density, urease activity and bacterial cell numbers all increased with time.

Bouropoulos et al (2000) investigated the formation of struvite from aqueous solutions, whereby reactant solutions of magnesium chloride and ammonium dihydrogen phosphate were mixed together at 25°C and samples withdrawn and examined by X-ray diffraction, scanning electron microscopy and FTIR spectroscopy. Struvite was exclusively precipitated at pH 8.5.

Some debate exists about the formation of struvite and its subsequent transformation to another compound newberyite ( $\text{MgHPO}_4 \cdot 3\text{H}_2\text{O}$ ) (Abbona et al 1982). There have been a few reports of newberyite deposition in human renal calculi (Sutor 1968). Babic-Ivancic et al (2004) investigated the formation of struvite in aqueous solutions under conditions similar to physiological at 37°C, over a wide range of pH values and observed its transformation into newberyite. Having chosen a system where the initial concentration of the reactants resulted in formation of both struvite and newberyite, they studied the system over a range of pH values. In the range pH 5.0–7.0, only newberyite formed. Upon mixing the reactants at pH 7.0, there was an immediate decrease in pH to 6.0 within the first minute of the process and only newberyite formed and remained since it is stable at pH 6.0. At pH 7.4, within the first minute, both struvite and newberyite formed, but at 5 hours only newberyite remained. At pH 8.0 the initial precipitate of struvite was 28.8 %wt and then 3.4 %wt

at 5 hours, whereas at pH 9.0 the initial precipitate increased from 52.6 %wt to 72.9 %wt at 5 hours. The authors suggested the reason for this might be the rate of nucleation for struvite being greater than that of newberyite.

#### 1.7.4.3 In-vivo struvite crystal growth:

Nickel et al (1987) have also performed in-vivo growth of struvite stones in a rat animal model. Rats were anaesthetised and via a laparotomy incision, two zinc discs were placed directly into the bladder. Seven days later the rats were anaesthetised again and catheterised for vesical infusion of a  $1 \times 10^8$  CFU/ml *Proteus mirabilis* bacterial infusion. Sequential struvite calculogenesis was investigated by direct ultrastructural observation and using microbiological techniques, when rats were sacrificed on days 0 to 8 and then days 15 and 30 after infusion of the bacterial suspension. The control group showed no significant calculus formation and there were no histological changes in the bladder or upper renal tracts. In the experimental group the urinary pH, urinary bacterial counts and urease activity increased rapidly. By 48 hours scanning electron microscopy showed the presence of struvite crystals within an extensive bacterial biofilm. Transmission electron microscopy (TEM) showed a layered stratification of these biofilm layers interspersed with layers of crystals. The biofilm layer was composed of dehydrated residue of the bacterial glycocalyx. By 30 days, all remaining rats had developed large bladder calculi, bilateral hydronephrosis and pyelonephritis, whilst 40% also had large renal staghorn calculi.

#### 1.7.5 Ultrastructure of human infected stones:

McLean et al (1989) investigated infected kidney stones removed from humans using transmission and analytical electron microscopy. TEM along with energy dispersive analysis of X-rays showed localised deposits of calcium, phosphate and magnesium close to bacterial cells. Bacterial exopolysaccharides were present, using ruthenium red staining, but only as a small percentage of the stone matrix. They concluded that the bacterial slime/exopolysaccharide production was intimately involved in the initiation of stone deposition.

#### 1.7.6 Manipulating struvite crystallisation in artificial urine:

Studies have shown variations in urease-induced activity and struvite deposition in different human urine samples. This effect was not thought to be due to urinary pH or the phosphate content and indicated that struvite crystallisation may be influenced by other compounds. Hedelin et al (1989) showed that zinc reduced and citrate promoted urease activity in synthetic urine. This influenced struvite and calcium phosphate precipitation, but these results could not be reproduced in human urine (five samples only) and they suggested caution should be taken by investigators when extrapolating from results obtained in synthetic urine to the situation in human voided urine.

McLean et al (1990) concluded that inhibitors of calcium oxalate crystallisation, such as chondroitin sulphate A and heparin sulphate, had no effect in reducing struvite precipitation. Although citrate did not inhibit struvite crystal formation, it did reduce the rate at which struvite crystals formed, due to the fact that octahedral crystals formed slowly as compared with X-shaped crystals associated with rapid growth.

They concluded that the physico-chemical basis for struvite stone precipitation was quite different from calcium oxalate formation.

#### 1.7.7 Manipulating struvite crystallisation in human urine:

Choong et al (2001) described the nucleation pH for stone formation (the pH at which calcium salt precipitation occurred in patients undergoing long-term catheterisation). Two groups of patients were examined, those whose catheters blocked ('blockers') and those whose catheters did not ('non-blockers'). They showed that the nucleation pH ( $\text{pH}_n$ ) was 7.66 and the voided pH ( $\text{pH}_v$ ) 6.26 in the 'non-blockers'. In the 'blockers' group the  $\text{pH}_n$  was similar 7.58, however the  $\text{pH}_v$  was more alkaline at 7.85. Thus the voided pH of 'blockers' was more similar to the nucleation pH.

Continuing on from this Suller et al (2005) investigated methods of manipulating the  $\text{pH}_n$  of the urine with a view to maintaining more of the calcium and magnesium salts in solution, despite more alkaline conditions. Both in-vitro urine dilution and in-vivo dilution (due to increased oral consumption) naturally caused a decrease in urinary  $[\text{Ca}^{2+}]$  and  $[\text{Mg}^{2+}]$  - measured using atomic absorption spectroscopy - and actually increased the  $\text{pH}_n$  of both  $\text{Ca}^{2+}$  and  $\text{Mg}^{2+}$ . In-vitro addition of varying amounts of  $\text{Ca}^{2+}$  and  $\text{Mg}^{2+}$  to collected urine samples to create a concentration range of 0-200  $\mu\text{g/ml}$ , showed that at higher concentrations of both ions, the  $\text{pH}_n$  of both decreased. Addition of pyrophosphate,  $\text{Na}^+$  or  $\text{Cl}^-$  had little effect on  $\text{pH}_n$ . In-vitro addition of citrate to urine and in-vivo increase in urinary citrate concentration (due to increased oral consumption) both showed that there was an increase in  $\text{pH}_n$ . The presence of bacterial cells did not encourage precipitation of salts. 'Debris' in the urine, consisting of desquamated epithelial cells, leucocytes and bacteria, (Clapham et al, 1990) varies

between patients and had been proposed to possibly act as nucleation sites for crystal development and growth, but Suller et al (2005) showed that there was no change in the  $\text{pH}_n$ . They concluded that increasing fluid intake along with increased citric acid consumption may reduce the extent of encrustation.

Subsequent experiments in a laboratory model of *Proteus mirabilis* infection confirmed that dilute, citrate-containing urine with a nucleation pH greater than 8.3 did not favour crystalline biofilm formation (Stickler 2006).

#### 1.8 BACTERIOLOGY ASSOCIATED WITH STRUVITE STONES:

Bacteria which are urease producers include species of *Proteus*, *Staphylococcus*, *Pseudomonas*, and *Klebsiella*. *Escherichia coli* rarely or never produce urease, whereas *Proteus* species always do (Table 1.2; Griffith, 1978).

There have been relatively few bacteriological studies of patients who have undergone surgical removal of renal calculi. Thompson et al (1973) showed that 77% of calculi removed showed bacterial growth. This was in contrast with Dajani et al (1983) who showed that of 142 stones, only 14% were infected. Lewi et al (1984) showed that out of 63 patients undergoing removal of intrarenal calculi, 17 patients had struvite calculi, 58% of which had a positive pre-operative MSU, 76% had positive culture from aspirated pelvic urine, and 82% demonstrated significant bacterial culture from the stone itself. Overall infection rates (for all 63 patients) were 29%, 30% and 38% respectively.

Table 1.2: A list of urease-producing bacteria (from Griffith, 1978).

Organism	% of bacterial isolates showing positive indication of urease activity
<i>Proteus vulgaris</i>	99.6
<i>Proteus mirabilis</i>	98.7
<i>Proteus morgani</i>	91.8
<i>Proteus rettgeri</i>	99.0
<i>Providencia al caliifaciens</i>	99.0
<i>Providencia stuarti</i>	97.1
<i>Klebsiella pneumoniae</i>	63.6
<i>Pseudomonas aeruginosa</i>	32.6
<i>Serratia marescens</i>	29.0
<i>Serratia liquefaciens</i>	5.0
<i>Enterobacter aerogenes</i>	2.6
<i>Citrobacter freundii</i>	0
<i>Escherichia. coli</i>	0

In the above studies, the commonest organism isolated was *Proteus mirabilis* in the ‘struvite’ group and *Escherichia coli* in the ‘calcium oxalate’ group. Interestingly in two patients within each group, the urine culture differed from the stone and pelvic urine cultures, reflecting possible secondary infection of the bladder urine, following antibiotic treatments, suggesting that pelvic urine more accurately reflects the urine environment in which the stone forms and bacteria grow. McCartney et al (1985) showed similarly that in 24 patients studied, 42 % were shown to have struvite calculi. Of this group, 57 % had positive cultures in per-operative mid-stream urine, 71 % had

positive pelvic urine culture and 86 % had positive stone culture. They also showed that bacteria were present deep within the stone, because bacterial cultures from when the stones were crushed were significantly higher than when the stones were just washed and the resultant washings cultured.

Two studies suggested different bacteriological overviews. Bratell et al (1990) showed that in a significant number of patients with infection / magnesium ammonium phosphate stones, no urease-producing organism could be cultured, however *Escherichia coli* was frequently cultured from the stone. This raised the possibility that *Escherichia coli* could be involved in stone formation. Hugosson et al (1990) showed that in 215 patients, of those with struvite calculi, only 48% grew urease-secreting organisms from stone culture, again suggesting that urease-producing organisms were not obligatory for this type of stone formation. Gault et al (1995) also showed that out of 36 patients with struvite calculi, 31 had negative stone cultures and 20 had negative urine cultures.

*Ureaplasma urealyticum* is also found in the lower urinary tract of sexually active individuals. It is thought that it invades the upper urinary tract, and then stone formation results in the kidney due to its urease-producing activity. In-vitro experiments have shown struvite crystallisation when synthetic urine has been inoculated with *Ureaplasma urealyticum* (Grenabo et al, 1984). In-vivo experiments showed that inoculation of *Ureaplasma urealyticum* into the bladder of rats resulted in rapid bladder stone formation (Grenabo et al, 1985). A study by Hedelin et al (1984) showed that *Ureaplasma urealyticum* was cultured in seven patients with infection stones. Four of these seven patients showed no other urease-producing organism,

showing that it can be present as the only urease-producing organism and may be associated with stone formation. The presence of *Ureaplasma urealyticum* can go unnoticed since it is not detected by routine cultures or urine cultures in the presence of renal calculi (Hedelin et al, 2002). It can however cause significant problems with rapid large stone formation and recurrent stones (Grenabo et al, 1986).

Thus, there remain some questions regarding the bacteriology of stones Rodman (1999):

1. Voided urine may not be representative of urine within the renal pelvis and hence voided urine cultures may therefore be an inaccurate reflection of the true scenario within the kidney. For this reason, removed stones should always be cultured directly.
2. When mid-stream urine samples are sent for analysis, laboratories may be missing or ignoring organisms growing small numbers of colonies, since it is common practice to label counts of <10,000 or <50,000 as 'not significant'. However, smaller colony numbers will provide very useful information and all organisms, regardless of number, should be grown and recorded in such patients.
3. The biofilm matrix creates a micro-environment which prevents organisms from being shed into the surrounding urine and makes it difficult to treat the infection.
4. As mentioned previously, urea-splitting bacteria are not always cultured from struvite stones, such as *Ureaplasma urealyticum* (Clerc et al, 1984).

## 1.9 CLINICAL IMPLICATIONS OF STRUVITE STONES

### 1.9.1 Survival rates and sepsis:

Staghorn calculi are branched calculi that sit in the renal collecting system, filling the renal pelvis, with branches that extend into the calices. They are usually infection-induced and can grow rapidly. They can be asymptomatic, however patients usually present with recurrent cystitis and abdominal radiographs identify staghorn calculi. An untreated staghorn calculus can destroy the kidney and result in life-threatening sepsis (Griffith, 1978; Ganpule et al, 2008).

Priestley et al (1949) first pointed out that staghorn calculi were rarely unassociated with severe urinary symptoms, and they showed that it was better to remove the stone rather than a nephrectomy, but still better than doing nothing. At this time some felt that staghorn calculi were generally silent and that patients were better left alone. Singh et al (1973) stated that if staghorn stones were silent, this was a very rare occurrence (0.05%). They showed that of 54 patients with 'untreated' staghorn calculi, 81% had pain, 48% had haematuria and 79% had infection. Forty-five patients had unilateral, whilst nine patients had bilateral staghorn calculi. Of the 45 patients with unilateral staghorn calculi, 16 out of 20 patients (80%) survived with primary nephrectomy, as did nine out of 12 patients (75%) with delayed nephrectomy, but only four of 13 patients (31%) survived with no surgical treatment. They confirmed that patients who had a nephrectomy fared better than those in whom a stone was left in-situ, and that a stone in-situ not only increases the risk of pyonephrosis within that kidney, but also poses a constant threat to the other kidney. Singh et al (1973) compared these figures with 81 out of 86 patients (94%) surviving after they

performed extended pyelolithotomy to remove staghorn calculi. 70 patients had unilateral stones and 16 patients had bilateral calculi. Of the 103 kidneys operated on, only three (3%) required nephrectomy and 13 (13%) recurred.

Grenabo et al (1985) conducted a retrospective study of 391 stone cases. 66% of stones were calcium stones, 30% were infection stones, 4% were uric acid stones and 1% were cystine stones. Of the infection cohort, 10% were staghorn stones. They found that the infection stones placed a greater strain on the patient. 61% of the infection stones were recurrent stones as compared to 48% of the calcium stones. Spontaneous passage of the stone was more common with calcium stones (42%) than with infection stones (12%). Kidney stone surgery was performed in 60% of patients with infection stones compared with 23% of patients with calcium stones. A positive urine culture was found in 15% of calcium stone cases in contrast with 63% of the infection stone cases.

Struvite staghorn calculi can form a real threat to the kidney and hence their presence is an indication for active treatment in most individuals (Segura, 1997). Staghorn struvite stones can be embedded with gram-negative bacteria, which can also produce endotoxins. Sepsis syndrome may occur after surgical therapy or endoscopic manipulation of infected or staghorn calculi (McAleer et al, 2002). Sepsis can occur, despite perioperative antibiotic use, possibly due to bacteremia or endotoxemia. Perinephric abscess can be a common manifestation of a renal staghorn stone. Patients may present with signs of sepsis, flank pain and discharge and this may then lead to diagnosis of a perinephric abscess secondary to a staghorn stone (Tsukagoshi et al, 2006).

Though it is fairly well-known that the main component of staghorn calculi are magnesium ammonium phosphate and carbonate apatite (Resnick et al, 1980), it is thought that a large proportion of patients with staghorn stone disease may have a metabolic abnormality contributing to their stone formation (Resnick, 1981). Wall et al (1986) showed that 21 out of 31 patients with renal staghorn disease had magnesium ammonium phosphate within the stone, however calcium phosphate was the most common constituent in 30 of the 31 patients. They also showed that 24 hour urine analysis was normal in only three of the 31 patients, and they suggested that a metabolic evaluation of all patients with staghorn stones was required post-operatively to decrease the high recurrence rate in these patients.

#### 1.9.2 Renal function impairment:

Vargas et al (1982) clinically evaluated 95 patients (105 kidneys) with staghorn calculi. Complications occurred in 53 per cent of the patients (20% had pyonephrosis, 8% had xanthogranulomatous pyelonephritis, 20% had severe/end-stage pyelonephritis or renal failure, and 5% had a perinephric abscess). They suggested complete removal of the calculus early in the course of the disease in order to prevent complications and renal deterioration.

Kristensen et al (1987) showed that of 75 patients with struvite stones, 52 were women. They suggested that women presented themselves with infection rather than stone passage, which is more commonly the presentation in men. Women are also less frequently hypercalciuric and have a higher frequency of surgery and contralateral stone formation compared to men. They concluded the primary struvite

nephrolithiasis was a serious form of stone disease and that both men and women were at high risk for reduced glomerular filtration rate, especially once a staghorn calculus had formed.

Worcester et al (2003) showed that females had a two-fold risk above that of males for losing the kidney, and that kidney loss did not worsen stone disease. They also showed that there was an accelerated rate of loss of creatinine clearance among stone formers in general as compared to normal subjects. Their study showed that the stones that led to kidney loss were frequently struvite stones or stones producing a large mass effect in the kidney.

Worcester et al (2006) investigated renal function in different stone formers. 1,856 stone formers were compared with 153 normal individuals. They showed that creatinine clearance was decreased in all stone formers, compared to normal subjects, but was particularly low in cystine and struvite stone formers.

### 1.9.3 Encrustation and blockage of urethral catheters:

Urethral catheters can be inserted for a short period (e.g. monitoring urine output) or long-term catheterisation may be used for patients with incontinence or where other methods of management have been excluded. Long-term catheterisation carries an increased risk of urinary tract infection and catheter encrustation (blockage). This can create a large and continual demand on hospital and community health services. A postal survey by Kohler-Ockmore et al (1996) showed that of 467 patients with long-term catheters, there were 506 emergency referrals during a six-month period. Detailed study of 54 patients showed that 48% suffered catheter blockage, 37% had

urine by-passing the catheter and 30% had haematuria. They concluded that the prevalence and morbidity associated with long-term catheterisation caused considerable pressure on district and hospital nursing services and that further research was required to reduce catheter blockage and encrustation.

Catheters allow external bacteria to have easy access to the bladder and thus catheterisation results in bacteriuria. The catheter may be disconnected from the collection tube and bacteriuria has been associated with such interruptions (Warren, 2001). Bacteria contaminating the lumen of the drainage tube, from the catheter bag, can ascend into the bag, to the collection tube and up the catheter. Bacteria that enter the catheterised urinary tract are able to multiply to high concentrations within a day (Stark & Maki, 1984). Warren et al (1994) suggested that complications of long-term catheter-associated bacteriuria could be divided into two groups. The first includes symptomatic urinary tract infections and pyelonephritis (Warren et al, 1987). The second group includes urinary obstruction, urinary tract stones, and chronic pyelonephritis.

Cox & Hukins (1989) showed hydroxyapatite and struvite deposition onto catheter materials, using scanning electron microscopy, in the presence of urease. Morgan et al (2009) studied the encrustation of silver Foley catheters in six patients undergoing long-term catheterisation. They showed that after being in-situ for 11 days, there was clear occlusion of one catheter with extensive deposits of crystalline material with the presence of apatite and struvite. Encrustation was visible around the eye-holes of the catheter and these crystalline deposits were revealed to be the bacterial biofilm. They suggested that layers of microcrystalline material are deposited onto the catheter

surface and then bacteria attach to these layers and grow into mature biofilms. The silver catheters used had been claimed resistant to bacterial colonisation (Davenport & Keeley, 2005). However, the above study showed this not be the case and suggested that in order to prevent catheter encrustation, it was essential to prevent the pH of urine rising above that at which crystals form.

Stickler et al (1993) indicated that *Proteus mirabilis* was the species most commonly recovered from patients' encrusted catheters. Sabbuba et al (2003) developed a method for genotyping *Proteus mirabilis* and identified that the same genotype persisted in a patient's urinary tract despite many catheter changes, courses of antibiotics and even periods when the patient was not catheterised. They also showed that the strains of *Proteus mirabilis* from catheter encrustations were identical to those in the bladder stones (Sabbuba et al, 2004). *Proteus mirabilis* is an enteric organism and analysis by Mathur et al (2005) showed that bacteria from faecal and catheter biofilm isolates from the same patients were identical.

Stickler (2008) suggested that biological, physical and chemical factors were causative in the formation of biofilms as follows.

Biological factors: initially the prosthetic device (e.g. catheter) is rapidly coated by a film of host proteins from the urine. Bacteria then attach to the proteins, via their fimbriae (Ong et al, 2008).

Physical factors: scanning electron microscopy has shown that catheter surfaces are rough and irregular in nature (Cox, 1990). Scanning electron microscopy showed the eye-holes in catheters to be particularly vulnerable to bacterial colonisation (Stickler et al, 2003).

Chemical factors: an alkaline urine has been shown to promote biofilm formation (Stickler et al, 2006). The nucleation pH is the pH at which urine becomes turbid due to crystallisation of struvite and apatite. Choong et al (2001) showed that catheters become encrusted if the pH of the urine is greater than the nucleation pH.

Strategies to prevent catheter encrustation include: dilution of urine by increasing fluid intake; increasing the urinary concentration of citrate; raising the nucleation pH (Suller et al, 2005) and; triclosan, a biocide used to inflate the catheter balloon and shown to inhibit biofilm formation; Jones et al, 2005). Norberg et al (1983) suggested monitoring the time taken for patients' catheters to block and then implementing a schedule for catheter replacement, specific to that patient, so that the catheter may be changed prior to the predicted time of blockage. An alternative approach is a simple sensor in the drainage system which signals the early encrustation and *Proteus mirabilis* infection, thus indicating need for change of catheter (Stickler et al, 2006).

#### 1.9.4 Ureteric Stent Encrustation:

Ureteric stent encrustation is less commonly associated with infection (Shaw et al, 2005) and is most commonly composed of calcium oxalate, whereas urethral catheter encrustation is often composed of struvite. Keane et al (1994) examined ureteric stents from 40 patients. They found that 58% of stents were encrusted and 28% of stents had a significant biofilm. The most common biofilm organism isolated was *Enterococcus faecalis* and not *Proteus sp.*

The manifestation of stent encrustation may include painful hydronephrosis and if prolonged can lead to irreversible renal damage, as well as development of sepsis

proximal to the obstruction with subsequent more rapid renal impairment. These circumstances may necessitate change of stent or urgent nephrostomy insertion. Occasionally if encrustation is very severe, it can be quite difficult removing the stent and may require several complex operative procedures in a specialist centre (Shaw et al., 2005).

Different types of stents have been used to try and minimise encrustation. Silicone was the first generation polymer to be used, but these were replaced by polyethylene and subsequently the third generation polymer polyurethane, which has excellent properties (Venkatesan et al, 2010a). Approaches to reduce bacterial adherence and encrustation include coating the stents with different materials or blending antiencrustation agents into the polymer. Coatings include hyaluronic acid, hydrogel, heparin and silver. More research is being conducted on the effect of uropathogens on in-vitro encrustation of ureteral stents (Venkatesan et al, 2010b). Triclosan, an antimicrobial agent, has also been incorporated into ureteric stent materials. However, Cadieux et al (2009) showed that there was no clinical benefit in terms of urine and stent cultures, or overall symptoms when compared with controls. They felt that triclosan-eluting stents alone were not sufficient to reduce associated infections.

#### 1.9.5 Metabolic syndrome

The metabolic syndrome consists of a cluster of physical and laboratory abnormalities including hypertension, hyperglycemia, hyperlipidemia and abdominal obesity (Peralta et al, 2006). West et al (2008) showed that the prevalence of stones increased amongst subjects with more metabolic syndrome traits, showing an association between stone formation and the metabolic syndrome. In particular, uric acid

nephrolithiasis is associated with the metabolic syndrome. A low urinary pH is required for uric acid stone formation and urinary acidity is recognized to be one of the features observed in the metabolic syndrome. This acidity is thought to be due to increased acid excretion, and impaired buffering due to defective urinary ammonium excretion (Sakhaee & Maalouf, 2008a).

Abate et al (2004) showed that a possible renal manifestation of insulin resistance was a low urinary pH and ammonium concentration. The concentration of urinary ammonium was measured using a glutamate dehydrogenase method. Sakhaee (2008b) suggested we needed to further our understanding of the mechanisms linking nephrolithiasis and the metabolic syndrome in order to develop more effective preventive and therapeutic treatment strategies.

#### 1.9.6 Summary:

The management strategy for patients with struvite stones was outlined above (section 1.7.2). However, at present there are no truly effective treatments to prevent or treat struvite stones. Problems are associated with:

- Bacteria are embedded within the layers of the stone and matrix – since antibiotics are unable to penetrate deep within the stone, they are ineffective.
- Once a patient is said to be rendered stone-free, even a small remaining nidus not evident at operation or on imaging can cause recurrence
- At present the only real treatment strategy is prevention of infections once a patient is stone free.
- There are no current monitoring strategies apart from urine cultures.

- The physical chemistry of  $\text{NH}_4^+$  and  $\text{Mg}^{2+}$  in the aqueous environment of urine is not known. For example, the urinary concentration of these reactants are not routinely measured and the conditions that result in crystallisation are therefore unclear.

### **1.10 THE USE OF ION-SELECTIVE ELECTRODES IN MONITORING URINE COMPOSITION.**

A new generation of potentiometric ion-selective electrodes has played an integral part in aiding our understanding of the physico-chemical basis for stone formation. Langley & Fry (1995) measure the ionised fraction of  $\text{Ca}^{2+}$  in urine, the variation in the concentration in urine samples from stone-formers and control patients and introduction of the concept of nucleation pH at which calcium salts crystallise in urine. Previously theoretical calculations were used to calculate urinary  $\text{Ca}^{2+}$  using computer programs such as Equil2 (Werness et al, 1985). Langley & Fry (1995) showed a poor correlation between the measured  $\text{Ca}^{2+}$  concentration using ion-selective electrodes and calculation methods, such as with Equil2. They suggested that calculations relied on accurate knowledge of the concentration of all  $\text{Ca}^{2+}$ -binding ligands and of their binding constants in urine, and that the poor correlation between the two methods further demonstrated that our knowledge of  $\text{Ca}^{2+}$ -binding ligands in urine was incomplete. They suggested that spot urinary measurements of  $\text{Ca}^{2+}$  concentration at a standard pH provided a more discriminative test than total calcium (ionised and bound) for the presence of urinary tract stones.

Ion-selective electrodes for  $\text{NH}_4^+$  and  $\text{Mg}^{2+}$  have been developed but have not been used for extensive measurement of urinary concentrations.  $\text{NH}_4^+$ -selective electrodes have been based on the ionophore nonactin and used for analysis of water and plasma samples, for example (Cooke & Jensen, 1983; Schwarz et al., 2000), but more recently other ionophores have been devised based on crown ether structures (Benco et al., 2003; Chandra et al., 2006). A recent study used  $\text{NH}_4^+$ -selective electrodes for the determination of nitrogen-containing substances (urea and creatinine) in urine samples but did not undertake an extensive analysis of urinary  $[\text{NH}_4^+]$  (Gutiérrez et al., 2008).

$\text{Mg}^{2+}$ -selective electrodes have been made from several neutral ionophores and used to measure ionised  $[\text{Mg}^{2+}]$  in biological samples such as plasma and serum (Rouilly et al., 1990; Brookes & Fry, 1993; Hafen et al., 1996). However, their use in urine samples has not been reported. One problem with  $\text{Mg}^{2+}$ -selective electrodes has been a poor selectivity with respect to  $\text{Ca}^{2+}$ .

A major objective of this thesis was to develop  $\text{NH}_4^+$ -selective and  $\text{Mg}^{2+}$ -selective electrodes for use in urine samples and to ascertain whether differences existed in the concentration of these ions using urine samples from struvite stone formers and stone-free controls

## 1.11 HYPOTHESES, AIMS AND OBJECTIVES OF THE THESIS.

There has been considerable research into in-vitro struvite crystal growth in artificial urine. However there has been less work investigating crystal growth in human urine or with in vivo animal studies. Furthermore, there has been no research involving characterisation of human urine from struvite stone-formers. The goal of this project was to understand the reasons for struvite stone formation in the human urinary tract and aid us in creating future treatments and possible preventative medications.

### 1.11.1 Hypotheses

The  $\text{NH}_4^+$  and  $\text{Mg}^{2+}$  concentrations in urine from stone-formers are different from that in control subjects.

The  $\text{NH}_4^+$  and  $\text{Mg}^{2+}$  concentrations in urine show a significant dependence on pH, and will increase the possibility of crystallisation as urine pH increases.

### 1.11.2 Aims and experimental objectives of the thesis

Development and characterisation of an  $\text{NH}_4^+$ -selective electrode at room temperature and at 37°C

Determination of selectivity coefficients of the  $\text{NH}_4^+$ -selective electrode against interferent ions.

Development and characterisation of a  $\text{Mg}^{2+}$ -selective electrode at room temperature and at 37°C.

Determination of selectivity coefficients of the  $\text{Mg}^{2+}$ -selective electrode against interferent ions.

Measurement of the  $\text{NH}_4^+$  and  $\text{Mg}^{2+}$  concentrations of urine from normal subjects at room temperature and  $37^\circ\text{C}$ .

Measurement of the pH-dependence of the urinary  $[\text{NH}_4^+]$  at room temperature and  $37^\circ\text{C}$ .

Validation of the  $\text{NH}_4^+$ -selective electrode data against colour spectrophotometry

Validation of the  $\text{NH}_4^+$ -selective electrode data against an empirical calculation method

Measurement of the  $\text{NH}_4^+$  and  $\text{Mg}^{2+}$  concentrations of urine from patients with staghorn stones or urinary tract stone disease.

## **CHAPTER 2**

### **METHODS AND PATIENT SAMPLES**

#### **2.1 PATIENT GROUPS:**

Healthy individuals from the laboratory were recruited for normal urine samples. Patients were recruited from those attending the Urology Stone Unit at University College Hospital. Patients were predominantly attending for a urological procedure including percutaneous nephrolithotomy and ureteroscopy, except for three patients who attended outpatient clinics.

A further group of patients were recruited from the renal stone clinic at the Royal Free Hospital, London. This is a specialised clinic dealing with patients with recurrent stones and problematic stones.

Prior to taking the urine sample, a consent form and patient information sheet (see appendix) were completed. The patient information sheet included the patient's personal details, information on their urological history, previous urological procedures, previous knowledge of stone type, and prior urinary tract infections. A past medical history, drug history and allergies, were also recorded. At this point the patient was assigned a number, which was written on the patient information sheet and consent form, to allow for confidentiality. Subsequent data handling and construction of experimental groups used only the patient number.

## **2.2 URINE COLLECTION AND CLINICAL BIOCHEMISTRY:**

### 2.2.1 Urine collection.

Because all but three patients were attending for urological procedures, all urine samples were collected between 7.15 and 8.00 a.m. By taking early morning urine samples, two purposes were served. Firstly, this allowed better comparison of urine samples by reducing variability of urine biochemistry during the day. Secondly, since patients had all been nil-by-mouth from the previous night, as a requirement for their clinical procedure, this reduced the effect that diet and fluid intake may have had on urinary constituents. Samples were collected in sterile MSU (mid-stream urine) bottles. Each patient provided about 20-40 ml of urine. The MSU bottles were then labelled with the patient's assigned number.

### 2.2.2 Urine storage:

After sample collection, urine samples were temporarily stored in a portable cooling container for transport back to the laboratory. Ice packs were present within the cooling container to maintain a cool (4°C) environment for transport.

### 2.2.3 Clinical Biochemistry:

For each patient, a mid-stream urine sample was sent to microbiology to investigate for evidence of current urinary infection. A sample was also sent to the clinical biochemistry department to measure urinary  $[Na^+]$  and  $[K^+]$  with a commercial ion-selective analyser (Orion); creatinine and urea with a Sequential Multiple Analyzer (SMA6, Technicon Instruments) and osmolality by freezing point depression.

## 2.3 MANUFACTURE OF ION-SELECTIVE ELECTRODES

### 2.3.1 General procedure for the manufacture of ion-selective plastics:

The ion-selective membrane is the key component of the ion-selective electrode. The ion-selective membrane is a plastic generated by mixing an ion-selective ligand with a polyvinylchloride (PVC) solution and a plasticiser to permit the ligand to disperse evenly within the PVC solution. Prior to manufacture of the ion-selective plastics, all the glass bottles/pots and equipment were cleaned with tetrahydrofuran (THF). The source of all chemicals in this thesis was the Sigma Chemical Company.

Firstly, one 10 ml glass bottle (Pot 1) was cleaned with THF and allowed to dry. High molecular weight PVC, in the form of a dry powder, was added to the pot and was dissolved in THF: see Table 2.1. The mixture was slowly, but continuously stirred for 10-20 minutes to ensure that all the PVC was dissolved. To a second glass bottle (Pot 2) was added the ion-selective ligand and plasticiser, which was then stirred slowly for about ten minutes to ensure adequate mixing of these two components. Different plasticisers were used for different ion-selective plastics, see Table 2.1.

For all ion-selective ligands, except that for  $\text{NH}_4^+$ , K-tetrakischlorophenylborate (KtClPhB) was also added to the ionophore/plasticiser mixture. This material confers a significant conductance to the eventual ion-selective plastic, enabling electrodes with a lower resistance (about 1 M $\Omega$ ) to be manufactured, thus reducing electrical noise in the experimental system, thus permitting the signal-to-noise ratio to be greatly increased. KtClPhB was omitted from the  $\text{NH}_4^+$ -selective electrodes as the salt confers a significant

$K^+$ -selectivity to the resulting ion-selective plastic and it was important to reduce this already significant property of the  $NH_4^+$ -selective electrode. For the remaining ion-selective plastics where  $K^+$ -interference was less significant the molar ratio of KtClPhB to the primary ion ionophore was  $<1.0$ .

Finally the PVC solution was added to the ionophore/plasticiser/(KtClPhB) mix and again slowly stirred for about five minutes. The final composition of the mixture (w/w) was plasticiser:PVC:ionophore:(KtClPhB) of 66%:33%:1%:0.4%.

The pot containing the mixture was covered with aluminium foil, to prevent light oxidising the THF, and the solvent was then allowed to evaporate slowly over several days. The slow evaporation was achieved by placing, under pressure, about fifty layers of fine filter paper over the mouth of the glass bottle to minimise the evaporation space. A clear, solid plastic, with no visible precipitations, resulted and could be stored in the dark, using silver foil around the container, for several months prior to preparation of the ion-selective electrodes.

Table 2.1 lists the materials used to manufacture ion-selective plastics for different ions measured in this thesis.

Table 2.1. Components of the different ion-selective plastics used to manufacture ion-selective electrodes.

Primary ion	Pot 1		Pot 2				
	High mw PVC	THF	Selective ionophore	KtClPhB	NB	DBS	EHS
NH <sub>4</sub> <sup>+</sup>	700 mg	6ml	2.4 mg nonactin	-	-	144 mg	-
K <sup>+</sup>	300 mg	7ml	3.2 mg valinomycin	0.3 mg	200 mg	-	596 mg
Mg <sup>2+</sup>	165mg	6ml	5.5 mg ETH 5506/7025	3.0 mg	-	-	330 mg
Ca <sup>2+</sup>	95mg	6ml	10 mg ETH 1001	2.5 mg	-	-	190 mg

PVC: polyvinylchloride

THF: tetrahydrofuran

NB: nitrobenzene

DBS: dibutyl sebacate

EHS: bis (2-ethylhexyl) sebacate

KtClPhB: potassium tetrakis(p-chlorophenyl)-borate

### 2.3.2 Manufacture of the electrode template:

The main part of the electrode was made of a five-cm length of hollow PVC tubing, 0.8 mm inside, 1.0 mm outside diameter. PVC tubing was flexible and was sufficiently supportive when placed in the apparatus. A length (2-3 mm) of ceramic plug (frequentite, Morgan Matroc, Worcestershire, UK) that had been reduced in diameter to fit tightly into the bore of the PVC tube was wedged into the tubing and the exposed ceramic plug surface smoothed down using fine-grade sandpaper. The ceramic rod acted as surface on which the ion-selective membrane could be applied. By being porous, the ceramic rod allowed the filling solution, within the electrode, to diffuse through the rod and come into

close contact with the ion-selective membrane. This system formed the template for both the reference and ion-selective electrodes.

### 2.3.3 Coating the electrode template with the ion-selective membrane:

The ion-selective plastic was first re-dissolved with THF. Only a small amount of THF was required (about 1 ml). The resulting solution was left to stir very slowly, in order to allow the THF to evaporate. Once the mixture was of a suitable consistency (e.g. treacle-like), the electrode templates were dipped into it. The aim was to coat the exposed ceramic rod and the distal part of the PVC tube to form a continuous coating. The tip of the electrode template was held in the solution for 1-2 seconds, and then raised above the solution for a further 10 seconds to allow any remaining solvent to evaporate slowly and so leave a uniform coat of ion-selective plastic. This process was repeated twice more at 15-minute intervals ensuring that the electrodes received an adequate coating of the ion-selective membrane. Care was taken to remove air bubbles from the dipped coating, by touching the tip of the electrode against the side-wall of the glass pot. The electrodes were left to dry in open air for 2-3 days, allowing the plastic ion-selective membrane to form around the distal tip of the electrode. Usually batches of five electrodes were dipped once the ion-selective plastic had been re-dissolved. The ion-selective plastic solution was allowed to re-form a solid that could be subsequently re-used.

### 2.3.4 Ion-selective electrode filling solutions:

The bore of the PVC tube that formed the ion-selective electrode was filled with a solution of known concentration of the primary ion. Thus, the voltage across the ion-selective plastic membrane was a function only of the ion activity gradient and hence the

activity of the ion in the test solution into which the ion-selective electrode was placed. Generally the concentration of the primary ion was similar to that in the test solutions so that excessively large voltages across the ion-selective membrane were not generated. In addition, the total cation concentration of the filling solution was about 150 mM so that excessive osmotic gradients across the electrode were also minimised, thus limiting water flux across the membrane.

Each of the stock filling solutions was saturated with AgCl, by adding a small amount of solid AgCl to them. This minimised the filling solution from dissolving away the AgCl on the Ag/AgCl electrode (section 2.3.5) and therefore limited voltage drift at the interface between the filling solution and Ag/AgCl electrode. When filling the electrodes, care was taken to ensure that the column of fluid was continuous, without any air bubbles, to allow good contact between the Ag/AgCl electrode and the ion-selective membrane. Bubbles were removed by gently flicking the electrode after injecting the filling solution.

#### 2.3.5 Manufacture of reference electrodes:

The reference electrode was made using an electrode template, with no coating, and filling it with a 3 M KCl solution, saturated with AgCl. The ceramic rod again provided a good porous support for a stable liquid junction potential between the filling solution and the test solution.

Table 2.2. Composition of filling solutions used with the different ion-selective electrodes.

Ion-selective Electrode	Filling Solution	Reference Electrode
NH <sub>4</sub> <sup>+</sup> -selective electrode	1 mM NH <sub>4</sub> Cl /150 mM NaCl Saturated with AgCl	3 M KCl
K <sup>+</sup> -selective electrode	4 mM KCl /146 mM NaCl Saturated with AgCl	3 M KCl
Mg <sup>2+</sup> -selective electrode	1 mM MgCl <sub>2</sub> / 150 mM NaCl Saturated with AgCl	3 M KCl
Ca <sup>2+</sup> -selective electrode	1 mM CaCl <sub>2</sub> / 150 mM NaCl Saturated with AgCl	3 M KCl

### 2.3.6 Manufacture of the Ag/AgCl electrodes:

These electrodes were used to connect the filling solutions within the ion-selective and the reference electrodes to a voltmeter. A coating of AgCl over a bare silver (Ag) wire electrodes provides a large surface area of conductor for the electrode size and minimises polarisation at the electrode surface, thus reducing electronic drift. A 6-cm length of Shellac-coated Ag wire (25 µm diameter) was prepared by scraping away the coating from a 2-cm length of one end with a blunt scalpel blade, revealing the bare Ag wire. Only the terminal region of the Shellac coating was removed for AgCl coating, as this was the region that made contact with the ion-selective filling solution (below). Leaving the coating on the remainder of the Ag wire external to the electrode ensured that water vapour in the air did not condense onto the Ag electrode. The extreme part of the other

end was similarly cleaned to permit a solder connection to a wire and hence connection with a voltmeter – see Figure 2.1, section 2.3.7).

Several bare Ag wires were coated with AgCl in a batch. To coat the Ag wire with AgCl the bare ends were first cleaned by connecting them to the cathode of a 9 V battery. The anode of the battery was connected to a 2 mm diameter Ag rod and the system immersed in 100mM KCl for 30 seconds, causing the silver bare wires to generate bubbles as water was hydrolysed. At the anode, the Ag rod gained a coarse, white granular layer of AgCl. This process served to clean the silver wires of surface impurities. The coarse AgCl deposit was scraped from the silver rod with fine emery paper and the system re-immersed in fresh 100 mM KCl solution. The polarity on the system was now reversed with the Ag wires now attached to the anode so that they would be coated with AgCl. To generate a more stable AgCl coating, the current through the system was reduced by placing a large (220 k $\Omega$ ) resistor in the circuit. The AgCl coat developed over 40-45 minutes and appeared as a brown/purple deposit on the wire. The coated electrodes were then removed and stored in a dry container until they were required for use.

### 2.3.7 Experimental Arrangement:

An electrochemical cell was created by measuring the potential difference (p.d.) between the ion-selective electrode and reference electrode when both were immersed in the test solution. The p.d. was measured with a differential amplifier manufactured in the laboratory, using high input impedance operational amplifiers as input stages (J-FETs, input impedance  $10^{12}$   $\Omega$ , RadioSpares, UK). The high input impedance was significantly greater than the impedance of the ion-selective electrodes (1-10 M $\Omega$ ), ensuring that the

differential amplifier did not affect the p.d. generated by the ion-selective/reference electrode pair. The differential amplifier output was connected to a liquid-crystal numerical display and the values recorded. A schematic of the arrangement is shown in figure 2.1.

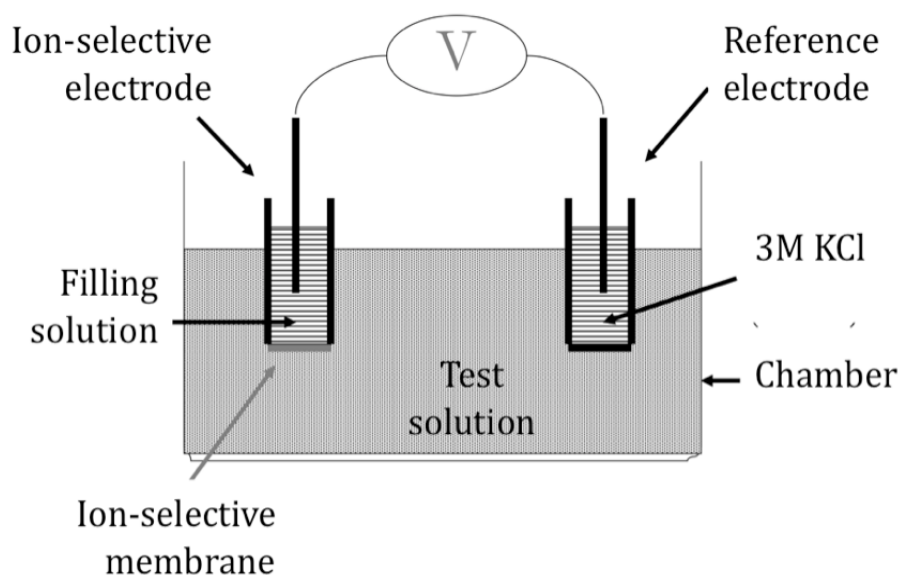


Figure 2.1. A schematic diagram of the electrochemical cell used for the measurement of ion activities with ion-selective electrodes.

The test chamber in which the electrodes were dipped was a 4 ml Perspex water-jacketted holder (Figure 2.2). Water was circulated through a water-jacket at 25 or 37°C. A commercial glass pH combination electrode was also immersed into the chamber through a side-wall so that the pH of the test solution could be continually monitored. A Perspex insert formed the top of the test chamber with small holes drilled through it. These holes held the ion-selective and reference electrodes so that only the tips were immersed in the test solution. An additional hole enabled a needle from a Hamilton Microlitre syringe

(10-100  $\mu\text{l}$ ) to be inserted into the test solution for the addition of calibrating solutions. The insert also minimised evaporation of the test solution for the duration of the recording – up to 30 minutes. The chamber was placed on a magnetic stirrer and a small Teflon-coated magnetic bar in the test chamber allowed adequate mixing throughout the measurement protocols.



Figure 2.2: Test chamber: A – side view with combination pH electrode projecting from the left-hand side. The chamber sits on top of a rotating magnetic chamber to allow rotation of the magnetic Teflon-coated bar placed in the test solution B – top view of experimental chamber.

## 2.4 CALIBRATION OF ION-SELECTIVE ELECTRODES

### 2.4.1 Calibration solutions:

The ion-selective electrodes were calibrated in a base solution of 150 mM NaCl or 140 mM NaCl + 10 mM 4-(2-hydroxyethyl)-1-piperazine ethane-sulphonic acid (MES) buffered to pH 6.0. Aliquots of aqueous stock calibrating solutions were added to the base solution, appropriate to the electrode being tested. Below is a list of the different calibration solutions used:

$\text{NH}_4^+$ -selective electrode: 100 mM and 1 M  $\text{NH}_4\text{Cl}$  solutions.

$\text{K}^+$ -selective electrode: 100 mM and 1 M  $\text{KCl}$  solutions.

$\text{Ca}^{2+}$ -selective electrode: 100 mM and 1 M  $\text{CaCl}_2$  solutions.

$\text{Mg}^{2+}$ -selective electrode: 100 mM and 1 M  $\text{MgCl}_2$  solutions.

#### 2.4.2 Manufacture of calibrating solutions:

Using the example of 1 M and 100 mM  $\text{NH}_4\text{Cl}$ : the molar weight of  $\text{NH}_4\text{Cl}$  is 53.49g. Therefore to create a 1 M solution, 53.49 g of  $\text{NH}_4\text{Cl}$  would need to be dissolved in one litre of water. Using a weighing boat and calibrated scales, 1.07g of  $\text{NH}_4\text{Cl}$  was weighed and dissolved in 20ml of deionised water. To measure out 20 ml of water accurately, a P5000 (R75275N) pipette was used to measure 5 ml and this was then added into the weighing boat to allow the  $\text{NH}_4\text{Cl}$  to dissolve, prior to pouring the solution into a sterile 20 ml plastic container. A further three measures of 5 ml of water were pipetted and used to rinse the weighing boat prior to transfer to the final plastic container, thus ensuring that the entire weighed salt was present in the final solution. This method therefore made a stock of 1 M solution  $\text{NH}_4\text{Cl}$ .

To make a 100 mM  $\text{NH}_4\text{Cl}$  solution, 2 ml of the 1 M  $\text{NH}_4\text{Cl}$  was diluted with 18ml of deionised water and stored in a cleaned plastic bottle. The same procedure was followed to manufacture the  $\text{KCl}$ ,  $\text{CaCl}_2$  and  $\text{MgCl}_2$  solutions.

#### 2.4.3 Experimental Protocol:

Aliquots of stock solution were added to change the concentration of the primary ion between 0.1 and 40 or 80 mM (see Table 2.3). The actual concentration of the primary

ion took into account the small increase of total volume with each incremental addition of stock solution. This is represented in the 'calculated conc' column in Table 2.3.

Table 2.3. Example of a calibration protocol for the  $\text{NH}_4^+$ -selective electrode

Concentration of $\text{NH}_4\text{Cl}$ (mM)	Quantity of 100 mM $\text{NH}_4\text{Cl}$ added, $\mu\text{l}$	Quantity of 1 M $\text{NH}_4\text{Cl}$ added, $\mu\text{l}$	Calculated conc (mM)
0	-	-	
0.1	4	-	0.10
0.2	4	-	0.20
0.4	8	-	0.40
1.0	24	-	0.99
2.0	40	-	1.96
4.0	-	8	3.91
10.0	-	24	9.73
20.0	-	40	19.3
30.0	-	40	28.6
40.0	-	40	37.8

## 2.5 THEORY OF IONIC SOLUTIONS AND THE CALCULATION OF SELECTIVITY COEFFICIENTS.

### 2.5.1 Concentration and ionic activity

The quantity of solute in a given volume or weight of solvent defines concentration. The Systeme Internationale (S.I.) unit of molality,  $m$ , is the number of moles of solute.kg<sup>-1</sup> solvent. The definition of molarity,  $c$ , is the number of moles of solute.litre<sup>-1</sup> solvent. In this thesis units of molarity are used.

When a salt is added to a suitable solvent, such as water, the solute components tend to dissociate into its constituent ions. Arrhenius theory proposes that an equilibrium exists between undissociated solute molecules and ions which arise from electrolytic dissociation. For strong acids and bases and salts such as NaCl and KCl this dissociation is almost complete but not complete. The effective concentration of an ion in solution is termed the activity,  $a$ . The relationship between concentration,  $c$ , and activity for any ion,  $i$ , is

$$a_i = \gamma_i \cdot c_i \quad 1$$

where  $\gamma_i$  is termed the activity coefficient. Ion-selective electrodes measure the activity rather than concentration of an ion in solution, which would be proportional to concentration if  $\gamma_i$  is constant. The value of  $\gamma_i$  is however dependent on a number of solution properties including the concentration of the ion itself, the temperature of the solution and the ionic strength,  $I$ , of the solution: where  $I = \frac{1}{2} \sum cz^2$  of each ionic

constituent ion (valency,  $z$ ) in the solution. The relationship between  $\gamma_i$  and solution parameters is given by the Debye-Hückel equation:

$$\ln \gamma_i = -Az_i^2 \sqrt{I} \quad 2$$

where  $A$  is a function of absolute temperature and at 25°C has a value of 1.172 mol<sup>-1/2</sup>.kg<sup>1/2</sup>. For the variation of temperature and ionic strength experienced in these experiments  $\gamma_i$  varies little and so ionic activity will be considered throughout to be proportional to ionic concentration. All values of ionic concentration will therefore be proportionately related to the concentration of calibration solutions.

2.5.2 The relationship between electrode potential and ion activity – the Nikolsky equation.

The potential difference between the ion-selective and reference electrodes is given by the Nikolsky equation (equation 3): where  $R$  is the gas constant (8.314 J.°K<sup>-1</sup>.mole<sup>-1</sup>),  $T$  is the absolute temperature (°K) and  $F$  is the Faraday constant (96,500 coulombs.J<sup>-1</sup>) and  $z$  is the valency of the primary ion ( $z=1$  for NH<sub>4</sub><sup>+</sup>, K<sup>+</sup>, Na<sup>+</sup>, H<sup>+</sup>;  $z=2$  for Ca<sup>2+</sup>, Mg<sup>2+</sup>). The variable  $E^0$  is a constant.

$$E = E^0 + \frac{RT}{zF} \ln \left( a_{NH_4} + \sum_{j=k,l,m..} k_{NH_4 j}^{pot} a_j^{z^*} \right)$$

$$E = E^0 + 2.303 \frac{RT}{zF} \left( a_{NH_4} + \sum_{j=k,l,m} k_{NH_4 j}^{pot} a_j^{z^*} \right) \quad 3$$

The term  $z^*$  as the exponent in the  $a_j$  term on the right-hand side of the equation is the ratio of valencies of the primary ion,  $i$ , and the interferent ion,  $j$  ( $=k,l,m,\dots$ ). For primary and interferent ions of the same valency  $z^*=1$ . This will be the case for the most

important interferent ions for the respective  $\text{NH}_4^+$ -selective and  $\text{Mg}^{2+}$ -selective electrodes in this study and so will be set to unity here with no loss of generality.

$k_{ij}^{pot}$  is the potentiometric selectivity coefficient for the  $j$ th interferent ion ( $j=k,l,m\dots$ ),  $\text{Na}^+$ ,  $\text{H}^+$ ,  $\text{K}^+$ ,  $\text{Ca}^{2+}$ ,  $\text{Mg}^{2+}$ , etc with respect to the primary ion,  $i$ , (e.g.  $\text{NH}_4^+$ ). Here the activity,  $a$ , of the primary and interferent ions are used in place of their respective concentrations. The values of  $k_{ij}^{pot}$  are quoted in the text as  $\log k_{ij}^{pot}$  values.

A plot of p.d. ( $E$ ) as a function of the logarithm ( $\log_{10}$ ) of the primary ion concentration would yield a straight-line (Nernstian) plot if the electrode was perfectly selective to the primary ion. The slope of the plot would be 61.5 mV or 58.5 mV for a 10-fold increase in concentration of a monovalent primary ion, at 37.5 and 25°C respectively. An ideal electrode for a divalent primary ion would generate a 31.5 mV and 28.5 mV increase over a 10-fold increase in concentration of the primary ion, at 37.5 and 25°C respectively.

However at lower concentrations of the primary ion, ion-selective electrode responses deviate from such a linear response as evidenced by a reduction of slope. This is due to significant effects of other, interferent, ions on the electrode response, the effect of which is to cause an apparent increase in the concentration of the primary ion in the electrode response. For accurate measurement of the primary ion concentration the magnitude of the interferent effect must be determined. This is achieved by estimation of the potentiometric selectivity coefficient,  $k_{ij}^{pot}$ , for each ion in conjunction with the Nikolsky equation.

There are two standard methods for the estimation of  $k_{ij}^{pot}$  values: the separate solution method (SSM) and the fixed interference method (FIM).

1. Separate solution method: this compares the p.d. generated by a pure solution of the primary ion,  $E_i$ , with the p.d. generated by a pure solution of the interferent ion,  $E_j$ .

The selectivity coefficient is then calculated from the Nikolsky equation:

$$k_{ij}^{pot} = 10^{\frac{(E_i - E_j)z_i F}{2.303RT}} \frac{a_i}{(a_j)^{z_i/z_j}} \quad 4$$

This method is not the method of choice since the concentration of the interferent ion and concentration of the primary ion may be quite different in biological solutions.

2. Fixed interference method: this is the method recommended by the International Union of Physical and Applied Chemistry (IUPAC) for determining selectivity coefficients ( $k_{ij}^{pot}$ ) of interferent ions. The concentration of the interferent ion is kept constant and the response of the ion-selective electrode to varying concentrations of the primary ion is measured. In effect, the ion-selective electrode is calibrated in a background solution that has a constant concentration of interferent ion. This is the recommended method since the chosen concentrations of the primary and interferent ions can be similar to the concentrations found in biological solutions.

Figure 2.3 shows a calibration curve of an ion-selective electrode in a background solution with a particular concentration of interferent ion. At higher concentrations of the primary ion,  $i$ , the calibration curve approaches a Nernstian straight line with a slope  $RT/z_i F$ . At the lowest concentrations of the primary ion, the calibration curve approaches

a horizontal line, because the fixed concentration of the interferent ion contributes more than the primary ion in generating the resultant p.d. At intermediate primary ion concentrations the slope of the plot is between these two extremes. At a certain primary ion concentration the slope is half the predicted Nernstian value, i.e. the primary ion and the interferent ion both contribute equally to the ion-selective electrode p.d. This concentration of the primary ion is known as the limit of detection and may be obtained by extrapolating the two linear sections of the calibration curve to the concentration at which they meet. At this point, where  $E_i=E_j$ , then the Nikolsky equation reduces to:

$$k_{ij}^{pot} = \frac{a_i}{(a_j)^{z_i/z_j}} \quad 5$$

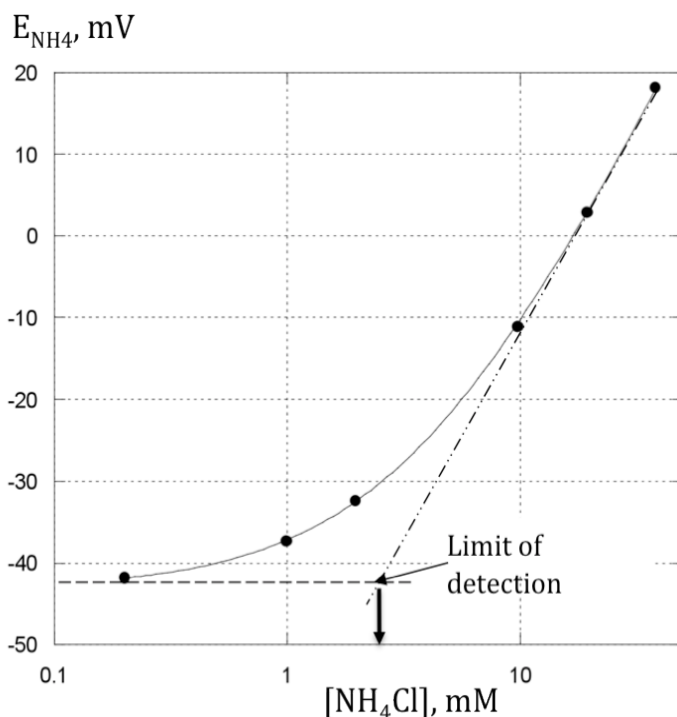


Figure 2.3: Sample calibration curve for an  $\text{NH}_4^+$ -selective electrode, calibrated in a solution of 140 mM NaCl + 25 mM KCl. The horizontal hashed line corresponds to the horizontal section of the curve and the diagonal line to the Nernstian slope at higher  $[\text{NH}_4^+]$ . The concentration where the two hashed lines meet is the limit of detection.

2.5.3 Experimental protocol for calculating potentiometric selectivity coefficients,  $k_{ij}^{pot}$  for an ion-selective electrode:

The general method will use the example for a  $\text{NH}_4^+$ -selective electrode. Specific variations for other ion-selective electrodes will be enunciated later. Note that although the Nikolsky equation uses values for ion activity,  $a$ , for practical purposes the concentration,  $c$ , of primary and interferent ions are used for the calculation of  $k_{ij}^{pot}$  values. This does not reduce the generality of the situation assuming that the relationship between ion activity and concentration remains unchanged (see section 2.5.2).

The electrode was calibrated in known concentrations of each potential interferent ion in a base solution of 140 mM NaCl, 10 mM HEPES, adjusted to pH 6 with NaOH, i.e. the total  $[\text{Na}^+]$  was approximately 150 mM. In the first instance calibration was carried out in the base solution to estimate the interference from  $\text{Na}^+$ . Next another potential interferent cation of known final concentration was added, as the  $\text{Cl}^-$  salt, to this background solution. The ion-selective electrode was then re-calibrated.

The Nikolsky equation assumes that each interferent ion is transported independently of others. Thus, the  $k_{ij}^{pot}$  values for separate interferent ions are linearly independent, i.e. the term  $k_{ik}^{pot} a_k + k_{il}^{pot} a_l + k_{im}^{pot} a_m \dots$  may be calculated from the calibration curve, where  $k$ ,  $m$ ,  $n$  represent different interferent ions.

Thus, data from the calibration curves were fitted to the general equation.

$$E = m_1 + s \log(c_i + m_2) \quad 6$$

where  $E$  is the recorded p.d.;  $c_i$  is the concentration of the primary ion;  $m_1$  is a constant equivalent to  $E^0$ , and  $m_2$  is a constant equivalent to  $\sum_{j=k,l,m,\dots} k_{ij}^{pot} c_j$ . Thus, calibration in the base solution yielded a value for  $m_2 = k_{iNa}^{pot} c_{Na}$  and subsequent calibrations in solutions of further interferent ions enabled  $k_{ij}^{pot}$  values for these ions also to be calculated.

For the  $\text{NH}_4^+$ -ion-selective electrode the major potential interferent was  $\text{K}^+$  and calibrations of these electrodes were repeated in four different  $\text{K}^+$  concentrations (2 mM, 5 mM, 25 mM and 50 mM).  $\text{Ca}^{2+}$  interference was evaluated by calibrating the electrode in a background solution containing 2 mM and 5 mM  $\text{CaCl}_2$  (experiments were repeated three times for each concentration of  $\text{Ca}^{2+}$ ). The quantities of solution added to produce the concentrations of the interferent ions in the background 140mM NaCl solution is shown in Table 2.4.

Table 2.4 Composition of solutions for determination of potentiometric selectivity coefficients for  $\text{NH}_4^+$ -selective electrodes.

Interferent ion	Solution added to 140mM NaCl	Concentration of interferent ion achieved in chamber (mM)
$\text{Na}^+$	-	140 mM
$\text{K}^+$	8 $\mu\text{l}$ 1 M KCl	2 mM
	20 $\mu\text{l}$ 1 M KCl	5 mM
	100 $\mu\text{l}$ 1 M KCl	25 mM
	200 $\mu\text{l}$ 1 M KCl	50 mM
$\text{Ca}^{2+}$	8 $\mu\text{l}$ 1 M $\text{CaCl}_2$	2 mM
	20 $\mu\text{l}$ 1 M $\text{CaCl}_2$	5 mM

A similar protocol was used to measure the potentiometric selectivity coefficients for  $K^+$ ,  $Mg^{2+}$ , and  $Ca^{2+}$ -selective electrodes.

For  $K^+$ -selective electrodes calibration was carried out in additional  $Mg^{2+}$ -containing solution (2 mM) and  $NH_4Cl$  (25 and 50 mM).

For  $Mg^{2+}$ -selective electrodes the most serious interferent ion was  $Ca^{2+}$ . Electrodes were calibrated first in 140 mM  $NaCl$ /10 mM HEPES (pH 6.0) and then in additional 1 mM  $CaCl_2$  solution.

For  $Ca^{2+}$ -selective electrodes calibration was carried out in additional K-containing solution (50-200 mM) and  $NH_4Cl$  (40 mM).

#### 2.5.4 Effect of pH on ion-selective responses:

Potentiometric selectivity coefficients were not calculated for  $H^+$  as above due to the low concentration of  $[H^+]$  and the fact that due to large concentrations of  $H^+$  buffers this ion was not in simple equilibrium with the ion-selective electrode.

Electrodes were calibrated in solutions of varying pH over a range likely to be encountered during experiments. The three chosen solutions were: 140 mM  $NaCl$ /10 mM HEPES adjusted to pH 7.5; 140 mM  $NaCl$ /10 mM HEPES adjusted to pH 6.5; 140 mM  $NaCl$ /10 mM MES adjusted to pH 5.5.

Note: MES; 2-(N-morpholino)ethanesulfonic acid  
HEPES; (4-(2-hydroxyethyl)-1-piperazineethanesulfonic acid)

### 2.5.2 The effects of altered osmolality on ion-selective electrode responses:

Because the osmolality of urine varies several-fold and thus might cause water fluxes across the ion-selective layer, it was important to determine any effect such solutions may have on electrode responses.

The  $\text{NH}_4^+$  ion-selective electrode was calibrated in a variety of solutions to examine the effects of osmolality on response. To increase the osmolality of the solution without increasing the ionic activity of the solution, sucrose was chosen since it is an unionised in solution. The protocol used and the effect on osmolality is shown in Table 2.5. Experiments were repeated three times for each solution and conducted at room temperature.

Table 2.5. Solution composition to test the effect of changes to solution osmolality on ion-selective electrode response.

Background Solution (mM)	Sucrose Conc (mM)	Total Osmolality (mOsm)	Effects on resultant solution
150 mM NaCl	-	300	N $\text{Na}^+$ / N Osm
50 mM NaCl	-	100	$\downarrow \text{Na}^+$ / $\downarrow$ Osm
300 mM NaCl	-	600	$\uparrow \text{Na}^+$ / $\uparrow$ Osm
150 mM NaCl	300 mM	600	N $\text{Na}^+$ / $\uparrow$ Osm
50 mM NaCl	200 mM	300	$\downarrow \text{Na}^+$ / N Osm

2.5.3 Effect of temperature on ion-selective  $\text{NH}_4^+$  and  $\text{K}^+$ -selective electrode responses:  $\text{NH}_4^+$ -selective electrodes were calibrated in a solution of 140 mM NaCl and 10 mM MES, which was adjusted to pH 6.0. Experiments were repeated 24 times at 37°C and compared with 40 calibrations of the electrode in a similar solution at room temperature.

Because  $\text{K}^+$  was the major interferent ion on the  $\text{NH}_4^+$ -selective electrodes they were calibrated in four different  $\text{K}^+$  concentrations (2 mM, 5 mM, 25 mM and 50 mM) at 37°C to calculate the  $k_{\text{NH}_4^+\text{K}}$  selectivity coefficient at this temperature.

$\text{K}^+$ -selective electrodes were also calibrated in 140 mM NaCl/10 mM MES (pH 6.0) at 37°C and compared to responses obtained at room temperature.

## 2.6 EXPERIMENTAL PROTOCOLS

2.6.1 Estimation of urinary  $[\text{NH}_4^+]$ .

2.6.1.1 Measurements from the  $\text{NH}_4^+$ -selective electrode.

The experimental chamber was first cleaned thoroughly with three washouts of deionised water and the  $\text{NH}_4^+$ -selective electrode was set up as described above (section 2.3.7). The electrode was then calibrated in a background solution of 150 mM NaCl or 140 mM NaCl/10 mM MES (pH 6): this was repeated three times until the calibration curves were similar. The chamber was washed out between calibrations with water and prior to urinary testing.

To measure urinary  $[\text{NH}_4^+]$ , a 4-ml aliquot of urine was accurately instilled into the chamber through the top and the system allowed to equilibrate. The p.d. of the ion-selective/reference electrodes system was then recorded using the voltmeter at the existing pH. Control experiments showed that the pH of the urine sample was constant ( $\pm 0.02$  pH units) after voiding for up to three hours if the sample was kept in tightly-stoppered plastic bottles and stored at  $4^\circ\text{C}$ . Henceforth this pH will be called voided pH. After recording the readings with urine the chamber was then washed out three times with deionised water prior to testing the next urine sample. The electrode was then re-calibrated after three urinary samples had been tested.

Drift within the system was seen as a gradual change in the p.d. recorded in a solution containing a constant concentration of the primary ion. There was little drift within the system, but if it was present then a systematic examination of the experimental setup was undertaken to identify the cause. Firstly, connections between Ag/AgCl electrodes and recording wires were checked and these electrodes were changed. If the drift persisted the ion-selective electrode or reference electrode or both were changed. These measures usually resolved any drift within the system. An electrode drift of less than 1.0 mV per hour was deemed acceptable for the  $\text{NH}_4^+$ -selective electrode, as the calibration and urine testing protocol was generally complete in 30 minutes.

#### 2.6.1.2 Measurement of urinary $[\text{K}^+]$

Because  $\text{K}^+$  ions caused significant interference with the  $\text{NH}_4^+$ -selective electrode, urinary  $[\text{K}^+]$  was measured separately with a valinomycin-based  $\text{K}^+$ -selective electrode. The interference from  $\text{NH}_4^+$  on this electrode was negligible (see Results) and hence the

[K<sup>+</sup>] could be measured accurately in the presence of a significant [NH<sub>4</sub><sup>+</sup>]. The method for measuring the urinary [K<sup>+</sup>] was the same as for measuring the urinary [NH<sub>4</sub><sup>+</sup>] (section 2.6.1.1).

Initially the estimation of urinary [NH<sub>4</sub><sup>+</sup>] and urinary [K<sup>+</sup>] was done separately: first the NH<sub>4</sub><sup>+</sup> electrode was calibrated, then the urine samples tested; second the K<sup>+</sup> electrode was calibrated and then the same urine samples tested. We later modified our technique and developed the following experimental arrangement to measure both ion concentrations simultaneously (Figure 2.4). This had several advantages:

- i) the time for the experimental protocol was shortened and hence minimised any problems of drift:
- ii) the same reference electrode was used at the same time to eliminate any systematic effect that urine samples may have had on the reference electrode potential.
- iii) the voided pH was the same for measurement of [NH<sub>4</sub><sup>+</sup>] and [K<sup>+</sup>] to avoid any possible effect of altered pH on these two ionic measurements.

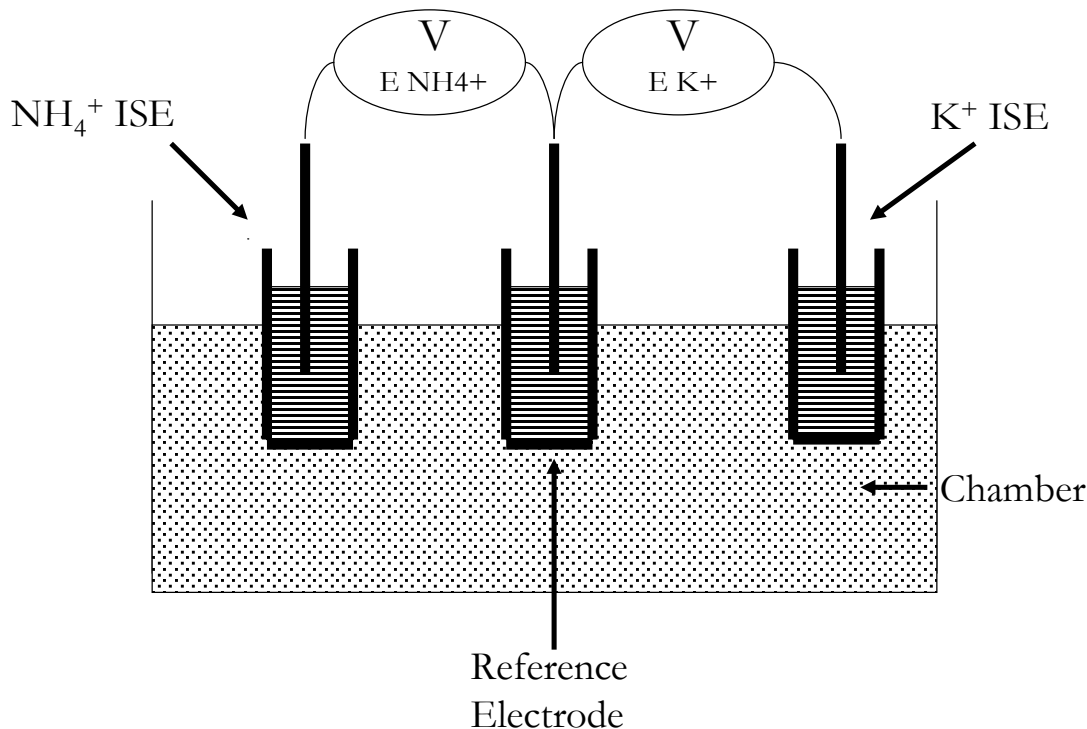


Figure 2.4: The experimental arrangement with two ion-selective electrodes in the chamber for simultaneous measurement of [NH<sub>4</sub><sup>+</sup>] and [K<sup>+</sup>].

#### 2.6.1.3 Protocol to measure urinary [NH<sub>4</sub><sup>+</sup>] from calibration curves:

- i) The mean calibration curve of the NH<sub>4</sub><sup>+</sup>-selective electrode was plotted (figure 2.5) and the potentiometric selectivity coefficient for Na<sup>+</sup>,  $k_{NH_4Na}^{pot}$ , estimated using equation 6 – section 2.5.3

$$E = m_1 + s \log(c_i + m_2) \quad 6$$

where the constant  $m_1$  is equivalent to the electrode constant,  $E^0$  and the constant  $m_2$  is equivalent to  $a_{Na} * k_{NH_4Na}^{pot}$ ; here  $a_{Na}$  was set at 150 mM. The term  $s$  is the slope factor of the electrode and was set to values of 58.5 or 61.5 (mV per 10-fold change of primary ion concentration) at room temperature and 37°C respectively.

ii) The  $E_{\text{NH}_4}$  reading from the  $\text{NH}_4^+$ -selective electrode when in the urine sample was converted to an equivalent  $[\text{NH}_4^+]$  (figure 2.5). This value will be an overestimate as the  $E_{\text{NH}_4}$  has a contribution from  $\text{Na}^+$  in the urine sample, and more significantly  $\text{K}^+$  in the sample.

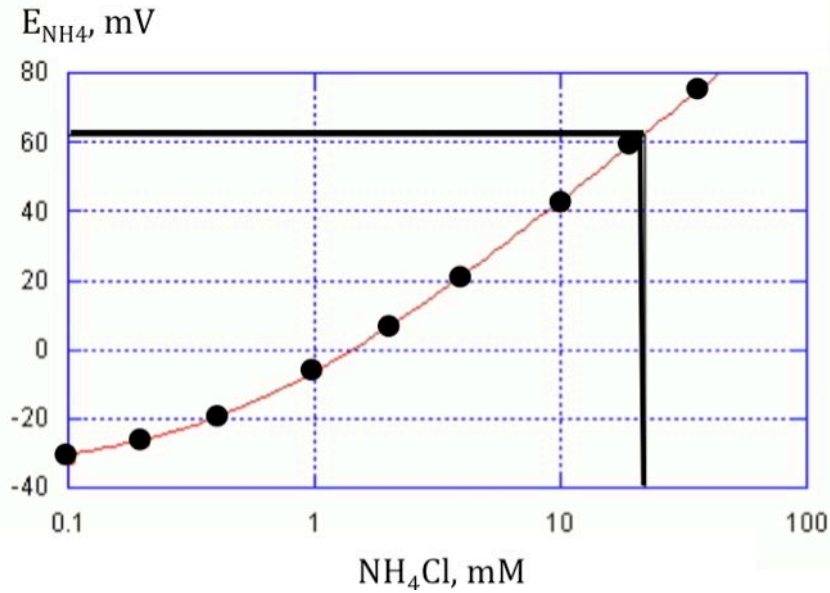


Figure 2.5. A sample calibration curve used to estimate the  $[\text{NH}_4^+]$  in a urine sample. The thick black horizontal line shows the  $E_{\text{NH}_4}$  value in the urine sample and the extension to the x-axis shows the uncorrected value of  $[\text{NH}_4^+]$  – see text for details.

- iii) The urine  $[\text{K}^+]$  was calculated from the  $\text{K}^+$ -selective electrode calibration curve.
- iv) The product  $a_{\text{K}} k_{\text{NH}_4\text{K}}^{\text{pot}}$  was calculated
- v) The Nikolsky equation was employed using terms for interferent ions only for  $\text{Na}^+$  and  $\text{K}^+$  and rearranged to yield a value for the  $a_{\text{NH}_4}$ .  $a_{\text{NH}_4}$  was made equivalent to  $[\text{NH}_4^+]$  according to section 2.5.1.

$$E_{\text{NH}_4} = E^0 + s \log(a_{\text{NH}_4} + k_{\text{NH}_4\text{Na}}^{\text{pot}} a_{\text{Na}} + k_{\text{NH}_4\text{K}}^{\text{pot}} a_{\text{K}}) \quad 7$$

re-arranging

$$a_{NH_4} = 10^{\frac{(E_{NH_4} - E^0)}{s}} - (k_{NH_4Na}^{pot} a_{Na} + k_{NH_4K}^{pot} a_K) \quad 7a$$

Values of  $[NH_4^+]$  were recorded along with the  $[K^+]$ , urine pH and temperature.

#### 2.6.1.4 Protocol to measure urinary $[Mg^{2+}]$ from calibration curves:

Exactly the same procedure was followed to calculate the  $[Mg^{2+}]$  in urine samples using  $Mg^{2+}$ -selective and  $Ca^{2+}$ -selective electrodes. In this case  $Ca^{2+}$  were the most serious interferent ion. In addition the slope factor,  $s$ , was divided by two as required for divalent ions.

#### 2.6.2 Effects of storage on urinary $[NH_4^+]$ :

Experimental protocol:

Urine samples from seven healthy subjects were used. A 20 ml sample was collected and divided into two 10 ml aliquots. One aliquot was tested immediately for urinary  $[NH_4^+]$  and  $[K^+]$  (designated time = 0), which were measured at room temperature. This 10 ml aliquot was then left on the bench at room temperature. The other 10 ml aliquot was frozen immediately to be tested after one week (designated time = 7 days).

The other 10 ml aliquot of urine, which was left on the bench, was tested for urinary  $[NH_4^+]$  and  $[K^+]$  after 1 hour, 2 hour and 7 days. This therefore permitted comparison of the urinary  $[NH_4^+]$  and  $[K^+]$  at time = 7 days between the sample left at room temperature and the sample which had been frozen. We were also able to assess the effects of freezing samples as a method of storage, by comparing the frozen sample urinary concentrations with the concentrations measured immediately after voiding at time = 0.

## 2.7 VALIDATION OF $\text{NH}_4^+$ -SELECTIVE ELECTRODE DATA AGAINST COLOUR SPECTROPHOTOMETRY

Urine samples were taken from 28 healthy subjects and were tested immediately for urinary  $[\text{NH}_4^+]$  and  $[\text{K}^+]$  using the respective ion-selective electrodes. At the same time, an aliquot of the urinary sample was stored in the freezer for testing at a later stage.

The values of urinary  $[\text{NH}_4^+]$  obtained using ISEs were compared to those using a conventional spectrophotometric assay on stored ( $-20^\circ\text{C}$ ) urine samples as above. Urinary  $[\text{NH}_4^+]$  was measured using a phenol-hypochlorite reaction detection method (Weatherburn, 1967). Urine samples were diluted (1/80) by the addition of trichloroacetic acid (15% final) and centrifuged at 10,000 rpm for 10 minutes at  $4^\circ\text{C}$  to remove any dissolved protein. The supernatant (50  $\mu\text{l}$ ) was incubated in a 96-well plate at  $30^\circ\text{C}$  for 3 hours in 200  $\mu\text{l}$  of a solution containing: phenol, 10 mM; Na hypochlorite, 10 mM; Na nitroprusside, 10 mM as a catalyst; and NaOH, 0.5 mM. Ammonium ions react with alkaline phenol to produce indophenol which has an intense blue color. The concentration was determined against a standard curve of  $\text{NH}_4\text{Cl}$  solutions over the range 5 – 200  $\mu\text{M}$  measured at 630 nm in a 96-well plate reader (Tecan Sunrise, Austria). All determinations were at  $25^\circ\text{C}$ .

## 2.8 ALGORITHM TO CALCULATE URINARY $[\text{NH}_4^+]$ .

The algorithm to estimate urinary  $[\text{NH}_4^+]$  is derived from calculation of the urinary anion gap (AG). The AG is calculated as the difference between the concentrations of the major cations ( $\text{Na}^+$  and  $\text{K}^+$ ) and the major anion ( $\text{Cl}^-$ ) (Hoge et al, 1974):

$$\text{Urine AG} = \text{Urine } (\text{Na}^+ + \text{K}^+ - \text{Cl}^-)$$

The urinary AG is used to help in the differential diagnosis of metabolic acidosis and is representative of the unmeasured ions in urine, the most important of which is  $\text{NH}_4^+$ .

In patients with a metabolic acidosis and a normal renal response, the urinary AG has a negative value, due to an increase of the urinary  $[\text{NH}_4^+]$ , as  $\text{NH}_4\text{Cl}$ , in order to excrete excess acid (Batlle et al. 1988). When patients are unable to excrete  $\text{NH}_4^+$  normally (e.g. renal failure, type 1 renal tubular acidosis), the urine AG has a positive value.

The urine  $[\text{NH}_4^+]$  can be estimated from calculation of the urine osmolal gap, which is the difference between the measured and calculated urine osmolality (Rose 1994). The calculation requires measurement of urine osmolality, the urine Na, K, urea nitrogen and glucose concentration (if dipstick positive for glucose). The calculated urine osmolality is then estimated:

$$\text{Calculated urine osmolality} = 2([\text{Na}] + [\text{K}]) + \frac{\text{urea nitrogen}}{2.8} + \frac{\text{glucose}}{18}$$

The multiple of 2 accounts for anions accompanying Na and K, and the divisors 2.8 and 18 reflect adjustments required to convert from routinely used units of mg/dl to mmol/l or mosmol/kg. The osmolal gap is then estimated:

$$\text{Osmolal gap} = \text{Measured osmolality} - \text{Calculated osmolality.}$$

The osmolal gap then approximates the concentration of ammonium salts and the  $[\text{NH}_4^+]$  itself will be half of this value, as the other half are anions accompanying  $\text{NH}_4^+$ . Thus,

$$\text{Urine } [\text{NH}_4^+] = 0.5 * \left( \text{Measured osmolality} - 2([\text{Na}] + [\text{K}]) + \frac{\text{urea}}{2.8} + \frac{\text{glucose}}{18} \right)$$

There are several variants for this calculation and the one used at the Royal Free Hospital, London, in the recurrent stone former clinic is:

$$\text{Urine } [\text{NH}_4^+] = 0.5 * (\text{Measured osmolality} - 2([\text{Na}] + [\text{K}]) + \text{urea})$$

We collected urine samples from patients attending the Renal Stone Clinic at the Royal Free Hospital. We calculated the urinary  $[\text{NH}_4^+]$  using the above formula, from the urinary Na, K, urea and osmolality. We also independently measured the urinary  $[\text{NH}_4^+]$  using the ISE technique so that a comparison could be made between the two methods for measuring urinary  $[\text{NH}_4^+]$ .

## 2.9 DATA PRESENTATION AND STATISTICAL ANALYSIS

Data are presented as mean values  $\pm$  standard deviation (SD), except in a number of cases specifically mentioned where median values and 25% and 75% interquartile ranges are quoted.

Comparison of two data sets was carried out using Student's *t*-test. When median values are quoted, comparison of data sets used a non-parametric Wilcoxon's test. For comparison of multiple data sets, analysis of variance was used. The null hypothesis was rejected when  $p < 0.05$ .

Curve-fitting of data sets to described functions used an iterative least-squares method with the program Kaleidagraph (Synergy software Inc). This program permitted writing the fitting function with an independent variable output in terms of a dependent variable and a number of parameters that used initial estimates. All functions are described in the text (Methods and Results chapters).

## CHAPTER 3

### RESULTS:

#### 3.1 Calibration of the $\text{NH}_4^+$ -selective electrode

Typical calibration data for the  $\text{NH}_4^+$ -selective electrode in 140 mM NaCl buffered to pH 6.0 with 10 mM MES is shown in Table 3.1. The table shows the nominal and calculated  $\text{NH}_4\text{Cl}$  concentration. The latter was calculated after consideration of the increased chamber volume following addition of the  $\text{NH}_4\text{Cl}$  aliquot. The corresponding calibration curve is displayed in Figure 3.1, below. All calibrations were performed at room temperature.

##### 3.1.1 Selectivity and sensitivity of the $\text{NH}_4^+$ -selective electrode:

The presence of other ions within a solution can affect the electrode response, and if significant will diminish the response of the electrode to the primary ion. Therefore the potentiometric selectivity coefficient  $k_{ij}^{\text{pot}}$  was determined experimentally for each possible interferent ion present in urine. This was performed using the fixed interference method described in the Methods. In figure 3.1 the data were fitted to the modified Nikolsky equation (equation 6, section 2.5.3):

$$E = m_1 + s \log(c_i + m_2) \quad 6$$

this allowed estimation of the potentiometric selectivity coefficient,  $k$ . In this case the only major interferent ion was  $\text{Na}^+$ . The value of the slope constant  $s$  was 58.5 mV per 10-fold change of  $[\text{NH}_4^+]$  and thus  $k$  is equivalent to  $k_{\text{NH}_4^+\text{Na}^+}^{\text{pot}}$ : in this example the value was 0.00247.

Table 3.1 Typical  $\text{NH}_4^+$ -selective electrode calibration data in a base solution of 140 mM NaCl, 10 mM MES solution (pH 6.0).  $\text{NH}_4\text{Cl}$  was added in aliquots to the base solution from a 0.1 or 1 M stock solution (section 2.4.3).

Nominal $[\text{NH}_4^+]$ (mM)	Actual $[\text{NH}_4^+]$ in the chamber (mM)	E $\text{NH}_4^+$ (mV)
0.100	0.100	-67.6
0.200	0.200	-62.0
0.400	0.398	-53.6
1.00	0.99	-38.3
2.00	1.96	-24.2
4.00	3.91	-10.4
10.0	9.73	12.0
20.0	19.3	29.0
30.0	28.6	38.7
40.0	37.8	45.6

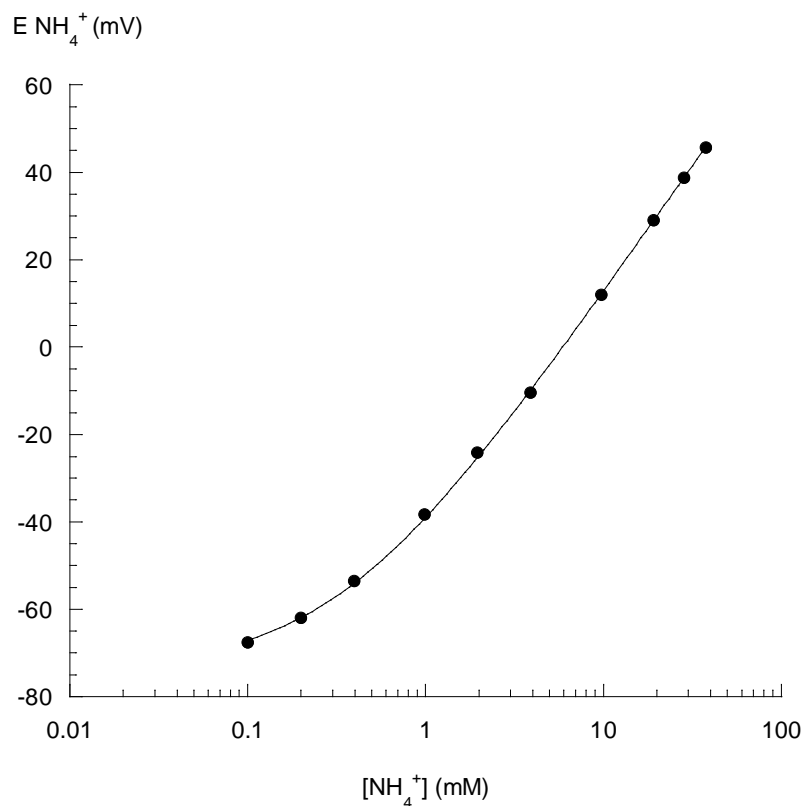


Figure 3.1. Typical calibration curve of a  $\text{NH}_4^+$ -selective electrode in 140 mM NaCl and 10 mM MES at pH 6.0. The total  $[\text{NH}_4^+]$  following each addition is plotted against the p.d. produced by the ion-selective/reference electrode pair, henceforth referred to as ISE. The line was fitted to the Nikolsky equation, see text for details:  $E_{\text{NH}_4} = E^0 + s \log_{10}([\text{NH}_4^+] + k)$  where the slope factor  $s=58.5$  mV per 10 fold change of  $[\text{NH}_4\text{Cl}]$ .

The ISE response to  $\text{NH}_4^+$  was good (i.e. roughly linear using the axes scale in Figure 3.1) in this base solution above a concentration of 1 mM.

Quantification of the interference from different ions on the ISE response permitted significant interferent ions to be identified. The concentration of these ions was

subsequently measured to allow subtraction of their influence on the  $\text{NH}_4^+$ -selective ISE response for each urine solution tested and thus permit evaluation of the true concentration of  $\text{NH}_4^+$ . The approach was to utilise the full Nikolsky equation - equation 3, section 2.5.2:

$$E_{\text{NH}_4} = E^0 + s \log_{10} (a_i + k_{ij}^{\text{pot}} (a_j)^{z_i/z_j} + k_{ik}^{\text{pot}} (a_k)^{z_i/z_k} \dots) \quad 3$$

where  $E^0$  is the constant;  $a_i$  is the concentration of the primary ion,  $\text{NH}_4^+$ ;  $a_j, a_k, \dots$  the concentrations of interferent ions; and  $k_{ij}^{\text{pot}}, k_{ik}^{\text{pot}}, \dots$  the selectivity coefficients of the respective interferent ions. The value of the selectivity coefficient can then be calculated from fitting the data to equation 3 using the calibration curve data as exemplified in Figure 3.1. For several interferent ions the value of one, say  $k_{ij}^{\text{pot}}$ , may first be calculated alone and then added to equation 3 for estimation of subsequent coefficients. Note: concentration values rather than activities,  $a$ , for each are used throughout - see Methods - and assumes that changes in the relationship between activity and coefficient is unaltered in any of the test and calibration solutions.

The smaller the value of  $k_{ij}^{\text{pot}}$  then the less is the interference of that ion on the ISE response. For the  $\text{NH}_4^+$ -selective electrode, the interferent ions of most concern were  $\text{Na}^+, \text{K}^+, \text{Ca}^{2+}$  and  $\text{H}^+$ . We examined the individual and combined effects of each of these ions on the  $\text{NH}_4^+$ -selective electrode. The values of each  $k_{ij}^{\text{pot}}$  will be tabulated together after individual values have been evaluated. The  $k_{ij}^{\text{pot}}$  values henceforth will be quoted as  $-\log k_{ij}^{\text{pot}}$  values for convenience. For the  $k_{\text{NH}_4\text{Na}}^{\text{pot}}$  value of 0.00247 obtained from Figure 3.1, the  $\log k_{ij}^{\text{pot}}$  was -2.607. An interpretation of the  $k_{ij}^{\text{pot}}$  value may be obtained from its

reciprocal, in this instance with a value of 404.9; this means the electrode is about 405-times more sensitive to  $\text{NH}_4^+$  than  $\text{Na}^+$ . For some interferent ions, because their influence on the ion-selective electrode was so small, it was not always possible to calculate a  $k_{ij}^{\text{pot}}$  value and hence in these experiments interference was described as ‘not detectable’.

### 3.1.2 $\text{Na}^+$ interference:

All calibration curves were performed in a background solution containing 140 mM NaCl +10 mM MES (at pH 6.0) –referred to as the baseline solution. Because  $\text{Na}^+$  was the predominant cation in all the calibration curves, the initial calibration was performed in the baseline solution to calculate the interference from  $\text{Na}^+$ , i.e. estimate  $\log k_{\text{NH}_4\text{Na}}^{\text{pot}}$ . This mean value was then substituted into the Nikolsky-Eisenmann equation 3 to permit calculation of the potentiometric selectivity coefficients of other interferent ions. From 40 determinations a value for  $\log k_{\text{NH}_4\text{Na}}^{\text{pot}}$  of  $-2.61 \pm 0.11$  was obtained. Where error bars have been included in the following figures, they may be too small to be visible.

### 3.1.3 $\text{K}^+$ interference:

Because  $\text{K}^+$  caused the greatest interference, the  $\text{NH}_4^+$ -selective electrode was tested in base solutions containing four different concentrations of KCl: 2, 5, 25 and 50 mM, to determine if the  $k_{\text{NH}_4\text{K}}^{\text{pot}}$  value itself was independent of the  $[\text{K}^+]$ . Ten  $\text{NH}_4^+$ -selective electrodes were calibrated in each of the four solutions, as well as the base solution, to calculate a mean  $\log k_{\text{NH}_4\text{K}}^{\text{pot}}$  for each concentration; the values are displayed in Table 3.2.

Figure 3.2 shows calibration curves in 2 and 5 mM KCl; figure 3.3 shows curves in 25 and 50 mM KCl; figure 3.4 combines curves from all KCl concentrations. Each calibration curve was normalised to 0 mV for the reading in 40 mM NH<sub>4</sub>Cl. The deviation from a relatively linear calibration curve in a zero-KCl solution, using the semi logarithmic axes as shown, was increasingly significant as the [K<sup>+</sup>] increased.

Table 3.2 shows that  $k_{NH_4K}^{pot}$  values were independent of the [K<sup>+</sup>], yielding a mean value of 0.141. This value was inserted into the Nikolsky equation with the appropriate [K<sup>+</sup>] for each urine sample for the determination of the true [NH<sub>4</sub><sup>+</sup>] in K<sup>+</sup>-containing urine.

Table 3.2. K<sup>+</sup> potentiometric selectivity coefficients of NH<sub>4</sub><sup>+</sup>-selective electrodes in the base-solution with varying background concentrations of K<sup>+</sup>.

[K <sup>+</sup> ]	NH <sub>4</sub> <sup>+</sup> -ISE (room temperature)			
	Mean log $k_{NH_4K}^{pot}$	Mean $k_{NH_4K}^{pot}$	Mean $k_{NH_4K}^{pot}$	Overall Mean $k_{NH_4K}^{pot}$
2mM	-0.84 ± 0.038	0.143	0.140	0.141
5mM	-0.86 ± 0.029	0.137		
25mM	-0.85 ± 0.010	0.141	0.141	
50mM	-0.85 ± 0.007	0.142		

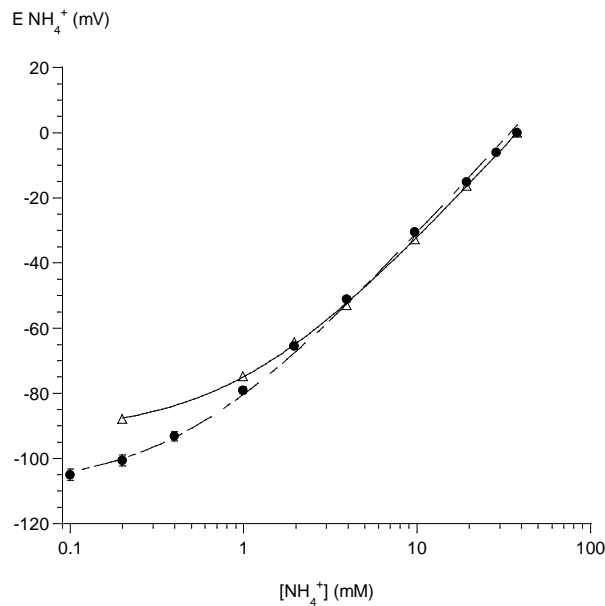
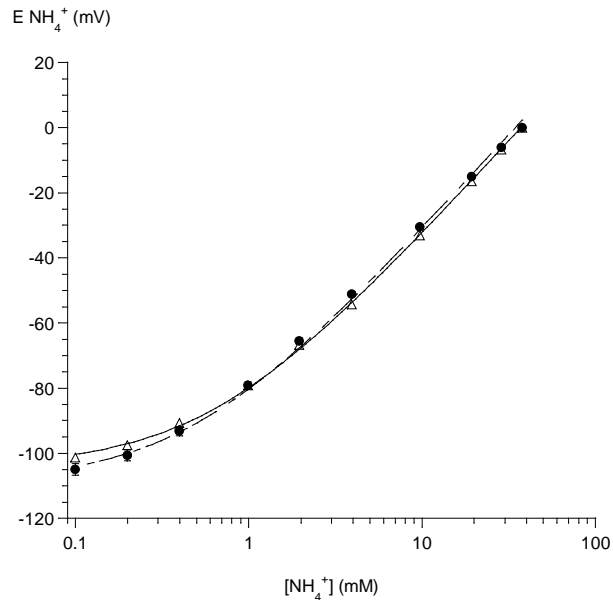


Figure 3.2. Calibration curves of an  $\text{NH}_4^+$ -selective electrode in a solution containing 140 mM NaCl + 10 mM MES + 2 mM KCl (upper graph), 140 mM NaCl + 10 mM MES + 5 mM KCl (lower graph). The closed circles represent determinations in base solution, the open triangles in the K-containing base solution. Individual calibration curves were normalized to 0 mV for the reading in 40 mM  $\text{NH}_4\text{Cl}$ . All solutions were at pH 6.0. Error bars have been added to calibration curves in base solution for both graphs.

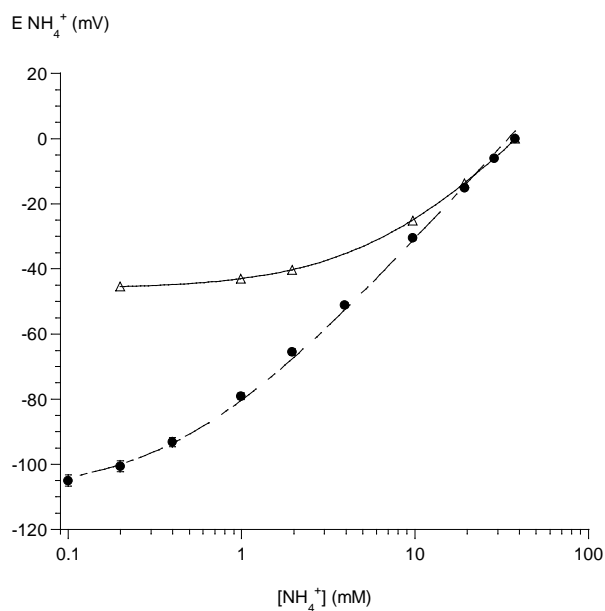
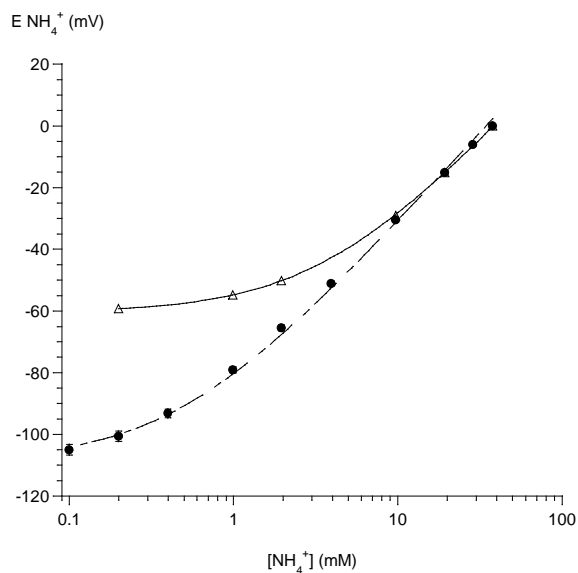


Figure 3.3. Calibration curves of an  $\text{NH}_4^+$ -selective electrode in a solution containing 140 mM NaCl + 10 mM MES + 25 mM KCl (upper graph), 140 mM NaCl + 10 mM MES + 50 mM KCl (lower graph). The closed circles represent determinations in base solution, the open triangles in the K-containing base solution. Individual calibration curves were normalized to 0 mV for the reading in 40 mM  $\text{NH}_4\text{Cl}$ . All solutions were at pH 6.0. Error bars have been added to calibration curves in base solution for both graphs.

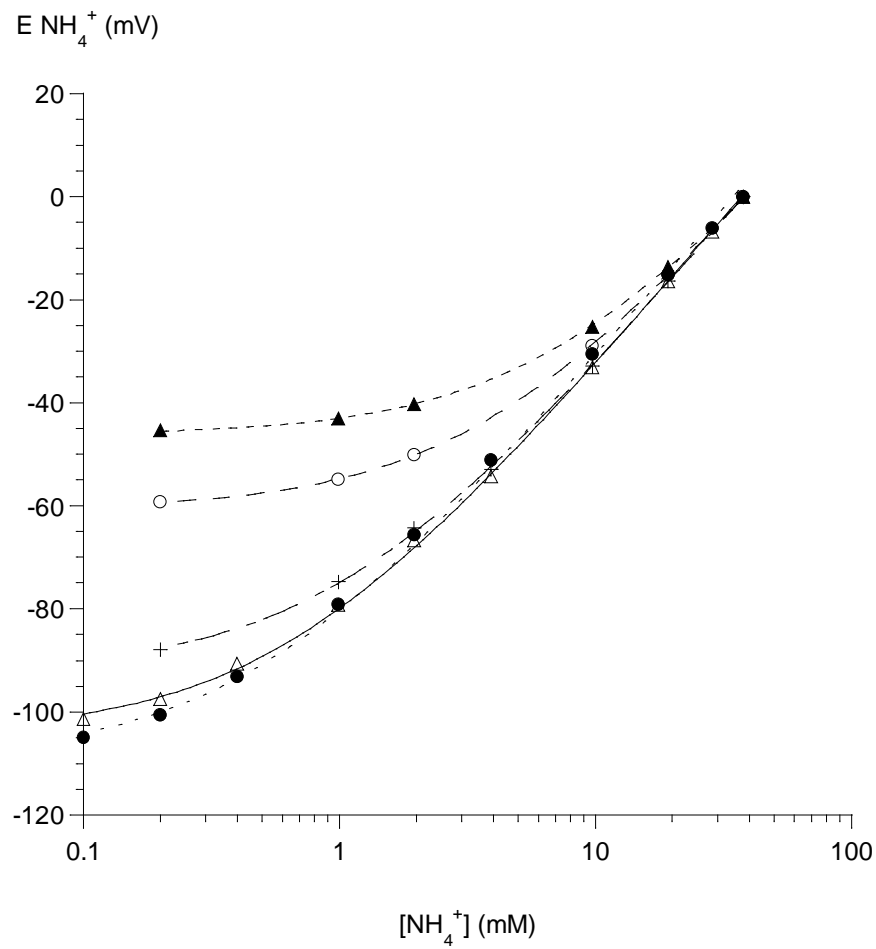


Figure 3.4. Calibration curves of the  $\text{NH}_4^+$ -selective electrode in the following solutions: 140 mM NaCl + 10 mM MES + 2 mM KCl (open triangles), 140 mM NaCl + 10 mM MES + 5 mM KCl (crosses), 140 mM NaCl + 10 mM MES + 25 mM KCl (open circles), 140 mM NaCl + 10 mM MES + 50 mM KCl (closed triangles). Each determination was performed 10 times, error omitted for clarity. The open circles were data obtained in base solution, 140 mM NaCl + 10 mM MES. The individual calibration curves were normalized to 0 mV for the reading in 40 mM  $\text{NH}_4\text{Cl}$ . All solutions were at pH 6.0.

### 3.1.4 Ca<sup>2+</sup> interference:

The NH<sub>4</sub><sup>+</sup>-selective electrode was calibrated in base solution containing either 2 mM or 5 mM CaCl<sub>2</sub>. The resulting mean calibration curves (n=3) for the two concentrations of Ca<sup>2+</sup> are shown in Figure 3.5. There was no significant effect on the calibration curve in base solution. Thus, there was no detectable interference from Ca<sup>2+</sup> on the NH<sub>4</sub><sup>+</sup>-selective electrode.

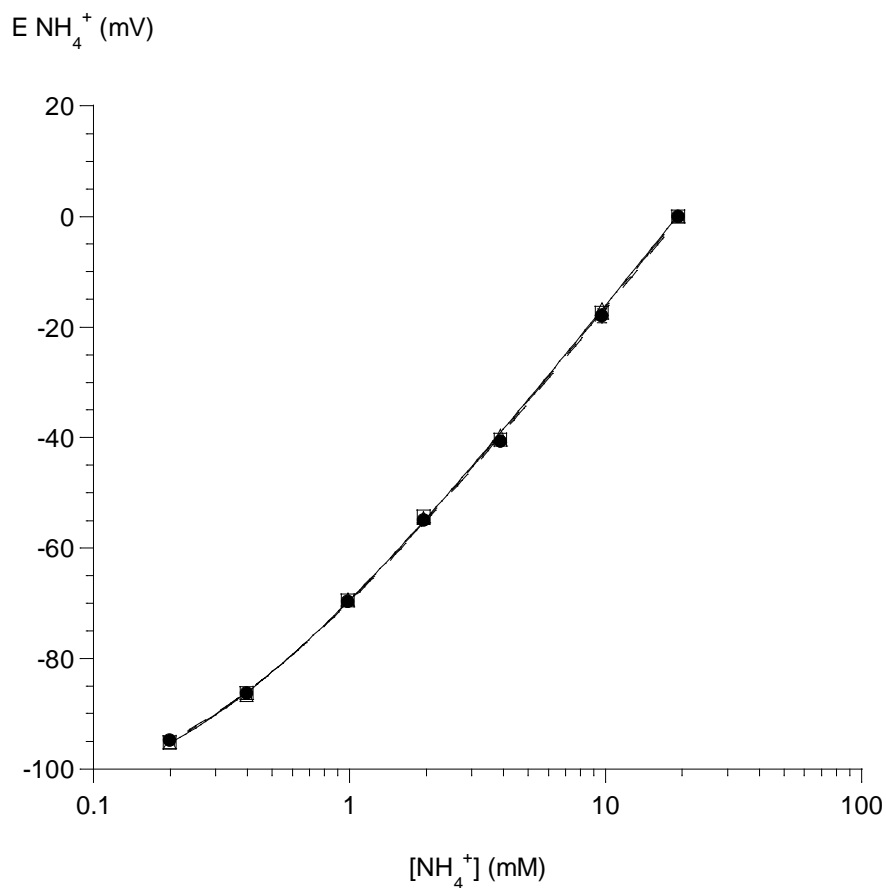


Figure 3.5. Calibration curves of the NH<sub>4</sub><sup>+</sup>-selective electrode in base solution (closed circles), base solution with 2 mM CaCl<sub>2</sub> (open triangles) and base solution with 5 mM CaCl<sub>2</sub> (open squares). Each determination was performed 3 times, error bars refer to data in base solution.

### 3.1.5 H<sup>+</sup> ion interference:

There was no detectable interference caused by H<sup>+</sup> ions on the NH<sub>4</sub><sup>+</sup>-selective electrode when the electrode was calibrated in three solutions of varying pH: 140 mM NaCl + 10 mM HEPES (pH 7.5), 140 mM NaCl + 10 mM HEPES (pH 6.5), and 140 mM NaCl + 10 mM MES (pH 5.5). The mean calibration curve for each pH is shown in Figure 3.6. All three calibration curves were not distinguishable from that in base solution (pH 6.0).

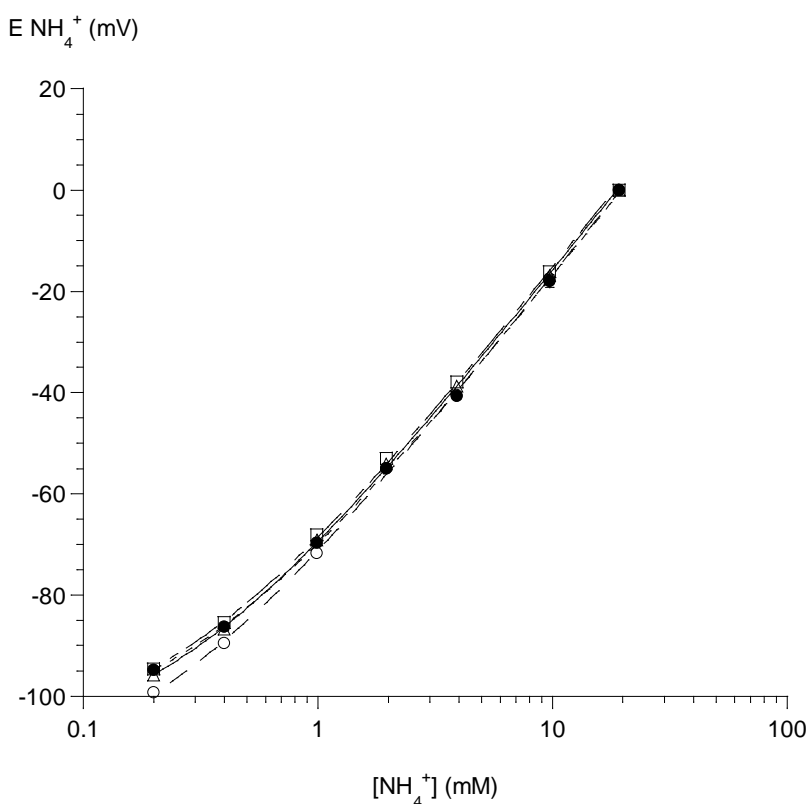


Figure 3.6. Calibration curves for the NH<sub>4</sub><sup>+</sup>-selective electrode in base solution (pH 6.0), 140 mM NaCl + 10 mM HEPES (pH 7.5, open triangles), 140 mM NaCl + 10 mM HEPES (pH 6.5, open squares) and 140 mM NaCl + 10 mM MES (pH 5.5, open circles). Each determination was performed 3 times. Error bars refer to data in the base solution.

Any pH-dependence was also examined in a K-containing solution to reflect more closely the situation in urine. Figure 3.7 shows in a solution containing 10 mM KCl there was also negligible interference from  $H^+$  over the same range of pH values from 5.5 to 7.5.

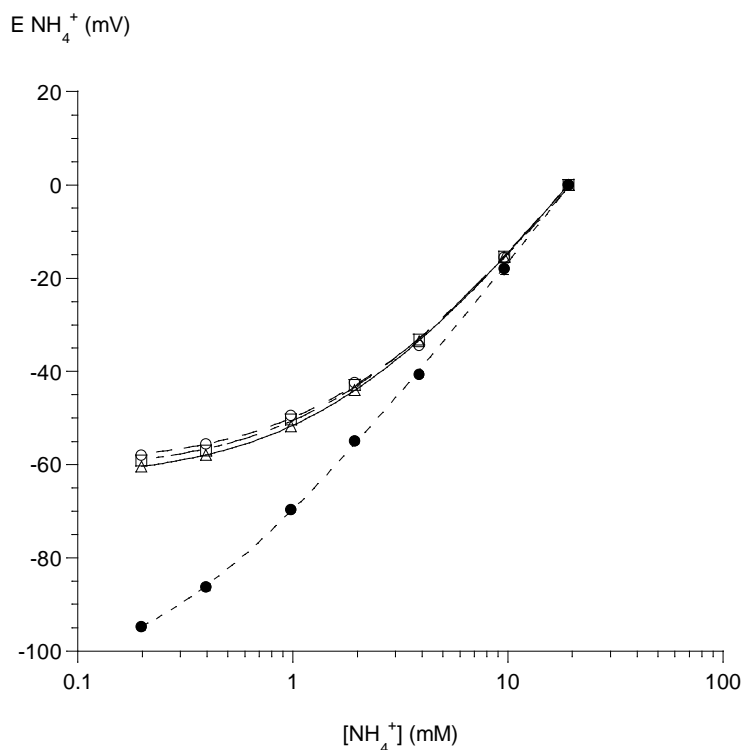


Figure 3.7. Calibration curves for the  $NH_4^+$ -selective electrode in a base solution containing 10 mM KCl and with pH varying from 5.5 to 7.5 using the same buffers as in Figure 3.6. Solutions were: pH 7.5 open triangles; pH 6.5 open squares; pH 5.5 open circles. Each determination was performed three times. Error bars refer to data in the base solution (pH 6.0 – no background KCl, closed circles).

Table 3.3 summarises the values of the potentiometric selectivity coefficients for the  $NH_4^+$ -selective ISE against potential interferent ions. It is seen that the  $NH_4^+$ -ISE has a 406-fold selectivity for  $NH_4^+$  over  $Na^+$ , and a 7-fold selectivity over  $K^+$ .

Table 3.3 Potentiometric selectivity coefficients for  $\text{NH}_4^+$  ion-selective electrodes against potential interferent ions, j, mean values  $\pm$ s.d. Values ( $\pm$ sd) for the  $\log k_{\text{NH}_4 j}^{\text{pot}}$ , as well as values of  $k_{\text{NH}_4 j}^{\text{pot}}$  and  $1/k_{\text{NH}_4 j}^{\text{pot}}$ , calculated from the mean  $\log k_{\text{NH}_4 j}^{\text{pot}}$  value. Not detectable means no significant deviation from the calibration in base solution alone was detected

Interferent ion	$\text{NH}_4^+$ -ISE (room temperature)		
	$\log k_{\text{NH}_4 j}^{\text{pot}}$	$k_{\text{NH}_4 j}^{\text{pot}}$	$1/k_{\text{NH}_4 j}^{\text{pot}}$
$\text{Na}^+$	$-2.61 \pm 0.11$	0.00247	405.5
$\text{K}^+$	$-0.85 \pm 0.0086$	0.141	7.1
$\text{H}^+$	not detectable	not detectable	-
$\text{Ca}^{2+}$	not detectable	not detectable	-

### 3.1.6 Determination of the effect of osmolality on the $\text{NH}_4^+$ -ISE response:

The osmolality and ionic strength of urine varies greatly. Therefore the sensitivity and selectivity of the  $\text{NH}_4^+$ -selective electrode was tested in solutions of varying osmolalities and differing ionic activities to determine if these affected the ISE response. This was done by estimating the potentiometric selectivity coefficient for  $\text{Na}^+$  (e.g.  $k_{\text{NH}_4 \text{Na}}^{\text{pot}}$ ), relative to the base-solution. Table 3.1.4 shows the solutions used for these experiments. A solution of low ionic strength and osmolality was achieved by replacing 150 mM NaCl with 50 mM NaCl in a base solution. A solution of normal osmolality but reduced ionic strength used a solution of 50 mM NaCl + 200 mM sucrose. Hyperosmolar solutions were achieved with addition to base solution of 300 mM sucrose (normal ionic strength) or a further 150 mM NaCl (raised ionic strength). Table 3.4 also shows the  $k_{\text{NH}_4 \text{Na}}^{\text{pot}}$  values (as  $\log k_{\text{NH}_4 \text{Na}}^{\text{pot}}$ ) in these various solutions. Figures 3.8 and 3.9 show calibration curves in

the different solutions. The values of  $\log k_{NH_4Na}^{pot}$  in the different solutions were not significantly different from the value in base solution and therefore it may be concluded that solution ionic strength and osmolality *per se* had no effect on the  $NH_4^+$ - selective ISE response.

Table 3.4: Values of  $\log k_{NH_4Na}^{pot}$  for the  $NH_4^+$ -selective electrode in solutions of varying osmolality and ionic activity

Solution	$\log k_{NH_4Na}^{pot}$
Base solution (150 mM Na)	-2.61±0.11
50 mM NaCl	-2.05 ± 0.13
50 mM NaCl + 200 mM Sucrose	-2.59 ± 0.07
300 mM NaCl	-2.77 ± 0.01
150 mM NaCl + 300 mM Sucrose	-2.77 ± 0.06

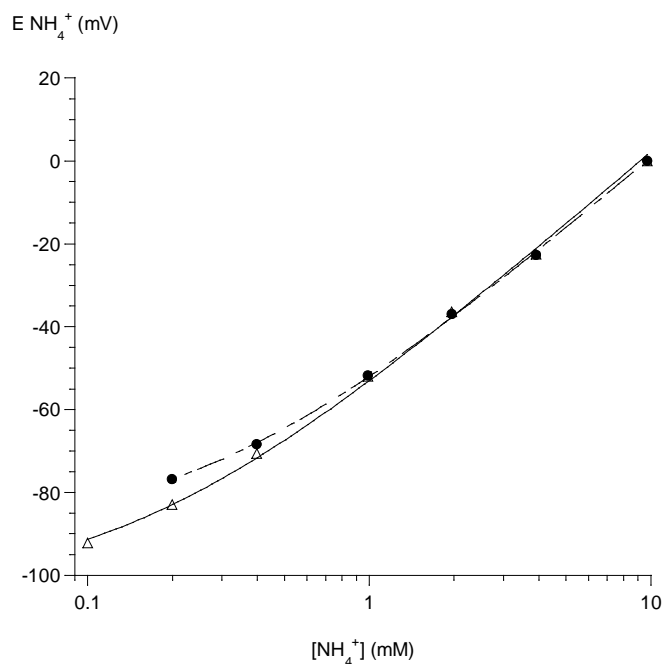
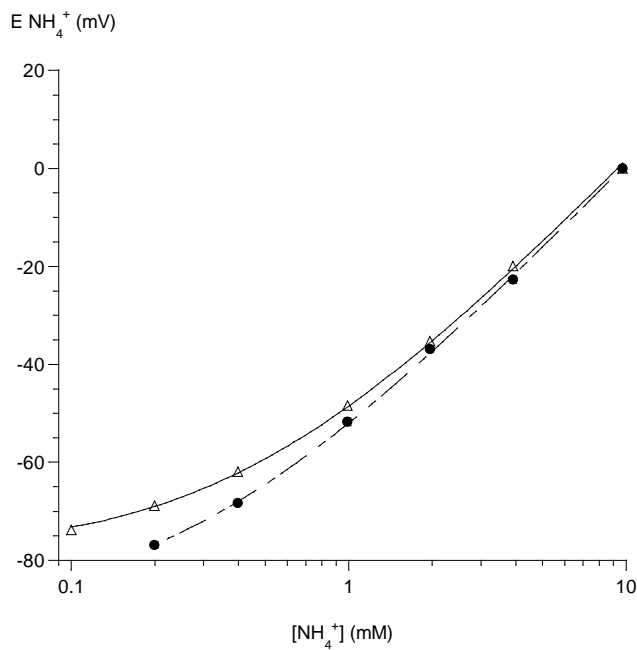


Figure 3.8. Calibration curves of the  $\text{NH}_4^+$ -selective electrode in: 50 mM NaCl (upper graph); 50 mM NaCl + 200 mM sucrose (lower graph) - open symbols - in comparison to base solution - closed symbols. All determinations were performed 3 times. Error bars refer to data from base solution.

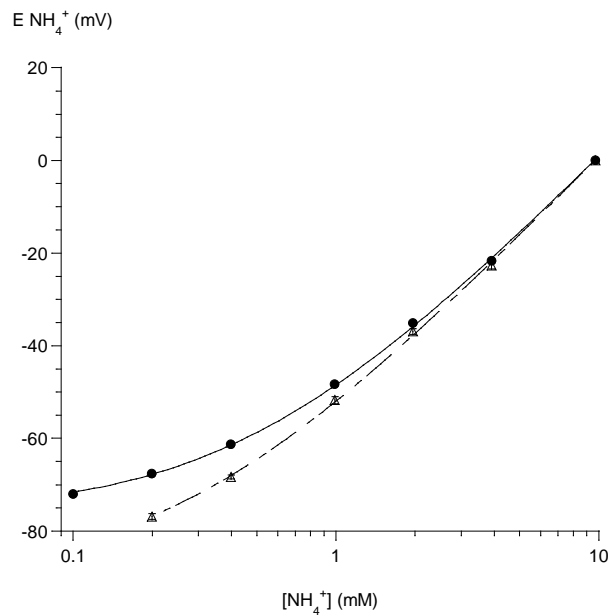
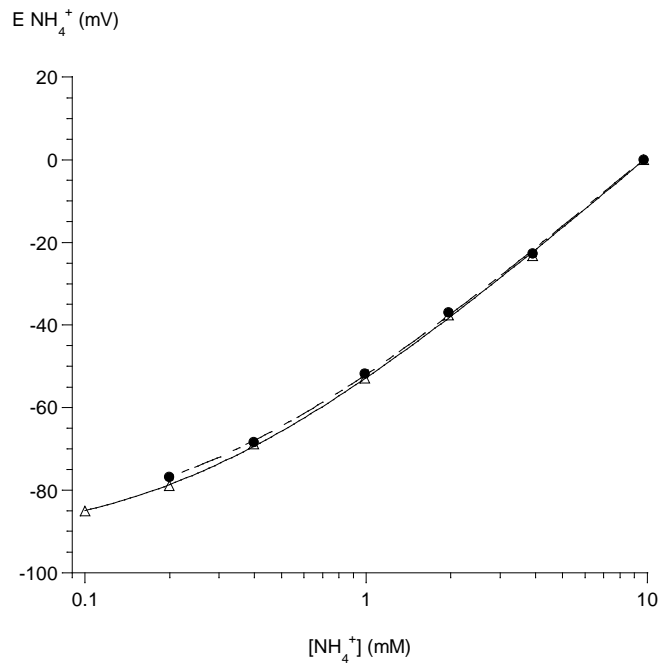


Figure 3.9. Calibration curves of the  $\text{NH}_4^+$ -selective electrode in: 150 mM NaCl + 300 mM sucrose (upper graph); 300mM NaCl only (lower graph) - open symbols - in comparison to base solution - closed symbols. All determinations were performed 3 times. Error bars refer to data from base solution.

### 3.2 Calibration of the K<sup>+</sup>-selective electrode:

Calibration of the K<sup>+</sup>-selective electrode was essential to determine if urinary [K<sup>+</sup>] could be measured sufficiently accurately to permit estimation of the [NH<sub>4</sub><sup>+</sup>] in the presence of interferent concentrations of K<sup>+</sup>.

#### 3.2.1 Calibration of K<sup>+</sup>-selective electrode:

Typical calibration data for a K<sup>+</sup>-selective electrode in 140 mM NaCl buffered to pH 6.0 with 10 mM MES is shown in table 3.5. The corresponding calibration curve is displayed in figure 3.10.

Table 3.5 Typical K<sup>+</sup>-selective electrode calibration data for calibration in 140 mM NaCl and 10 mM MES at pH 6.0.

Nominal [K <sup>+</sup> ], mM	Actual [K <sup>+</sup> ], mM	E K <sup>+</sup> (mV)
0.10	0.10	-49.1
0.20	0.20	-44.2
0.40	0.40	-37.5
1.0	0.99	-24.2
2.0	1.96	-11.5
4.0	3.91	3.4
10	9.73	27.6
20	19.3	45.4
30	28.6	55.6
40	37.8	63.8

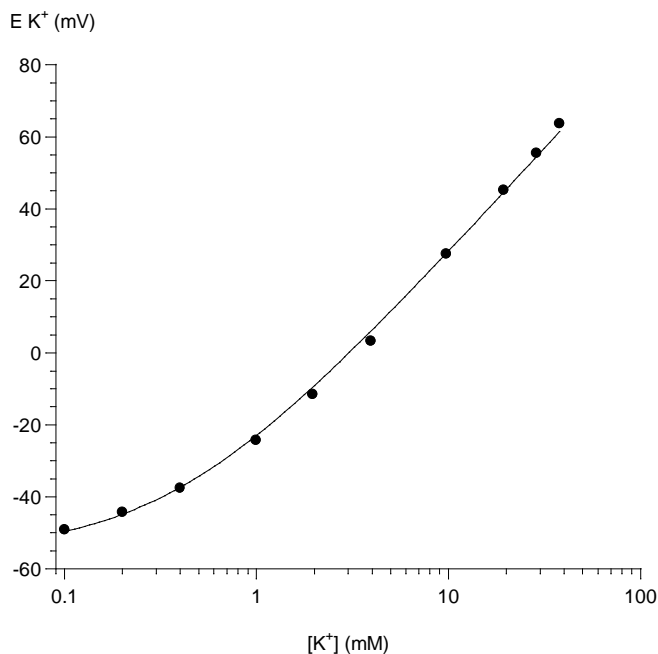


Figure 3.10: Typical calibration curve of a K<sup>+</sup>-selective electrode in 140 mM NaCl and 10 mM MES at pH 6.0.

### 3.2.2 Selectivity of the K<sup>+</sup>-selective electrode:

For the K<sup>+</sup>-selective electrode, the interferent ions of most concern were Na<sup>+</sup>, NH<sub>4</sub><sup>+</sup>, Ca<sup>2+</sup> and H<sup>+</sup>. We examined the individual and combined effects of each of these ions on the K<sup>+</sup>-selective electrode using the methods as for the NH<sub>4</sub><sup>+</sup>-selective electrode.

### 3.2.3 Na<sup>+</sup> interference:

To calculate Na<sup>+</sup> interference, 40 calibration curves were performed in a base solution containing 140 mM NaCl + 10 mM MES (at pH 6.0). The mean value for  $\log k_{KNa}^{pot}$  was  $-2.91 \pm 0.33$ . The anti-logarithm of this value was equivalent to a mean  $k_{KNa}^{pot}$  value of 0.0012. This value was substituted into the Nikolsky-Eisenmann equation to calculate the potentiometric selectivity coefficients of the other interferent ions.

### 3.2.4. $\text{NH}_4^+$ interference:

The  $\text{K}^+$ -selective electrode was tested in two different solutions containing 25 mM and 50 mM background concentrations of  $\text{NH}_4\text{Cl}$ . The  $\text{K}^+$ -selective electrode was calibrated ten times in each solution to calculate a mean  $\log k_{\text{KNH}_4}^{\text{pot}}$  value of  $-1.63 \pm 0.06$ , equivalent to a mean  $k_{\text{KNH}_4}^{\text{pot}}$  value of 0.0232. A mean calibration curve was produced from the ten calibrations for each background concentration of  $\text{NH}_4^+$  and this was compared to a mean baseline calibration, see figure 3.11.

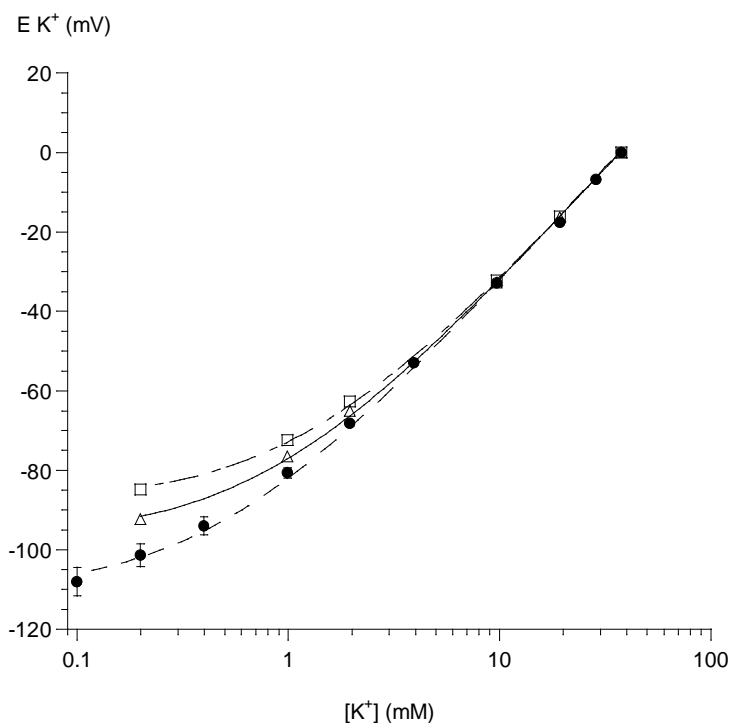


Figure 3.11. Mean calibration curves of a  $\text{K}^+$ -selective electrode in a solution containing 140 mM  $\text{NaCl}$  + 10 mM  $\text{MES}$  (closed circles – base solution), with a background of 25 mM  $\text{NH}_4\text{Cl}$  (open triangles), and background of 50 mM  $\text{NH}_4\text{Cl}$  (open squares). Each determination was performed ten times, error bars refer to data in base solution. All solutions were at pH 6.0.

The figure shows that  $\text{NH}_4^+$  at concentrations between 25 and 50 mM reduce the sensitivity of the  $\text{K}^+$ -selective electrode, but is significant only at  $[\text{K}^+]$  values less than 10 mM. However, the  $[\text{K}^+]$  values measured in urine were always greater than 10 mM (below, section 3.4.2). Thus, the measurement of urinary  $[\text{K}^+]$  will be sufficiently accurate and unaffected by the urinary  $[\text{NH}_4^+]$  to permit correction of the  $\text{NH}_4^+$  - electrode reading for the interference caused by  $\text{K}^+$ .

### 3.2.5 $\text{Ca}^{2+}$ interference:

There was no detectable interference from  $\text{Ca}^{2+}$  on the  $\text{K}^+$ -selective electrode when it was calibrated three times in a background concentration of 2 mM  $\text{CaCl}_2$ . The resulting mean calibration curves for the background concentration of  $\text{Ca}^{2+}$  are shown in figure 3.12.

### 3.2.6 $\text{H}^+$ ion interference:

There was no detectable interference caused by  $\text{H}^+$  ions on the  $\text{K}^+$ -selective electrode when the electrode was calibrated in three solutions of varying pH (7.5, 6.5, and 5.5). The mean calibration curve for each pH can be seen in figure 3.13.

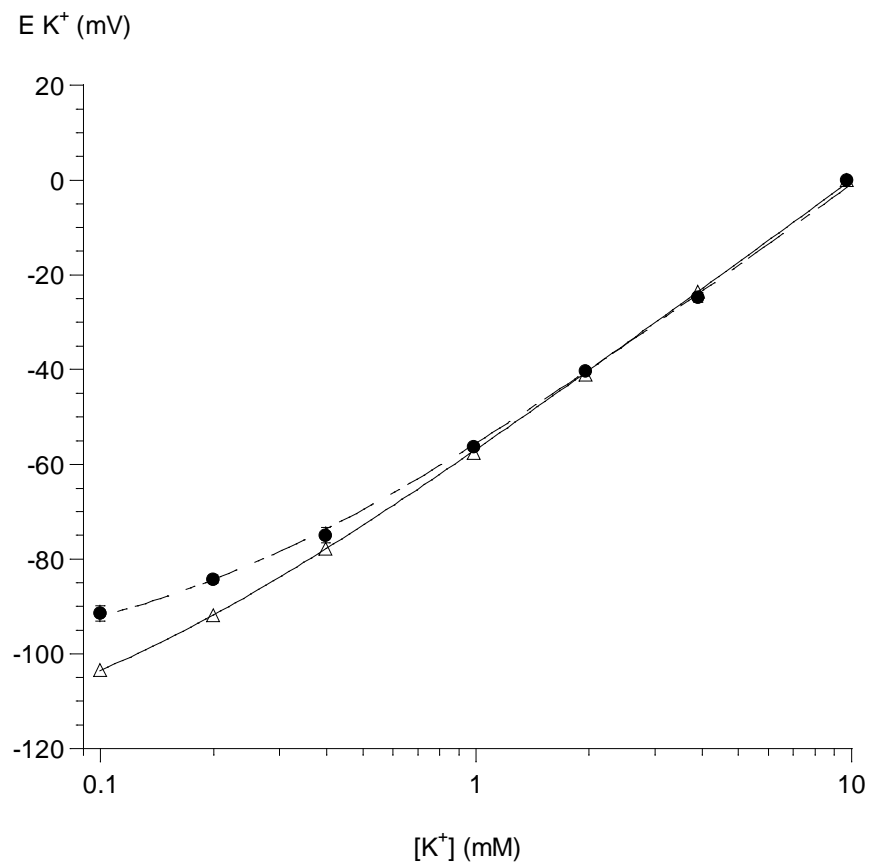


Figure 3.12. Mean calibration curves of  $K^+$ -selective electrodes in a base solution (open symbols) and in the solution containing also 2 mM  $CaCl_2$ . Error bars refer to data in base solution.

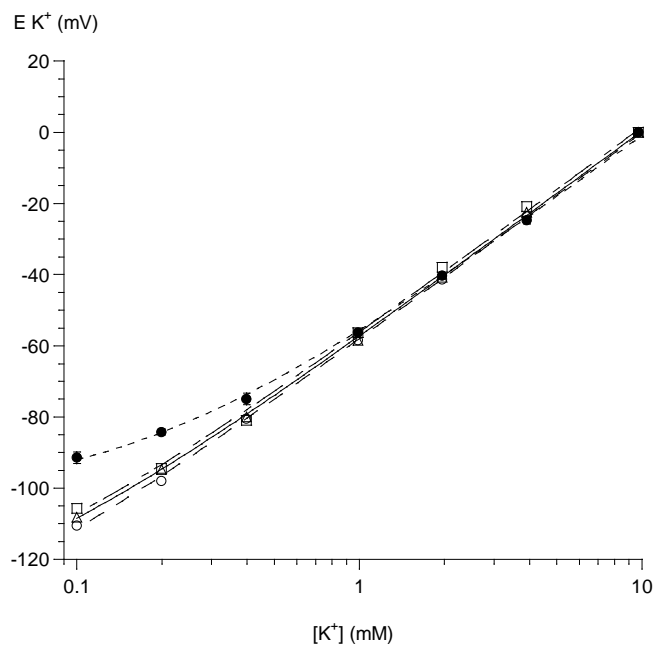


Figure 3.13. Mean calibration curves of  $K^+$ -selective electrodes in a base solution (closed symbols, pH 6) and in solutions buffered to pH 7.5 (open triangles), 6.5 (open squares) and 5.5 (open circles). All solutions contained 140 mM NaCl and 10 mM HEPES (pH 6.0, 6.5 and 7.5) or 10 mM MES (pH 5.5). Error bars refer to data in base solution.

The summarised values of  $\log k_{Kj}^{pot}$ ,  $k_{Kj}^{pot}$ ,  $1 / k_{Kj}^{pot}$  and are summarised in table 3.6.

Table 3.6. Values of  $\log k_{Kj}^{pot}$ ,  $k_{Kj}^{pot}$ ,  $1 / k_{Kj}^{pot}$  for the  $K^+$ -ISE against potential interferent ions, mean  $\pm$  s.d. Not detectable, no significant deviation from calibration in base solution.

	$K^+$ -ISE (room temperature)		
Interferent ion	$\log k_{Kj}^{pot}$	$k_{Kj}^{pot}$	$1 / k_{Kj}^{pot}$
$Na^+$	$-2.91 \pm 0.33$	0.0012	819.5
$NH_4^+$	$-1.63 \pm 0.06$	0.0232	43.1
$H^+$	not detectable	not detectable	-
$Ca^{2+}$	not detectable	not detectable	-

### 3.2.7 Determination of the effect of osmolality on the K<sup>+</sup>-selective electrode:

The K<sup>+</sup>-selective electrode was unaffected by changes in osmolality and ionic activity of the solution as seen by the unchanged  $k_{KNa}^{pot}$  values in the different solutions, using the protocols as described for similar measurements with the NH<sub>4</sub><sup>+</sup>-selective electrode, section 3.1.6. The values are summarized in table 3.7 and mean calibration curves shown in figure 3.14; they show that alterations to ionic strength and osmolality had no effect on the selectivity of the K<sup>+</sup>-ISE to K<sup>+</sup> in the presence of Na<sup>+</sup>.

Table 3.7. Values of  $\log k_{KNa}^{pot}$  and  $k_{KNa}^{pot}$  in solutions of varying ionic strength and osmolality – see section 3.1.6 for further details

Solution	$\log k_{KNa}^{pot}$
Base solution (150 mM Na)	-2.61±0.11
50 mM NaCl	-2.72±0.08
50 mM NaCl + 200 mM Sucrose	-2.88±0.25
300 mM NaCl	-3.87±0.12
150 mM NaCl + 300 mM Sucrose	-3.69±0.21

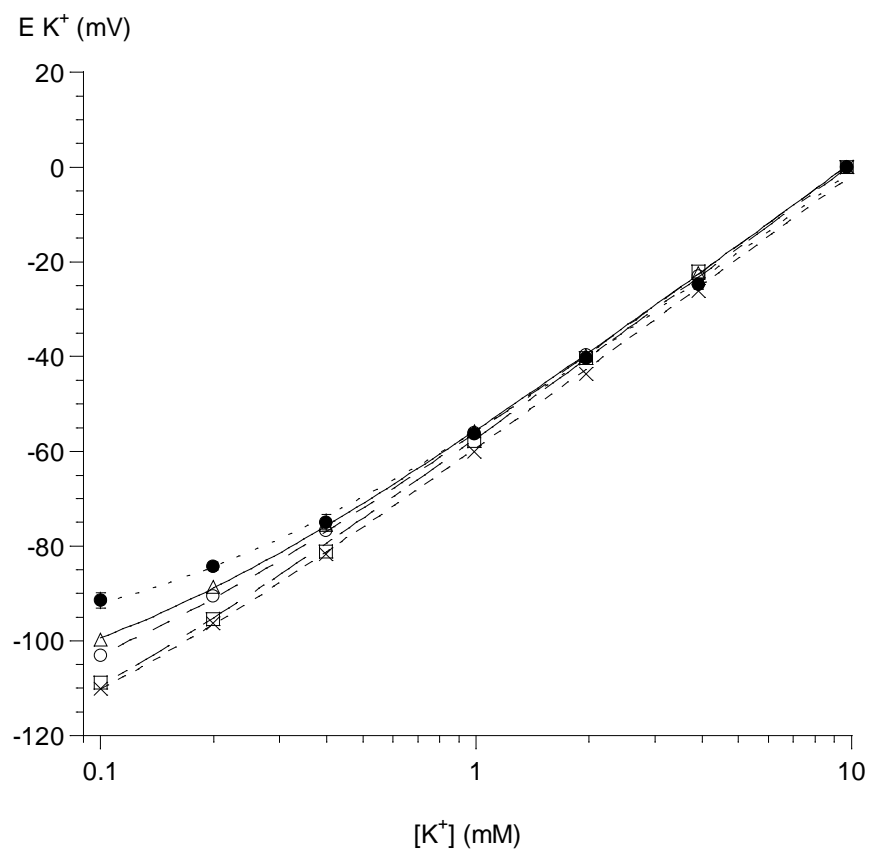


Figure 3.14. Calibration curves of the K<sup>+</sup>-selective electrode in base solution (150 mM Na, closed circles); 50 mM NaCl (open triangles); 50 mM NaCl + 200 mM sucrose (open circles); 300 mM NaCl (crosses); and 150mM NaCl + 300mM sucrose (open squares). All determinations were performed three times. Error bars refer to data in base solution.

### **3.3 Characteristics of Patient Groups and Normal Subjects**

- i) Normal subjects: these were entirely chosen from healthy members within the laboratory and with no history of renal stone disease / urological disease. The average age was 40 years and all were male. Only men were asked to provide samples for appropriateness and ease of providing a sample.
  
- ii) Patient subjects: patients who were attending the urology in-patient ward for a stone-related (on the whole) urology procedure were requested to take part. Volunteers who agreed were provided with a patient information sheet and a consent form to be completed and signed. Twenty-nine patients were able to provide urine samples, 28 were voided samples and one was a renal pelvic sample, obtained from flexible uretero-rensoscopy. Unfortunately we were unable to collect any more renal pelvic samples since there was usually too little urine within the renal pelvis for sampling either during flexible uretero-rensoscopy or during percutaneous nephrolithotomy (PCNL). The patient from whom a renal urine sample was obtained was because the person had a dilated renal pelvis or hydronephrosis allowing for more urine in the renal pelvis. Of the 28 patients, 14 each were male and female. For the female group the mean age was  $42.4 \pm 15.5$  years; for the male group the mean was  $52.1 \pm 14.6$  years.
  
- iii) Patient subjects: a second group of patients was examined who attended an outpatient appointment at the Renal Stone Clinic at the Royal Free Hospital. This is a specialised clinic dealing with patients with recurrent stones and

problematic stones. Following clinical biochemical analysis of their renal stone and a full assessment, they received personalised advice, including advice on their diet, with a view to prevent further stone episodes.

### **3.4 Urinary $[\text{NH}_4^+]$ and $[\text{K}^+]$ measurements using the $\text{NH}_4^+$ - and $\text{K}^+$ -selective electrodes at room temperature:**

Urine from normal subjects (group I, section 3.3): Measurements were made by placing both ion-selective electrodes into the recording chamber and then adding a 4 ml sample of urine. A p.d. was recorded for each electrode.

#### 3.4.1 Sample calculations. Urinary $[\text{K}^+]$ measurement:

Due to the lack of significant interferent effects of other ions on the  $\text{K}^+$ -selective electrode response the  $\text{K}^+$  concentration of urine samples was calculated first. The electrode response may be approximated by a simplified version of the Nikolsky equation (equation 3, section 2.5.2) in which only the  $\text{Na}^+$  interference was taken into account:

$$E_K = E^0 + s \log_{10}([\text{K}^+]) \quad 7$$

Note that ion concentrations rather than activities have been substituted into equation 7, and the justification for doing this was described in section 2.5.3.

The mean urine  $[\text{Na}]$  was 52 mM, which yields a value for  $k_{\text{KNa}}^{\text{pot}}[\text{Na}]$  of  $0.0012 \times 52 = 0.0624$  mM. That is the  $\text{Na}^+$  in the urine sample will contribute to the  $\text{K}^+$ -selective electrode a potential equivalent to this concentration of  $\text{K}^+$ . In a worst case of urinary  $[\text{Na}] = 300$  mM the equivalent contribution would be equivalent to 0.36 mM  $\text{K}^+$ . For this

reason the effect of interferent ions was ignored and the electrode  $K^+$ -selective response curve described by the Nernst equation.

$$E_K = E^0 + s \log_{10}([K^+]) \quad 8$$

$E^0$  is merely an offset that moves the calibration curve along the y-axis but does not change the shape of the calibration curve and may be calculated from a fit of equation 7 to the calibration curve data at noting the value of  $E_K$  for 1 mM KCl, i.e. at 1 mM KCl  $E_K = E^0$  as  $s \log_{10}(K^+) = 0$  using a millimolar scale of concentrations. Thus from equation 8:

$$[K^+] = 10^{\frac{(56.2 - (-29.0))}{58.5}} \quad 9$$

As an example let the values from one urine sample be  $E_K = 56.2$  mV,  $E^0 = -29.0$  mV.

The slope factor  $s$  is 58.5 mV. From equation 9

$$[K^+] = 10^{\frac{(56.2 - (-29.0))}{58.5}} = 28.6 \text{ mM}$$

Note if the urinary Na interference was taken into account the value of the  $[K^+]$  would be corrected down to 28.4 mM in the worst case and 28.5 mM if the mean  $[Na]$  was used. In all subsequent data the  $[K^+]$  values have been reduced by 0.1 mM from initial calculations using equation 9.

### 3.4.2 Urinary $[NH_4^+]$ measurement:

$K^+$  was the major interferent ion with a  $k_{NH_4K}^{pot}$  value of 0.141. To calculate the true urinary  $[NH_4^+]$ , a direct urinary  $[K^+]$  measurement was required. Continuing with the above urine sample, where  $[K^+] = 28.5$  mM:

The  $E_{NH_4}$  reading from the  $NH_4^+$ -selective electrode was 43.5 mV and from the calibration curve  $E^0 = -21.0$  mV. The slope factor is again 58.5 mV for a monovalent ion.

The value of  $k_{NH_4K}^{pot} [K^+] = 4.0$  mM. Thus the Nikolsky equation becomes.

$$E_{NH_4} = E^0 + s \log_{10} ([NH_4^+ + k_{NH_4K}^{pot} [K^+]]) \quad 10$$

thus, 
$$\frac{E_{NH_4} - E^0}{s} = \log_{10} ([NH_4^+ + k_{NH_4K}^{pot} [K^+]])$$

and 
$$10^{\frac{E_{NH_4} - E^0}{s}} = ([NH_4^+ + 4.02])$$

$$[NH_4^+] = \left( 10^{\frac{43.5 - (-21.0)}{58.5}} \right) - 4.0 = 8.7 \text{ mM}$$

From this example it can be seen that correction for the  $[K^+]$  is essential; if it was ignored the apparent  $[NH_4^+] = 12.7$  mM.

Note the contribution from the urine  $[Na^+]$  is small. For a  $k_{NH_4Na}^{pot} = 0.00247$  and a mean  $[Na^+] = 52$  mM the contribution to  $E_{NH_4}$  would be equivalent to 0.1 mM. This was not taken into account in subsequent calculations due to the much more significant interference from  $K^+$ .

### 3.4.3 Values of urinary $[NH_4^+]$ and $[K^+]$ at room temperature:

The urinary  $[NH_4^+]$  and  $[K^+]$  in 28 urine samples were:

$[NH_4^+]$ :  $26.6 \pm 11.5$  mM. Range, 8.7 - 55.2 mM

$[K^+]$ :  $44.8 \pm 16.9$  mM. Range 12.4 - 77.6 mM.

The pH of the samples was  $5.96 \pm 0.76$  (range 4.97-7.33). Individual values are shown in Table 3.8.

Table 3.8. Individual values of urinary  $[\text{NH}_4^+]$  and  $[\text{K}^+]$  at room temperature.

Urine Sample	$[\text{K}^+]$ , mM	$[\text{NH}_4^+]$ , mM	Urine Sample	$[\text{K}^+]$ , mM	$[\text{NH}_4^+]$ , mM
1	28.4	8.7	15	42.2	38.0
2	54.4	30.3	16	77.6	23.1
3	59.8	30.2	17	63.9	22.6
4	63.7	48.2	18	30.2	12.0
5	20.3	13.1	19	56.8	19.5
6	37.6	33.3	20	52.6	20.3
7	56.8	40.7	21	30.8	19.9
8	45.1	20.8	22	51.4	19.0
9	45.7	29.5	23	60.2	28.2
10	56.8	30.1	24	45.8	15.3
11	34.8	31.0	25	55.8	41.8
12	15.9	33.6	26	12.4	8.6
13	16.6	55.3	27	63.6	26.6
14	29.6	14.9	28	45.6	29.4

#### 3.4.4 The relationship between $[\text{NH}_4^+]$ and $[\text{K}^+]$ :

The urinary  $[\text{NH}_4^+]$  was plotted as a function of the urinary  $[\text{K}^+]$ , figure 3.15. There was no significant relationship between the two variables ( $r^2=0.040$ ).

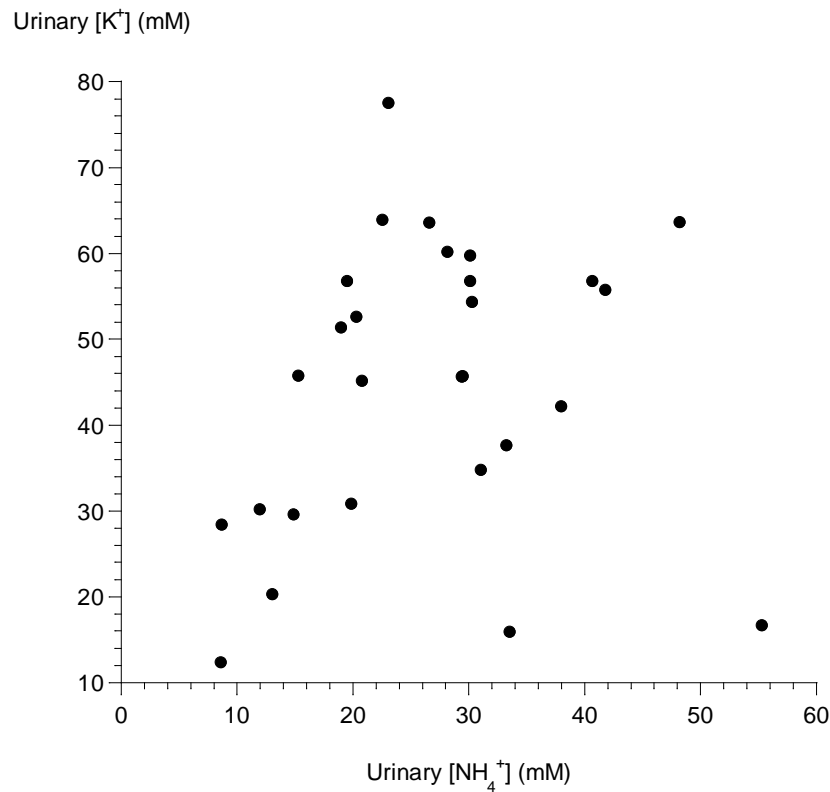


Figure 3.15. The relationship between urinary [NH<sub>4</sub><sup>+</sup>] and urinary [K<sup>+</sup>].

#### 3.4.5 Effects of storage on urinary [NH<sub>4</sub><sup>+</sup>] and [K<sup>+</sup>]:

If urine samples were to be obtained at distant centres it may be necessary to freeze the samples for subsequent storage and transport. To determine if freezing altered the urinary [NH<sub>4</sub><sup>+</sup>] and [K<sup>+</sup>], samples were frozen at -20°C for varying periods, thawed and then analysed. Seven samples were used to examine any effects of storage at -20 °C. Each sample was divided into two aliquots and one aliquot was analysed immediately after collection and kept at room temperature, whilst the other aliquot was kept in the freezer at -20 °C and then analysed after seven days of storage.

The mean value of urinary  $[\text{NH}_4^+]$  was  $20.9 \pm 13.6$  mM immediately after collection, day-0. The aliquot kept at room temperature was analysed on day 2 and day 7 and the mean values of urinary  $[\text{NH}_4^+]$  were  $21.7 \pm 12.0$  and  $29.2 \pm 16.5$  mM respectively – see Table 3.9. ANOVA using comparisons between the groups showed no significant difference between the values obtained at days 0, 2 and 7. Note: a non-parametric analysis of variance did reveal a significant increase of the median values for the values obtained from day 7 samples. The median values (25 and 75% interquartiles are also shown for the data in table 3.9.

Table 3.9: Effects of up to seven days storage at room temperature and  $-20^\circ\text{C}$  on urinary  $[\text{NH}_4^+]$ .

Urine Sample	Day 0 Room temp	Day 2, Room temp	Day 7, Room temp	Day 7, Frozen
1	18.3	21.7	49.6	16.9
2	36.2	35.7	-	42.8
3	42.5	38.6	47.2	36.3
4	3.3	4.6	7.8	3.5
5	15.5	20.6	30.4	16.7
6	14.5	14.1	18.6	14.6
7	16.1	16.6	21.5	13.1
Mean	$20.9 \pm 13.6$	$21.7 \pm 12.0$	$29.2 \pm 16.5$	$20.6 \pm 13.8$
Median	16.1 (15.0, 27.3)	20.6 (15.4, 28.7)	26.0 (19.3, 43.0)	16.7 (13.9, 26.6)

Table 3.9 also shows values of urinary  $[\text{NH}_4^+]$  after seven days frozen storage, the mean value was  $20.6 \pm 13.8$  mM. Paired *t*-test analysis showed no significant difference between these values and those at day 0. It may be concluded that storage for up to seven

days as a frozen sample had no effect on the value of urinary  $[\text{NH}_4^+]$ , whilst there was some evidence that storage at room temperature caused an increase. Storage as a frozen urine sample was therefore used for such subsequent analyses. Figure 3.16 shows the values of urinary  $[\text{NH}_4^+]$  when frozen for seven days, as a proportion of the values obtained at day 0.

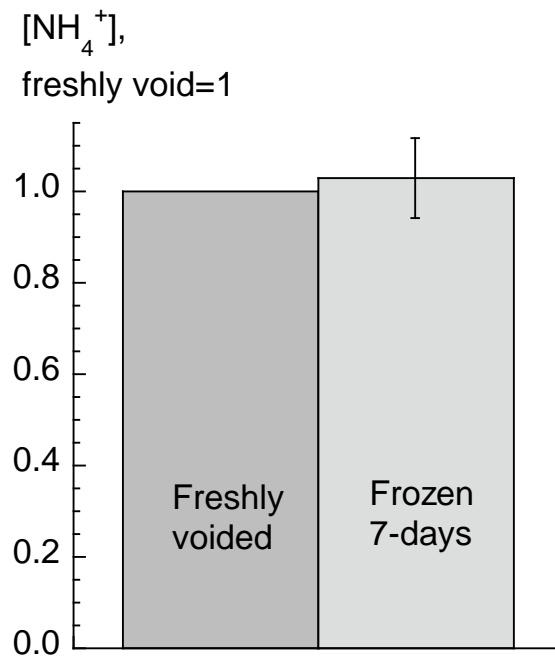


Figure 3.16: Urinary  $[\text{NH}_4^+]$  in freshly voided and 7-day stored, frozen samples. The values in the stored samples are expressed as a proportion of the freshly voided values in the same samples ( $n=7$ ). Mean data  $\pm$  s.d.

Table 3.10 shows values for urinary  $[\text{K}^+]$  at day 0 and after seven days frozen storage. The mean values were  $26.1 \pm 17.4$  and  $38.0 \pm 21.6$  mM respectively. Paired  $t$ -test analysis showed no significant difference between the two sets. However, one sample (sample 3) showed a very large increase after seven days and will have skewed the data set. A Wilcoxon rank test did show a significant difference ( $p=0.04$ ) between the two data sets.

A larger data set will be required to determine if the seven days frozen storage does lead to an increase of urinary  $[K^+]$ . There was no obvious cellular material in the urine samples and so the increase of urinary  $[K^+]$  if real is unlikely to result from cell lysis as a result of storage. The reproducibility of the  $K^+$ -selective electrode was very good and running the samples in duplicates was not required from reproducibility experiments.

Table 3.10. Urinary  $[K^+]$  measured at day 0 and after seven days frozen storage at  $-20^\circ\text{C}$ .

Urine sample	Time=0	7 days Frozen
1	50.9	50.1
2	47.0	55.1
3	12.4	66.3
4	7.9	10.5
5	32.7	46.5
6	16.6	18.4
7	15.0	19.2
Mean	$26.1 \pm 17.4$	$38.0 \pm 21.6$
Median	16.6 (13.7, 39.9)	46.5 (18.8, 52.6)

3.4.6 Validation of urinary  $[\text{NH}_4^+]$  measurements with a  $\text{NH}_4^+$ -selective electrode in comparison to colour spectrophotometry:

Figure 3.17 shows the relationship between values for  $[\text{NH}_4^+]$  in the 28 individual urine samples described above as determined both by colour spectrophotometry (CS) and ion-selective electrodes; the straight-line is the line of best fit close to the one of identity through the origin. The sample values showed a large variability to enable validation of the ISE determinations over a wide range of concentrations. The mean values were

26.3±12.5 by colour spectrophotometry and 26.6±11.5 mM by ion-selective electrode analysis, see table 3.11.

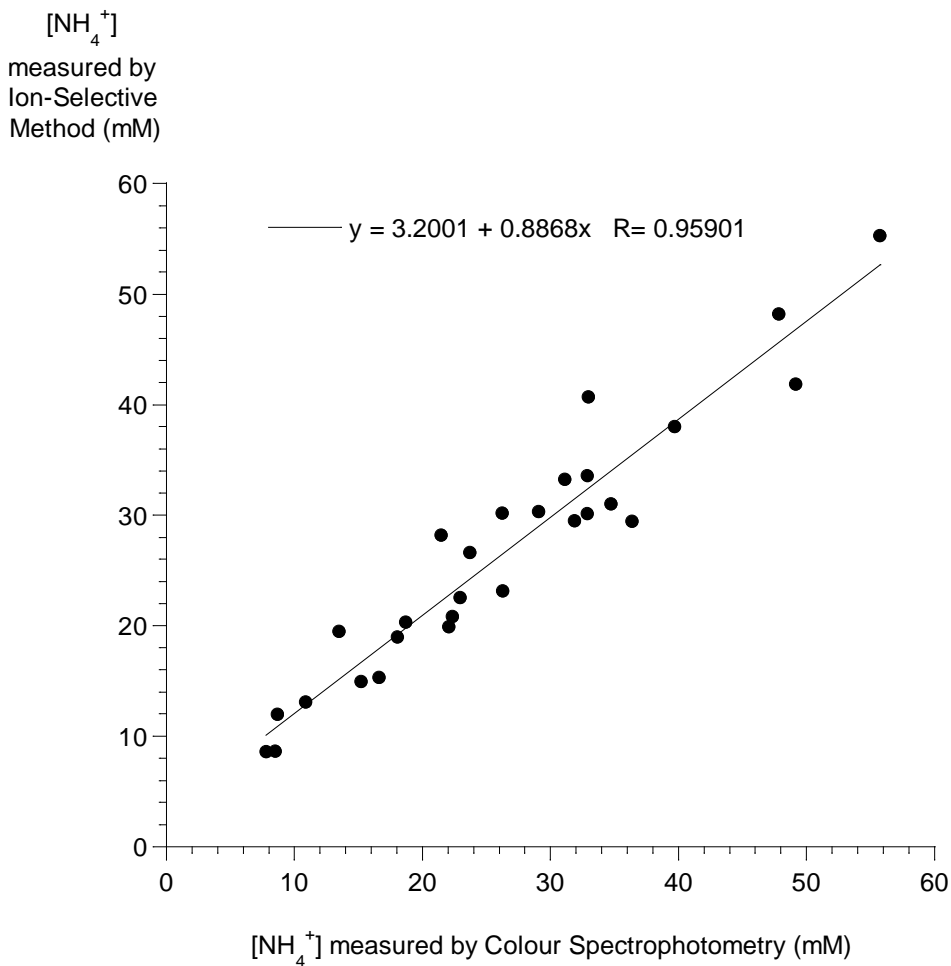


Figure 3.17: Comparison of urinary  $[\text{NH}_4^+]$  measurements using colour spectrophotometry (CS) and ion-selective electrodes (ISE). The straight-line is a line of best fit, close to the line of identity, through the origin.

The data fitted well a straight-line relationship and approximated well to the line of identity shown in figure 3.4.3. The ratio of  $[\text{NH}_4^+]$  as determined by ISE and CS,  $R_{[\text{NH}_4^+]}$ , was  $1.04 \pm 0.16$  and was not significantly different from identity. Moreover, there was no significant relationship between the value of  $R_{[\text{NH}_4^+]}$  as a function of the  $[\text{NH}_4^+]$

as determined by CS ( $r^2=0.152$ ), showing that the values measured by the two methods were consistent over the entire range.

Table 3.11.  $[\text{NH}_4^+]$  values from 28 samples as determined with CS and the ion-selective electrode. The ISE data are the same as shown in Table 3.8. Also shown are the pH values of the sample and the ratio of  $[\text{NH}_4^+]$  determined by ISE and CS,  $R_{\text{NH}_4^+}$ .

Urine Sample	CS $[\text{NH}_4^+]$ , mM	ISE $[\text{NH}_4^+]$ , mM	pH	$R_{\text{NH}_4^+}$	Urine Sample	CS $[\text{NH}_4^+]$ , mM	ISE $[\text{NH}_4^+]$ , mM	pH	$R_{\text{NH}_4^+}$
1	8.5	8.7	6.88	1.02	15	39.7	38.0	5.43	0.956
2	29.1	30.3	5.86	1.04	16	26.3	23.1	5.68	0.878
3	26.3	30.2	5.57	1.15	17	23.0	22.6	6.80	0.981
4	47.8	48.2	5.25	1.01	18	8.7	12.0	7.00	1.38
5	10.9	13.1	5.34	1.20	19	13.5	19.5	7.30	1.44
6	31.1	33.3	5.39	1.07	20	18.7	20.3	6.70	1.08
7	33.0	40.7	5.74	1.23	21	22.1	19.9	6.43	0.901
8	22.3	20.8	7.04	0.932	22	18.1	19.0	4.97	1.05
9	31.9	29.5	5.63	0.926	23	21.4	28.2	6.88	1.31
10	33.0	30.1	5.69	0.916	24	16.6	15.3	5.49	0.919
11	34.8	31.0	5.49	0.893	25	49.2	41.8	5.10	0.850
12	32.9	33.6	5.46	1.02	26	7.8	8.6	7.33	1.10
13	55.8	55.3	5.30	0.991	27	23.7	26.6	6.71	1.12
14	15.2	14.9	5.10	0.979	28	36.4	29.4	5.45	0.808
					Mean	26.3	26.6	5.96	1.04
					$\pm$ sd	$\pm$ 12.5	$\pm$ 11.5	$\pm$ 0.76	$\pm$ 0.16

The same comparison between values for urinary  $[\text{NH}_4^+]$  obtained by CS and ISE was also available for the seven frozen samples analysed above. The data are shown in Table 3.12 and also show similar values obtained by the two methods. The ratio,  $R_{\text{NH}_4^+}$  was

also not significantly different from unity, although the range of  $R_{\text{NH}_4^+}$  values was greater than above.

Table 3.12.  $[\text{NH}_4^+]$  values from seven samples frozen for seven days, as determined with CS and the ion-selective electrode. The ISE data are the same as shown in Table 3.9.

Urine Sample	CS $[\text{NH}_4^+]$ , mM	ISE $[\text{NH}_4^+]$ , mM	$R_{\text{NH}_4^+}$
1	17.9	16.9	0.94
2	34.6	42.8	1.24
3	45.0	36.3	0.81
4	2.4	3.5	1.46
5	10.8	16.7	1.55
6	8.5	14.6	1.72
7	12.3	13.1	1.07
Mean	18.8±15.4	20.6±13.8	1.25±0.34

#### 3.4.7 The pH-dependence of the $[\text{NH}_4^+]$ at room temperature:

Figure 3.18 shows the dependence of the urinary  $[\text{NH}_4^+]$  as a function of the voided pH, the  $[\text{NH}_4^+]$  values as determined by colour spectrophotometry and ion-selective electrodes are plotted. There was a significant negative association between voided pH and  $[\text{NH}_4^+]$ , whether the latter was estimated by colour spectrophotometry ( $r^2=0.340$ ) or with ion-selective electrodes ( $r^2=0.263$ ). Straight-lines through the values yielded slopes of  $-9.6 \text{ mmol}\cdot\text{l}^{-1} \text{ NH}_4^+\cdot\text{pH unit}^{-1}$  and  $-7.8 \text{ mmol}\cdot\text{l}^{-1} \text{ NH}_4^+\cdot\text{pH unit}^{-1}$  respectively. The figure shows that four samples seemed to form a separate group in the lower left-hand side of the plot (their significance is considered in the Discussion). Omission of these

values gave respective slopes of  $-13.5$  ( $r^2=0.792$ ) and  $-11.2$  ( $r^2=0.675$ )  $\text{mmoles.l}^{-1}$   $\text{NH}_4^+ \cdot \text{pH unit}^{-1}$ .

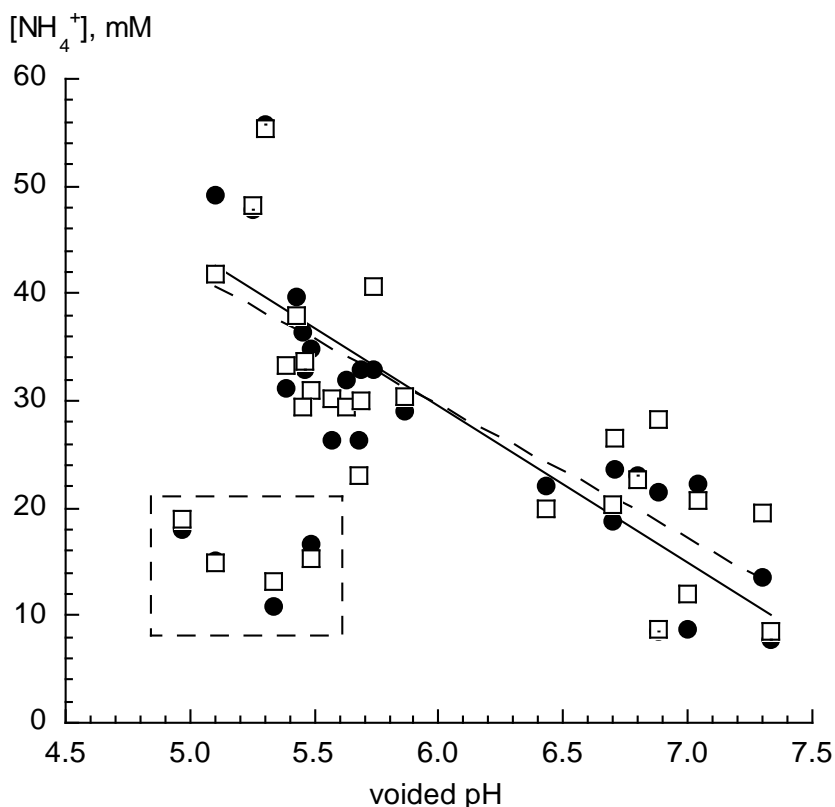


Figure 3.18. The variation of  $[\text{NH}_4^+]$  as a function of voided pH. The  $[\text{NH}_4^+]$  was measured by ion-selective electrodes (ISE, open squares) or colour spectrophotometry (CS, closed circles). The dotted line is through the ISE data, solid line through the CS data. The four boxed values were omitted from calculation of the straight-line plots.

#### 3.4.8 Summary of results at room temperature

1. The urinary  $[\text{NH}_4^+]$  was measured in 28 urine samples with a mean value of  $26.6 \pm 11.5$  mM. It was necessary to measure simultaneously the  $[\text{K}^+]$  as the concentration was large enough to affect significantly the electrode potential of the ion-selective electrode.

2. Storage of urine samples frozen at  $-20^{\circ}\text{C}$  for up to seven days had no significant effect on measured urinary  $[\text{NH}_4^+]$  values. However, there was some evidence that seven days storage at room temperature tended to increase urinary  $[\text{NH}_4^+]$ , although storage for two days did not. Urinary  $[\text{K}^+]$  values increase after seven days from storage.
3. The urinary  $[\text{NH}_4^+]$  measured with ion-selective electrodes was validated against a standard colour spectrophotometry method at room temperature. There was an excellent correlation between the values estimated by the two methods in the same urine samples.
4. Urinary  $[\text{NH}_4^+]$  decreased as a function of increasing voided pH. This was not reproduced by titrating individual urine samples from voided pH to pH 5.0 and 7.5.

### 3.5 Urinary $[\text{NH}_4^+]$ and $[\text{K}^+]$ measurements using the $\text{NH}_4^+$ - and $\text{K}^+$ -selective electrodes at $37^\circ\text{C}$ .

Urine from the urology patient group subjects (group ii, section 3.3): Measurement of  $[\text{NH}_4^+]$  and  $[\text{K}^+]$  was carried out at room temperature in part to permit validation of the ion-selective electrode technique against a standard colour spectrophotometry assay that is conventionally performed under this condition and also because many other clinical biochemical assays are carried out at room temperature. However, to measure  $[\text{NH}_4^+]$  and  $[\text{K}^+]$  under more physiological conditions and describe more precisely the conditions that might lead to stone (struvite) formation in situ also required measurements carried out at  $37^\circ\text{C}$ . To ensure accurate determination of the urinary  $[\text{NH}_4^+]$  at this temperature it was important to characterise the calibration curves at this temperature also, in particular to determine the temperature-dependence of the potentiometric selectivity coefficients.

#### 3.5.1 Calibration of $\text{NH}_4^+$ -selective electrode at $37^\circ\text{C}$ :

Typical calibration data for the  $\text{NH}_4^+$ -selective electrode in 140 mM NaCl buffered to pH 6.0 with 10 mM MES at  $37^\circ\text{C}$  are shown in Table 3.13. The corresponding calibration curve is displayed in figure 3.19 and is compared to a calibration curve performed at room temperature; data from Tables 3.1. The values of  $E_{\text{NH}_4}$  at 40 mM  $\text{NH}_4\text{Cl}$  have been normalised to zero mV to allow better comparison of the two curves. At lower  $[\text{NH}_4\text{Cl}]$  the calibration curve at  $37^\circ\text{C}$  deviated more from a Nernstian straight-line relationship indicating that interference from  $\text{Na}^+$  in this case was greater at the elevated temperature – section 3.5.2.

Table 3.13 Typical  $\text{NH}_4^+$ -selective electrode calibration data for calibration in 140 mM NaCl and 10 mM MES at pH 6.0 at 37°C.

Nominal [ $\text{NH}_4^+$ ], mM	Actual [ $\text{NH}_4^+$ ], mM	E $\text{NH}_4^+$ (mV)
0.200	0.200	-73.1
0.400	0.398	-65.0
1.00	0.99	-52.8
2.00	1.96	-40.0
4.00	3.91	-27.0
10.0	9.73	-5.6
20.0	19.27	12.0
30.0	28.6	22.4
40.0	37.8	29.8

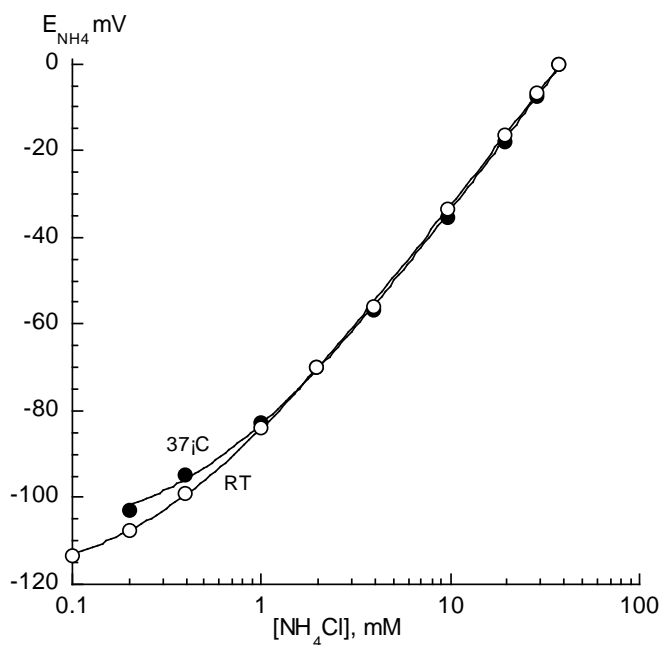


Figure 3.19. Calibration curve for  $\text{NH}_4^+$ -selective electrodes in 140 mM NaCl and 10 mM MES at pH 6.0 at room temperature (open symbols) and 37°C (closed symbols). Values have been normalized to 0 mV for the  $E_{\text{NH}_4}$  in 40 mM  $\text{NH}_4\text{Cl}$ . The lines are a fit of equation 6.

### 3.5.2 Selectivity of the $\text{NH}_4^+$ -selective electrode at 37°C:

To calculate  $\text{Na}^+$  interference on the  $\text{NH}_4^+$ -selective electrode at 37°C, 20 calibration curves were performed in a background solution containing 140 mM NaCl + 10 mM MES (pH 6.0) at 37°C. The mean  $\log k_{\text{NH}_4\text{Na}}^{\text{pot}}$  was  $-2.40 \pm 0.11$ , equivalent to a mean  $k_{\text{NH}_4\text{Na}}^{\text{pot}}$  value of 0.00402. The  $\log k_{\text{NH}_4\text{Na}}^{\text{pot}}$  value was significantly lower than obtained at room temperature, indicating greater interference from  $\text{Na}^+$  at the raised temperature.

To calculate  $\text{K}^+$  interference on the  $\text{NH}_4^+$ -selective electrode, 10 calibrations were performed in four baseline solutions containing 2 mM, 5 mM, 25 mM, and 50 mM KCl. The mean  $\log k_{\text{NH}_4\text{K}}^{\text{pot}}$  and  $k_{\text{NH}_4\text{K}}^{\text{pot}}$  values for each  $\text{K}^+$  concentration are shown in Table 3.14.

Table 3.14.  $k_{\text{NH}_4\text{K}}^{\text{pot}}$  values of the  $\text{NH}_4^+$ -selective electrode in four different background concentrations of  $\text{K}^+$  at room temperature and 37°C

K <sup>+</sup> concentration (mM)	NH <sub>4</sub> <sup>+</sup> -ISE			
	Room temperature			
	Mean $\log k_{\text{NH}_4\text{K}}^{\text{pot}}$	Mean $k_{\text{NH}_4\text{K}}^{\text{pot}}$	Mean $k_{\text{NH}_4\text{K}}^{\text{pot}}$	Overall Mean $k_{\text{NH}_4\text{K}}^{\text{pot}}$
2	$-0.84 \pm 0.038$	0.143	$0.140 \pm$	$0.141 \pm$ $0.025$
5	$-0.86 \pm 0.029$	0.137	0.003	
25	$-0.85 \pm 0.010$	0.141	$0.141 \pm$	
50	$-0.85 \pm 0.007$	0.142	0.008	
	37°C			
2	$-0.65 \pm 0.037$	0.224	$0.223 \pm$	$0.208 \pm$ $0.038$
5	$-0.65 \pm 0.015$	0.222	0.027	
25	$-0.71 \pm 0.013$	0.194	$0.195 \pm$	
50	$-0.71 \pm 0.008$	0.195	0.010	

The modulus of the values for  $-\log k_{NH_4K}^{pot}$  were smaller at 37°C than at room temperature, indicating a greater interference from  $K^+$  at the higher temperature. The mean  $-\log k_{NH_4K}^{pot}$  value from the 20 calibration curves in 25 mM and 50 mM KCl concentrations was  $-0.71 \pm 0.01$ , equivalent to a mean  $k_{NH_4K}^{pot}$  value of 0.195, and this figure was substituted into the Nikolsky equation with the urinary  $[K^+]$ , to obtain the contribution due to  $K^+$ , and thus evaluate the true urinary  $[NH_4^+]$ . At lower background concentrations of  $K^+$  (2 mM and 5 mM) the mean  $-\log k_{NH_4K}^{pot}$  value was significantly smaller ( $0.223 \pm 0.027$ ) indicating that  $K^+$  interference was greater. Thus the extent of interference from  $K^+$  is concentration-dependent, less at higher  $[K^+]$ . Because the mean  $[K^+]$  of the urine values was  $44.8 \text{ mM} \pm 16.9$ , the  $k_{NH_4K}^{pot}$  value of 0.195 (from the mean  $k_{NH_4K}^{pot}$  obtained from the 25 mM and 50 mM background KCl concentration calibration) was chosen to substitute into the Nikolsky equation to calculate the contribution due to  $K^+$ . The mean calibration curves in the four different  $[K^+]$  solutions, as well as the base solution, are shown in figure 3.20.

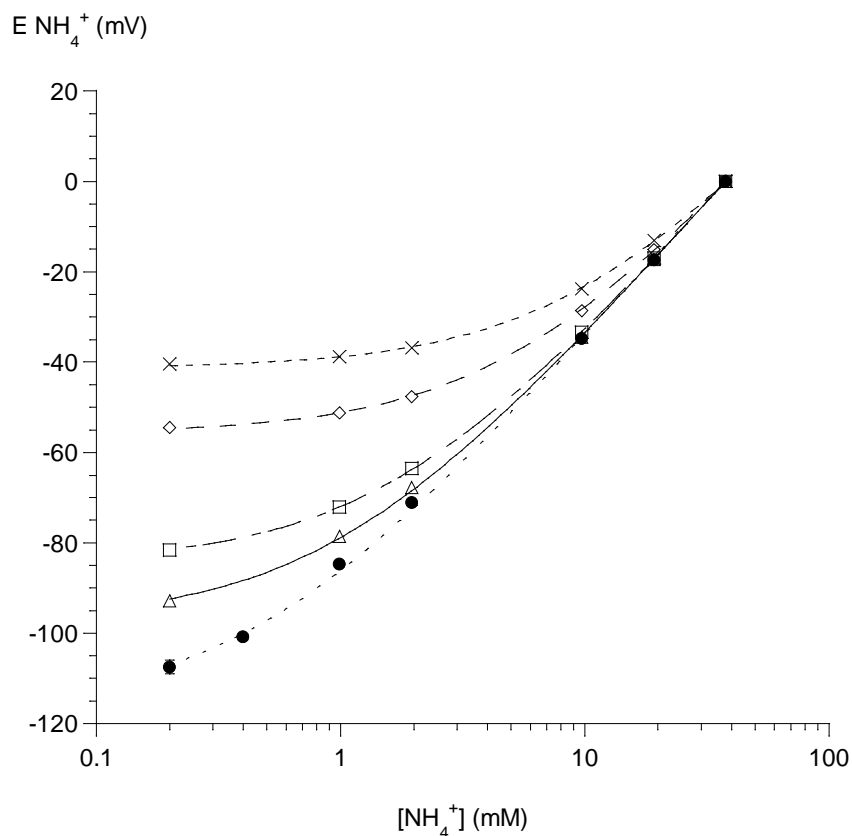


Figure 3.20. Calibration curves of  $\text{NH}_4^+$  selective electrode in 140 mM NaCl + 10 mM MES (base solution) (buffered to pH 6, open circles) and background concentrations of 2 mM (open triangles), 5 mM (open squares), 25 mM (open diamonds) and 50 mM (crosses) KCl at 37°C. Error bars refer to data in base solution.

### 3.5.3 Calibration and selectivity of $\text{K}^+$ -selective electrode at 37°C:

Typical calibration data for the  $\text{K}^+$ -selective electrode in 140 mM NaCl buffered to pH 6.0 with 10 mM MES at 37°C is shown in Table 3.15. The corresponding calibration curve is displayed in Figure 3.21 and is compared to a calibration curve performed at room temperature. The  $E_{\text{K}}$  values were normalised to 0 mV for the highest  $[\text{K}^+]$  used (40 mM) as in Figure 3.19.

Table 3.15. Sample  $K^+$ -selective electrode calibration data for calibration in 140 mM NaCl and 10 mM MES at pH 6.0 at 37°C

Nominal [K <sup>+</sup> ], mM	Actual [K <sup>+</sup> ], mM	E K <sup>+</sup> (mV)
0.1	0.10	28.3
0.2	0.20	33.3
0.4	0.40	40.9
1	0.99	59.7
2	1.97	74.6
4	3.91	88.9
10	9.73	111.3
20	19.3	128.8
30	28.6	138.3
40	37.8	146.3

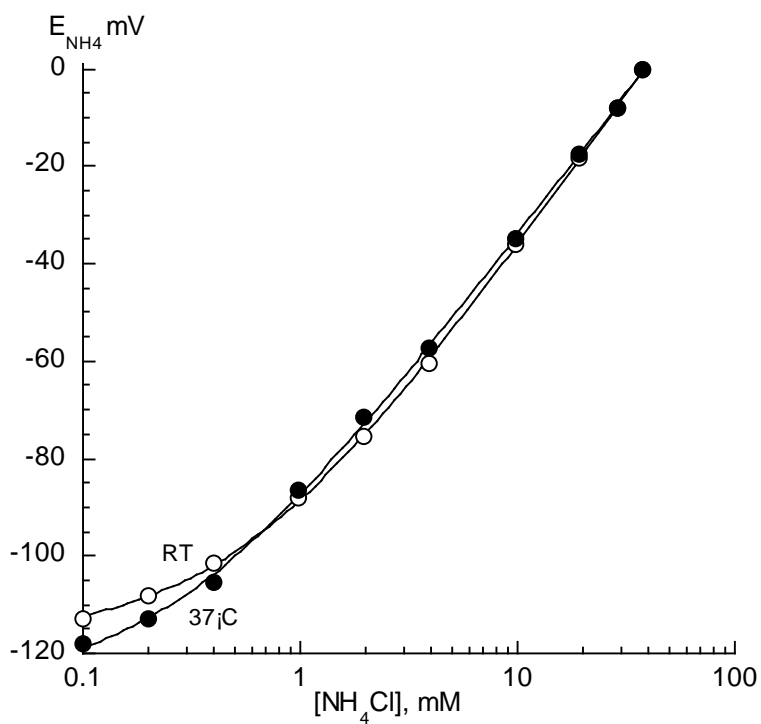


Figure 3.21. Mean calibration curves of  $K^+$ -selective electrodes in 140 mM NaCl and 10 mM MES (pH 6.0) at 37°C (closed symbols) and at room temperature (open symbols).

To calculate Na<sup>+</sup> interference on the K<sup>+</sup>-selective electrode at 37°C, 20 calibration curves were performed in a background solution containing 140 mM NaCl + 10 mM MES (pH 6.0) at 37°C. The mean  $\log k_{\text{KNa}}^{\text{pot}}$  was  $-2.76 \pm 0.10$ , equivalent to a mean  $k_{\text{KNa}}^{\text{pot}}$  value of 0.00173, i.e. the K<sup>+</sup>-selective electrode is 578 times more selective for K<sup>+</sup> than Na<sup>+</sup> at 37°C. This selectivity for K<sup>+</sup> compared to Na<sup>+</sup> was not significantly different from the value at room temperature, section 3.2.2.

To calculate NH<sub>4</sub><sup>+</sup> interference on the K<sup>+</sup>-selective electrode, 10 calibrations were performed in two baseline solutions containing 25 mM, and 50 mM NH<sub>4</sub>Cl. The mean  $\log k_{\text{KNH}_4}^{\text{pot}}$  and  $k_{\text{KNH}_4}^{\text{pot}}$  values for each K<sup>+</sup> concentration are shown in Table 3.16.

Table 3.16. Comparison of NH<sub>4</sub><sup>+</sup> interference values,  $\log k_{\text{KNH}_4}^{\text{pot}}$ , on the K<sup>+</sup>-selective electrode in 25 and 50 mM NH<sub>4</sub>Cl at room temperature and 37°C

Background [NH <sub>4</sub> <sup>+</sup> ] (mM)	K <sup>+</sup> - ISE		
	ROOM TEMPERATURE		
	Mean $\log k_{\text{KNH}_4}^{\text{pot}}$	$k_{\text{KNH}_4}^{\text{pot}}$	Overall Mean $k_{\text{KNH}_4}^{\text{pot}}$
25	$-1.580 \pm 0.038$	0.026	$0.023 \pm 0.064$
50	$-1.689 \pm 0.025$	0.020	
	37°C		
25	$-1.577 \pm 0.030$	0.026	$0.025 \pm 0.035$
50	$-1.611 \pm 0.032$	0.024	

The mean  $\log k_{\text{KNH}_4}^{\text{pot}}$  value from the 20 calibration curves in 25 mM and 50 mM KCl concentrations was  $-1.59 \pm 0.035$ , equivalent to a mean  $k_{\text{KNH}_4}^{\text{pot}}$  value of 0.025, meaning that

the  $K^+$ -selective electrode is 40 times more selective for  $K^+$  than for  $NH_4^+$ . This interference is not significantly different from that measured at room temperature, section 3.2.2. The mean calibration curves in the two solutions are shown in figure 3.22.

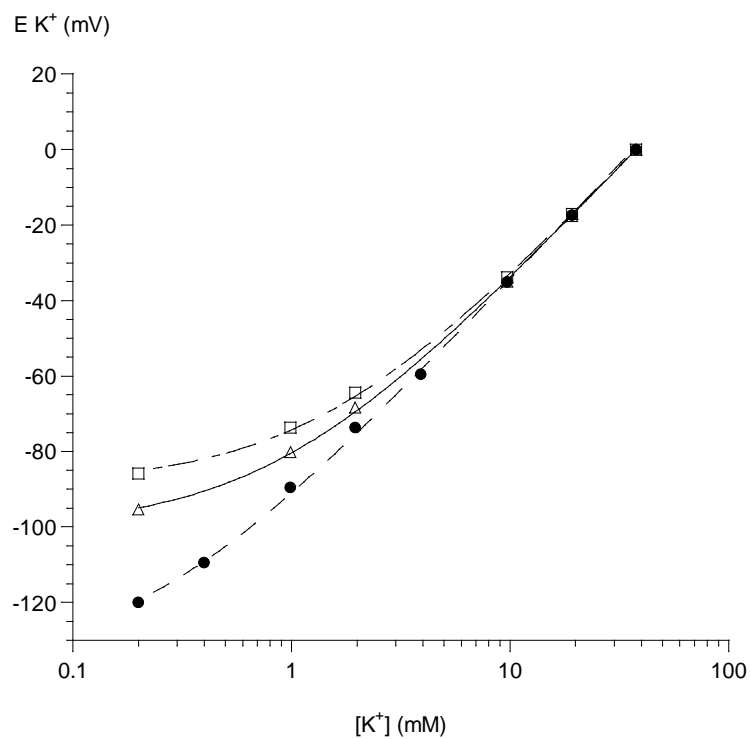


Figure 3.22. Mean calibration curves of the  $K^+$ -selective electrode in 140 mM NaCl + 10 mM MES (buffered to pH 6, closed circles) and in a background concentration of 25 mM (open triangles) and 50 mM (open squares)  $NH_4Cl$  at  $37^\circ C$ . Error bars refer to data in base solution.

### 3.6 Values of urinary $[\text{NH}_4^+]$ and $[\text{K}^+]$ measured at 37°C:

Twenty-four patients attending the in-patient ward for urology operations were recruited. Each was nil-by-mouth from midnight to reduce the effects of dietary intake on urinary  $\text{NH}_4^+$ . Samples were obtained between 7 and 8 am, to minimise diurnal variability.

#### 3.6.1 Urinary values of $[\text{NH}_4^+]$ and $[\text{K}^+]$ :

Urinary  $[\text{NH}_4^+]$  and  $[\text{K}^+]$  were  $15.0 \pm 9.8$  and  $35.9 \pm 15.8$  mM respectively, n=28. The ranges of values were 1.12 - 44.1 and 11.2 - 72.3 mM respectively. The voided pH of the samples was  $6.70 \pm 0.92$  (range 5.50 - 8.52). These values are shown in table 3.17.

Table 3.17. Individual values of urinary  $[\text{NH}_4^+]$ ,  $[\text{K}^+]$  and voided pH at 37°C.

Urine Sample	$[\text{K}^+]$ , mM	$[\text{NH}_4^+]$ , mM	Voided pH	Urine Sample	$[\text{K}^+]$ , mM	$[\text{NH}_4^+]$ , mM	Voided pH
1	12.9	7.3	6.10	13	51.0	14.2	7.55
2	28.9	25.3	8.20	14	44.6	16.3	6.85
3	72.3	44.1	5.65	15	35.4	13.6	6.21
4	28.5	11.2	5.60	16	44.4	11.1	6.85
5	50.6	24.6	5.68	17	19.7	13.1	6.48
6	45.4	18.8	5.64	18	32.8	17.4	7.27
7	38.0	1.1	7.70	19	28.9	4.6	6.60
8	26.0	19.0	6.10	20	40.9	4.7	6.37
9	37.4	7.0	5.50	21	11.2	18.8	8.10
10	24.9	34.1	6.93	22	25.4	15.3	5.30
11	22.0	14.8	8.52	23	47.2	6.6	7.55
12	22.0	12.5	6.97	24	71.3	6.5	6.96
				Mean	35.9	15.0	6.70
				$\pm$ sd	15.8	9.8	0.92

### 3.6.2 The relationship between urinary $[\text{NH}_4^+]$ and $[\text{K}^+]$ .

Figure 3.23 plots the value of urinary  $[\text{NH}_4^+]$  as a function urinary  $[\text{K}^+]$  at voided pH.

There was no significant relationship between the two variables. This lack of significant relationship was also observed at room temperature (section 3.4.3).

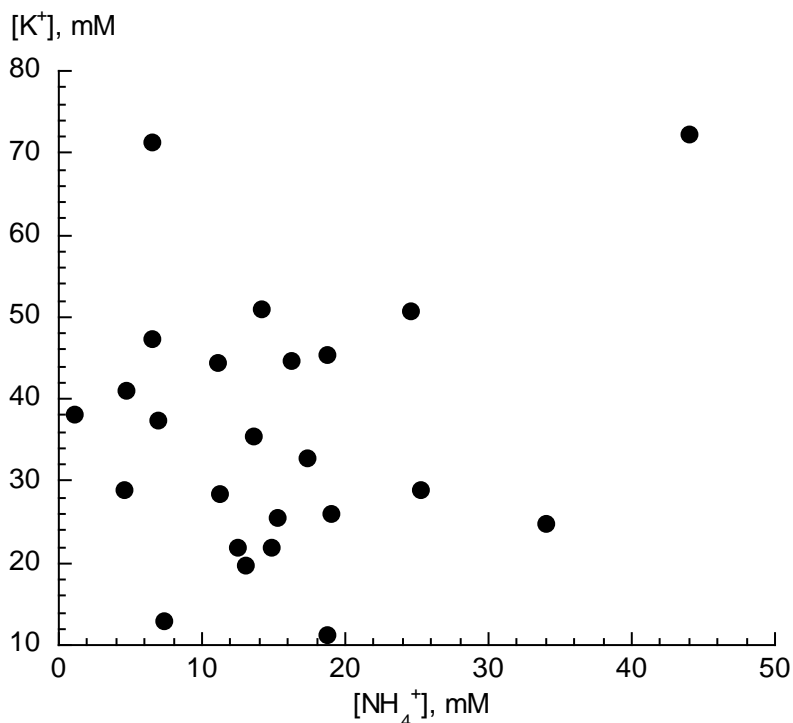


Figure 3.23: The relationship between urinary  $[\text{K}^+]$  and urinary  $[\text{NH}_4^+]$  at the voided pH of urine.

### 3.6.3 The pH dependence of urinary $[\text{NH}_4^+]$ at 37°C.

The variability of urinary  $[\text{NH}_4^+]$  as a function of voided pH at 37°C was plotted, as it was for room temperature data (Figure 3.18, section 3.4.7). The relationship is shown in Figure 3.24.

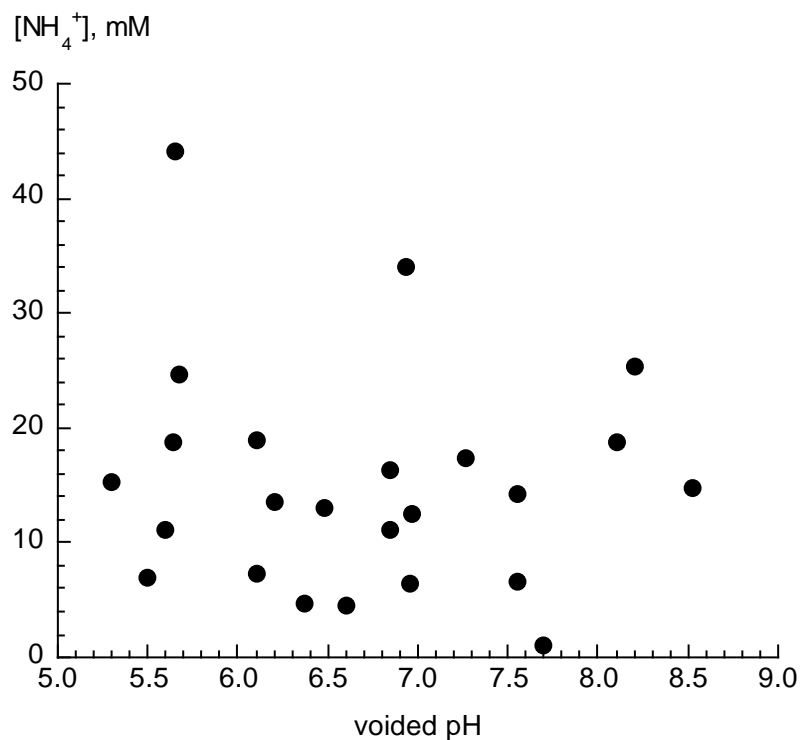


Figure 3.24. Urinary  $[\text{NH}_4^+]$  plotted as a function of voided pH, measured at  $37^\circ\text{C}$ .

A negative relationship between the two variables was recorded, as for measurements at room temperature. However, the association failed to achieve statistical significance at  $37^\circ\text{C}$  ( $r^2 = -0.066$ ).

#### 3.6.4 Effect of adjusting urinary pH to 6.0 on urinary $[\text{NH}_4^+]$ and $[\text{K}^+]$ :

The difference at room temperature and  $37^\circ\text{C}$  regarding the pH-dependency of the  $[\text{NH}_4^+]$  may reflect intrinsic variability of the data between samples as a trend was observed at  $37^\circ\text{C}$  and a strong relationship at room temperature. The potential pH-dependence of the value of the urinary  $[\text{NH}_4^+]$  at  $37^\circ\text{C}$  was further investigated by altering the pH of individual samples and successively measuring the  $[\text{NH}_4^+]$ .

The data from urine samples at 37°C (Table 3.17) are also shown in Tables 3.18 and 3.19, but in this instance values for urinary  $[\text{NH}_4^+]$  and  $[\text{K}^+]$  are also shown when pH was adjusted to pH 6.0. Each urine sample was divided into two aliquots. The first was tested at voided pH for urinary  $[\text{NH}_4^+]$  and  $[\text{K}^+]$  as above. The pH of the second aliquot was adjusted to 6.0 by addition of NaOH or HCl. The objective was to analyse the effect of pH on the values of  $[\text{NH}_4^+]$  and  $[\text{K}^+]$  and to determine the variability of the values at a fixed pH value.

Urinary  $[\text{NH}_4^+]$  and  $[\text{K}^+]$  in the 24 urine samples were significantly greater (paired *t*-test) at pH 6.0 than at the voided pH, i.e.  $6.70 \pm 0.92$ . The values at pH 6.0 were  $19.1 \pm 12.4$  and  $40.8 \pm 17.6$  mM respectively. The ranges of values were 3.4–49.3 and 17.4–90.5 mM respectively and individual results are shown in Table 3.18 and 3.19. Shown are the values of urinary  $[\text{NH}_4^+]$  and  $[\text{K}^+]$  as well as the change of  $[\text{NH}_4^+]$  and  $[\text{K}^+]$  ( $\Delta[\text{NH}_4^+]$  and  $\Delta[\text{K}^+]$ ) as the pH was adjusted. Negative values for  $\Delta[\text{NH}_4^+]$  and  $\Delta[\text{K}^+]$  mean that the concentration was less at pH 6.0 than at voided pH. For the  $\Delta\text{pH}$  values, these are negative if the pH was adjusted in an alkaline direction to achieve pH 6.0 and *vice versa*. The summaries at the bottom of the tables show mean ( $\pm\text{SD}$ ) and median (25,75% IQs) values, as the data sets appear skewed.

Table 3.18. Values of urinary  $[\text{NH}_4^+]$  at voided pH and pH 6.0 and the change of  $[\text{NH}_4^+]$ ,  $\Delta[\text{NH}_4^+]$ . Values of voided pH and  $\Delta\text{pH}$  to achieve pH=6.0 are also listed

Urine Sample	$[\text{NH}_4^+]$ , mM		$\Delta[\text{NH}_4^+]$	Voided pH	$\Delta\text{pH}$
	Void pH	pH 6.0			
1	7.3	5.4	-1.9	6.10	0.10
2	25.3	45.8	20.5	8.20	2.20
3	44.1	37.1	-7.0	5.65	-0.35
4	11.2	9.2	-2.0	5.60	-0.40
5	24.6	23.9	-0.7	5.68	-0.32
6	18.8	12.3	-6.5	5.64	-0.36
7	1.1	3.4	2.3	7.70	1.70
8	19.0	21.8	2.8	6.10	0.10
9	7.0	9.5	2.5	5.50	-0.50
10	34.1	41.1	7.0	6.93	0.93
11	14.8	21.9	7.1	8.52	3.52
12	12.5	13.8	1.3	6.97	0.97
13	14.2	17.6	3.4	7.55	1.55
14	16.3	18.5	2.2	6.85	0.85
15	13.6	15.0	1.4	6.21	0.21
16	11.1	15.3	4.2	6.85	0.85
17	13.1	15.6	2.5	6.48	0.48
18	17.4	18.6	1.2	7.27	1.27
19	4.6	5.9	1.3	6.60	0.60
20	4.7	11.0	6.3	6.37	0.37
21	18.8	49.3	30.5	8.10	2.10
22	15.3	22.0	6.7	5.30	-0.70
23	6.6	12.9	6.3	7.55	1.55
24	6.5	12.5	6.0	6.96	0.96
Mean (SD)	15.1±9.7	19.1±12.4	4.1±7.7	6.70±0.92	0.74±1.02
Median (IQ)	13.9 (7.2,18.8)	15.5 (12.0,21.9)	2.5 (1.3,6.3)	6.72 (6.00,7.34)	1.02 (-0.01,1.34)

Table 3.19. Values of urinary  $[K^+]$  at voided pH and pH 6.0 and the change of  $[K^+]$ ,  $\Delta[K^+]$ . Values of voided pH and  $\Delta$ pH to achieve pH=6.0 are also listed

Urine Sample	$[K^+]$ , mM		$\Delta[K^+]$	Voided pH	$\Delta$ pH
	Void pH	pH 6.0			
1	12.9	18.6	5.7	6.10	0.10
2	28.9	38.6	9.7	8.20	2.20
3	72.3	90.5	18.2	5.65	-0.35
4	28.5	39.5	11	5.60	-0.40
5	50.6	67.8	17.2	5.68	-0.32
6	45.4	46.9	1.5	5.64	-0.36
7	38.0	48.2	10.2	7.70	1.70
8	26.0	19.1	-6.9	6.10	0.10
9	37.4	40.7	3.3	5.50	-0.50
10	24.9	30.1	5.2	6.93	0.93
11	22.0	33.6	11.6	8.52	3.52
12	22.0	28.1	6.1	6.97	0.97
13	51.0	53.1	2.1	7.55	1.55
14	44.6	40.8	-3.8	6.85	0.85
15	35.4	33.4	-2	6.21	0.21
16	44.4	44.5	0.1	6.85	0.85
17	19.7	17.4	-2.3	6.48	0.48
18	32.8	47.4	14.6	7.27	1.27
19	28.9	37.7	8.8	6.60	0.60
20	40.9	44.7	3.8	6.37	0.37
21	11.2	18.4	7.2	8.10	2.10
22	25.4	21.5	-3.9	5.30	-0.70
23	47.2	51.0	3.8	7.55	1.55
24	71.3	67.5	-3.8	6.96	0.96
Mean (SD)	35.9±15.7	40.8±17.6	4.9±6.9	6.70±0.92	0.74±1.02
Median (IQ)	34.1 (25.2,44.8)	40.1 (29.6,47.6)	4.5 (-0.4,9.8)	6.72 (6.00,7.34)	1.02 (-0.01,1.34)

The data for the  $\Delta[\text{NH}_4^+]$  and  $\Delta[\text{K}^+]$  as a function of  $\Delta\text{pH}$  are plotted in Figure 3.25 (urinary  $[\text{NH}_4^+]$ ) and Figure 3.26 (urinary  $[\text{K}^+]$ ). Figure 3.25 shows that an increase of  $[\text{NH}_4^+]$  (positive  $\Delta[\text{NH}_4^+]$ ) was significantly associated with acidification of the urine (positive  $\Delta\text{pH}$ :  $r^2=0.396$ ,  $p<0.05$ ). Figure 3.26 shows a similar plot for the change of  $[\text{K}^+]$  ( $\Delta[\text{K}^+]$ ) where no significant relationship was observed with  $\Delta\text{pH}$  ( $r^2=0.023$ ). Thus, as the urine was made more acid the  $[\text{NH}_4^+]$  increased (or the  $[\text{NH}_4^+]$  decreased as urine was alkalinised).

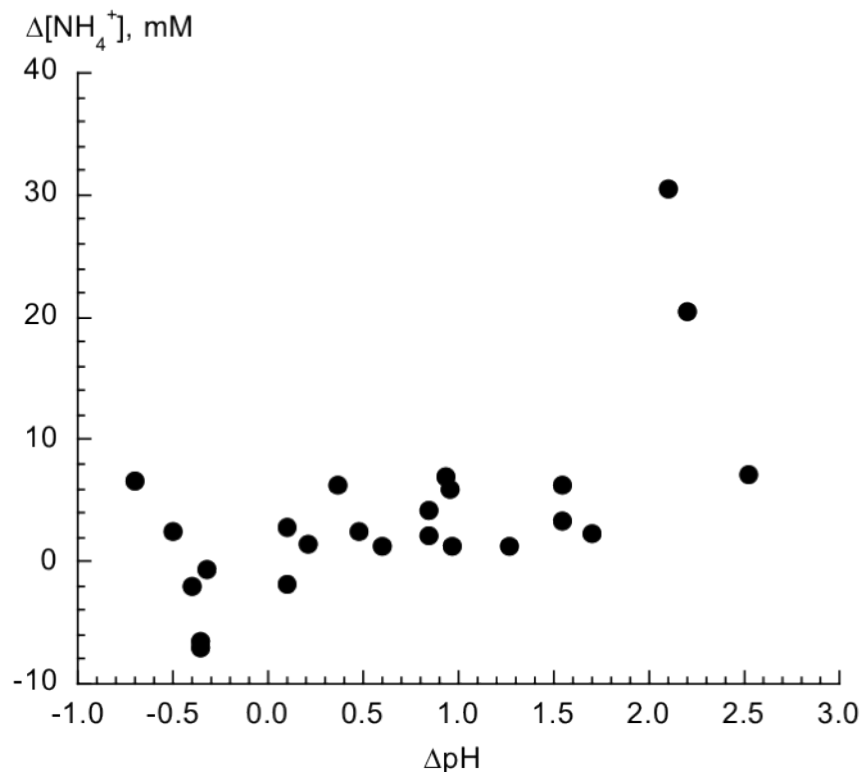


Figure 3.25. Change of urinary  $[\text{NH}_4^+]$ ,  $\Delta[\text{NH}_4^+]$ , as a function of alteration of pH,  $\Delta\text{pH}$ , from the voided value to pH 6.0.

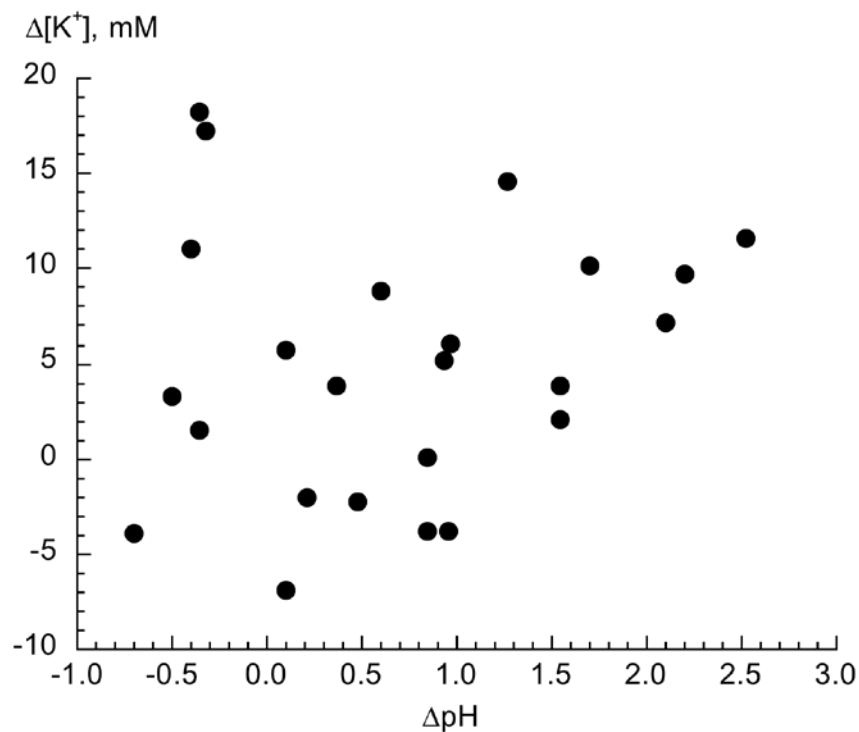


Figure 3.26. Change of urinary  $[K^+]$ ,  $\Delta[K^+]$ , as a function of alteration of pH,  $\Delta pH$ , from the voided value to pH 6.0.

### 3.6.5 Summary of results at 37°C

1. The  $NH_4^+$  and  $K^+$ -selective electrodes showed a similar performance at 37°C as at room temperatures. There was slight variation in the selectivity to interferent ions but did not limit their use in urine samples. Of most significance was a concentration-dependence on the interference of  $K^+$  on the  $NH_4^+$ -selective electrodes.
2. The urinary  $[NH_4^+]$  was measured in 24 urine samples with a mean value of  $15.1 \pm 9.7$  mM at the voided pH ( $6.70 \pm 0.92$ ). The urinary  $[K^+]$  in the same samples was  $35.9 \pm 15.8$  mM.
3. There was no significant relationship between urinary  $[NH_4^+]$  and voided pH as measured at room temperature. However, if the pH was adjusted to pH 6.0 mean

urinary  $[\text{NH}_4^+]$  increased. There was significant relationship between the change of urine pH and urinary  $[\text{NH}_4^+]$ : if pH was reduced urinary  $[\text{NH}_4^+]$  increased and if pH was increased urinary  $[\text{NH}_4^+]$  decreased. There was no dependence of urinary  $[\text{K}^+]$  on voided pH or changes to urine pH.

### **3.7 Urinary $[\text{NH}_4^+]$ and $[\text{K}^+]$ from patients at a Renal Stone Clinic:** (group iii, section 3.3):

#### 3.7.1 Measured values of urinary $[\text{NH}_4^+]$ and $[\text{K}^+]$ at room temperature and 37°C.

This group of patients represented a different cohort or people and it was of interest to determine if the measured urinary  $[\text{NH}_4^+]$  and  $[\text{K}^+]$  values, measured at 37°C and room temperature, were different from the previous groups. In addition, because these measurements were carried out at the two temperatures on the same samples any temperature-dependence was more easily compared. Table 3.20 shows the values of urinary  $[\text{NH}_4^+]$  and  $[\text{K}^+]$  measured at both room temperature and at 37°C and the mean values are summarised in Figure 3.26. The urinary osmolality and voided pH were also measured and recorded in Table 3.20.

Table 3.20: Urinary values of  $[\text{NH}_4^+]$  and  $[\text{K}^+]$  measured at room temperature and  $37^\circ\text{C}$  from patients attending the renal stone clinic (RFH).

Urine Sample	$[\text{NH}_4^+]$	$[\text{NH}_4^+]$ mM 37°C	$[\text{K}^+]$ mM	$[\text{K}^+]$ mM 37°C	Urine osmolality mOsm.kg <sup>-1</sup>	Voided pH
	mM RT		RT			
1	29.9	33.1	40.2	54.8	804	5.44
2	15.8	17.4	42.7	49.0	664	6.83
3	14.2	13.9	33.9	39.4	464	5.78
4	11.8	11.1	44.9	64.2	575	7.74
5	5.7	4.9	10.0	10.6	177	7.33
6	4.8	3.5	29.2	35.5	321	
7	9.3	8.7	22.9	25.0	238	6.99
8	10.3	9.5	31.9	33.1	495	5.05
9	5.6	1.6	41.0	59.6	516	7.90
10	4.8	2.7	36.4	44.3	432	8.24
11	14.5	11.2	47.8	72.4	833	7.50
12	2.9	2.8	7.6	8.3	87	6.00
13	27.2	30.9	26.9	38.8	840	5.08
14	8.3	6.7	52.0	58.3	463	7.38
15	25.6	28.9	24.9	33.8	458	6.61
16	5.0	3.9	56.2	65.0	474	6.96
17	4.9	5.0	7.9	7.9	110	6.89
18	26.8	30.6	32.3	45.7	584	5.85
19	12.8	14.9	18.9	31.8	461	6.97
20	11.7	9.8	29.2	35.4	631	6.34
21	34.3	38.4	29.6	41.7	970	5.79
22	14.2	13.5	26.5	35.8	395	6.37
23	14.4	13.0	20.1	22.0	636	7.55
24	16.1	15.2	24.0	25.2	183	5.15
Mean	13.8	13.8	30.7	39.1	492	6.60
SD	8.9	10.8	13.0	17.7	234	0.94

The mean values are summarized in figure 3.27.

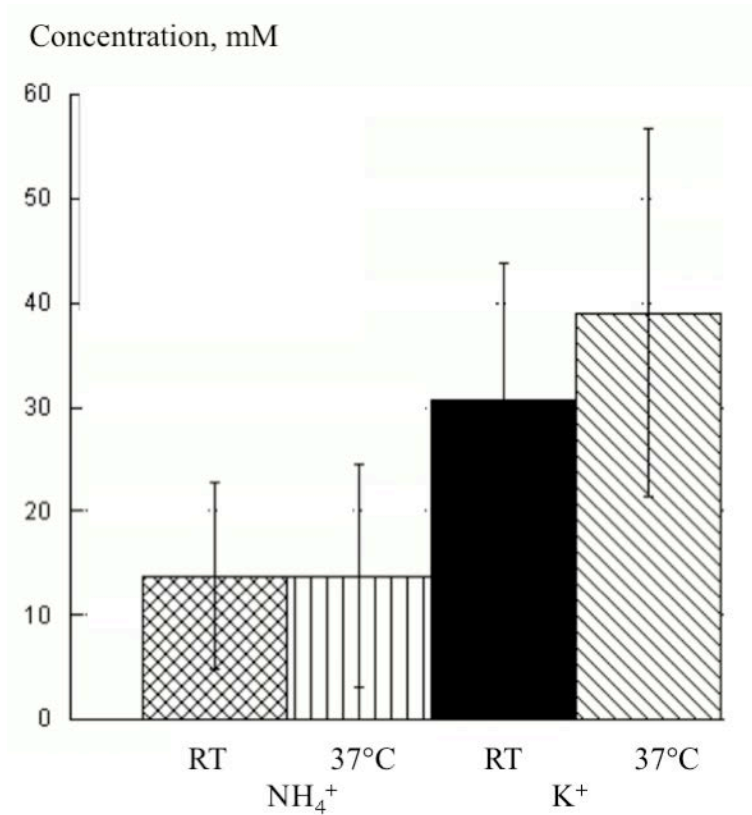


Figure 3.27 Urinary  $[\text{NH}_4^+]$  and  $[\text{K}^+]$  at room temperature and 37°C. Mean values  $\pm$  SD.

There was no significant difference between the urinary  $[\text{NH}_4^+]$  measurements made at room temperature and those made at 37°C; however, the urinary  $\text{K}^+$  values were significantly higher (Student's paired  $t$ -tests).

Figure 3.28 shows the relationship between the  $[\text{NH}_4^+]$  measurements at the two temperatures, with a good correlation between the two sets of data ( $r^2 = 0.98$ ). The figure also shows the line of identity (solid line) and the best-fit line (dotted line). The two were not exactly superimposable with the best-fit line having a positive intercept on the abscissa (2.8 mM) and a slope of 1.20.

$$[\text{NH}_4^+]@37^\circ\text{C} = 1.20*[\text{NH}_4^+]@RT - 2.78$$

Thus  $[\text{NH}_4^+]@37^\circ\text{C} = [\text{NH}_4^+]@RT$  at 13.9 mM, which is almost the mean value (table 3.7.1). At values lower than this  $[\text{NH}_4^+]@RT$  tends to overestimate  $[\text{NH}_4^+]@37^\circ\text{C}$  and underestimate it at higher values. For the highest value at RT (34.3 mM) this represented an estimated underestimate of 4.1 mM at  $37^\circ\text{C}$ , whilst for the lowest value at RT (2.9 mM) it represented an overestimate of 2.2 mM.

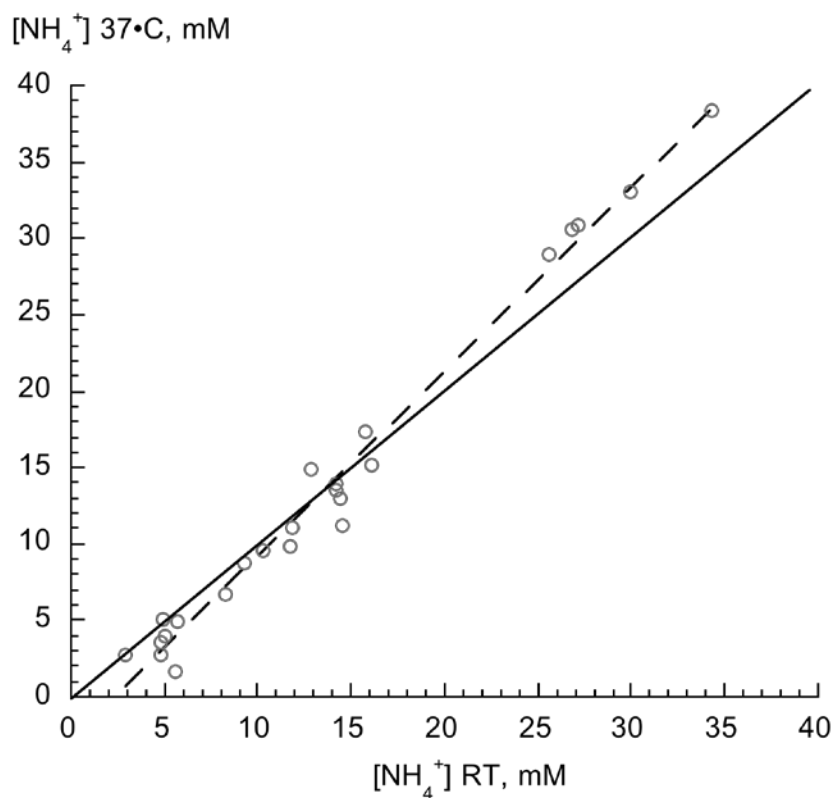


Figure 3.28. The  $[\text{NH}_4^+]$  measured at  $37^\circ\text{C}$  and at room temperature from urine samples of patients at the Renal Stone Clinic. The line of identity (solid line) and the best-fit line (dotted line) are shown

For the  $[\text{K}^+]$  measurements there was a greater discrepancy between the two data sets, as evidenced by the paired  $t$ -test comparison above, although there was also a significantly significant association between the two sets of data ( $r^2=0.91$ ). Figure 3.29 plots the paired

[K<sup>+</sup>] values at RT and 37°C; the line of best-fit showed an intercept on the abscissa at 0.7 mM, but with a slope of 1.30. Thus equivalent values were obtained at 2.4 mM. In this case the highest and lowest values at RT (56.2 and 7.6 mM) were underestimated compared to calculated values at 37°C by 14.2 and 1.5 mM respectively.

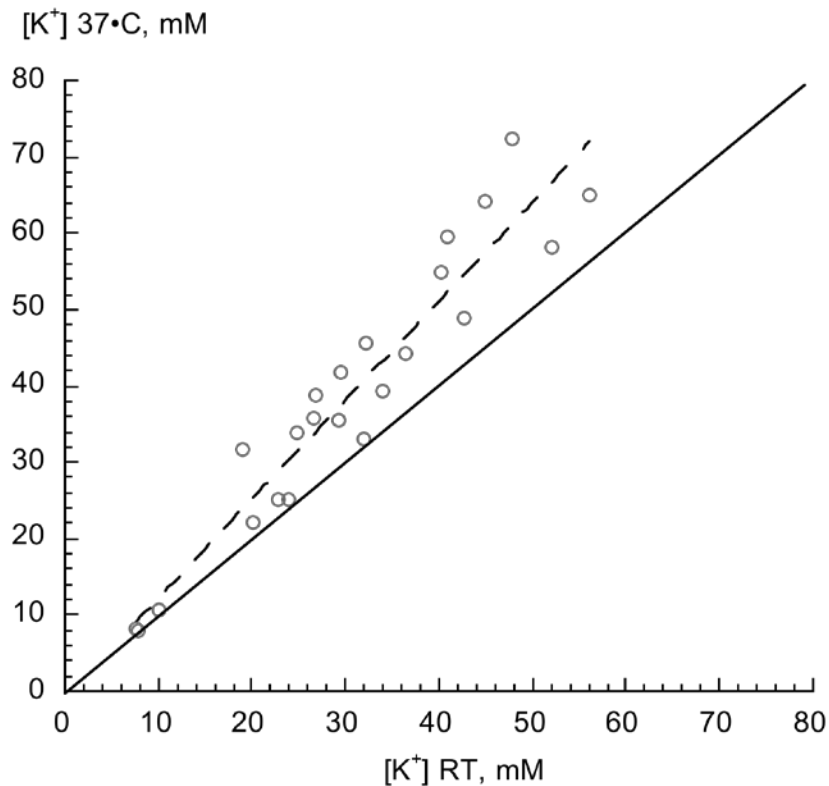


Figure 3.29. The [K<sup>+</sup>] measured at 37°C and at room temperature from urine samples of patients at the Renal Stone Clinic. The line of identity (solid line) and the best-fit line (dotted line) are shown.

### 3.7.2 The dependence of urinary [NH<sub>4</sub><sup>+</sup>] and [K<sup>+</sup>] on urine osmolality.

Figure 3.30 and 3.31 show a positive association between urine osmolality and urinary [NH<sub>4</sub><sup>+</sup>] ( $r^2=0.487, 0.311$ ; ion-selective data at room temperature and 37°C respectively) and [K<sup>+</sup>] ( $r^2=0.307, 0.368$ ; room temperature and 37°C).

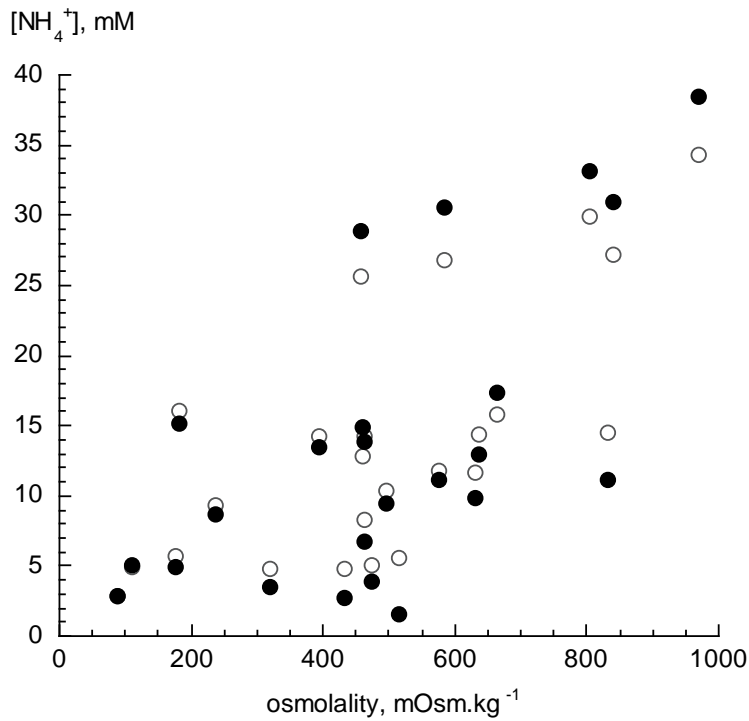


Fig 3.30. The association between urinary [NH<sub>4</sub><sup>+</sup>] and osmolality. The [NH<sub>4</sub><sup>+</sup>] values were measured at room temperature (open circles) or at 37°C (closed circles).

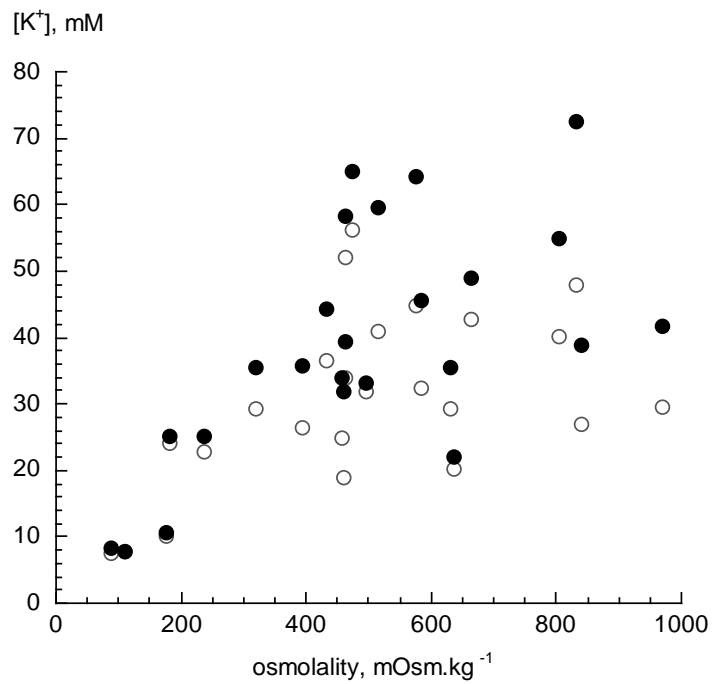


Fig 3.31. The association between urinary [K<sup>+</sup>] and osmolality. The [K<sup>+</sup>] values were measured at room temperature (open circles) or at 37°C (closed circles).

### 3.7.3 The dependence of urinary $[\text{NH}_4^+]$ and $[\text{K}^+]$ on urine voided pH.

Previous sections determined any association between values of urinary  $[\text{NH}_4^+]$  and  $[\text{K}^+]$  and voided pH and this was also possible in samples from this cohort of patients. Figure 3.32 shows a significant negative association between urinary  $[\text{NH}_4^+]$  and voided pH, whether  $[\text{NH}_4^+]$  was measured at room temperature ( $r^2=0.25$ ,  $p=0.015$ ) or at  $37^\circ\text{C}$  ( $r^2=0.34$ ,  $p=0.003$ ).

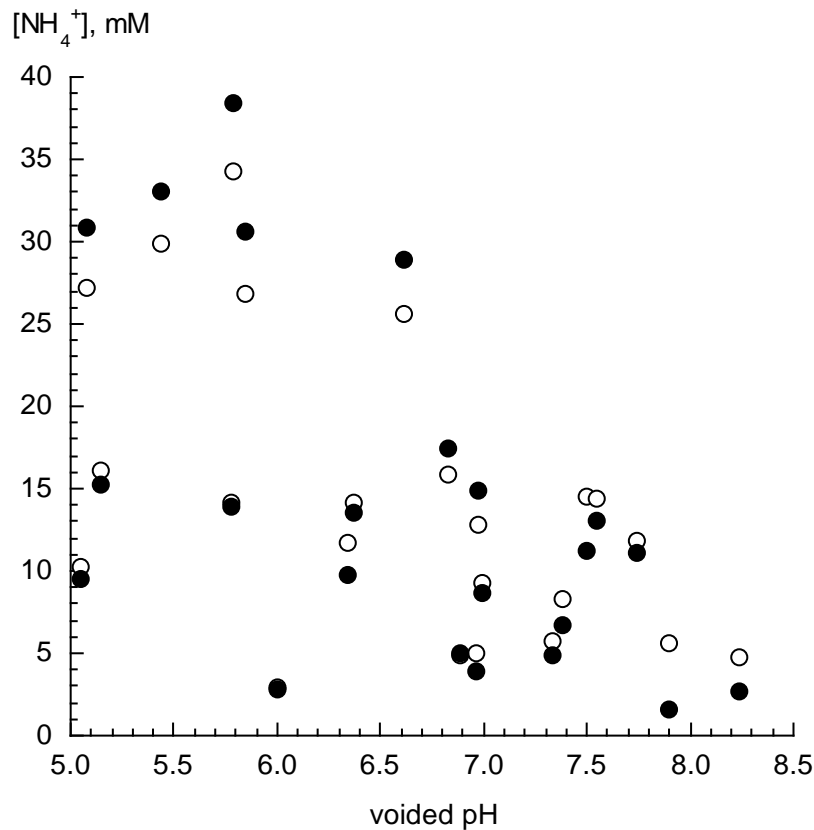


Fig 3.32. The association between urinary  $[\text{NH}_4^+]$  and voided pH. The  $[\text{NH}_4^+]$  values were measured at room temperature (open circles) or at  $37^\circ\text{C}$  (closed circles).

The values of urinary  $[\text{K}^+]$  as a function of voided pH are shown in Figure 3.33 and no significant relationship was observed at room temperature ( $r^2=0.04$ ,  $p=\text{NS}$ ) or at  $37^\circ\text{C}$  ( $r^2=0.05$ ,  $p=\text{NS}$ ).

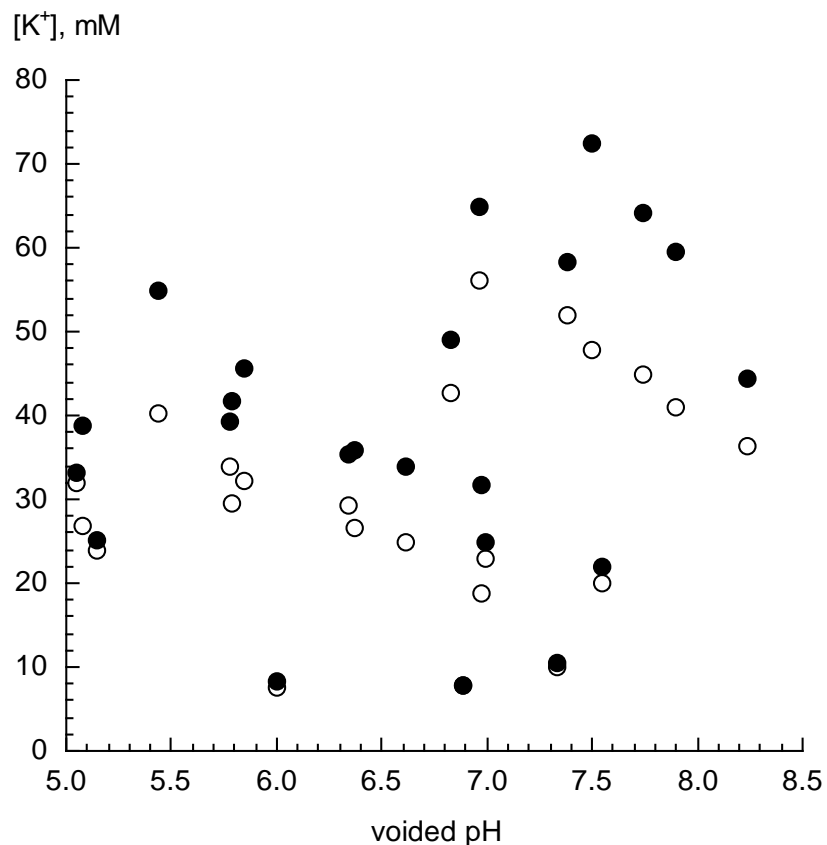


Fig 3.33. The association between urinary [K<sup>+</sup>] and voided pH. The [K<sup>+</sup>] values were measured at room temperature (open circles) or at 37°C (closed circles).

#### 3.7.4 Summary of measured urinary [NH<sub>4</sub><sup>+</sup>] and [K<sup>+</sup>].

The data in sections 3.4 and 3.6 have demonstrated urinary [NH<sub>4</sub><sup>+</sup>] and [K<sup>+</sup>] at the two temperatures using urine samples from a non-stone forming population. The data in section 3.7 used samples from a stone-forming group. It was of interest to determine if there were differences in values between samples from the two cohorts of volunteers.

Table 3.21 shows these data.

Table 3.21 Values of urinary  $[\text{NH}_4^+]$  and  $[\text{K}^+]$  in urine samples from a non-stone forming and a stone-forming cohort of volunteers, \*  $p < 0.05$  non-stone former vs stone formers at RT.

	Non-stone formers	Stone formers		
		RFH patients (stone clinic)		UCLH patients(operative)
	Room temp	Room temp	37°C	37°C
$[\text{NH}_4^+]$ , mM	26.1±11.5 *	13.8±8.9	13.8±10.8	15.0±9.8
$[\text{K}^+]$ , mM	44.8±16.9	30.7±13.0	39.1±17.7	35.9±15.8
Voided pH	5.96±0.76 *	6.60±0.94	6.60±0.94	6.70±0.92

The urinary  $[\text{NH}_4^+]$  and voided pH were significantly different in the non-stone formers samples measured at room temperature. Because the voided pH was significantly more acid in the latter group this may account for the significantly greater  $[\text{NH}_4^+]$ . In addition, the increased alkalinity of urine in the stone formers group may certainly be contributory to their increased stone deposition (see Discussion, section 4.6.4).

Figure 3.34 provides further evidence that all four sets of data came from similar groups. All the data summarized in Table 3.21 are plotted as a function of voided pH. It is difficult to separate any individual data set apart from the remainder. This plot emphasizes the crucial importance of recording voided pH when measuring urinary  $[\text{NH}_4^+]$ , if it is not possible to standardize the pH prior to the measurement. The plot also indicates that there was no difference per se in the values of urinary  $[\text{NH}_4^+]$  in samples from a non-stone forming and stone forming group.

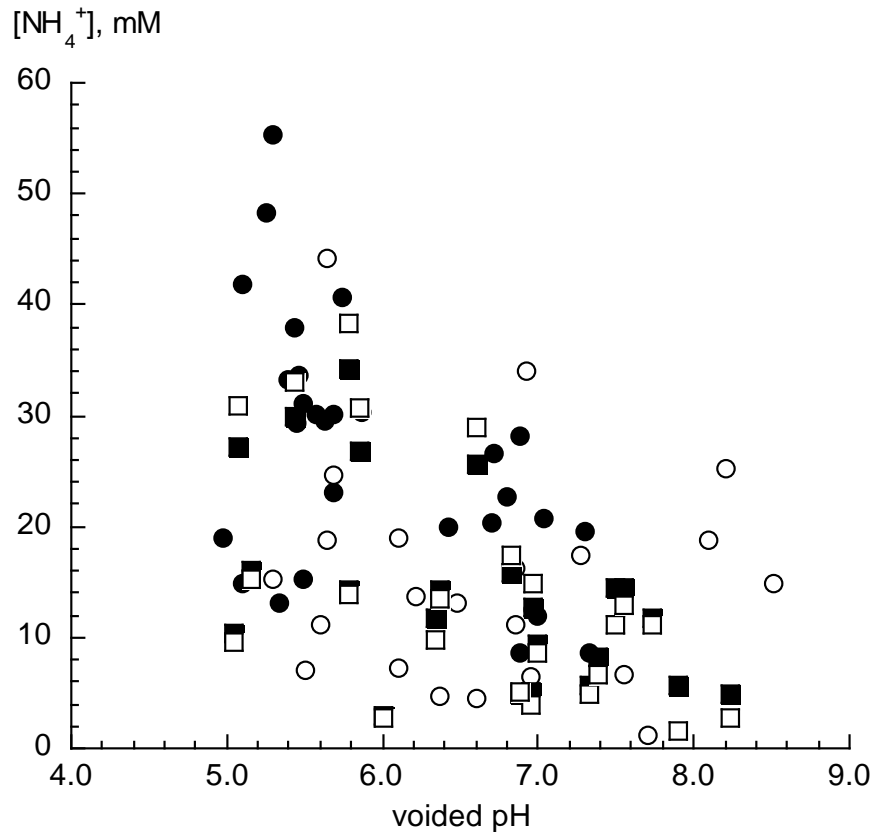


Fig 3.34. The association between urinary  $[\text{NH}_4^+]$  and voided pH in urine samples analysed at room temperature (closed symbols) and at  $37^\circ\text{C}$  (open symbols): non-stone formers (closed circles), RFH stone formers at room temperature (closed squares), RFH stone formers at  $37^\circ\text{C}$  (open squares), and UCLH stone formers at  $37^\circ\text{C}$  (open circles).

### 3.7.5 Validation of the algorithm for calculation of the urinary $[\text{NH}_4^+]$ :

Table 3.22 shows urinary values of  $[\text{NH}_4^+]$  measured by the  $\text{NH}_4^+$ -selective electrode and the values obtained by the algorithm to calculate urinary values, see Methods, section 2.8. Some values produced by the algorithm were negative suggesting that it is not an accurate estimate of the urinary  $[\text{NH}_4^+]$ . The measured values obtained at room temperature were used, although similar conclusion in the analysis below were obtained if the data at  $37^\circ\text{C}$  were used.

Table 3.22: Calculated urinary  $[\text{NH}_4^+]$  compared to ion-selective electrode values

Urine Sample	Calculated $[\text{NH}_4^+]$ (mM)	ISE $[\text{NH}_4^+]$ (mM)	Urinary pH	Urine Sample	Calculated $[\text{NH}_4^+]$ (mM)	ISE $[\text{NH}_4^+]$ (mM)	Urinary pH
1	28.0	29.9	5.44	13	30.0	27.2	5.08
2	5.0	15.8	6.83	14	-7.0	8.3	7.38
3	21.5	14.2	5.78	15	25.5	25.6	6.61
4	-8.5	11.8	7.74	16	-4.0	5.0	6.96
5	0	5.7	7.33	17	2.0	4.9	6.89
6	-4.5	4.8	-	18	30.0	26.8	5.85
7	8.0	9.3	6.99	19	11.0	12.8	6.97
8	7.5	10.3	5.05	20	15.0	11.7	6.34
9	8.5	5.6	7.90	21	49.5	34.3	5.79
10	-3.5	4.8	8.24	22	18.0	14.2	6.37
11	4.0	14.5	7.50	23	-2.5	14.4	7.55
12	2.0	2.9	6.00	24	11.0	16.1	5.15
				Mean	10.3	13.8	6.60
				SD	14.5	8.9	0.94

Figure 3.35 shows a plot of the calculated values as a function of the measured values. Apart from the negative calculated values the association was significant ( $r^2=0.54$ ), but the straight-line fit has a slope of 1.41 with an intercept on the y-axis of -9.1 mM.

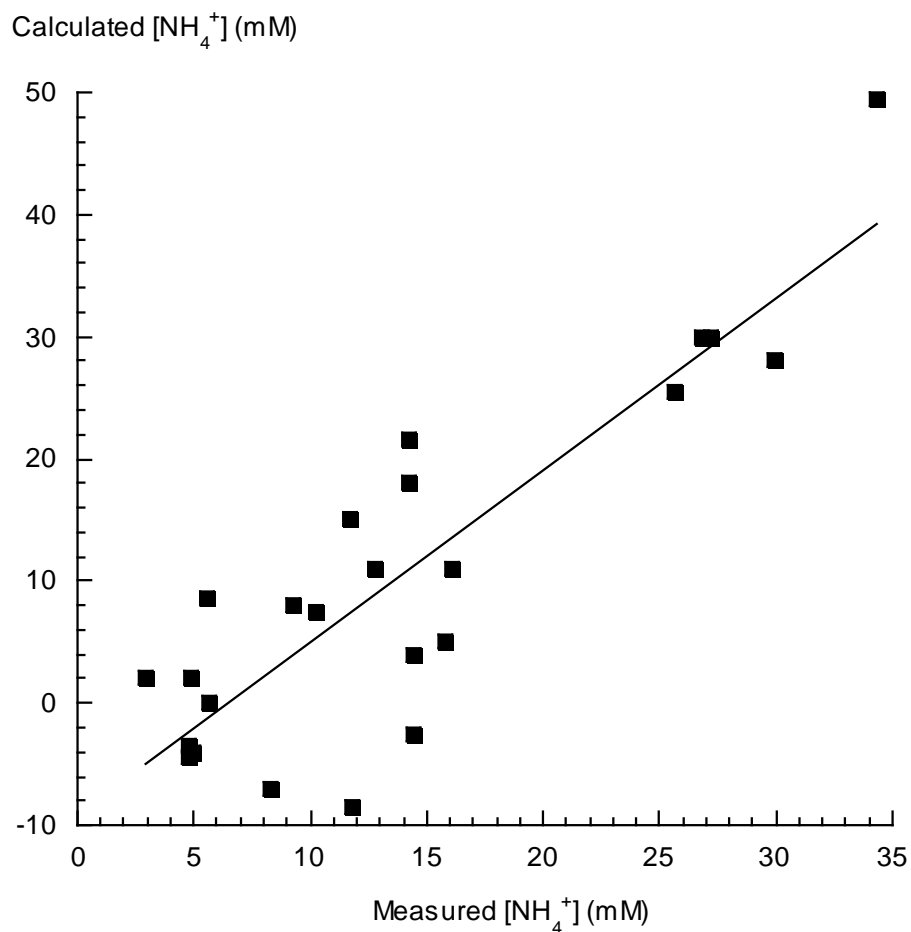


Figure 3.35. Calculated values of urinary [NH<sub>4</sub><sup>+</sup>] as a function of measured values using an ion-selective electrode.

Figure 3.36 plots the differences between the calculated and measured values as a function of the measured [NH<sub>4</sub><sup>+</sup>]. In most cases the calculated value was smaller than the measured value. However, there was no significant association between the two values ( $r^2=0.20$ ) so that the difference is not a proportional error between the two values.

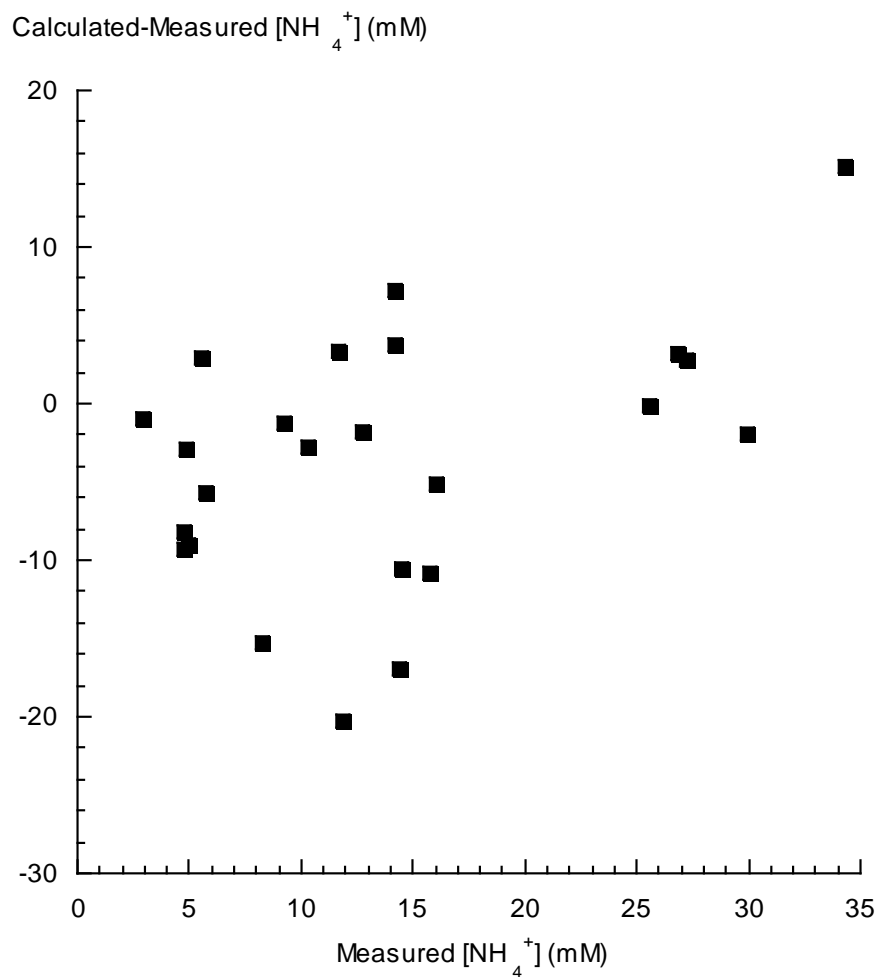


Figure 3.36. The difference between calculated and measured values of urinary  $[\text{NH}_4^+]$  as a function of measured values.

Figure 3.37 plots the difference between the calculated and measured values as a function of urinary pH. At pH values above 6.0 there was a systematic and growing deviation between the two values. This suggests there is an in-built error in the calculation algorithm that is pH-dependent, or that the measured values have an error inherent in the pH-dependence of the ion-selective electrodes. The latter possibility is considered less likely due to the rigorous attempts to correct for any such behaviour.

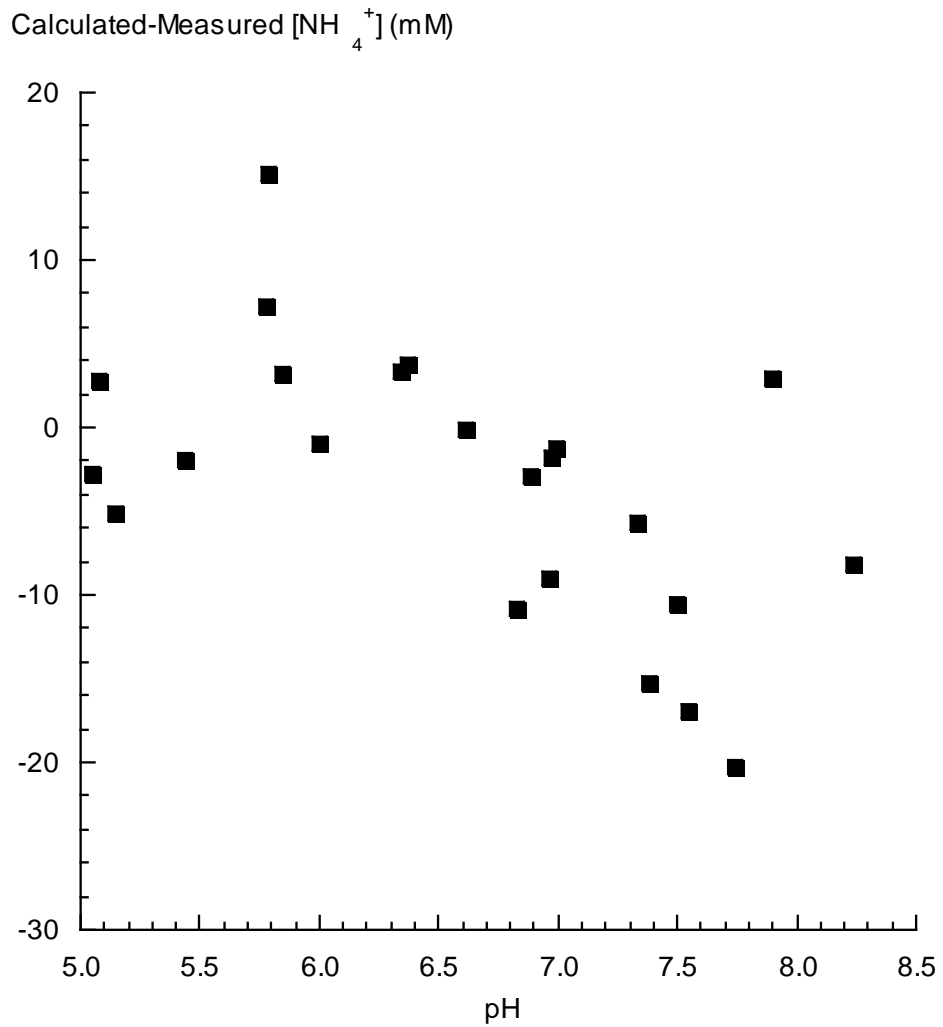


Figure 3.37. The difference between calculated and measured values of urinary  $[\text{NH}_4^+]$  as a function of urine pH.

Finally, figure 3.38 plots the pH-dependence of the calculated and measured values of urinary  $[\text{NH}_4^+]$  values. In both cases pH declined significantly as a function of increasing pH, with  $r^2$  values of 0.42 and 0.30 respectively.

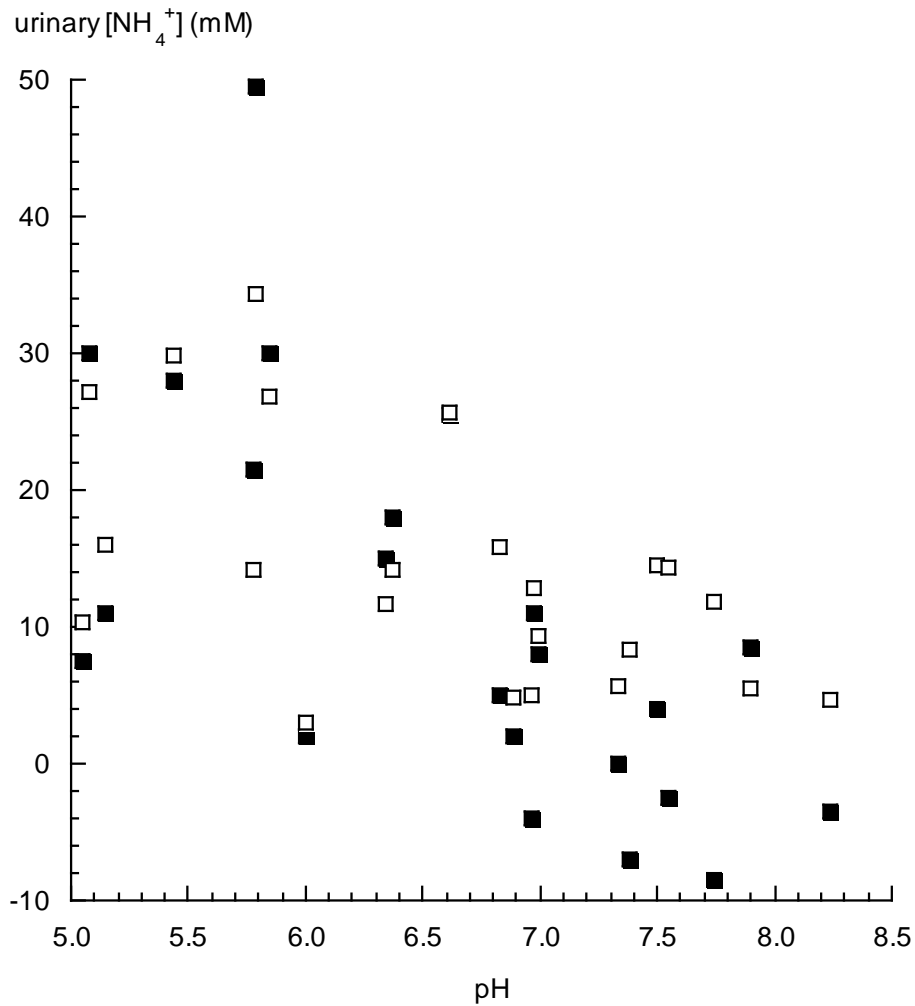


Figure 3.38. Calculated (closed symbols) and measured (open symbols) values of urinary [NH<sub>4</sub><sup>+</sup>] as a function of urine pH.

### 3.7.6 Urinary [NH<sub>4</sub><sup>+</sup>] in 'struvite' vs 'non-struvite' patients:

Analysis was performed on the sub-groups within patients attending for an operation at UCLH. The mean urinary [NH<sub>4</sub><sup>+</sup>] was unchanged (15.0, 15.3 and 15.2 mM) amongst the three sub-groups (those with various stones, previous struvite stones and those currently presenting with struvite stones).

Table 3.23. Urinalysis of patients with struvite and non-struvite stones.

Urine Sample	[NH <sub>4</sub> <sup>+</sup> ]	[K <sup>+</sup> ]	Voiding pH	Stone type	Current previous	Gender	Age
<b>Various stones</b>							
1	7.3	12.9	6.10	CaOx/CaPO <sub>4</sub>	current	F	26
3	44.1	72.3	5.65	Urate (99%) / CaOx	current	M	63
4	11.2	28.5	5.60	CaOx (100%)	current	F	34
5	24.6	50.6	5.68	Operation cancelled	-	M	54
6	18.8	45.4	5.64	CaOx (99%)/CaPO <sub>4</sub>	previous	F	55
13	14.2	51.0	7.55	CaOx/CaPO <sub>4</sub>	previous	F	48
14	16.3	44.6	6.85	CaOx (98%)/CaPO <sub>4</sub>	current	M	47
15	13.6	35.4	6.21	CaOx (97%)/CaPO <sub>4</sub>	current	M	52
16	11.1	44.4	6.85	no stone	previous	F	15
17	13.1	19.7	6.48	stones - cystinuria	previous	M	32
18	17.4	32.8	7.27	no stone	-	F	43
20	4.7	40.9	6.37	CaPO <sub>4</sub> (79%)/ CaOx	current	F	44
23	6.6	47.2	7.55	CaOx (89%) / CaPO <sub>4</sub>	current	M	40
24	6.5	71.3	6.96	Bladder TCC	-	M	60
<b>Mean</b>	<b>15.0</b>	<b>42.7</b>	<b>6.5</b>	-	-	-	<b>44</b>
<b>Previous Struvite</b>							
7	1.1	38.0	7.70	Struvite (13%)/CaPO <sub>4</sub>	previous	F	55
8	19.0	26.0	6.10	Struvite (80%)/CaPO <sub>4</sub>	previous	F	22
9	7.0	37.4	5.50	Struvite (36%)/CaPO <sub>4</sub>	previous	F	56
10	34.1	24.9	6.93	Struvite(27%)/CaPO <sub>4</sub>	previous	F	42
<b>Mean</b>	<b>15.3</b>	<b>31.6</b>	<b>6.6</b>	-	-	-	<b>44</b>
<b>Current Struvite</b>							
2	25.3	28.9	8.20	Struvite (22%)/CaPO <sub>4</sub>	current	M	67
11	14.8	22.0	8.52	Struvite (37%)/CaPO <sub>4</sub>	current	F	73
19	4.6	28.9	6.60	Struvite (7%)/CaPO <sub>4</sub>	current	F	48
21	18.8	11.2	8.10	Struvite (20%)/CaPO <sub>4</sub>	current	F	32
22	15.3	25.4	5.30	Struvite (37%)/CaPO <sub>4</sub>	current	M	47
12	12.5	22.0	6.97	Struvite (34%)/CaPO <sub>4</sub>	current	M	49
<b>Mean</b>	<b>15.2</b>	<b>23.1</b>	<b>7.3</b>	-	-	-	<b>53</b>

Urinary [K<sup>+</sup>] was lower in patients with previous / current struvite stones as compared to those with other stones. Mean pH was higher in patients with current / previous struvite stones (7.3 / 6.6) as compared to those with other stones (6.5). Five out of six patients with current struvite stones also presented with staghorn stones, and including those with previous struvite stones was eight out of ten. In ten of the total twenty four patients

cultures were performed on the stones. Four cultures were returned with a result other than ‘no growth’ and all were present within the group of patients with current struvite stones (one positive with *Strep milleri*, one with *Proteus*; one with fecal flora; and one culture showed mixed growth of doubtful significance).

### 3.8 Measurements with a $Mg^{2+}$ ion-selective electrode:

#### 3.8.1 Calibration of the $Mg^{2+}$ -selective electrode:

Typical calibration data for the  $Mg^{2+}$ -selective electrode in 140 mM NaCl buffered to pH 6.0 with 10 mM MES is shown in Table 3.24. All experiments are at 37°C. The concentration of Mg in the reaction chamber took into account any dilutional effect caused by adding significant volumes of  $MgCl_2$  solution during the calibration procedure.

Table 3.24: Sample  $Mg^{2+}$ -selective electrode calibration data in a medium containing 140 mM NaCl and 10 mM MES at pH 6.0. The values of  $E_{Mg}$  are offset to zero mV at the highest [Mg].

$[Mg^{2+}]$ added (mmol/l)	$[Mg^{2+}]$ in the chamber (mM)	$E_{Mg}$ , mV
0.1	0.10	-34.9
0.2	0.20	-32.8
0.4	0.40	-30.2
1	0.99	-25.8
2	1.96	-21.7
4	3.91	-17.5
10	9.73	-10.7
20	19.27	-5.3
40	37.81	0

Figure 3.39 shows the calibration plotted as a calibration curve and fit to the equation (see also section 3.1)

$$E_{Mg} = E^0 + m \log_{10}([Mg^{2+}] + k)$$

where  $E^0$  is a constant;  $m$  the slope ( $RT/zF$ ) factor and  $k$  a constant that is equivalent to the sum of the potentiometric selectivity constant to other ions, here mainly  $Na^+$ .

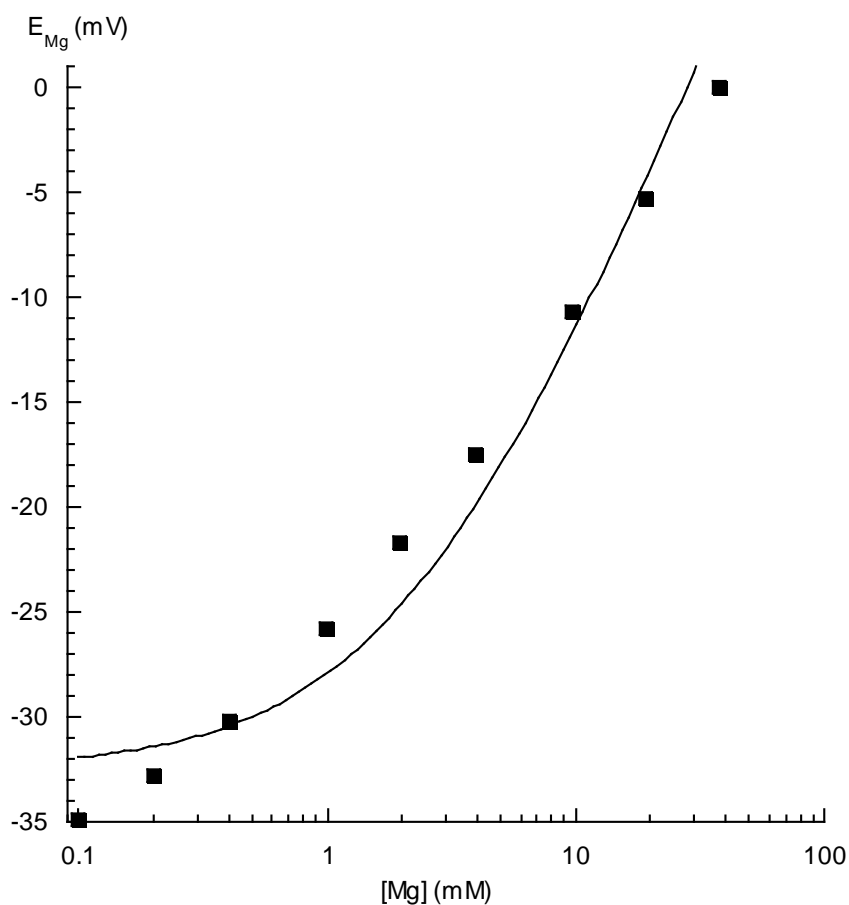


Figure 3.39. Sample calibration curve of a  $Mg^{2+}$ -selective electrode in 140mM NaCl and 10mM MES at pH 6.0.

In Figure 3.39 the value of  $m$  was set to 29 mV per 10-fold change of the  $[Mg^{2+}]$ . The calibration curve shows that the data were a relatively poor fit to the above equation.

This necessitated calculating carefully the potentiometric selectivity coefficients for different ions, and for each ion-selective electrode, and subtracting their effect from the overall electrode response at each experiment.

When used in the base solution of 140 mM NaCl, 10 mM MES the value of the potentiometric selectivity coefficient,  $k_{ij}^{\text{pot}}$  to  $\text{Na}^+$  expressed as the logarithm of the value,  $\log k_{\text{MgNa}}^{\text{pot}}$  was  $-1.59 \pm 0.15$ , i.e. the mean value of  $k_{\text{MgNa}}^{\text{pot}}$  was 0.025. This was calculated from 40 calibrations in the base solution.

### 3.8.2 Selectivity of the $\text{Mg}^{2+}$ -selective electrode and use of a $\text{Ca}^{2+}$ -selective electrode:

The most interferent ion was potentially  $\text{Ca}^{2+}$ , and its effect as well as the effect of  $\text{Na}^+$  and  $\text{K}^+$  were all estimated by the methods and procedures described in detail above (sections 3.1 and 3.2). Figure 3.40 shows examples of calibration curves of a  $\text{Mg}^{2+}$ -selective electrode in the absence and presence of 1 mM  $\text{CaCl}_2$ .

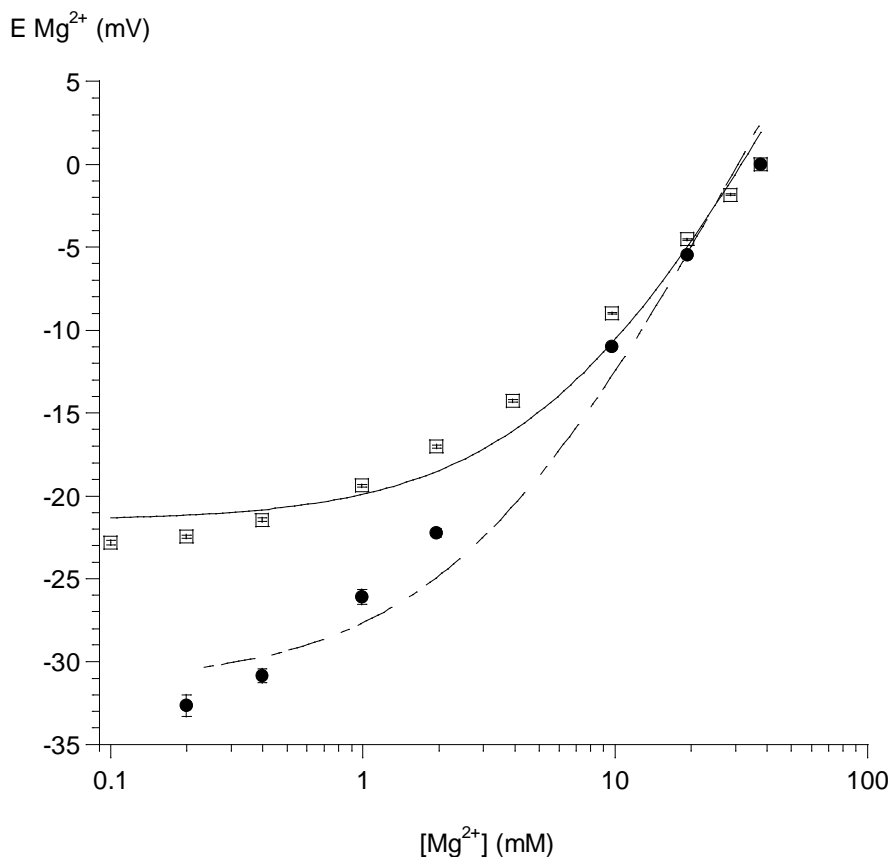


Figure 3.40. Mean calibration curves of the  $\text{Mg}^{2+}$ -selective electrode in 140mM NaCl and 10mM MES at pH 6.0, in the absence (closed symbols) or presence (open symbols) of 1 mM  $\text{CaCl}_2$ . Each determination was performed ten times. All calibrations were performed at  $37^\circ\text{C}$ . Error bars have been included for both curves.

The mean value of  $\log k_{\text{MgCa}}^{\text{pot}}$  as determined from ten experiments was  $0.66 \pm 0.02$ . A value less than unity means that the electrode is more selective to the ‘interferent’ ion than  $\text{Mg}^{2+}$ . As with  $\text{K}^+$  interference on the  $\text{NH}_4^+$  electrode, this necessitated separate measurement of the  $[\text{Ca}^{2+}]$  with a  $\text{Ca}^{2+}$ -ion-selective electrode, which was relatively unaffected by  $\text{Mg}^{2+}$ , to allow the interferent effect of varying  $[\text{Ca}^{2+}]$  on the electrode response to be subtracted.

Table 3.25 shows data for a  $\text{Ca}^{2+}$ -selective electrode

Table 3.25. Data for a sample calibration of a  $\text{Ca}^{2+}$ -selective electrode in 140 mM NaCl and 10 mM MES at pH 6.0. The values of  $E_{\text{Ca}}$  are offset to zero mV at the highest [Ca].

$[\text{Ca}^{2+}]$ added (mmol/l)	$[\text{Ca}^{2+}]$ in the chamber (mM)	$E_{\text{Ca}}$ , mV
0.2	0.20	-64.7
1	0.99	-49.1
2	1.96	-41
10	9.73	-19.7
20	19.3	-9.6
40	37.8	0

The data are plotted in Figure 3.41 and show a more selective response to the primary ion,  $\text{Ca}^{2+}$ , over this range. 40 calibrations were performed in 140 mM NaCl base solution and the  $\log k_{\text{CaNa}}^{\text{pot}}$  was  $-3.58 \pm 0.59$ , showing that the  $\text{Ca}^{2+}$ -selective electrode had good selectivity for  $\text{Ca}^{2+}$  over  $\text{Na}^+$ . Moreover, the calibration curve was unaffected by the presence of  $\text{MgCl}_2$ , 1-5 mM. Therefore the  $\text{Ca}^{2+}$ -selective electrode may be used to measure the  $[\text{Ca}^{2+}]$  in urine samples and used to subtract the interferent effect on the  $\text{Mg}^{2+}$ -selective electrode response.

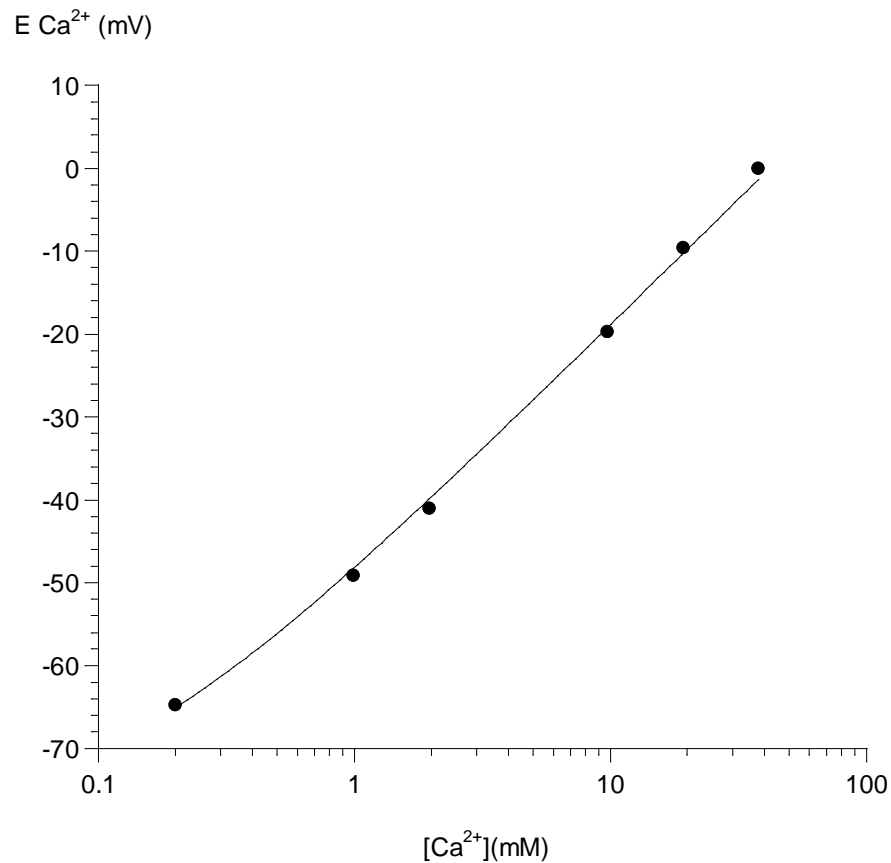


Figure 3.41. Sample calibration curves of a  $\text{Ca}^{2+}$ -selective electrode in 140mM NaCl and 10mM MES at pH 6.0. The line is calculated through the data points as in figure 3.38

Figures 3.42 shows the response of the electrode to inclusion of a large [K] in the calibrating solution (200 mM). The data show that the  $\text{K}^+$  interference is about the same as that from  $\text{Na}^+$ .

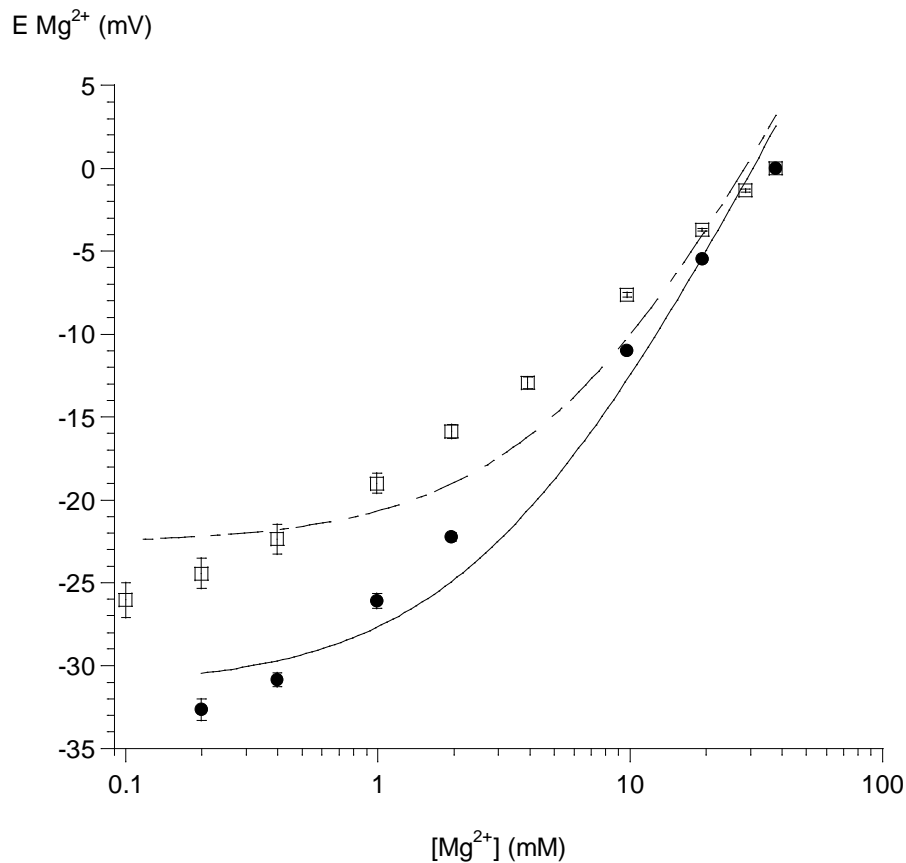


Figure 3.42. Mean calibration curves of a  $\text{Mg}^{2+}$ -selective electrode in 140mM NaCl and 10mM MES in the absence (closed circles) and presence (open circles) of 200 mM KCl. The lines are calculated through the data points as in figure 3.38. Determinations were performed 3 times at 37°C, error bars are shown for both curves.

The calibration was carried with a high concentration of K as with smaller concentrations, up to 50 mM, and significant interferent effect was not consistently observed.

Table 3.26 shows a summary of the interference estimations to  $\text{Ca}^{2+}$ ,  $\text{Na}^{+}$  and  $\text{K}^{+}$  from the above experiments.  $\text{Ca}^{2+}$  is the most interferent ion and requires monitoring along with

the use of the  $Mg^{2+}$ -selective electrode. Although significant, the effects of  $Na^+$  and  $K$  were more than two orders of magnitude smaller. In subsequent measurements averaged values of the  $[Na]$  and  $[K]$  were used in the Nikolsky equation to subtract away interferent effects of these ions.

Table 3.26 Values of the  $\log k_{ij}^{pot}$  (mean  $\pm$  sd,  $n=10$ ) for the  $Mg^{2+}$ -selective electrode in the presence of  $Ca^{2+}$ ,  $Na^+$  and  $K^+$  as interferent ions. The mean value of  $\log k_{ij}^{pot}$  is transformed to  $k_{ij}^{pot}$  and  $1/k_{ij}^{pot}$  values. The value is  $1/k_{ij}^{pot}$  a measure of the fold-selectivity for  $Mg^{2+}$  over the interferent ion.

Interferent ion	$Mg^{2+}$ -ISE (room temperature)		
	$\text{Log } k_{ij}^{pot}$	$k_{ij}^{pot}$	$1 / k_{ij}^{pot}$
$Na^+$	$-1.59 \pm 0.15$	0.025	39.35
$Ca^{2+}$	$0.66 \pm 0.02$	4.532	0.22
$K^+$	$-1.50 \pm 0.08$	0.031	31.82
$H^+$	$2.71 \pm 0.05$	517.261	0.002

Figure 3.43 shows the effect of a pH change on the  $Mg^{2+}$ -selective electrode response.

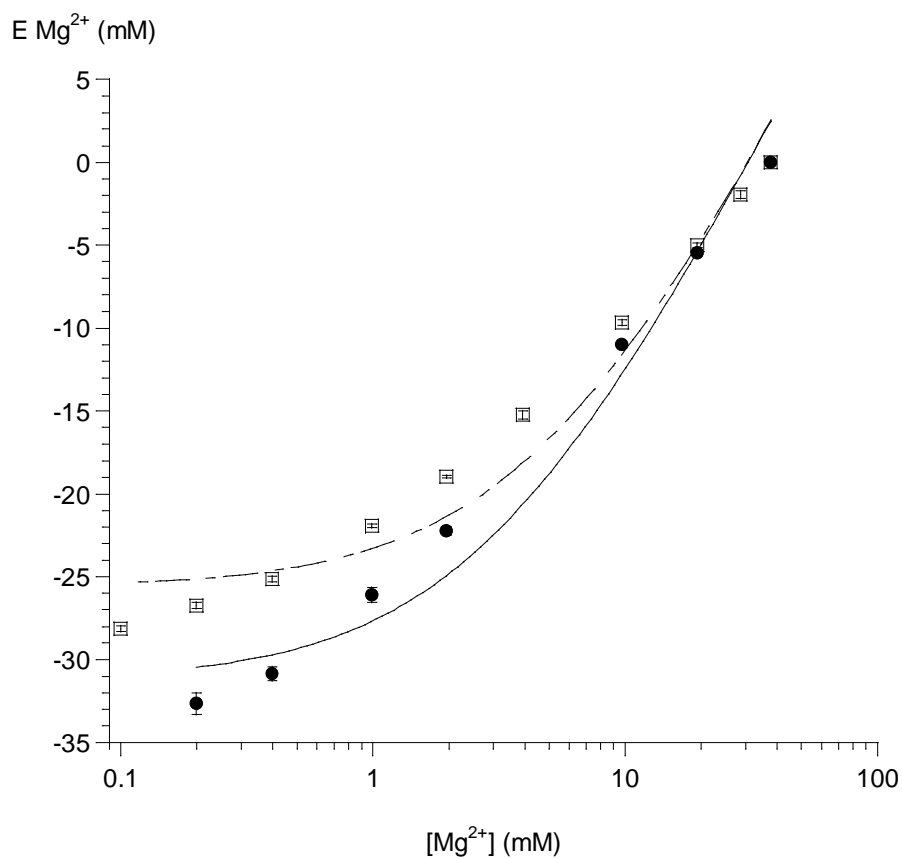


Figure 3.43 Sample calibration curves of a  $\text{Mg}^{2+}$ -selective electrode in 140mM NaCl and 10mM MES at control pH (6.0, closed circles) and at pH 5.5 (open squares). The lines are calculated through the data points as in figure 3.38. Each determination was performed three times at 37°C. Error bars are shown for both curves.

### 3.8.3 Values of urinary $[Mg^{2+}]$ :

Table 3.27 shows values of urinary  $[Mg^{2+}]$  as estimated using the  $Mg^{2+}$ -selective electrode at voided pH and after titration to pH 6.0. Reliable experiments using urine samples of 14 separate subjects were possible. Median values and 25%, 75% interquartiles are quoted because of the large variation of data.

Table 3.27. Values of urinary  $[Mg^{2+}]$  at voided pH and after adjustment to pH 6.0.

Urine sample	$[Mg^{2+}]$ , mM voided pH	$[Ca^{2+}]$ mM voided pH	$[Mg^{2+}]$ mM pH 6.0	$[Ca^{2+}]$ mM pH 6.0	Urinary $[Na^+]$ mM	Urinary $[K^+]$ mM	Urinary osm mOsm	Urinary [creat] mM	Voided pH
1	1.3	0.3	3.4	0.2	14	6	64	895	6.10
2	37.4	0.2	16.7	0.1	62	77	668	8488	5.64
3	7.1	0.02	9.4	0.1	26	52	249	3235	7.70
4	13.9	0.002	9.0	0.03	55	46	440	10419	5.50
5	4.9	0.2	11.6	0.7	58	36	439	11313	6.93
6	9.0	0.0	15.0	0.005	45	36	289	6564	8.52
7	21.5	0.4	14.9	0.6	44	74	544	11281	6.85
8	14.5	1.4	19.2	0.4	145	56	584	5881	6.85
9	11.3	0.4	10.4	0.2	47	14	257	3944	6.48
10	7.5	0.8	14.7	1.9	95	37	510	7731	7.27
11	3.5	0.4	11.5	0.8	69	44	430	6119	6.37
12	3.2	0.0	57.6	0.2	46	33	352	2981	8.10
13	8.7	0.3	21.8	1.0	107	59	521	9769	7.55
14	14.9	0.1	19.7	0.4	96	103	265	8604	6.96
Median	8.9	0.25	14.8	0.3	56.5	45	434.5	7148	6.89
25, 75% interquartiles	5.5, 14.4	0.04, 0.4	10.7, 18.6	0.13, 0.68	45.3, 88.5	36, 58.3	271, 518.3	4428, 9478	6.40, 7.48

There was no significant association between the value of  $[\text{Mg}^{2+}]$  and voided pH. However, a paired non-parametric rank test (Kruskal-Wallis) indicated that the values  $[\text{Mg}^{2+}]$  were marginally significantly greater ( $p=0.048$ ) when the pH was titrated to 6.0.

Figure 3.44 plots the change of the  $[\text{Mg}^{2+}]$ ,  $\Delta[\text{Mg}^{2+}]$ , as a function of the change of pH,  $\Delta\text{pH}$  required to bring the value to  $\text{pH}=6.0$  – negative  $\Delta\text{pH}$  values indicate the urine was alkalinized. In this plot the data pair for sample 12 in Table 3.27 was omitted. There was a significant association ( $r^2=0.324$ ,  $p=0.042$ ), indicating that acidifying the urine ( $+\Delta\text{pH}$ ) increased the  $[\text{Mg}^{2+}]$ , probably by increasing the ionized fraction of the total urinary  $[\text{Mg}]$ .

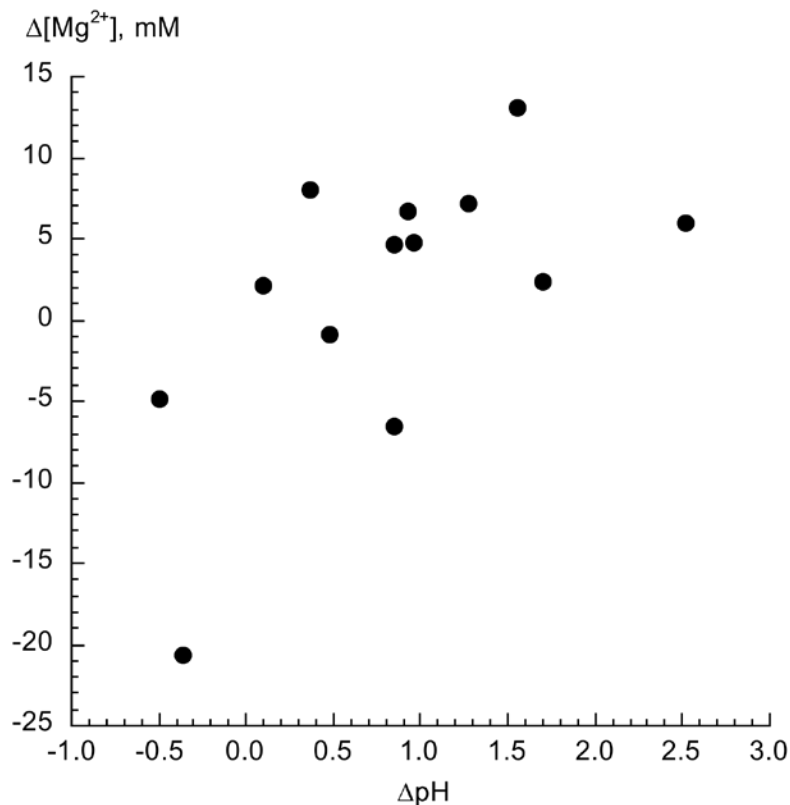


Figure 3.44. Values of  $\Delta[\text{Mg}^{2+}]$  as a function of  $\Delta\text{pH}$  as urine pH is normalized to  $\text{pH}=6.0$  from the voided value. Negative values indicate urine was alkalinized to achieve  $\text{pH}=6.0$ .

## **CHAPTER 4**

### **DISCUSSION**

#### **4.1 URINARY TRACT STONES**

##### 4.1.1 The clinical problem.

Urolithiasis is a common disorder, with calcium oxalate / phosphate stones being the commonest type and 10% of Caucasian men developing a kidney stone by the age of 70. The peak incidence is between age 20 and 40, with males more commonly affected than females (Finlayson, 1974) and a family history of stones increases the likelihood of stones (Curhan et al, 1997) Renal stones are rare in black Americans, black Africans, native-Americans and Australian aborigines in comparison to Asians and Caucasians. This high incidence of renal stones is exemplified by their occurrence in the United States, the British Isles, Scandinavian countries, Mediterranean countries and central Europe (Finlayson, 1974) and in addition are more common in hot climates (Prince et al, 1960). Crystalluria has been shown to be greater during the summer months (Hallson et al, 1977) due to increased sweating, during high temperatures, leading to concentrated urine and urinary crystal formation.

Increased incidence of renal calculi is associated with a more 'affluent' diet (increased animal protein, refined sugar and salt and a lack of dietary fibre is also thought to contribute to stone formation (Robertson et al, 1978). Most importantly, a low fluid intake predisposes to stone formation and an increased water intake causes urinary dilution of the constituents that may precipitate as well as reducing the average time of residence of free crystal particles in the urine (Finlayson, 1974). Sedentary

occupations (Lonsdale, 1968) and stress (Najem, 1997) have also been associated with stone disease.

#### 4.1.2 Struvite stones:

Struvite stones pose a significant clinical problem and are often found in staghorn calculi, which can grow rapidly. Untreated staghorn calculi can destroy the kidney and result in life-threatening sepsis (Griffith, 1978; Ganpule et al, 2008) and are often associated with pain, haematuria and infection (Singh et al, 1973). Conservative treatment, with a mean follow-up of 7.8 years, was used in 61 patients with staghorn calculi (Koga et al, 1991), with chronic renal failure developing in 22 cases and 7 deaths from uraemia. Other complications included severe hydronephrosis, renal abscess and xanthogranulomatous pyelonephritis, with early stone removal being advised. Lechevallier et al (2008) also advocate no role for conservative treatment of staghorn stones. Nephrectomy was considered the treatment of choice, particularly in unilateral large stones in older patients (Moore et al, 1976). Extended pyelolithotomy was shown to be a safe and appropriate form of treatment of unilateral staghorn stones, without compromising the contralateral kidney and that even with incomplete clearance regrowth of stone within the kidney was not an inevitability (Woodhouse et al, 1981). More recently, the main mode of therapy for staghorn calculi has been percutaneous nephrolithotomy (PCNL) (Saad et al, 1993) and combination therapy with extracorporeal shock wave lithotripsy (ESWL) (Lam et al, 1992). The American Urological Association nephrolithiasis guidelines panel recommended a combination of percutaneous stone removal and shock wave lithotripsy (Segura et al, 1994). Current European Association of Urology Urolithiasis guidelines (EAU Guidelines) recommend PCNL, ESWL and then laparoscopic or open surgery. However, open

surgery is still recommended for the management of complex staghorn stone disease, particularly in developing countries, due to high patient load and limited resources (Agrawal et al, 2009). Honeck et al (2009) also suggested that open stone surgery still plays an important role in the management of complex stones with high stone burden and anatomical variations.

Sepsis syndrome (McAleer et al, 2002), perinephric abscess (Tsukagoshi et al, 2006) and increased recurrence rates (Grenabo et al, 1985) are serious clinical manifestations of struvite stone formation.

Renal impairment is often associated with staghorn calculi (Vargas et al, 1982; Kristensen et al, 1987). An accelerated rate of loss of creatinine clearance has been shown among stone formers in general as compared to normal subjects (Worcester et al, 2003; Worcester et al, 2006) with kidney loss being frequently associated with struvite stone cases or very large stones.

Long-term catheterisation carries an increased risk of urinary tract infection and catheter encrustation (blockage) and can create a huge constant demand on hospital and community health services. Struvite and hydroxyapatite deposition have been identified in catheter encrustation (Cox, 1989; Morgan, 2009). Ureteric stent encrustation is less commonly associated with infection (Shaw et al, 2005) and is most commonly composed of calcium oxalate

The metabolic syndrome has also been associated with stone formation (West et al, 2008). Uric acid nephrolithiasis has particularly been associated with the metabolic

syndrome and a low urinary pH due to defective urinary  $\text{NH}_4^+$  excretion (Sakhaee et al, 2008a).  $\text{NH}_4^+$ -selective electrodes would again provide a useful tool in monitoring such patients.

Struvite stones are composed of magnesium ammonium phosphate, and account for 5-20% of all urinary stones (Griffith, 1978; Sharma et al, 1989). They are thought to be associated with urinary tract infections caused by 'urease' secreting bacteria (Griffith, 1978; Bichler et al, 2002).

For struvite to form, fluid within the urinary tract must contain  $\text{NH}_4^+$  and trivalent phosphate ions ( $\text{PO}_4^{3-}$ ) at the same time. Struvite forms only under abnormal physiological conditions, because renal tubules only generate  $\text{NH}_4^+$  when the organism is trying to excrete an acid load and trivalent phosphate is almost absent in acid urine. Non-physiological conditions, created by urease-secreting bacteria, are generally required for struvite to precipitate. The alkalinisation of urine by the urease reaction causes the formation of  $\text{NH}_4^+$ , as well as carbonate ions ( $\text{CO}_3^{2-}$ ), and also the formation of  $\text{PO}_4^{3-}$ . This environment in turn causes struvite and carbonate apatite formation (Rodman, 1999; Miano et al, 2007). However Rodman (1999) suggested that struvite could also form in the absence of urea-splitting bacteria, since it has been possible to form struvite crystals *in vitro* in acidic solutions (pH 6) even though the morphology of the resultant crystals was slightly different, suggesting that a different set of physico-chemical conditions was present to cause crystallisation. At present, very little is known about the physico-chemical conditions that result in struvite crystallisation. This lack of understanding has two bases: i) the particular ionised concentrations of the reactants (e.g.  $\text{Mg}^{2+}$ ,  $\text{NH}_4^+$ , and phosphate) in the urine are unknown; ii) the prevailing chemical conditions that would modulate crystallisation are also unclear (e.g. pH, osmolality, other urinary constituents). Urinary pH is determined by many different factors and there is a complex buffering system, involving various different buffers. However it is only urinary  $\text{NH}_4^+$ , along with  $\text{Mg}^{2+}$ , and phosphate that will eventually determine whether struvite crystals form. Through determining the actual urinary  $[\text{NH}_4^+]$ , we can further understand the

relationship between urinary pH and  $[\text{NH}_4^+]$ , as well as the impact of other buffering systems. Recent advances in the development of ion-selective electrodes allows accurate determination of urinary constituents in small (<1ml) undiluted samples to better understand the physico-chemical basis for struvite crystallisation, as well as provide us with a tool for monitoring patients who are recurrent struvite stone formers.

## 4.2 CHARACTERISATION OF THE $\text{NH}_4^+$ ELECTRODE:

### 4.2.1 The $\text{NH}_4^+$ -selective electrode:

The  $\text{NH}_4^+$ -selective ligand studied previously for use in ion-selective electrodes has been the natural antibiotic nonactin, incorporated into plasticised poly(vinyl chloride) (PVC) membranes (Buhlmann et al, 1998). The main problem has been selectivity of the ligand for  $\text{NH}_4^+$  over  $\text{K}^+$  ions. Various attempts at improving selectivity by varying the amount of nonactin and using different plasticisers were made in order to improve the conductivity of  $\text{NH}_4^+$  ions through the membrane (Ghauri et al, 1994).

The  $\text{NH}_4^+$ -ion-selective electrode used in these studies was made of Ammonium Ionophore I, nonactin (1% w/w; ETH 09877 – Fluka) with  $\geq 95\%$  purity of the primary agent; CAS (Chemical Abstracts Service) number 6833-84-7.

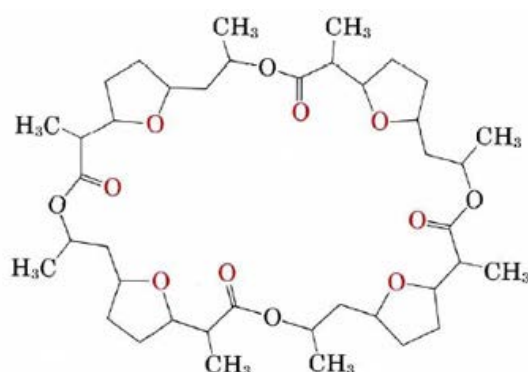


Figure 4.1. The structure of nonactin (<http://chemed.chem.wisc.edu>)

The agent is a ring-shaped molecule with a central region that can accommodate  $\text{NH}_4^+$  by interacting with the eight inward-facing oxygen atoms.

To enable the ionophore to be distributed evenly in the PVC matrix and render the plastic supple and therefore less prone to fracture a plasticiser is used: in this case it was bis(2-ethylhexyl) sebacate (CAS number 122-62-3).

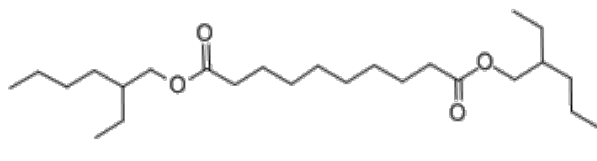


Figure 4.2. The structure of bis(2-ethylhexyl) sebacate

With this combination, the electrode behaved in a reasonably Nernstian fashion within an  $[\text{NH}_4^+]$  range, commonly seen and expected to include values found in urine (0.4–50 mM). Calibration of the electrode in 140 mM NaCl (buffered to pH 6.0) at 37°C produced a mean slope of 53.8mV per decade (10-fold change of the primary ion concentration) between 2 mM and 20 mM  $\text{NH}_4\text{Cl}$  concentrations. This increased to 56.8mV when the range of  $\text{NH}_4\text{Cl}$  concentrations was 4-40 mM. The ideal slope for a monovalent cation should be 61.5mV per decade at 37°C.

At 25°C, the mean slope was 52.2mV per decade between 2-20 mM  $\text{NH}_4\text{Cl}$  and 51.7mV per decade between 4-40 mM  $\text{NH}_4\text{Cl}$  concentrations. The ideal slope should be 59.1mV at 25°C. Our values obtained compared favourably with previously studied  $\text{NH}_4^+$ -selective electrodes which have been reported to have slopes between 51.0 and 57.5 mV per decade at 25°C (Guibalt et al, 1969; Ghauri et al, 1994).

An important factor in the sensitivity of ion-selective electrodes is the type of plasticiser used and for this bis(1-butylpentyl)adipate (CAS: 77916-77-9) was also utilised. This molecule is similar in being a long chain hydrocarbon with several coordinating oxygen atoms as the plasticiser and found that there was no real significant difference in the way the electrodes responded.

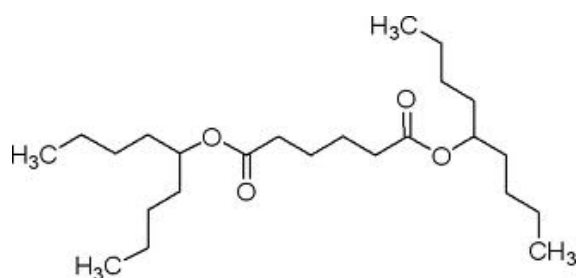


Figure 4.3. The structure of bis(1-butylpentyl)adipate

The main limitation has been that although nonactin-based ion-selective electrodes have reasonable  $\text{NH}_4^+/\text{Na}^+$  selectivity there is poorer selectivity over  $\text{K}^+$ . One study found mean values for  $\log k_{\text{NH}_4\text{Na}}^{\text{pot}} = -2.4$  and for  $\log k_{\text{NH}_4\text{K}}^{\text{pot}} = -0.9$  (Benco et al, 2003). This study showed comparable selectivity over  $\text{Na}^+$  and  $\text{K}^+$  ( $\log k_{\text{NH}_4\text{Na}}^{\text{pot}} = -2.61$ ; and  $\log k_{\text{NH}_4\text{K}}^{\text{pot}} = -0.85$ ).

There have been other attempts to develop new synthetic ionophores with higher  $\text{NH}_4^+$  selectivity. The selectivity of the ionophore has been attributed to its tetrahedral geometry and its ability to donate four hydrogen bonds to stabilise the cation. Benco et al (2003) synthesised ‘ammonium ionophore IV’ incorporating hydrogen bond donors in tetrahedrally symmetric complexation sites. They used nitrophenyl octyl ether (NPOE) and dioctyl phthalate (DOP) as the plasticisers. They also investigated the effect of a lipophilic ionic additive, potassium tetrakis(4-chlorophenyl)borate

(KtpCIPB), which was added to two of the four preparations. Their study showed two main effects: firstly the NPOE plasticiser consistently produced slopes closest to Nernstian conditions as compared to DOP, and this was attributable to the higher polarity that NPOE imparts to the membrane, thus reducing intramolecular hydrogen bonding and allowing for more efficient  $\text{NH}_4^+$  complexation (Gallo et al, 1993). Secondly the addition of KtpCIPB resulted in significant deviation from Nernstian behaviour and reduced the selectivity, particularly over the divalent cations. The use of KtpCIPB in the  $\text{NH}_4^+$ -selective electrodes used in this study was also avoided for the above reason. Overall the above studies showed that optimum electrode characteristics were obtained with NPOE as a plasticiser and omission of KtpCIPB. The response to  $\text{NH}_4^+$  over  $\text{Na}^+$  or  $\text{K}^+$  produced somewhat inferior values of  $\log k_{\text{NH}_4\text{Na}}^{\text{pot}}$  (-2.1) and  $\log k_{\text{NH}_4\text{K}}^{\text{pot}}$  (-0.6). As with the electrodes used in this study excellent selectivity over divalent cations ( $\text{Ca}^{2+}$  and  $\text{Mg}^{2+}$ ) was shown. Thus, although this study slightly improved on the selectivity characteristics of an  $\text{NH}_4^+$ -selective electrode over common divalent cations, interference by  $\text{K}^+$ , in particular, requires its separate determination to account for any interferent effects.

Our study also showed that the  $\text{NH}_4^+$ -selective electrode showed equivalent Nernstian responses over wide range of pH variation (5.5, 6.5, and 7.5), and in effect interference from  $\text{H}^+$  ions was not detectable. The importance of the pH-dependence of  $[\text{NH}_4^+]$  in urinary samples will be discussed below.

The osmolality and ionic strength of urine varies greatly. Therefore the sensitivity and selectivity of the  $\text{NH}_4^+$ -selective electrode was tested in solutions of varying osmolalities and differing ionic activities to determine if these affected the ISE

response. Since the values of  $\log k_{NH_4Na}^{pot}$  in the different solutions were not significantly different from the value in base solution, it may be concluded that solution ionic strength and osmolality *per se* had no effect on the  $NH_4^+$ -selective electrode response.

#### 4.2.2 $K^+$ -selective electrode:

In view of the interference caused by  $K^+$  ions on the  $NH_4^+$ -selective electrode, it was necessary to measure urinary  $[K^+]$  to subtract the interferent contribution from the electrode response and thus measure accurately the urinary  $[NH_4^+]$ . A  $K^+$ -selective electrode was constructed and characterised. Valinomycin was used as a  $K^+$ -selective ionophore and has been used previously to measure  $[K^+]$  in urine and blood samples.

The valinomycin  $K^+$ -selective electrode showed a Nernstian response, with a mean slope of 54.4 mV per decade at 37°C. This value was similar to others reported in similar  $Na^+$ -based calibration solutions; – between 57.3 and 59.7mV (Band et al, 1978; Hill et al, 1978; Jenny et al, 1980).

The  $K^+$ -selective electrodes were calibrated in the presence of different potentially interferent ions. Interference from  $Na^+$  ions was negligible and the interference from  $NH_4^+$  ions was minimal (mean  $\log k_{KNa}^{pot} = -2.91$ ; mean  $\log k_{KNH_4}^{pot} = -1.63$ ). Despite the small interference from  $Na^+$ , because of the potentially high  $[Na^+]$  any effect was factored out. The value of  $\log k_{KNa}^{pot}$  means that the  $K^+$ -selective electrode was 819 times more selective for  $K^+$  ions than  $Na^+$  ions. An upper limit of the urinary  $[Na^+]$  150 mM was assumed and was equivalent to an apparent change of  $[K^+] = 0.18$  mM. This value was subtracted from the calculated values of  $[K^+]$  to obtain the final quoted

value and that used to correct the  $\text{NH}_4^+$ -selective electrode estimation. This in turn led to a correction of the  $[\text{NH}_4^+]$  of 0.01 – 1.16 mM over the quoted range of values between 0.4 and 50 mM).

These experiments also showed that there was no detectable interference from  $\text{Ca}^{2+}$  on the  $\text{K}^+$ -selective electrode, nor was the electrode affected by changes to pH, ionic activity or osmolality of the calibrating solution.

### **4.3 URINARY MEASUREMENT OF $\text{NH}_4^+$**

#### 4.3.1 Values of urinary $[\text{NH}_4^+]$ at room temperature

This study has made the first measurements of urinary  $[\text{NH}_4^+]$  with an ion-selective electrode. The study had several aims:

- to determine any effect of pH and temperature on urinary  $[\text{NH}_4^+]$
- to determine if the urinary  $[\text{NH}_4^+]$  was different in control subjects and those with urinary tract stones.

The method also provided a more rapid and cost-effective method than those previously used.

From 28 normal subjects, the urinary  $[\text{NH}_4^+]$  and  $[\text{K}^+]$  were  $26.6 \pm 11.5$  and  $44.8 \pm 16.9$  mM respectively. The ranges of values were 8.7-55.2 and 12.4-77.6 mM respectively. The pH of the samples was  $5.96 \pm 0.76$  (range 4.97-7.33).

The results showed that there was no relationship between urinary  $[\text{NH}_4^+]$  and  $[\text{K}^+]$ . By comparing different methods of storage of the urine samples, it was also demonstrated that storing samples in a freezer did not significantly alter the urinary

[NH<sub>4</sub><sup>+</sup>]. Paired *t*-test analysis also showed no significant difference for urinary [K<sup>+</sup>] however, one sample showed a very large increase after seven days, thus skewing the data set and a Wilcoxon rank test did show a significant difference (*p*=0.04) between the two data sets. A larger data set will be required to determine if the seven days frozen storage does lead to an increase of urinary [K<sup>+</sup>], since only 7 samples were tested. There was no obvious cellular material in the urine samples and so the increase of urinary [K<sup>+</sup>] if real is unlikely to result from cell lysis as a result of storage.

Since storage at room temperature did not significantly alter the urinary [NH<sub>4</sub><sup>+</sup>] it was therefore possible to transport urine samples from distant centres and store them by freezing the specimens. This allowed the urinary [NH<sub>4</sub><sup>+</sup>] and [K<sup>+</sup>] to be measured later without the problem of concentrations altering with storage.

#### 4.3.2 Comparison with other methods

The above values are similar to other reported values. Miller et al (2000) tested for abnormalities in acid-base regulation in hypertensive patients. They compared indices of urinary acid secretion, which included urinary pH and urinary [NH<sub>4</sub><sup>+</sup>], in hypertensive compared to normotensive patients. The measurement of urinary [NH<sub>4</sub><sup>+</sup>] was based on the Berthelot reaction, a method to detect nitrogen content of samples and often also used for the detection of urea by producing a blue dye formed NH<sub>3</sub> in the presence of Na phenate and Na nitroprusside (Bergquist and Searcy (1963). Samples required dilution to 1/20 with distilled water and a standard curve of ammonium chloride was prepared in double-distilled water. Phenol nitroprusside reagent was added to sample and standard tubes. After further stirring, alkaline hypochlorite solution was added and the solutions placed in a water bath (37°C) for 40 min. After adding a further 1 ml of distilled water, samples and standards were

measured by absorption spectrophotometry at 630 nm. The urinary  $\text{NH}_4^+$  excretion rate was  $24.6 \pm 7.7$  in the normotensive group and  $23.1 \pm 10.2$  mmol/24h in the hypertensive group, concentrations were not reported.

Other methods of measuring urinary ammonium are even more labour-intensive and more amenable to error. These include the glutamate dehydrogenase method to measure urinary  $[\text{NH}_4^+]$  (Abate et al, 2004).

Gravimetric measurements have also been previously used to estimate urinary  $[\text{NH}_4^+]$ . This has involved precipitating the  $\text{NH}_4^+$  out of solution using sodium tetraphenylborate. The solid precipitate, ammonium tetraphenylborate is then filtered out, washed and dried to remove any moisture. The precipitate is then weighed and the amount of ammonium in the original sample can then be calculated from the mass of the precipitate and its chemical composition or analysed by spectrophotometry (Kiss-Eröss et al., 1970). However, the method is unreliable as tetraphenylborate also precipitates  $\text{K}^+$  which must be excluded from the final analysis.

Cunarro et al (1974) compared four different methods for measuring urinary  $[\text{NH}_4^+]$ .

i) The Conway microdiffusion technique involved placing urine in the outer chamber of a Conway microdiffusion dish, with  $\text{K}_2\text{CO}_3$  on the opposite side and boric acid (with bromocresol green) in a central chamber. The  $\text{K}_2\text{CO}_3$  and urine were mixed, followed by back titration with  $\text{H}_2\text{SO}_4$ . The urinary  $[\text{NH}_4^+]$  was calculated from the amount of  $[\text{H}^+]$  used. This technique is a variant used by others to detect  $[\text{NH}_4^+]$  by mixing samples with phenol and hypochlorite (Russell, 1944).

ii) An ammonia specific electrode is a gas detecting electrode which responds to the partial pressure of dissolved ammonia gas, and related to the concentration of ammonia using Henry's law (the amount of a given gas dissolved in a given type and volume of liquid is directly proportional to the partial pressure of that gas in that liquid). All the  $\text{NH}_4^+$  in the solution is first converted to  $\text{NH}_3$ , by the addition of NaOH to elevate the pH to 13. Measurements are conducted immediately since ammonia gas is lost once alkali is added.

iii) A further method, formalin-titrimetric method (see Ninan et al., 1990), requires that a 10 ml urine sample is mixed with an equivalent volume of HCl, and all dissolved  $\text{CO}_2$  is removed using a vacuum. Titration to pH 7.4 is performed using NaOH and titratable acidity calculated. Formaldehyde solution is then added to the mixture and again titration to pH 7.4 is performed with NaOH, and the  $[\text{NH}_4^+]$  calculated from the amount of NaOH used.

iv) Finally the Berthelot reaction, as described above was also used.

Two different urine samples were analysed six times by each technique for comparison of the four methods of measuring urinary  $[\text{NH}_4^+]$ . The study concluded that the methods were fairly specific for urinary  $\text{NH}_4^+$ . However, the speed of each of the techniques varied greatly. It was suggested that in an eight-hour working day, a maximum of 50 determinations could be performed using the Conway technique and formalin-titration method, 100 determinations with the ammonia electrode, and possibly 200 determinations with the Berthelot reaction. However, this output would be labour- and equipment-intensive and this represent a significant investment.

The advantages of the potentiometric ion-selective electrode technique used in this study was the ability to make immediate and accurate determinations of urinary  $[\text{NH}_4^+]$ . The apparatus took about 20 minutes to prepare, including time for baseline calibrations. To perform a determination on an individual urine sample required only two minutes, including the time for washing out the chamber before and after the determination, making this technique very fast to perform. Most importantly, the urine samples are undiluted, meaning there was less chance of errors being introduced.

Szmidt-Adjide et al (2008) investigated an enzymatic method for measuring urinary  $[\text{NH}_4^+]$  using a particular ammonium reagent on an Olympus (R) AU 2700 analyzer. They showed a good correlation between this method and results obtained from a formula calculation based upon the modified urine osmolal gap (Hafen et al., 1996). However, a potential error introduction was again the fact that urine samples were diluted to 1/100. Furthermore, a brief search for the price of an Olympus AU 2700 analyzer revealed that it cost \$272,000. In contrast, ion-selective electrodes are cheap to produce, fairly robust and require very little maintenance. The set-up cost for ion-selective apparatus is fairly low and many hundreds / thousands of electrodes may be produced at a time again at very low cost.

#### **4.4 VALIDATION OF THE $\text{NH}_4^+$ -SELECTIVE ELECTRODE FOR USE IN URINE**

To ensure that the use of an ion-selective electrode method provided a reliable and accurate measurement of urinary  $[\text{NH}_4^+]$  it was necessary to validate it against an established method. The choice of a standardised method was problematical due to

the fact that urinary  $[\text{NH}_4^+]$  is not routinely measured. A conventional spectrophotometric assay was chosen (Weatherburn, 1967) as it was well-validated in different settings and available. The method measures urinary  $[\text{NH}_4^+]$  using a phenol-hypochlorite reaction detection method and urine samples were diluted (1/80) and centrifuged. The supernatant was then incubated for three hours in a solution containing phenol. The resulting blue colour of the solution was interpreted using spectrophotometric absorption against a standard curve. The whole process took about four to five hours to perform.

A good correlation between the two methods was demonstrated, which confirmed that an ion-selective electrode method to measure urinary  $[\text{NH}_4^+]$  was accurate, but also demonstrated several other advantages over colour spectrophotometry:

- ion-selective electrodes are cheap, robust, and easily produced. Their within batch and between batch reproducibility is very good and many electrodes can be produced in a single batch. The greatest cost is the ion-selective ionophore itself, but this is small compared to the cost of the equipment required for colour spectrophotometry.
- ion-selective electrodes produce an instant reading, so that individual reading can be checked, whereas colour spectrophotometry requires four to five hours before data are available.
- a single ion-selective electrode may be used on multiple occasions and over days and weeks. The ability to carry out rapid and instant calibrations combined with the longevity of the electrode ensures reproducible and consistent responses..

- ion-selective electrodes may be used with undiluted urine samples. By contrast colour spectrophotometry requires that the urine is diluted. This may not only introduce inaccuracies, but will also change the chemical environment of the measured ion i.e. dilute also other moieties that affect the value of the primary ion.
- ion-selective electrodes measure the ionised fraction of the ion in solution. Other analytical techniques, including colour spectrophotometry, measure both the bound and freely ionised fraction and thus do not estimate the chemically/biologically active fraction.

#### **4.5 URINARY MEASUREMENT OF $[\text{NH}_4^+]$ AT $37^\circ\text{C}$**

Many of the measurements of urinary  $[\text{NH}_4^+]$  in this thesis were carried out at room temperature because validation against more standardised techniques are also performed under this condition. However, to understand the more physiological conditions under which struvite stone formation occurs, measurements were also carried out at  $37^\circ\text{C}$ . Both the  $\text{NH}_4^+$ - and  $\text{K}^+$ -selective electrodes were therefore characterised at  $37^\circ\text{C}$  to determine the temperature-dependence of the potentiometric selectivity coefficients.

##### **4.5.1 Characterisation of the $\text{NH}_4^+$ -selective electrode at $37^\circ\text{C}$ :**

At lower  $\text{NH}_4\text{Cl}$  concentrations in the calibration solution, the curve relating concentration to potential difference generated by the  $\text{NH}_4^+$ -selective electrode at  $37^\circ\text{C}$  deviated more than at room temperature from an ideal Nernstian relationship. This indicated that interference from  $\text{Na}^+$  was greater at the elevated temperature.

However the true interference was still negligible as suggested by a the mean  $\log k_{\text{NH}_4\text{Na}}^{\text{pot}}$  value of  $-2.40 \pm 0.11$ .

$\text{K}^+$  interference was also greater on the  $\text{NH}_4^+$ -selective electrode at  $37^\circ\text{C}$  compared to room temperature calibrations. The  $\log k_{\text{NH}_4\text{K}}^{\text{pot}}$  was significantly smaller at  $-0.68 \pm 0.08$  at  $37^\circ\text{C}$ , compared to  $-0.85 \pm 0.08$  at room temperature. Of interest also was that the extent of interference from  $\text{K}^+$  was concentration-dependent; this was less at higher  $[\text{K}^+]$  (25 and 50 mM;  $\log k_{\text{NH}_4\text{K}}^{\text{pot}}$   $-0.73 \pm 0.02$ ) compared to lower background concentrations (2 and 5 mM;  $\log k_{\text{NH}_4\text{K}}^{\text{pot}}$   $-0.65 \pm 0.06$ ). This makes correction for the interference of  $\text{K}^+$  on the  $\text{NH}_4^+$ -selective electrode more difficult. In this study the 25-50 mM  $k_{\text{pot}}$  was used (0.195).

#### 4.5.2 Characterisation of $\text{K}^+$ -selective electrode at $37^\circ\text{C}$ :

Interference from  $\text{Na}^+$  on the  $\text{K}^+$ -selective electrode at  $37^\circ\text{C}$  was not significantly different from that at room temperature ( $\log k_{\text{KNa}}^{\text{pot}}$   $-2.76 \pm 0.10$  at  $37^\circ\text{C}$ ;  $\log k_{\text{KNa}}^{\text{pot}}$   $-2.91 \pm 0.33$  at room temperature).

Similarly, interference from  $\text{NH}_4^+$  on the  $\text{K}^+$ -selective electrode at  $37^\circ\text{C}$  was not significantly different from that at room temperature ( $\log k_{\text{KNH}_4}^{\text{pot}}$   $-1.59 \pm 0.04$ , at  $37^\circ\text{C}$ ;  $\log k_{\text{KNH}_4}^{\text{pot}}$   $-1.63 \pm 0.06$  at room temperature).

#### 4.5.3 Urinary measurements of $[\text{NH}_4^+]$ at $37^\circ\text{C}$ .

Urine samples were obtained from twenty-four patients attending the in-patient ward for urology operations. Since patients were nil-by-mouth from midnight the effects of

dietary intake on urinary  $[\text{NH}_4^+]$  were reduced. Diurnal variability was also minimised because all samples were obtained at the same time (between 7 and 8 am).

Urinary  $[\text{NH}_4^+]$  and  $[\text{K}^+]$  were  $15.0 \pm 9.8$  and  $35.9 \pm 15.8$  mM respectively. The ranges of values were 1.12-44.1 and 11.2-72.3 mM respectively. The voided pH of the samples was  $6.70 \pm 0.92$  (range 5.50-8.52). There was no significant relationship between urinary  $[\text{NH}_4^+]$  and urinary  $[\text{K}^+]$  at  $37^\circ\text{C}$ .

#### 4.5.4 pH dependence of urinary $[\text{NH}_4^+]$

Determination of any dependence of urinary  $[\text{NH}_4^+]$  on pH was an important objective of the thesis as struvite stones forms in an alkaline environment within the urinary tract. At room temperature, there was a significant negative association between voided pH and  $[\text{NH}_4^+]$  - whether estimated by colour spectrophotometry ( $r^2=0.792$ ) or with ion-selective electrodes ( $r^2=0.675$ ). Four samples that seem to form a separate group and were excluded from the final analysis, figure 3.18. However, these urine samples were found to be very abnormal and there was no particular reason, since samples of the same individuals on different occasions were normal.. In a small number of samples pH was artificially altered to determine if a similar relationship could be generated in individual samples. However, this was not observed in the small sample set that was used.

At  $37^\circ\text{C}$ , the negative relationship between voided pH and urinary  $[\text{NH}_4^+]$  was absent. The pH of individual urine samples was artificially altered and any changes in  $[\text{NH}_4^+]$  measured, as carried out in the smaller set at room temperature. In this case acidification of urine increased the  $[\text{NH}_4^+]$ , similar to observed between voided pH

and  $[\text{NH}_4^+]$  at room temperature. Although a general trend is present, i.e. acidification of urine increases the  $[\text{NH}_4^+]$ , the manner in which this was demonstrated at the two temperatures remains to be ascertained.

However, the range of pH values over which the  $[\text{NH}_4^+]$  cannot be explained solely on the fact that the  $\text{NH}_3/\text{NH}_4^+$  pair is acting as a simple buffer. The pK of the reaction



is 9.23. At this pH the concentration of  $\text{NH}_3$  and  $\text{NH}_4^+$  would be equal. At pH 6.23 the  $[\text{NH}_4^+]$  is 1000-times greater than the  $[\text{NH}_3]$  and even at pH 7.23 the  $[\text{NH}_4^+]$  is 100-times greater than the  $[\text{NH}_3]$ . Thus if the total ammonia pool ( $\text{NH}_4^+$  and  $\text{NH}_3$ ) in a urine sample remains constant, altering the pH in the range 6.0-7.0 will have only a trivial effect on the  $[\text{NH}_4^+]$  if only a change of the equilibrium was constant. To have such significant changes as recorded in these experiments could only be explained by a non-equilibrium process whereby alkalisation of the urine was removing  $\text{H}^+$  by other buffers continually forcing the equilibrium reaction above to the formation of  $\text{NH}_3$ . The indication is that the  $[\text{NH}_4^+]$  altered by about 10 mmol/l per pH unit at room temperature (figure 3.18) and less so at 37°C (figure 3.24) when pH was altered between pH 5.5-7.0. Another urinary buffer with a pK value near this pH range would achieve such a non-equilibrium shift of  $[\text{NH}_4^+]$ . A major future objective will be to determine the nature of this buffer system as its manipulation will have profound effects on the urinary  $[\text{NH}_4^+]$ , and potentially the ability to form struvite crystals in urine. A candidate is urinary phosphate as the reaction:



has a pK value of 7.2 (Gomori, 1959) and a concentration of about 1-30 mmol/l in urine (Themelis et al., 2004), i.e. similar to the change of  $[\text{NH}_4^+]$  documented above. For the formation of struvite crystals, the urine must be super-saturated with  $\text{Mg}^{2+}$ ,  $\text{NH}_4^+$  and  $\text{PO}_4^{3-}$  ions.  $\text{Mg}^{2+}$  will be discussed later,  $\text{NH}_4^+$  is pH dependent as described above and  $\text{H}_2\text{PO}_4^- / \text{HPO}_4^-$  ions have the above pK value. However  $\text{PO}_4^{3-}$  ions begin to form logarithmically once the pH goes above 8-9 causing a rapid increase in the  $\text{PO}_4^{3-}$  ion concentration. However at pH 7, the  $[\text{NH}_4^+]$  is less than what would be expected for super-saturation with this ion, hence the function of the urease-secreting bacteria, in firstly increasing  $\text{NH}_3$  production and secondly increasing the pH / alkalinising the urine, thus leading to rapid increase in  $\text{PO}_4^{3-}$  ions, which subsequently leads to struvite deposition. Thus potentially the  $\text{PO}_4^{3-}$  ions appear to be a driving force for struvite crystallisation.

#### **4.6 URINARY MEASUREMENTS FROM PATIENTS ATTENDING A RENAL STONE CLINIC**

Urine samples were obtained from patients attending a renal stone clinic at the Royal Free Hospital. All patients attending this clinic were recurrent stone formers or at risk of further stone formation. Samples were used to compare values of urinary  $[\text{NH}_4^+]$  and  $[\text{K}^+]$  in this set of patients with those from other cohorts. In addition, urine samples from this patient cohort underwent routine urinalysis and therefore afforded the opportunity to determine the effect on urine osmolality on  $[\text{NH}_4^+]$  and  $[\text{K}^+]$ . Finally, an algorithm used to estimate urinary  $[\text{NH}_4^+]$  in these patients could be validated against measured values using the ion-selective electrode.

#### 4.6.1 Effect of temperature on urinary measurements of $[\text{NH}_4^+]$ and $[\text{K}^+]$ :

Previous experiments to characterise the  $\text{NH}_4^+$ -selective electrode showed that interference from  $\text{Na}^+$  was greater at  $37^\circ\text{C}$ , but still negligible.  $\text{K}^+$  interference was also greater and concentration dependent (i.e. less interference at higher background concentrations of  $\text{K}^+$ ). As mentioned above, the interference of  $\text{Na}^+$  and  $\text{NH}_4^+$  on the  $\text{K}^+$ -selective electrode at  $37^\circ\text{C}$  was not significantly different from that at room temperature.

Comparison of urinary measurements of  $[\text{NH}_4^+]$  and  $[\text{K}^+]$ , made at  $37^\circ\text{C}$  and room temperature, for each urine sample, importantly showed that there was no significant difference between the  $[\text{NH}_4^+]$  measurements. However the  $[\text{K}^+]$  measurements were significantly higher suggesting that the measurements made at room temperature underestimated the measurements made at  $37^\circ\text{C}$ , but this did not affect the  $[\text{NH}_4^+]$  measurements.

#### 4.6.2 The dependence of urinary $[\text{NH}_4^+]$ and $[\text{K}^+]$ on urine osmolality:

A positive association was seen between urinary osmolality and urinary  $[\text{NH}_4^+]$  and  $[\text{K}^+]$ . This may be expected as when the urine becomes more concentrated the urinary  $[\text{NH}_4^+]$  and  $[\text{K}^+]$  increases.

#### 4.6.3 The dependence of urinary $[\text{NH}_4^+]$ and $[\text{K}^+]$ on voided pH:

As described above, we confirmed the same significant negative association between urinary  $[\text{NH}_4^+]$  and voided pH within this cohort of patients. There was no significant relationship between urinary  $[\text{K}^+]$  and voided pH.

#### 4.6.4 Differences between stone-formers and non-stone formers

One objective of the study was to determine if a single test for urinary  $[\text{NH}_4^+]$  might distinguish between normal control and stone-formers. This was carried out in Table 3.21 and showed that actually the urinary  $[\text{NH}_4^+]$  for non-stone formers was significantly greater. The table is reproduced here for convenience.

Table 3.21 Values of urinary  $[\text{NH}_4^+]$  and  $[\text{K}^+]$  in urine samples from a non-stone forming and a stone-forming cohort of volunteers. \*  $p < 0.05$  non-stone former vs stone formers at RT.

	Non-stone formers	Stone formers		
		RFH patients (stone clinic)		UCLH patients (operative)
	Room temp	Room temp	37°C	37°C
$[\text{NH}_4^+]$ , mM	26.1±11.5 *	13.8±8.9	13.8±10.8	15.0±9.8
$[\text{K}^+]$ , mM	44.8±16.9	30.7±13.0	39.1±17.7	35.9±15.8
Voided pH	5.96±0.76 *	6.60±0.94	6.60±0.94	6.70±0.92

However, it is clear that other variables also were different, i.e. the voided pH and the  $[\text{K}^+]$ , an increase of pH raised the  $[\text{NH}_4^+]$  and an increase of  $[\text{K}^+]$  was consistent with increased osmolality and hence an increase of the  $[\text{NH}_4^+]$ . Therefore, a single spot-test of the urinary  $[\text{NH}_4^+]$  would be insufficient to distinguish between a stone-former and non-stone former on the basis of the measurements.

An approximate attempt to reduce the effect of these confounders is as follows, from the room temperature data:

1. Figure 3.18 showed that the  $[\text{NH}_4^+]$  decreased by  $11.2 \text{ mmol.l}^{-1} \cdot \text{pH unit}^{-1}$ . Voided pH was 0.74 units less in non-stone formers and would *per se* increase  $[\text{NH}_4^+]$  by 8.3 mM

2. Figures 3.29 and 3.30 show that  $[\text{NH}_4^+]$  increased by 0.035 mM/mosmol and  $[\text{K}^+]$  by 0.067 mM/mosmol if linear fits are assumed; i.e.  $[\text{NH}_4^+]$  increases by 1 mM per 1.9 mM increase of  $[\text{K}^+]$ . As non-stone formers  $[\text{K}^+]$  was 14.1 mM greater this is per se is equivalent to an increased  $[\text{NH}_4^+]$  of 7.4 mM
3. Subtracting these two values from the measured 26.6 mM  $[\text{NH}_4^+]$  yields a mean value of 10.9 mM for non-stone formers  $[\text{NH}_4^+]$  in comparison to the value of 13.8 mM for stone-formers.

A similar calculation may be carried out for the comparison of  $[\text{NH}_4^+]$  in urine samples from struvite and Ca oxalate stone formers (section 3.6.5).

The  $[\text{NH}_4^+]$  in the two groups:  $16.8 \pm 9.0$  vs  $15.0 \pm 10.0$  mM (struvite vs Ca oxalate)

The  $[\text{K}^+]$  in the two groups:  $26.5 \pm 7.7$  vs  $42.7 \pm 16.7$  mM

Normalisation around an equivalent  $[\text{K}^+]$  in the two groups would increase the  $[\text{NH}_4^+]$  in the struvite group from a mean of 16.8 mM to 25.3 mM in comparison to the mean value of 15.0 mM in the Ca oxalate group.

Although these are approximate calculations it shows the importance of matching the osmolality and pH when comparing measured values of  $[\text{NH}_4^+]$  between groups. However, an in vitro model found no relation between urine osmolality or ammonia with urease-induced crystallization (Hugosson et al., 1990) Accumulation of more data will determine if such a linearly independent approach is valid to correct for these confounders.

#### 4.6.5 Validation of the $\text{NH}_4^+$ -selective electrode against a standard algorithm:

A standard algorithm was used to calculate urinary  $[\text{NH}_4^+]$  (Hoge et al., 1994)

$$\text{Urine } [\text{NH}_4^+] = 0.5 * \left( \text{Measured osmolality} - 2([\text{Na}] + [\text{K}]) + \frac{\text{urea}}{2} \right)$$

and these values compared to measured values. The mean calculated urinary  $[\text{NH}_4^+]$  was  $10.3 \pm 14.5$  mM (range -8.5 – 49.5 mM) compared with a mean ISE urinary  $[\text{NH}_4^+]$  measurement of  $13.8 \pm 8.9$  mM (range 2.9 – 34.3 mM). The calculated method produced negative values which suggested inaccuracies with this method. There was however a significant association between the calculated and ISE method ( $r^2=0.54$ ). The calculated value was smaller than the measured value in most cases, but this was not a proportional error between the two values. As the pH rose above 6.0, there was a growing deviation between the two values, suggesting an in-built error in the calculation algorithm that is pH-dependent. On the whole, the calculated algorithm provides an alternative method for estimation of urinary  $[\text{NH}_4^+]$ , despite the inaccuracies, however, the ion-selective electrode provides a more accurate measurement. Refinements of the algorithm will be possible using the ion-selective electrode data as a basis for empirical correction of the formula. Though we made preliminary attempts at refining the formula, further focused attempts will be required to produce an even more accurate formula.

#### **4.7 CHARACTERISATION OF MAGNESIUM ELECTRODE:**

Magnesium is the fourth most abundant cation in the human body and the second most common cation in the intracellular fluid (Quamme, 1986). Magnesium is an extremely important intracellular cation and a cofactor in essential biological systems (Aikawa, 1980; Flink et al, 1987).

Plasma  $[\text{Mg}^{2+}]$  depends on intake and renal excretion, which is regulated mainly in the thick ascending limb of the loop of Henle. 25% of reabsorption occurs in the proximal convoluted tubule, with 60% occurring in the loop of Henle and 10-15% occurring in the distal convoluted tubule. The hormonal control exhibited over other ions (e.g.  $\text{K}^+$ ,  $\text{Ca}^{2+}$ ) is lacking for magnesium and therefore a negative magnesium balance results in a prompt decrease in plasma  $[\text{Mg}^{2+}]$  and *vice versa* (de Rouffignac et al, 1994; Kelepouris, 1998; Quamme et al, 2000; Dai et al, 2001;).

A close relationship between hypokalaemia and hypomagnesaemia has been identified (Whang et al, 1981), and both can induce ventricular arrhythmias (Whang, 1987). Altura (1994a) highlighted the need for a sensitive  $\text{Mg}^{2+}$ -selective electrode, for measuring the ionised free  $\text{Mg}^{2+}$ , which is physiologically the most important fraction. Subsequently  $\text{Mg}^{2+}$ -selective electrode were characterised to measure ionised  $[\text{Mg}^{2+}]$  (Altura et al, 1994b; Marsoner et al, 1994) and its uses in the critical care setting (Altura et al, 1994c).

Measurements of  $[\text{Mg}^{2+}]$  in undiluted blood samples were also achieved by Rouilly et al (1990) using  $\text{Mg}^{2+}$ -selective ionophores. The  $\text{Mg}^{2+}$ -selective ionophore used was ETH 5282, and was mixed (by weight) with 33% polyvinyl chloride (Fluka), and 65% to 66% o-nitrophenyl octyl ether (NPOE; Fluka), plus potassium tetrakis(p-chlorophenyl)-borate (KTPC1PB; Fluka). The main problem was selectivity over  $\text{Ca}^{2+}$ , and a  $\log k_{\text{MgCa}}^{\text{pot}}$  of -1.05 was obtained. International workshops have taken place to establish international standards for the measurement of ionised magnesium (Fleisher, 1994). The parameters and working mechanism to aid developing these electrodes have also been investigated (Eugster et al, 1991).

Three commercial analysers (Rehak et al, 1996) are available currently which measure the free  $[Mg^{2+}]$  and  $[Ca^{2+}]$  in blood, plasma serum. The instruments are the AVL 988-4 (AVL, Graz, Austria), the Microlyte 6 (KONE, Espoo, Finland), and the Nova CRT (Nova, Waltham, MA). They all use the  $[Ca^{2+}]$  to subsequently correct for the selectivity of the  $Mg^{2+}$ -selective electrode for  $Ca^{2+}$ . These instruments have not been used in undiluted urine samples.

We initially used ETH 4030 as the  $Mg^{2+}$ -selective ionophore, but there was no response seen with changes in  $[Mg^{2+}]$ . ETH 4030 had been used by Maj-Zurawska et al (1989), where the  $k_{MgCa}^{pot}$  was 1.0 and the  $k_{MgNa}^{pot}$  was  $1.6 \times 10^{-4}$ . Hu et al (1989) investigated ETH 5214, another  $Mg^{2+}$ -selective ionophore, and found that  $\log k_{MgCa}^{pot}$  ranged between 0.6 and 1.0 and the  $\log k_{MgNa}^{pot}$  ranged between -2.0 and -2.3.

ETH 7025 has been found to be a good  $Mg^{2+}$ -selective ionophore (Eugster et al, 1993). Seven ion-selective membranes were made using differing amounts of ion-selective ionophore, PVC and plasticiser. The  $\log k_{MgCa}^{pot}$  ranged between -0.8 and -1.4, showing fairly good selectivity for  $Mg^{2+}$  over interferent ions.

The  $Mg^{2+}$ -ion-selective electrode used in the current study was made of Magnesium Ionophore VI, (1% w/w; ETH 5506 – Fluka) with  $\geq 95\%$  purity of the primary agent. Other constituents for the  $Mg^{2+}$ -selective membrane included 165mg high MW PVC, 6ml tetrahydrofuran, 330 mg of bis (2-ethylhexyl) sebacate and 3.0 mg potassium tetrakis(p-chlorophenyl)-borate (KTPC1PB). The response of the  $Mg^{2+}$ -ion-selective

electrode was poorer at lower  $[\text{Mg}^{2+}]$ . Calibration of the electrode in buffered NaCl solutions at 37°C yielded a slope of 10.4 mV per decade ( $n=10$ ), between 0.2-2.0 mM  $\text{MgCl}_2$ , and this was 16.7 mV per decade between 2.0-20 mM  $\text{MgCl}_2$  ( $n=10$ ). The ideal slope for a divalent cation should be 30.75mV per decade at 37°C.  $\text{MgCl}_2$ .

Selectivity for  $\text{Mg}^{2+}$  over  $\text{Na}^+$  was evaluated from 40 calibrations in the base solution (140 mM NaCl) and the  $\log k_{\text{MgNa}}^{\text{pot}}$  was  $-1.59 \pm 0.15$ , with a mean  $k_{\text{MgNa}}^{\text{pot}}$  value of 0.025 (i.e. the  $\text{Mg}^{2+}$ -ion-selective electrode was 40 times more selective for  $\text{Mg}^{2+}$  than  $\text{Na}^+$ ). O'Donnell et al (1993) studied ETH 5506 and the ion-selective membrane constituents included 1% w/w ionophore, 33% w/w PVC and 66% w/w plasticiser (either *o*-NPOE (2-nitrophenyl octyl ether – Fluka) or ETH 5373). With the plasticiser ETH 5373, the  $\log k_{\text{MgNa}}^{\text{pot}}$  was -4.7, whereas with *o*-NPOE as the plasticiser, the  $\log k_{\text{MgNa}}^{\text{pot}}$  was -4.4.

In the current study, the most interferent ion was  $\text{Ca}^{2+}$ , and calibration curves of a  $\text{Mg}^{2+}$ -selective electrode in the presence of 1 mM  $\text{CaCl}_2$  were performed. The mean value of  $\log k_{\text{MgCa}}^{\text{pot}}$ , as determined from ten experiments, was  $0.66 \pm 0.02$ , suggesting that since this value is less than unity, the electrode is more selective for the 'interferent' ion ( $\text{Mg}^{2+}$ ). O'Donnell et al (1993), in their study, showed that with the plasticiser ETH 5373, the  $\log k_{\text{MgCa}}^{\text{pot}}$  was -1.9, whereas with *o*-NPOE as the plasticiser, the  $\log k_{\text{MgCa}}^{\text{pot}}$  was -1.7. The electrode used in the present study appeared more susceptible to interferent ions, than in O'Donnell's study (1993). The reason is unclear but possible reasons include the different plasticiser used in the current study

and varying ratios. Further experiments are necessary and should include using a different plasticiser.

#### **4.8 URINARY MEASUREMENT OF $[\text{Mg}^{2+}]$ AT 37°C:**

##### 4.8.1 Characterisation of the $\text{Ca}^{2+}$ -selective electrode at 37°C:

Separate measurement of urinary  $[\text{Ca}^{2+}]$  was carried out using a  $\text{Ca}^{2+}$ -ion-selective electrode, which was relatively unaffected by  $\text{Mg}^{2+}$ . This allowed the interferent effect of varying  $[\text{Ca}^{2+}]$  on the electrode response to be subtracted.

##### 4.8.2 Urinary measurements of $[\text{Mg}^{2+}]$ at 37°C:

Reliable experiments using urine samples of 14 separate subjects were possible. After subtracting the interferent effect of  $\text{Ca}^{2+}$ , the median urinary  $[\text{Mg}^{2+}]$  was 8.9 mM, with the 25% and 75% interquartiles being 5.5 and 14.4 mM respectively. The urinary  $[\text{Mg}^{2+}]$  was slightly increased from what might be expected, reflecting the poor selectivity of the  $\text{Mg}^{2+}$ -selective electrode for  $\text{Mg}^{2+}$ . The median voided pH was 6.89.

##### 4.8.3 pH dependence of urinary $[\text{Mg}^{2+}]$ :

There was no significant association between the value of  $[\text{Mg}^{2+}]$  and voided pH. However, urinary  $[\text{Mg}^{2+}]$  values were marginally significantly greater ( $p=0.048$ ) when the pH was titrated to 6.0. There was a significant association ( $r^2=0.324$ ) indicating that acidifying the urine increased the urinary  $[\text{Mg}^{2+}]$ , probably by increasing the ionized fraction of the total urinary  $[\text{Mg}]$ . This raises the possibility that as urinary pH changes, the urinary  $[\text{Mg}^{2+}]$  increases and drives struvite deposition.

Further experiments are required to reliably obtain accurate urinary  $[Mg^{2+}]$  and should include using different plasticisers, and trial of different  $Mg^{2+}$ -selective ionophores.

#### **4.9 CONCLUSION AND FUTURE STUDIES:**

Struvite stones account for 10-15% of renal stones and grow rapidly forming staghorn calculi. An understanding of the physico-chemical conditions causing struvite crystallization allows development of strategies to prevent their formation. This lack of understanding has two bases: i) the particular ionised concentrations of the reactants (e.g.  $Mg^{2+}$ ,  $NH_4^+$ , and phosphate) in the urine are unknown; ii) the prevailing chemical conditions that would modulate crystallisation are also unclear (e.g. pH, osmolality, other urinary constituents).

At present there are no current true effective treatments to prevent or treat struvite stones. Problems:

- The bacteria are within the layers of the stone and matrix – since antibiotics are unable to penetrate deep within the stone, they are ineffective.
- Once a patient is stone free, even a small remaining nidus can cause recurrence. At present there is no urinary monitoring strategy, apart from urinary cultures and prevention of infections, once the patient is stone free.
- The voided urine may not be representative of the urine within the renal pelvis and hence voided urine cultures may therefore be an inaccurate reflection of the true scenario within the kidney.
- Laboratories may be missing or ignoring organisms growing small numbers of colonies, and labelling them ‘not significant’, however this information may

be very useful and identifying all organisms regardless of count in such patients may be beneficial.

In the present study, we have:

- Developed and characterised an  $\text{NH}_4^+$ -selective electrode at room temperature and at  $37^\circ\text{C}$ .
- Determined the selectivity coefficients of the  $\text{NH}_4^+$ -selective electrode against interferent ions.
- Made the first measurements of urinary  $[\text{NH}_4^+]$  in undiluted urine from normal subjects at room temperature and  $37^\circ\text{C}$ .
- Measured the pH-dependence of the urinary  $[\text{NH}_4^+]$  at room temperature and  $37^\circ\text{C}$ .
- Validated the  $\text{NH}_4^+$ -selective electrode data against colour spectrophotometry.
- Validated the  $\text{NH}_4^+$ -selective electrode data against an empirical calculation method.
- Made measurements of the urinary  $[\text{NH}_4^+]$  from patients with staghorn stones and urinary tract stone disease.
- Developed and characterised of a  $\text{Mg}^{2+}$ -selective electrode at room temperature and at  $37^\circ\text{C}$  as well as determining the selectivity coefficients of this  $\text{Mg}^{2+}$ -selective electrode against interferent ions.
- Made measurements of urinary  $[\text{Mg}^{2+}]$  from normal subjects at room temperature and  $37^\circ\text{C}$  as well as from patients with urinary tract stone disease.

This present study has confirmed that the  $\text{NH}_4^+$ -selective electrode is stable and responds appropriately in urine, and that along with the  $\text{Mg}^{2+}$ -selective electrode, they

could realistically become useful tools for studying the behaviour of these ions and could become available in commercial analysers for use in routine urine analysis.

Future uses might include:

- Detecting urease secreting bacteria: currently it is possible to detect urease activity on urine samples but urine samples need to be sent to the laboratory, grown on specific media (can take 3-5 hours), and even so not all bacteria are detected. This would provide a rapid effective simple instant tool which might detect urease-secreting bacteria.
- Use as an adjunct with colourimetric urine dipstick.
- Use as a monitoring tool for patients seen in the outpatient clinic, particularly in those with known history of staghorn, struvite or, previous calcium stones (especially if associated with urinary tract infections). By monitoring the urinary  $[\text{NH}_4^+]$ , a rise in the  $[\text{NH}_4^+]$  might alert the clinician to institute prophylactic treatment (e.g. antibiotics).

Future studies could include:

- Testing the  $[\text{NH}_4^+]$  in urine samples containing urease secreting bacteria.
- Testing the  $[\text{NH}_4^+]$  in urine samples with patients with blocked catheters compared to unblocked catheters.
- Testing more urine samples from patients with staghorn stones.
- Comparing the urinary  $[\text{NH}_4^+]$  from voided urine samples with the urinary  $[\text{NH}_4^+]$  obtained directly from the collecting system (i.e. nephrostomy sample or sample obtained during PCNL).
- Further characterisation and trial of different ionophores for the  $\text{Mg}^{2+}$ -selective electrode.

**CHAPTER 5**

**APPENDIX**

**5.1 Consent Form**

**University College Hospitals NHS Trust **  
NHS Foundation Trust

**Directorate of Urology**  
Urology Department  
2B Maple House  
Ground Floor, Rosenheim Wing  
25 Grafton Way  
London WC1E 6DB

**Administrative Enquiries**  
Telephone: 020 7380 9179  
Fax: 020 7380 9303  
[www.uclh.org](http://www.uclh.org)

Centre Number:  
Patient ID Number:

UCLH Project ID number:  
Form version:

**CONSENT FORM**

Title of project: Measuring  $\text{NH}_4^+$  and  $\text{Mg}^{2+}$  concentrations in urine from patients with kidney stones.

Name of Principal investigator: Professor Chris Fry

**Please initial box**

1. I confirm that I have read and understood the information sheet dated ..... (version .....) for the above study and have had the opportunity to ask questions.
2. I confirm that I have had sufficient time to consider whether or not want to be included in the study
3. I understand that my participation is voluntary and that I am free to withdraw at any time, without giving any reason, without my medical care or legal rights being affected.
4. I understand that sections of any of my medical notes may be looked at by responsible individuals from (company name) or from regulatory authorities where it is relevant to my taking part in research. I give permission for these individuals to have access to my records.
5. I agree to take part in the above study.



## 5.2 Patient information sheet

# University College Hospitals NHS Trust NHS Foundation Trust

### Directorate of Urology

Urology Department  
2B Maple House  
Ground Floor, Rosenheim Wing  
25 Grafton Way  
London WC1E 6DB

### Administrative Enquiries

Telephone: 020 7380 9179  
Fax: 020 7380 9303  
[www.uclh.org](http://www.uclh.org)

Version:2  
Date: 2/01/07  
Project ID:

## Patient Information Sheet

### Measuring $\text{NH}_4^+$ and $\text{Mg}^{2+}$ concentrations in urine from patients with kidney stones.

You are being invited to take part in a research study. Before you decide, it is important for you to understand why the research is being done and what it will involve. Please take time to read the following information carefully and discuss it with others if you wish. Ask us if there is anything that is not clear or if you would like more information. Take time to decide whether or not you wish to take part.

#### **The purpose of the study:**

At the Institute of Urology, we are keen to understand the conditions under which large kidney stones form. By furthering our understanding of these conditions we aim to prevent these large stones from forming in the first place.

With recent advances in technology it has been possible, for the first time, to accurately measure the concentration of certain chemicals in the urine that are the building blocks for large kidney stones.

#### **Why have I been chosen?**

You were chosen to take part because you have a large kidney stone. By providing us with a sample of urine, we will be able to measure the concentration of these chemicals, which will help our understanding of why these stones form.

### **What is involved in the study?**

All you will be required to do is to provide us with a sample of urine (about 30ml) and answer a few questions about your urological and medical history with the research doctor. This should take no longer than 10 minutes.

If you are having an operation, your operation will not be changed in any way, by taking part in this study. During the operation, urine is routinely aspirated from the kidney and discarded. A small sample of urine will be allocated to our project.

### **What will happen to my urine sample?**

The urine sample will be taken to the laboratory and kept in the freezer. It will be tested for urinary ammonium and magnesium concentrations. After all the experiments have been conducted, the sample will be destroyed and not kept for future studies by us or any other group.

### **Benefits of taking part?**

You will not benefit directly from this study but by participating you will help to find treatments that prevent the condition occurring in others. Obviously, there are no risks or side effects from taking part in this study. Please be sure that you are entirely happy before you agree, and ask the doctor any questions you may wish, before signing the consent form.

### **Confidentiality:**

Professor Christopher Fry will be the custodian for the data generated at the Institute of Urology (0207 679 9376) and will be pleased to help if you need further information.

All information collected about you during the course of the research will be kept strictly confidential. Urine samples will be coded and any identifiable information will be removed so that you cannot be recognised from it. The results are likely to be published in a scientific journal and you will not be identified in any report/publication.

In the unlikely event should you wish to complain, you have a right to complain through the UCLH complaints procedure.

### **Organisation and Funding:**

The study is being carried out in conjunction with the Institute of Urology, University College London. The project is funded by the Royal College of Surgeons of England.

### **Withdrawal from the project:**

Your participation in the trial is entirely voluntary. If you do decide to take part you will be given this information sheet to keep and be asked to sign a consent form. If you decide to take part you are still free to withdraw at any time and without giving a reason. If you choose not to enter the trial, or to withdraw once entered, this will in no way affect

your future medical care. All information regarding your medical records will be treated as strictly confidential and will only be used for medical purposes. Participation in this study will in no way affect your legal rights.

**Ethics Review:**

The project has been reviewed by the National Hospital for Neurology and Neurosurgery and Institute of Neurology Joint Research Ethics Committee.

**Contact for further information:**

Should you require any further information, then please do not hesitate in contacting Professor Chris Fry or Senthyl Sellaturay at the Institute of Urology (0207 679 9376 / 9112).

We thank you for taking part in our study.

### 5.3 Parent information sheet

# University College Hospitals NHS Trust

NHS Foundation Trust

#### Directorate of Urology

Urology Department  
2B Maple House  
Ground Floor, Rosenheim Wing  
25 Grafton Way  
London WC1E 6DB

#### Administrative Enquiries

Telephone: 020 7380 9179  
Fax: 020 7380 9303  
[www.uclh.org](http://www.uclh.org)

Version:2  
Date: 2/01/07  
Project ID:

## Patient Information Sheet - PARENT

### Measuring $\text{NH}_4^+$ and $\text{Mg}^{2+}$ concentrations in urine from patients with kidney stones.

Your child is being invited to take part in a research study. Before you decide, it is important for you to understand why the research is being done and what it will involve. Please take time to read the following information carefully and discuss it with others if you wish. Ask us if there is anything that is not clear or if you would like more information. Take time to decide whether or not you wish your child to take part.

#### **The purpose of the study:**

At the Institute of Urology, we are keen to understand the conditions under which large kidney stones form. By furthering our understanding of these conditions we aim to prevent these large stones from forming in the first place.

With recent advances in technology it has been possible, for the first time, to accurately measure the concentration of certain chemicals in the urine that are the building blocks for large kidney stones.

#### **Why was my child chosen?**

Your child was chosen to take part because they have a large kidney stone. By providing us with a sample of urine, we will be able to measure the concentration of these chemicals, which will help our understanding of why these stones form.

### **What is involved in the study?**

All your child will be required to do is to provide us with a sample of urine (about 30ml) and for you to answer a few questions about your child's urological and medical history with the research doctor. This should take no longer than 10 minutes.

If your child is having an operation, the operation will not be changed in any way, by taking part in this study. During the operation, urine is routinely aspirated from the kidney and discarded. A small sample of urine will be allocated to our project.

### **What will happen to my urine sample?**

The urine sample will be taken to the laboratory and kept in the freezer. It will be tested for urinary ammonium and magnesium concentrations. After all the experiments have been conducted, the sample will be destroyed and not kept for future studies by us or any other group.

### **Benefits of taking part?**

Your child will not benefit directly from this study but by participating they will help to find treatments that prevent the condition occurring in others. Obviously, there are no risks or side effects from taking part in this study. Please be sure that you are entirely happy for your child to take part before you agree, and ask the doctor any questions you may wish, before signing the consent form.

### **Confidentiality:**

Professor Christopher Fry will be the custodian for the data generated at the Institute of Urology (0207 679 9376) and will be pleased to help if you need further information.

All information collected about your child during the course of the research will be kept strictly confidential. Urine samples will be coded and any identifiable information will be removed so that they cannot be recognised from it. The results are likely to be published in a scientific journal and your child will not be identified in any report/publication.

In the unlikely event should you wish to complain, you have a right to complain through the UCLH complaints procedure.

### **Organisation and Funding:**

The study is being carried out in conjunction with the Institute of Urology, University College London. The project is funded by the Royal College of Surgeons of England.

### **Withdrawal from the project:**

Your child's participation in the trial is entirely voluntary. If you decide that your child may take part, then you will be given this information sheet to keep and be asked to sign a consent form. If they take part you are still free to withdraw them at any time and without giving a reason. If you choose not to enter your child into the trial, or to withdraw them once entered, this will in no way affect your child's future medical care. All information regarding your child's medical records will be treated as strictly confidential and will only be used for medical purposes. Participation in this study will in no way affect you or your child's legal rights.

**Ethics Review:**

The project has been reviewed by the National Hospital for Neurology and Neurosurgery and Institute of Neurology Joint Research Ethics Committee.

**Contact for further information:**

Should you require any further information, then please do not hesitate in contacting Professor Chris Fry or Senthyl Sellaturay at the Institute of Urology (0207 679 9376 / 9112).

We thank you and your child for taking part in our study.

## 5.4 Control information sheet

# University College Hospitals NHS Trust NHS Foundation Trust

### Directorate of Urology

Urology Department  
2B Maple House  
Ground Floor, Rosenheim Wing  
25 Grafton Way  
London WC1E 6DB

### Administrative Enquiries

Telephone: 020 7380 9179

Fax: 020 7380 9303

[www.uclh.org](http://www.uclh.org)

Version:

Date:

Project ID:

## Patient Information Sheet - CONTROL

### Measuring $\text{NH}_4^+$ and $\text{Mg}^{2+}$ concentrations in urine from patients with kidney stones.

You are being invited to take part in a research study. Before you decide, it is important for you to understand why the research is being done and what it will involve. Please take time to read the following information carefully and discuss it with others if you wish. Ask us if there is anything that is not clear or if you would like more information. Take time to decide whether or not you wish to take part.

#### **The purpose of the study:**

At the Institute of Urology, we are keen to understand the conditions under which large kidney stones form. By furthering our understanding of these conditions we aim to prevent these large stones from forming in the first place.

With recent advances in technology it has been possible, for the first time, to accurately measure the concentration of certain chemicals in the urine that are the building blocks for large kidney stones.

#### **Why have I been chosen?**

You were chosen to take part to act as a control / normal volunteer because you do not have a large kidney stone. By providing us with a sample of urine, we will be able to measure the concentration of these chemicals in normal individuals and compare the

levels with patients who do have large kidney stones. This will help our understanding of why these stones form.

**What is involved in the study?**

All you will be required to do is to provide us with a sample of urine (about 30ml) and answer a few questions about your urological and medical history with the research doctor. This should take no longer than 10 minutes.

If you are having an operation, your operation will not be changed in any way, by taking part in this study. During the operation, urine is routinely aspirated from the kidney and discarded. A small sample of urine will be allocated to our project.

**What will happen to my urine sample?**

The urine sample will be taken to the laboratory and kept in the freezer. It will be tested for urinary ammonium and magnesium concentrations. After all the experiments have been conducted, the sample will be destroyed and not kept for future studies by us or any other group.

**Benefits of taking part?**

You will not benefit directly from this study but by participating you will help to find treatments that prevent the condition occurring in others. Obviously, there are no risks or side effects from taking part in this study. Please be sure that you are entirely happy before you agree, and ask the doctor any questions you may wish, before signing the consent form.

**Confidentiality:**

Professor Christopher Fry will be the custodian for the data generated at the Institute of Urology (0207 679 9376) and will be pleased to help if you need further information.

All information collected about you during the course of the research will be kept strictly confidential. Urine samples will be coded and any identifiable information will be removed so that you cannot be recognised from it. The results are likely to be published in a scientific journal and you will not be identified in any report/publication.

In the unlikely event should you wish to complain, you have a right to complain through the UCLH complaints procedure.

**Organisation and Funding:**

The study is being carried out in conjunction with the Institute of Urology, University College London. The project is funded by the Royal College of Surgeons of England.

**Withdrawal from the project:**

Your participation in the trial is entirely voluntary. If you do decide to take part you will be given this information sheet to keep and be asked to sign a consent form. If you decide to take part you are still free to withdraw at any time and without giving a reason.

If you choose not to enter the trial, or to withdraw once entered, this will in no way affect your future medical care. All information regarding your medical records will be treated as strictly confidential and will only be used for medical purposes. Participation in this study will in no way affect your legal rights.

**Ethics Review:**

The project has been reviewed by the National Hospital for Neurology and Neurosurgery and Institute of Neurology Joint Research Ethics Committee.

**Contact for further information:**

Should you require any further information, then please do not hesitate in contacting Professor Chris Fry or Senthyl Sellaturay at the Institute of Urology (0207 679 9376 / 9112).

We thank you for taking part in our study.

## 5.5 Patient Questionnaire

# Patient Questionnaire

Name:

Assigned Number:

Address:

Tel No:

Date of Birth:

Age:

Presenting Complaint:

Associated symptoms and length of time:

Associated urinary tract infections / how many:

How diagnosed:

Stone composition known or unknown:

Past medical history:

Drug history and allergies:

Diet modification:

## 5.6 Ethics Approval Letter

### The National Hospital for Neurology and Neurosurgery & Institute of Neurology Joint REC

Mr Senthly Vigna Sellaturay  
Research Fellow  
University College London,  
48, Riding House Street,  
London  
W1W 7EY  
Our Ref: 07L 109

Research & Development  
1st Floor, Maple House  
Ground Floor, Rosenheim Wing  
25 Grafton Way  
London  
WC1E 5DB  
Tel: 020 7380 9940  
Fax: 020 7380 9937  
Email: [sasha.vandayar@uclh.nhs.uk](mailto:sasha.vandayar@uclh.nhs.uk)  
Website: [www.uclh.nhs.uk](http://www.uclh.nhs.uk)

02 May 2007

Dear Mr Sellaturay

**Study title:** The physico-chemical basis of magnesium ammonium phosphate (struvite) kidney stone formation  
**REC reference:** 06/Q0512/103  
**Amendment number:** 1  
**Amendment date:** 04 April 2007

The above amendment was reviewed at the meeting of the Sub-Committee of the REC held on 01 May 2007.

#### Ethical opinion

The members of the Committee present gave a favourable ethical opinion of the amendment on the basis described in the notice of amendment form and supporting documentation.

#### Approved documents

The documents reviewed and approved at the meeting were:

Document	Version	Date
Notice of Substantial Amendment (non-CTIMPs)	1	04 April 2007

#### Membership of the Committee

The members of the Committee who were present at the meeting are listed on the attached sheet.

#### R&D approval

All investigators and research collaborators in the NHS should notify the R&D office for the relevant NHS care organisation of this amendment and check whether it affects R&D approval of the research.

The Committee is constituted in accordance with the Governance Arrangements for Research Ethics Committees (July 2001) and complies fully with the Standard Operating Procedures for Research Ethics Committees in the UK.

06/Q0512/103:

Please quote this number on all correspondence

Yours sincerely

**Sasha Vandayar**  
**Committee Co-ordinator**

E-mail: [Sasha.Vandayar@uclh.nhs.uk](mailto:Sasha.Vandayar@uclh.nhs.uk)

Enclosures List of names and professions of members who were present at the meeting and those who submitted written comments

Copy to: *R&D office for UCLH*

## CHAPTER 6

### REFERENCES

1. Abate N, Chandalia M, Cabo-Chan AV Jr, Moe OW, Sakhaee K. The metabolic syndrome and uric acid nephrolithiasis: novel features of renal manifestation of insulin resistance. *Kidney Int.* 2004; 65: 386-392.
2. Abbona F, Boistelle R. Growth morphology and crystal habit of struvite crystals ( $\text{MgNH}_4\text{PO}_4 \cdot 6\text{H}_2\text{O}$ ). *J Crystal Growth*, 1979; 46: 339-354.
3. Abbona F, Lundager Madsen HE, Boistelle R. Crystallisation of two magnesium phosphates, struvite and newberyite: effect of pH and concentration. *J Crystal Growth*, 1982; 57:6.
4. Aikawa JK. Magnesium. *West J Med.* 1980 Oct;133(4):333-4.
5. Agrawal MS, Singh SK, Singh H. Management of multiple/staghorn kidney stones: Open surgery versus PCNL (with or without ESWL). *Indian J Urol.* 2009 Apr;25(2):284-5.
6. Altura BM. Introduction: importance of Mg in physiology and medicine and the need for ion selective electrodes. *Scand J Clin Lab Invest Suppl.* 1994a;217:5-9.
7. Altura BT, Shirey TL, Young CC, Dell'Orfano K, Hiti J, Welsh R, Yeh Q, Barbour RL, Altura BM. Characterization of a new ion selective electrode for ionized magnesium in whole blood, plasma, serum, and aqueous samples. *Scand J Clin Lab Invest Suppl.* 1994b;217:21-36.
8. Altura BT, Burack JL, Cracco RQ, Galland L, Handwerker SM, Markell MS, Mauskop A, Memon ZS, Resnick LM, Zisbrod Z, et al. Clinical studies with the NOVA ISE for  $\text{IMg}^{2+}$ . *Scand J Clin Lab Invest Suppl.* 1994c;217:53-67.

9. Babic-Ivancic V, Kontrec J, Brecevic L. Formation and transformation of struvite and newberyite in aqueous solutions under conditions similar to physiological. *Urol Res*, 2004; 32: 350-356.
10. Baker PW, Coyle P, Bais R, Rofe AM. Influence of season, age and sex on renal stone formation in South Australia. *Med J Aust* 1993; 159: 390-392.
11. Band DM, Kratochvil J, Wilson PAP, Treasure T. Relationship between activity and concentration measurements of plasma potassium. *Analyst*. 1978; 103: 246-251.
12. Battle DC, Hizon M, Cohen E, Gutterman C, Gupta R. The use of the urinary anion gap in the diagnosis of hyperchloremic metabolic acidosis. *N Engl J Med*. 1988; 318: 594-599.
13. Benco JS, Nienaber HA, McGimpsey WG. Synthesis of an ammonium ionophore and its application in a planar ion-selective electrode. *Anal Chem*. 2003; 75: 152-156.
14. Bergquist LM, Searcy RL. Application of the Berthelot reaction for rapid detection of urea hydrolysis by *Proteus* strains. *J Bacteriol* 1963; 85: 954-955.
15. Bichler KH, Eipper E, Naber K, Braun V, Zimmermann R, Lahme S. Urinary infection stones. *Int J Antimicrob Agents*. 2002; 19: 488-498.
16. Bouropoulos NC, Koutsoukos PG. Spontaneous precipitation of struvite from aqueous solutions. *J Crystal Growth*, 2000; 213: 381-388.
17. Brookes CI, Fry CH. Ionised magnesium and calcium in plasma from healthy volunteers and patients undergoing cardiopulmonary bypass. *Br Heart J*. 1993; 69: 404-408.
18. Bratell S, Brorson JE, Grenabo L, Hedelin H, Pettersson S. The bacteriology of operated renal stones. *Eur Urol*. 1990; 17: 58-61.

19. Blandy J. The fate of the unoperated staghorn calculus. *Br J Urol.* 1973; 45: 581-585.
20. Brown CM, Purich DL. Physical chemical processes in kidney stone formation. In Coe FL, Flavus MJ (eds): *Disorders of bone and mineral metabolism.* New York, Raven Press, 1992, pp613-624.
21. Buhlmann P, Pretsch E, Bakker E. Carrier-based ion-selective electrodes and bulk optodes. 2. ionophores for potentiometric and optical sensors. *Chem Rev.* 1998; 98: 1593-1688.
22. Cadieux PA, Chew BH, Nott L, Seney S, Elwood CN, Wignall GR, Goneau LW, Denstedt JD. Use of triclosan-eluting ureteral stents in patients with long-term stents. *J Endourol.* 2009; 23: 1187-1194.
23. Chandra S, Buschbeck R, Lang H. A 15-crown-5-functionalized carbosilane dendrimer as ionophore for ammonium selective electrodes. *Talanta.* 2006; 70: 1087-1093.
24. Choong S, Wood S, Fry CH, Whitfield H. Catheter associated urinary tract infection and encrustation. *Int J Antimicrob Agents,* 2001; 17: 305-310.
25. Clapham I, McLean RJC, Nickel JC, Downey J, Costerton JW. The influence of bacteria on struvite crystal habit and its importance in urinary stone formation. *J Crystal Growth,* 1990; 104: 475.
26. Clerc M, Texier J, Bebear C. Experimental production of bladder calculi in rats by ureaplasma injection. *Ann Microbiol (Paris).* 1984; 135A: 135-140.
27. Cooke RJ, Jensen RL. Plasma ammonia concentration during the first six postnatal months, as measured with an ammonium-selective electrode. *Clin Chem.* 1983; 29: 1563-1564.
28. Cox AJ. Comparison of catheter surface morphologies. *Br J Urol.* 1990; 65: 55-60.

29. Cox AJ, Hukins DW. Morphology of mineral deposits on encrusted urinary catheters investigated by scanning electron microscopy. *J Urol*. 1989; 142: 1347-1350.
30. Cunarro JA, Weiner MW. A comparison of methods for measuring urinary ammonium. *Kid Int* 1974; 5: 303–305.
31. Curhan GC, Willett WC, Rimm EB, Stampfer MJ. Family history and risk of kidney stones. *J Am Soc Nephrol* 1997; 8: 1568-1573.
32. Dai LJ, Ritchie G, Kerstan D, Kang HS, Cole DE, Quamme GA. Magnesium transport in the renal distal convoluted tubule. *Physiol Rev*. 2001 Jan;81(1):51-84.
33. Dajani AM, Shehabi AA. Bacteriology and composition of infected stones. *Urology*. 1983; 21: 351-353.
34. Davenport K, Keeley FX. Evidence for the use of silver-alloy-coated urethral catheters. *J Hosp Infect*. 2005; 60: 298-303.
35. de Rouffignac C, Quamme G. Renal magnesium handling and its hormonal control. *Physiol Rev*. 1994 Apr;74(2):305-22.
36. European Association of Urology. Urolithiasis Guidelines. Retrieved February 22 2011 from <http://www.uroweb.org/gls/pdf/Urolithiasis%202010.pdf>
37. Eugster R, Rusterholz B, Schmid A, Spichiger UE, Simon W. Characterization procedure for ion-selective electrode assays of magnesium activity in aqueous solutions of physiological composition. *Clin Chem*. 1993 May;39(5):855-9.
38. Eugster R, Gehrig PM, Worf WE, Spichiger UE, Simon W. Selectivity modifying influence of anionic sites in neutral-carrier-based membrane electrodes. *Anal Chem*, 1991; 63:2285-9.
39. Finlayson B. Renal lithiasis in review. *Urol Clin North Am* 1974; 1: 181-212.

40. Fleisher M. Report of the first international workshop on unique magnesium-sensitive ion selective electrodes. *Scand J Clin Lab Invest Suppl.* 1994;217:97-8.
41. Flink EB, Aikawa JK, Whang R, Wacker WE. Hypomagnesemia. *West J Med.* 1987 Jul;147(1):86-7.
42. Gallo EA, Gellman SH. Hydrogen-bond-mediated folding in depsipeptide models of  $\beta$ -turns and  $\alpha$ -helical turns *J Am Chem Soc.*1993; 115: 9774-9788.
43. Ganpule AP, Desai M. Management of the staghorn calculus: multiple-tract versus single-tract percutaneous nephrolithotomy. *Curr Opin Urol.* 2008; 18: 220-223
44. Gault MH, Longrich LL, Crane G, Cooper R, Dow D, Best L, Stockall E, Brown W. Bacteriology of urinary tract stones. *J Urol.* 1995; 153: 1164-1170
45. Ghauri MS, Thomas, JDR. Evaluation of an ammonium ionophore for use in poly(vinyl chloride) membrane ion-selective electrodes: solvent mediator effects. *Analyst.* 1994; 119: 2323-2326.
46. Gomori F. *Methods in Enzymology.* Ed SP Colowick, NO Kaplan 1965; vol 1, pp 142-143. Academic Press, New York.
47. Grenabo L, Brorson JE, Hedelin H, Pettersson S. Ureaplasma urealyticum-induced crystallization of magnesium ammonium phosphate and calcium phosphates in synthetic urine. *J Urol.* 1984; 132: 795-799.
48. Grenabo L, Brorson JE, Hedelin H, Pettersson S. Concrement formation in the urinary bladder in rats inoculated with Ureaplasma urealyticum. *Urol Res.* 1985; 13: 195-198.
49. Grenabo L, Claes G, Hedelin H, Pettersson S. Rapidly recurrent renal calculi caused by Ureaplasma urealyticum: a case report. *J Urol.* 1986; 135: 995-997.
50. Grenabo L, Hedelin H, Pettersson S. The severity of infection stones compared to other stones in the upper urinary tract. *Scand J Urol Nephrol.* 1985; 19: 285-289.

51. Griffith DP. Struvite stones. *Kidney International*, 1978; 13: 372-382.
52. Griffith DP, Osborne CA. Infection (urease) stones. *Miner Electrolyte Metab.* 1987; 13: 278-285.
53. Guibalt GG, Smith RK, Montalvo JG. Use of ion-selective electrodes in enzymatic analysis. *Anal Chem.* 1969; 41: 600-605.
54. Gutiérrez M, Alegret S, del Valle M. Bioelectronic tongue for the simultaneous determination of urea, creatinine and alkaline ions in clinical samples. *Biosens Bioelectron.* 2008; 23: 795-802.
55. Hafen G, Laux-End R, Truttmann AC, Schibler A, McGuigan JA, Peheim E, Bianchetti MG. Plasma ionized magnesium during acute hyperventilation in humans. *Clin Sci (Lond).* 1996; 91: 347-351.
56. Hedelin H. Uropathogens and urinary tract concretion formation and catheter encrustations. *Int J Antimicrob Agents.* 2002; 19: 484-487.
57. Hedelin H, Brorson JE, Grenabo L, Pettersson S. *Ureaplasma urealyticum* and upper urinary tract stones. *Br J Urol.* 1984; 56: 244-249
58. Hedelin H, Grenabo L, Hugosson J, Pettersson S. The influence of zinc and citrate on urease-induced urine crystallisation. *Urol Res*, 1989; 17: 177-180.
59. Hill JL, Gettes LS, Lynch MR, Herbert NC. Flexible valinomycin electrodes for on-line determination of intravascular and myocardial  $K^+$ . *Am J Physiol.* 1978; 235: H455-H459.
60. Hoge JH, Hazenberg HJ, Gipsa CH. Determination of ammonia in urine with an ammonium electrode and with a direct method. *Clinica Chimica Acta*; 55: 273-279.

61. Honeck P, Wendt-Nordahl G, Krombach P, Bach T, Häcker A, Alken P, Michel MS. Does open stone surgery still play a role in the treatment of urolithiasis? Data of a primary urolithiasis center. *J Endourol.* 2009 Jul;23(7):1209-12.
62. Hu ZM, Bühner T, Müller M, Rusterholz B, Rouilly M, Simon W. Intracellular magnesium ion selective microelectrode based on a neutral carrier. *Anal Chem.* 1989 Mar 15;61(6):574-6.
63. Hugosson J, Grenabo L, Hedelin H, Pettersson S, Seeberg S. Bacteriology of upper urinary tract stones. *J Urol.* 1990; 143: 965-968.
64. Hugosson J, Grenabo L, Hedelin H, Pettersson S, Tarfusser I. How variations in the composition of urine influence urease-induced crystallization. *Urol Res* 1990; 18: 413-417.
65. Jenny HB, Riess C, Amman D, Magyar B, Asper R, Simon W. Determination of K<sup>+</sup> in diluted and undiluted urine with ion-selective electrodes. *Mikrochimica acta.* 1980. 11: 309-315.
66. Jones GL, Russell AD, Caliskan Z, Stickler DJ. A strategy for the control of catheter blockage by crystalline *Proteus mirabilis* biofilm using the antibacterial agent triclosan. *Eur Urol.* 2005; 48: 838-845.
67. Keane PF, Bonner MC, Johnston SR, Zafar A, Gorman SP. Characterization of biofilm and encrustation on ureteric stents in vivo. *Br J Urol.* 1994; 73: 687-691.
68. Kelepouris E, Agus ZS. Hypomagnesemia: renal magnesium handling. *Semin Nephrol.* 1998 Jan;18(1):58-73.
69. Kiss-Eröss K, Erdey L, Buzás I. Investigation of alkali metal and ammonium tetraphenylborates by infrared spectrophotometry. *Talanta.* 1970; 17: 1209-1212.
70. Koga S, Arakaki Y, Matsuoka M, Ohyama C. Staghorn calculi--long-term results of management. *Br J Urol.* 1991 Aug;68(2):122-4.

71. Kohler-Ockmore J, Feneley RC. Long-term catheterization of the bladder: prevalence and morbidity. *Br J Urol.* 1996; 77: 347-351.
72. Kristensen C, Parks JH, Lindheimer M, Coe FL. Reduced glomerular filtration rate and hypercalciuria in primary struvite nephrolithiasis. *Kidney Int.* 1987; 32: 749-753.
73. Lam HS, Lingeman JE, Mosbaugh PG, Steele RE, Knapp PM, Scott JW, Newman DM. Evolution of the technique of combination therapy for staghorn calculi: a decreasing role for extracorporeal shock wave lithotripsy. *J Urol.* 1992 Sep;148(3 Pt 2):1058-62.
74. Langley SEM, Fry CH. Differences in the free  $\text{Ca}^{2+}$  in undiluted urine from stone formers and normal subjects using a new generation of ion-selective electrodes. *Br J Urol,* 1995; 75: 288-295.
75. Lechevallier E, Traxer O, Saussine C. Chronic renal failure and urinary stone. *Prog Urol.* 2008 Dec;18(12):1027-9. [Article in French]
76. Leusmann DB. A classification of urinary calculi with respect to their composition and micromorphology. *Scand J Urol,* 1991; 25: 141-150.
77. Lewi HJ, White A, Hutchinson AG, Scott R. The bacteriology of the urine and renal calculi. *Urol Res.* 1984; 12: 107-109.
78. Lonsdale K. Human stones. *Science* 1968; 159: 1199-1207.
79. Maj-Zurawska M, Rouilly M, Morf WE, Simon W. Determination of magnesium and calcium in water with ion-selective electrodes. *Analytica Chimica Acta.* 1989; 218: 47-59.
80. Marsoner HJ, Spichiger UE, Ritter C, Sachs C, Ghahramani M, Offenbacher H, Kroneis H, Kindermans C, Dechaux M. Measurement of ionized magnesium with

- neutral carrier based ISE's. Progress and results with the AVL 988-4 magnesium analyzer. *Scand J Clin Lab Invest Suppl.* 1994;217:45-51.
81. Mathur S, Sabbuba NA, Suller MT, Stickler DJ, Feneley RC. Genotyping of urinary and fecal *Proteus mirabilis* isolates from individuals with long-term urinary catheters. *Eur J Clin Microbiol Infect Dis.* 2005; 24: 643-644.
  82. McAleer IM, Kaplan GW, Bradley JS, Carroll SF. Staghorn calculus endotoxin expression in sepsis. *Urology.* 2002; 59: 601.
  83. McCartney AC, Clark J, Lewi HJ. Bacteriological study of renal calculi. *Eur J Clin Microbiol.* 1985; 4: 553-555.
  84. McLean RJC, Downey J, Clapham L, Nickel JC. A simple technique for studying struvite crystal growth in-vitro. *Urological research,* 1990; 18: 39-43.
  85. McLean RJC, Downey J, Clapham L, Nickel JC. Influence of chondroitin sulphate, heparin sulphate, and citrate on proteus mirabilis-induced struvite crystallisation in-vitro. *J Urol,* 1990; 144: 1267-1271.
  86. McLean RJC, Nickel JC, Beveridge TJ, Costerton JW. Observations of the ultrastructure of infected kidney stones. *J Med Microbiol,* 1989; 29: 1-7.
  87. McLean RJC, Nickel JC, Noakes VC, Costerton JW. An in-vitro ultrastructural study of infectious kidney stone genesis. *Infection and immunity,* 1985; 49: 805-811.
  88. Menon M, Resnick MI. Urinary lithiasis: aetiology, diagnosis and medical management. In *Cambells Urology 8<sup>th</sup> Ed.* 2002. Vol IV, Ch 96: 3229-3305.
  89. Miano R, Germani S, Vespasiani G. Stones and urinary tract infections. *Urol Int.* 2007; 79 Suppl 1: 32-36.
  90. Moores WK, O'Boyle PJ. Staghorn calculi of the kidneys. A. Clinical review. *Eur Urol.* 1976;2(5):216-220.

91. Morgan SD, Rigby D, Stickler DJ. A study of the structure of the crystalline bacterial biofilms that can encrust and block silver Foley catheters. *Urol Res.* 2009; 37: 89-93.
92. Najem GR, Seebode JJ, Samady AJ, Feuerman M, Friedman L. Stressful life events and risk of symptomatic kidney stones. *Int J Epidemiol* 1997; 26: 1017-1023.
93. Nickel JC, Olson M, McLean RJC, Grant SK, Costerton JW. An ecological study of infected urinary stone genesis in an animal model. *Br J Urol*, 1987; 59: 21-30.
94. Ninan KN, Madhavan A, Sadhana R. A rapid non-aqueous titrimetric estimation of ammonium perchlorate in pyrotechnic compositions. *Propellants, Explosives, Pyrotechnics* 1990; 15: 8-10.
95. Norberg B, Norberg A, Parkhede U. The spontaneous variation of catheter life in long-stay geriatric inpatients with indwelling catheters. *Gerontology.* 1983; 29: 332-335.
96. O'Donnell J, Li H, Rusterholz B, Pedrazza U, Simon W. Development of magnesium selective ionophores. *Analytica Chimica Acta.* 1993; 281: 129-134.
97. Ogata T, Akakura K, Mizoguchi K, Mikami K, Nozumi K, Ito H. Annual changes of the incidence and clinical characteristics of magnesium ammonium phosphate urinary stones. *Int J Urol.* 2003; 10: 1-5.
98. Ong CL, Ulett GC, Mabbett AN, Beatson SA, Webb RI, Monaghan W, Nimmo GR, Looke DF, McEwan AG, Schembri MA. Identification of type 3 fimbriae in uropathogenic *Escherichia coli* reveals a role in biofilm formation. *J Bacteriol.* 2008;190: 1054-1063.
99. Parry ES, Lister IS. Sunlight and hypercalciuria. *Lancet* 1975; 1: 1063-1065.
100. Peralta CA, Kurella M, Lo JC, Chertow GM. The metabolic syndrome and chronic kidney disease. *Curr Opin Nephrol Hypertens.* 2006;15: 361-365.

101. Priestley JT, Dunn JH. Branched renal calculi. *J Urol*. 1949; 61:194-203.
102. Prince CL, Scardino PL. A statistical analysis of ureteral calculi. *J Urol* 1960; 83: 561-565.
103. Quamme GA. Renal handling of magnesium: drug and hormone interactions. *Magnesium*. 1986;5(5-6):248-72.
104. Quamme GA, de Rouffignac C. Epithelial magnesium transport and regulation by the kidney. *Front Biosci*. 2000 Aug 1;5:D694-711.
105. Rehak NN, Cecco SA, Niemela JE, Hristova EN, Elin RJ. Linearity and stability of the AVL and Nova magnesium and calcium ion-selective electrodes. *Clin Chem*. 1996 Jun;42(6 Pt 1):880-7.
106. Resnick MI. Evaluation and management of infection stones. *Urol Clin North Am*. 1981; 8: 265-276.
107. Resnick MI, Boyce WH. Bilateral staghorn calculi--patient evaluation and management. *J Urol*. 1980; 123: 338-341.
108. Robertson WG. The scientific basis of urinary stone formation. In *Scientific basis of urology*, 2004; 2<sup>nd</sup> ed. Ch 10: 205-227.
109. Robertson WG, Peacock M. Risk factors in calcium stone formation. In *Proceedings of the VII International Congress of Urology*. (Barcelo R., ed.) Basle: Karger.
110. Robertson WG, Peacock M, Heyburn PJ, Hanes FA, Rutherford A, Clementson E, Swaminathan R, Clark PB. Should recurrent calcium oxalate stone-formers become vegetarians? *Br J Urol* 1979; 51: 427-431.
111. Rodman JS. Struvite stones. *Nephron*, 1999; 81(suppl 1): 50-59.
112. Rose, BD. *Clinical Physiology of Acid-Base and Electrolyte Disorders*, 4th ed, McGraw-Hill, New York, 1994, pp. 551-553.

113. Rouilly M, Rusterholz B, Spichiger UE, Simon W. Neutral ionophore-based selective electrode for assaying the activity of magnesium in undiluted blood serum. *Clin Chem.* 1990; 36: 466-469.
114. Russell JA. The colorimetric estimation of small amounts of ammonia by the phenol-hypochlorite reaction. *J Biol Chem* 1944; 156: 457-461.
115. Saad F, Faucher R, Mauffette F, Paquin JM, Perreault JP, Valiquette L. Staghorn calculi treated by percutaneous nephrolithotomy: risk factors for recurrence. *Urology.* 1993 Feb;41(2):141-3.
116. Sabbuba NA, Mahenthalingam E, Stickler DJ. Molecular epidemiology of *Proteus mirabilis* infections of the catheterized urinary tract. *J Clin Microbiol.* 2003; 41: 4961-4965.
117. Sabbuba NA, Stickler DJ, Mahenthalingam E, Painter DJ, Parkin J, Feneley RC. Genotyping demonstrates that the strains of *Proteus mirabilis* from bladder stones and catheter encrustations of patients undergoing long-term bladder catheterization are identical. *J Urol.* 2004; 171: 1925-1928.
118. Sakhaee K. Nephrolithiasis as a systemic disorder. *Curr Opin Nephrol Hypertens.* 2008; 17: 304-309.
119. Sakhaee K, Maalouf NM. Metabolic syndrome and uric acid nephrolithiasis. *Semin Nephrol.* 2008; 28: 174-180.
120. Schwarz J, Kaden H, Pausch G. Development of miniaturized potentiometric nitrate- and ammonium selective electrodes for applications in water monitoring. *Fresenius J Anal Chem.* 2000; 367: 396-398
121. Segura JW, Preminger GM, Assimos DG, Dretler SP, Kahn RI, Lingeman JE, Macaluso JN Jr, McCullough DL. Nephrolithiasis Clinical Guidelines Panel summary report on the management of staghorn calculi. *The American Urological*

- Association Nephrolithiasis Clinical Guidelines Panel. *J Urol.* 1994 Jun;151(6):1648-51.
122. Segura JW. Staghorn calculi. *Urol Clin North Am.* 1997; 24: 71-80.
123. Sharma RN, Shah I, Gupta S, Sharma P, Beigh AA. Thermogravimetric analysis of urinary stones. *Br J Urol* 1989; 64: 564-566.
124. Shaw GL, Choong SK, Fry C. Encrustation of biomaterials in the urinary tract. *Urol Res.* 2005; 33: 17-22.
125. Singh M, Chapman R, Tresidder Wall I, Hellgren E, Larsson L, Tiselius HG. Biochemical risk factors in patients with renal staghorn stone disease. *Urology.* 1986; 28: 377-380.
126. Stark RP, Maki DG. Bacteriuria in the catheterized patient. What quantitative level of bacteriuria is relevant? *N Engl J Med.* 1984; 311: 560-564.
127. Stickler DJ. Bacterial biofilms in patients with indwelling urinary catheters. *Nat Clin Pract Urol.* 2008; 5: 598-608.
128. Stickler D, Ganderton L, King J, Nettleton J, Winters C. *Proteus mirabilis* biofilms and the encrustation of urethral catheters. *Urol Res.* 1993; 21: 407-411.
129. Stickler DJ, Jones SM, Adusei GO, Waters MG, Cloete J, Mathur S, Feneley RC. A clinical assessment of the performance of a sensor to detect crystalline biofilm formation on indwelling bladder catheters. *BJU Int.* 2006; 98: 1244-1249.
130. Stickler DJ, Lear JC, Morris NS, Macleod SM, Downer A, Cadd DH, Feast WJ. Observations on the adherence of *Proteus mirabilis* onto polymer surfaces. *J Appl Microbiol.* 2006; 100: 1028-1033.
131. Stickler DJ, Morgan SD. Modulation of crystalline *Proteus mirabilis* biofilm development on urinary catheters. *J Med Microbiol.* 2006; 55: 489-494.

132. Stickler D, Young R, Jones G, Sabbuba N, Morris N. Why are Foley catheters so vulnerable to encrustation and blockage by crystalline bacterial biofilm? *Urol Res.* 2003; 31: 306-311.
133. Stratful I, Scrimshaw MD, Lester JN. Conditions influencing the precipitation of magnesium ammonium phosphate. *Water Res.* 2001; 35: 4191-4199.
134. Suller MTE, Anthony VJ, Mathur S, Feneley RCL, Greenman J, Stickler DJ. Factors modulating the pH at which calcium and magnesium phosphates precipitate from human urine. *Urol Res*, 2005; 33: 254-260.
135. Sutor DJ. Newberyite –its formation in human urinary calculi. *Nature*, 1968; 218: 295.
136. Themelis DG, Economou A, Tsiomlektisis A, Tzanavarasa PD. Direct determination of phosphate in urine by sequential-injection analysis with single on-line dilution–calibration method and photometric detection. *Anal Biochem* 2004; 330: 193-198.
137. Thom JA, Morris JE, Bishop A, Blacklock NJ. Effect of dietary sucrose on urinary calcium oxalate activity product. In *Urinary Calculus*, p103. (Brockis JG, Finlayson B eds.) Littleton, Mass: PSG Publishing Co.
138. Thompson RB, Stamey TA. Bacteriology of infected stones. *Urology.* 1973; 2: 627-633.
139. Tsukagoshi D, Dinkovski B, Dasan S, Jethwa J. Perinephric abscess secondary to a staghorn calculus presenting as a subcutaneous abscess. *CJEM.* 2006; 8: 285-288.
140. Uribarri J, Oh MS, Carroll HJ. The first kidney stone. *Ann Intern Med* 1989; 111; 1006-1009.
141. Vargas AD, Bragin SD, Mendez R. Staghorn calculis: its clinical presentation, complications and management. *J Urol.* 1982; 127: 860-862.

142. Venkatesan N, Shroff S, Jayachandran K, Doble M. Polymers as ureteral stents. *J Endourol.* 2010; 24: 191-198.
143. Venkatesan N, Shroff S, Jeyachandran K, Doble M. Effect of uropathogens on in vitro encrustation of polyurethane double J ureteral stents. *Urol Res.* 2010; 39: 29-37.
144. Warren JW. Catheter-associated urinary tract infections. *Int J Antimicrob Agents.* 2001; 17: 299-303.
145. Warren JW, Damron D, Tenney JH, Hoopes JM, Deforge B, Muncie HL Jr. Fever, bacteremia, and death as complications of bacteriuria in women with long-term urethral catheters. *J Infect Dis.* 1987; 155: 1151-1158.
146. Warren JW, Muncie HL Jr, Hebel JR, Hall-Craggs M. Long-term urethral catheterization increases risk of chronic pyelonephritis and renal inflammation. *J Am Geriatr Soc.* 1994; 42: 1286-1290
147. Weatherburn MW. Phenol-hypochlorite reaction for determination of ammonia. *Anal Chem.* 1967; 39: 971-974.
148. Werness P, Brown C, Smith L, Finlayson B. Equil2: a basic computer program for the calculation of urinary saturation. *J Urol,* 1985; 134: 1242-1244.
149. West B, Luke A, Durazo-Arvizu RA, Cao G, Shoham D, Kramer H. Metabolic syndrome and self-reported history of kidney stones: the National Health and Nutrition Examination Survey (NHANES III) 1988-1994. *Am J Kidney Dis.* 2008; 51: 741-747.
150. Whang R, Oei TO, Aikawa JK, Ryan MP, Watanabe A, Chrysant SG, Fryer A. Magnesium and potassium interrelationships, experimental and clinical. *Acta Med Scand Suppl.* 1981;647:139-44.

151. Whang R. Magnesium deficiency: pathogenesis, prevalence, and clinical implications. *Am J Med.* 1987 Mar 20;82(3A):24-9.
152. Woodhouse CR, Farrell CR, Paris AM, Blandy JP. The place of extended pyelolithotomy (Gil-Vernet Operation) in the management of renal staghorn calculi. *Br J Urol.* 1981 Dec;53(6):520-3.
153. Worcester EM, Parks JH, Evan AP, Coe FL. Renal function in patients with nephrolithiasis. *J Urol.* 2006; 176: 600-603;
154. Worcester E, Parks JH, Josephson MA, Thisted RA, Coe FL. Causes and consequences of kidney loss in patients with nephrolithiasis. *Kidney Int.* 2003; 64: 2204-2213.